

UNCLASSIFIED

AD NUMBER
AD865310
NEW LIMITATION CHANGE
TO Approved for public release, distribution unlimited
FROM Distribution authorized to U.S. Gov't. agencies and their contractors; Critical Technology; DEC 1969. Other requests shall be referred to Air Force Flight Dynamics Laboratory, Attn: FDCS, Wright-Patterson AFB, OH 45433.
AUTHORITY
affdl ltr, 6 apr 1972

THIS PAGE IS UNCLASSIFIED

AFFDL-TR-68-164

AD 865310

**AIRCRAFT LOAD ALLEVIATION AND MODE  
STABILIZATION (LAMS) FLIGHT  
DEMONSTRATION TEST ANALYSIS**

*MR. P. M. BURRIS*

*The Boeing Co.*

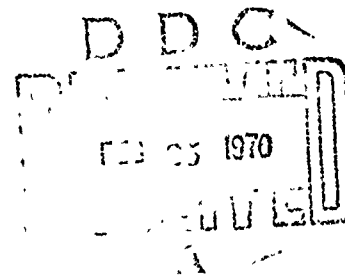
*and*

*MR. M. A. BENDER*

*Honeywell, Inc.*

TECHNICAL REPORT AFFDL-TR-68-164

DECEMBER 1969



This document is subject to special export controls and each transmittal to foreign governments or foreign nationals may be made only with prior approval of Air Force Flight Dynamics Laboratory (FDCS), Wright-Patterson Air Force Base, Ohio 45433.

Reproduced by the  
CLEARINGHOUSE  
for Federal Scientific & Technical  
Information Springfield Va. 22151

**AIR FORCE FLIGHT DYNAMICS LABORATORY  
AIR FORCE SYSTEMS COMMAND  
WRIGHT-PATTERSON AIR FORCE BASE, OHIO**

NOTICE

When Government drawings, specifications, or other data are used for any purpose other than in connection with a definitely related Government procurement operation, the United States Government thereby incurs no responsibility nor any obligation whatsoever; and the fact that the Government may have formulated, furnished, or in any way supplied the said drawings, specifications, or other data, is not to be regarded by implication or otherwise as in any manner licensing the holder or any other person or corporation, or conveying any rights or permission to manufacture, use, or sell any patented invention that may in any way be related thereto.

This document is subject to special export controls and each transmittal to foreign governments or foreign nationals may be made only with prior approval of Air Force Flight Dynamics Laboratory (FDCS), Wright-Patterson Air Force Base, Ohio 45433.

2

2FSTI	WHIP SECTION <input type="checkbox"/>
DCG	REP SECTION <input checked="" type="checkbox"/>
UN-ANNOUNCED	
JUSTIFICATION	
BY	
DATE TO BE AVAILABLE	
DIST.	

Copies of this report should not be returned unless return is required by security considerations, contractual obligations, or notice on a specific document.

**AIRCRAFT LOAD ALLEVIATION AND MODE  
STABILIZATION (LAMS) FLIGHT  
DEMONSTRATION TEST ANALYSIS**

**MR. P. M. BURRIS**

*The Boeing Co.*

*and*

**MR. M. A. BENDER**

*Honeywell, Inc.*

This document is subject to special export controls and each transmittal to foreign governments or foreign nationals may be made only with prior approval of Air Force Flight Dynamics Laboratory (FDCS), Wright-Patterson Air Force Base, Ohio 45433.

## FOREWORD

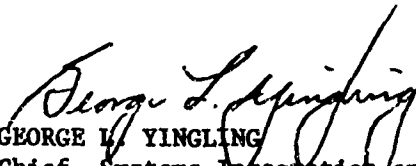
This report was prepared for the Air Force Flight Dynamics Laboratory through joint effort of The Boeing Company, Wichita Division, Wichita, Kansas, and Honeywell, Inc., Aerospace Division, Minneapolis, Minnesota, in fulfillment of Contract AF33(615)-3753.

The work was administered and the program was conducted under the direction of Mr. R. P. Johannes (FDCS) during the period June 1966 through December 1968.

The program reported herein was made possible only through the dedicated and enthusiastic support of all those who participated which are too numerous to mention. The activity was directed by Mr. P. M. Burris, Boeing Engineering Manager, and Mr. M. A. Bender, Honeywell Project Manager. Mr. R. L. McDougal, Lockheed-Georgia Company, Marietta, Georgia, contributed significantly to the C-5A analyses.

The report is identified internally at The Boeing Company, Wichita Division, as D3-7902-2.

This technical report has been reviewed and is approved.

  
GEORGE L. YINGLING  
Chief, Systems Integration and  
Flight Experimentation Branch  
Flight Control Division  
Air Force Flight Dynamics Laboratory

## ABSTRACT

The Load Alleviation and Mode Stabilization (LAMS) program was conducted to demonstrate the capabilities of an advanced flight control system (FCS) to alleviate gust loads and control structural modes on a large flexible aircraft using existing aerodynamic control surfaces as force producers.

The analysis, design, and flight demonstration of the flight control system was directed toward three discrete flight conditions contained in a hypothetical mission profile of the B-52E test aircraft. The FCS was designed to alleviate structural loads while flying through atmospheric turbulence.

The LAMS-FCS was produced as hardware and installed on the test vehicle, B-52E AF56-632. Test vehicle modifications included the addition of hydraulically powered controls, a fly-by-wire (FBW) pilot station, associated electronics and analog computers at the test engineer's stations, instrumentation for system evaluation, and the LAMS flight controller.

Flight demonstration of the LAMS-FCS was conducted to provide a comparison of analytical and experimental data. The results obtained showed that the LAMS-FCS provided significant reduction in fatigue damage rates.

In addition, a LAMS C-5A study was included in the program. This portion of the program was to analytically demonstrate that the technology developed for the B-52 could be applied to another aircraft. The C-5A study was conducted for one flight condition in the C-5A mission profile. Significant reductions in fatigue damage rates and fuselage accelerations were predicted by the LAMS C-5A analyses.

This abstract is subject to special export controls and each transmittal to foreign governments or foreign nationals may be made only with prior approval of the Air Force Flight Dynamics Laboratory (FFDL), Wright-Patterson Air Force Base, Ohio 45433.

## CONTENTS

	<u>PAGE</u>
1.0 INTRODUCTION	17
1.1 Background	17
1.2 Purpose	17
1.3 Objectives	18
1.4 Report Contents	18
2.0 SUMMARY	19
2.1 Introduction	19
2.2 Aircraft Configuration and Modification	19
2.3 System Performance	22
2.4 Hardware Performance	31
3.0 AIRCRAFT CONFIGURATION AND MODIFICATION	32
3.1 Monitor Pilot Control System	32
3.2 Evaluation Pilot Control System	32
3.3 Flight Engineer Station	34
3.4 Instrumentation	35
3.5 Baseline SAS	35
3.6 LAMS-FCS	44
4.0 SYSTEM PERFORMANCE	48
4.1 Flutter Boundary and Dynamic Response Testing	48
4.2 Aerodynamic Testing	52
4.3 Structural Response to Turbulence	64
5.0 HARDWARE PERFORMANCE	121
5.1 Aircraft Control System Ground Vibration Test	121
5.2 Hydraulic Actuator Performance	128
5.3 Hydraulic Power System Performance	139
5.4 Evaluation Pilot Feel System	143
5.5 Electrical/Electronics System	147
5.6 Baseline SAS	148
5.7 LAMS-FCS	150
5.8 System Checkout	154
6.0 CONCLUSIONS	170
6.1 Conclusions, LAMS Program	170
6.2 Conclusions, LAMS B-52 Flight Demonstration Test Analyses	170
7.0 REFERENCES	172

## FIGURES

<u>FIGURE</u>		<u>PAGE</u>
1	LAMS Document Organization	16
2	B-52E Aircraft Geometry	20
3	Electronics Profile	21
4	Flight Region For The Revised LAMS-FCS	25
5	Dutch Roll Handling Qualities	26
6	Pilot Control System	33
7	Transducer Locations	37
8	Load And Stress Measurement Locations	40
9	Baseline SASS Rate Gyro Locations	41
10	Baseline Pitch SAS Block Diagram	42
11	Baseline Roll And Yaw SAS Block Diagram	43
12	LAMS Longitudinal Flight Control System Block Diagram	45
13	LAMS-FCS Rate Gyro Locations	46
14	LAMS Lateral-Directional Flight Control System Block Diagram	47
15	Dynamic Response Testing Initial LAMS-FCS Wing Tip Vertical Displacement	50
16	Dynamic Response Testing Modified LAMS-FCS Wing Tip Vertical Displacement	51
17	Short Period Response - Flight Test Data - Flight Condition 1	53
18	Short Period Response - Flight Test Data - Flight Condition 2	54
19	Short Period Response - Flight Test Data - Flight Condition 3	55
20	Symmetrical Spoiler Effectiveness - LAMS-FCS Spoilers - Flight Condition 1	57
21	Symmetrical Aileron Effectiveness - Flight Condition 1	58
22	Spoiler Roll Response - Flight Condition 1	60

<u>FIGURE</u>		<u>PAGE</u>
23	Aileron Roll Response - Flight Condition 1	61
24	Elevator Effectiveness - Flight Condition 1	62
25	Rudder Effectiveness - Flight Condition 1	63
26	Signal to Noise Comparison	66
27	Coherency Function Between Pilot And Gust Inputs	68
28	Normalized Gust Spectra	69
29	Coherency Function Between Vertical And Lateral Components	70
30	Frequency Response Function - BS 1222 Vertical Bending Moment	72
31	Frequency Response Function - BS 1412 Vertical Bending Moment	73
32	Frequency Response Function - SBL 56 Vertical Bending Moment	74
33	Frequency Response Function - WS 222 Vertical Bending Moment	75
34	Frequency Response Function - WS 222 Chordwise Bending Moment	76
35	Frequency Response Function - WS 820 Vertical Bending Moment	77
36	Frequency Response Function - WS 820 Chordwise Bending Moment	78
37	Frequency Response Function - WS 974 Vertical Bending Moment	79
38	Frequency Response Function - WS 974 Chordwise Bending Moment	80
39	Frequency Response Function - BS 172 Vertical Acceleration	81
40	Frequency Response Function - BS 860 Vertical Acceleration	82
41	Frequency Response Function - BS 1655 Vertical Acceleration	83

<u>FIGURE</u>		<u>PAGE</u>
42	Frequency Response Function - Elevator Angular Displacement	84
43	Frequency Response Function - Aileron Angular Displacement	85
44	Frequency Response Function - Spoiler Angular Displacement	86
45	Frequency Response Function - FS 135 Side Bending Moment	87
46	Frequency Response Function - BS 1222 Side Bending Moment	88
47	Frequency Response Function - BS 1412 Side Bending Moment	89
48	Frequency Response Function - WS 222 Vertical Bending Moment	90
49	Frequency Response Function - WS 222 Chordwise Bending Moment	91
50	Frequency Response Function - WS 820 Vertical Bending Moment	92
51	Frequency Response Function - WS 820 Chordwise Bending Moment	93
52	Frequency Response Function - WS 974 Vertical Bending Moment	94
53	Frequency Response Function - WS 974 Chordwise Bending Moment	95
54	Frequency Response Function - SEL 56 Vertical Bending Moment	96
55	Frequency Response Function - BS 172 Side Acceleration	97
56	Frequency Response Function - BS 860 Side Acceleration	98
57	Frequency Response Function - BS 1655 Side Acceleration	99
58	Frequency Response Function - Rudder Angular Displacement	100

<u>FIGURE</u>		<u>PAGE</u>
59	Frequency Response Function - Aileron Angular Displacement	101
60	Wing RMS Vertical Bending Moment Due to Vertical Gust	103
61	Fuselage RMS Vertical Bending Moment Due to Vertical Gust	104
62	Fuselage RMS Vertical Acceleration Due to Vertical Gust	105
63	Wing RMS Chordwise Bending Moment Due to Lateral Gust	106
64	Fuselage RMS Side Bending Moment Due to Lateral Gust	107
65	Fuselage RMS Side Acceleration Due to Lateral Gust	108
66	Vertical Acceleration FSD - BS 172	120
67	Directional Manual Control System Dynamics - Monitor Pilot	122
68	Longitudinal Manual Control System Dynamic - Monitor Pilot	123
69	Frequency Response - Aileron Against Actuator	125
70	Frequency Response - Shaker On Aileron AMVIA	126
71	Frequency Response - Monitor Pilot Roll Axis Control System	127
72	Frequency Response - Monitor Pilot Roll Axis Control System - Spoiler Disconnected	129
73	Actuator Maximum Surface Amplitude Limits For Linear Response To Sinusoidal Inputs	130
74	Aileron Actuator Frequency Response	131
75	Aileron Auxiliary Actuator Open Loop Frequency Response	132
76	Aileron Actuator Step Response	133
77	Aileron Actuator Hysteresis	133
78	LAMS Spoiler Actuator Frequency Response	135

<u>FIGURE</u>		<u>PAGE</u>
79	LAMS Spoiler Actuator Step Response	136
80	LAMS Spoiler Actuator Hysteresis	136
81	FBW Spoiler Actuator Open Loop Frequency Response	137
82	Rudder Actuator Frequency Response	138
83	Rudder Actuator Step Response	140
84	Rudder Actuator Hysteresis	140
85	Elevator Actuator Frequency Response	141
86	Elevator Actuator Step Response	142
87	Elevator Actuator Hysteresis	142
88	Evaluation Pilot Rudder Pedal Feel System Preload And Spring Gradient	144
89	Evaluation Pilot Control Column Feel System Pre- load And Spring Gradient	145
90	Evaluation Pilot Control Wheel Feel System Pre- load And Spring Gradient	146
91	Function Generator Sine Wave Output	149
92	Open Loop Frequency Response - Baseline Pitch SAS FC-2	151
93	Open Loop Frequency Response - Baseline Roll SAS FC-2	152
94	Open Loop Frequency Response - Baseline Yaw SAS FC-2	153
95	LAMS-FCS Open Loop Frequency Response - Elevator To WBL 720 Roll Rate Gyro	155
96	LAMS-FCS Open Loop Frequency Response - Aileron To WBL 720 Roll Rate Gyro	156
97	LAMS-FCS Open Loop Frequency Response - Spoiler To WBL 720 Roll Rate Gyro	157
98	LAMS-FCS Open Loop Frequency Response - Elevator To BS 566 Pitch Rate Gyro	158
99	LAMS-FCS Open Loop Frequency Response - Aileron To BS 566 Pitch Rate Gyro	159

FIGUREPAGE

100	LAMS-FCS Open Loop Frequency Response - Spoiler To BS 566 Pitch Rate Gyro	160
101	LAMS-FCS Open Loop Frequency Response - Elevator To BS 1377 Pitch Rate Gyro	161
102	LAMS-FCS Open Loop Frequency Response - Aileron To BS 1377 Pitch Rate Gyro	162
103	LAMS-FCS Open Loop Frequency Response - Spoiler To BS 1377 Pitch Rate Gyro	153
104	LAMS-FCS Open Loop Frequency Response - Elevator to Evaluation Pilot Column	164
105	LAMS-FCS Open Loop Frequency Response - Rudder To BS 695 Yaw Rate Gyro	165
106	LAMS-FCS Open Loop Frequency Response - Aileron To BS 805 Roll Rate Gyro	166
107	LAMS-FCS Open Loop Frequency Response - Aileron To Evaluation Pilot Wheel	167

TABLES

<u>TABLE</u>		<u>PAGE</u>
I	Flutter Test Configurations	23
II	Relative Peak Incremental Stresses	28
III	Relative Fatigue Damage Rates	29
IV	Relative RMS Accelerations	30
V	Instrumentation (Available At Interpatch Panel)	36
VI	Instrumentation (Not Available At Interpatch Panel)	38
VII	Vertical Gust A's - Raw Time History Data	109
VIII	Vertical Gust A's - Calculated	110
IX	Vertical Gust A's - Theoretical	111
X	Lateral Gust A's - Raw Time History Data	112
XI	Lateral Gust A's - Calculated	113
XII	Lateral Gust A's - Theoretical	114
XIII	Vertical Gust N <sub>0</sub> 's - Calculated	115
XIV	Vertical Gust N <sub>0</sub> 's - Theoretical	116
XV	Lateral Gust N <sub>0</sub> 's - Calculated	117
XVI	Lateral Gust N <sub>0</sub> 's - Theoretical	118

## NOMENCLATURE

### SYMBOLS

AF	Air Force	
AF	Aft fuselage	
A/P	Airplane	
Aux Act	Auxiliary Actuator	
$A_y$	Normalized $\sigma_y$	
	$A_y = \frac{\epsilon_y}{\sigma_y} \sigma_{gust}^2$	
BBL	Body buttock line	
BS	Body Station	
BWL	Body water line	
CBM	Chordwise bending moment	inch-lbs
CPS	Cycles per second	
DVM	Digital volt meter	
DEG	Degree	
ECP	Engineering Change Proposal	
FBW	Fly-by-wire	
FC	Flight condition	
FCS	Flight control system	
FS	Fin station	
FPS	Feet per second	
Ft	Feet	
GW	Airplane gross weight	lbs
GPM	Gallons per minute	
In	Inches	
KEAS	Knots equivalent airspeed	

SYMBOLS

KIAS	Knots indicated airspeed
KIPS	Thousand pounds
L.H.	Left Hand
Lbs.	Pounds
LSS	Left stabilizer station
$N_{O_y}$	Zero crossing of y with positive slope

$$N_{O_y} = \frac{1}{2\pi} \frac{\sigma_y^2}{\sigma_y^2}^{\frac{1}{2}} \quad \text{cps}$$

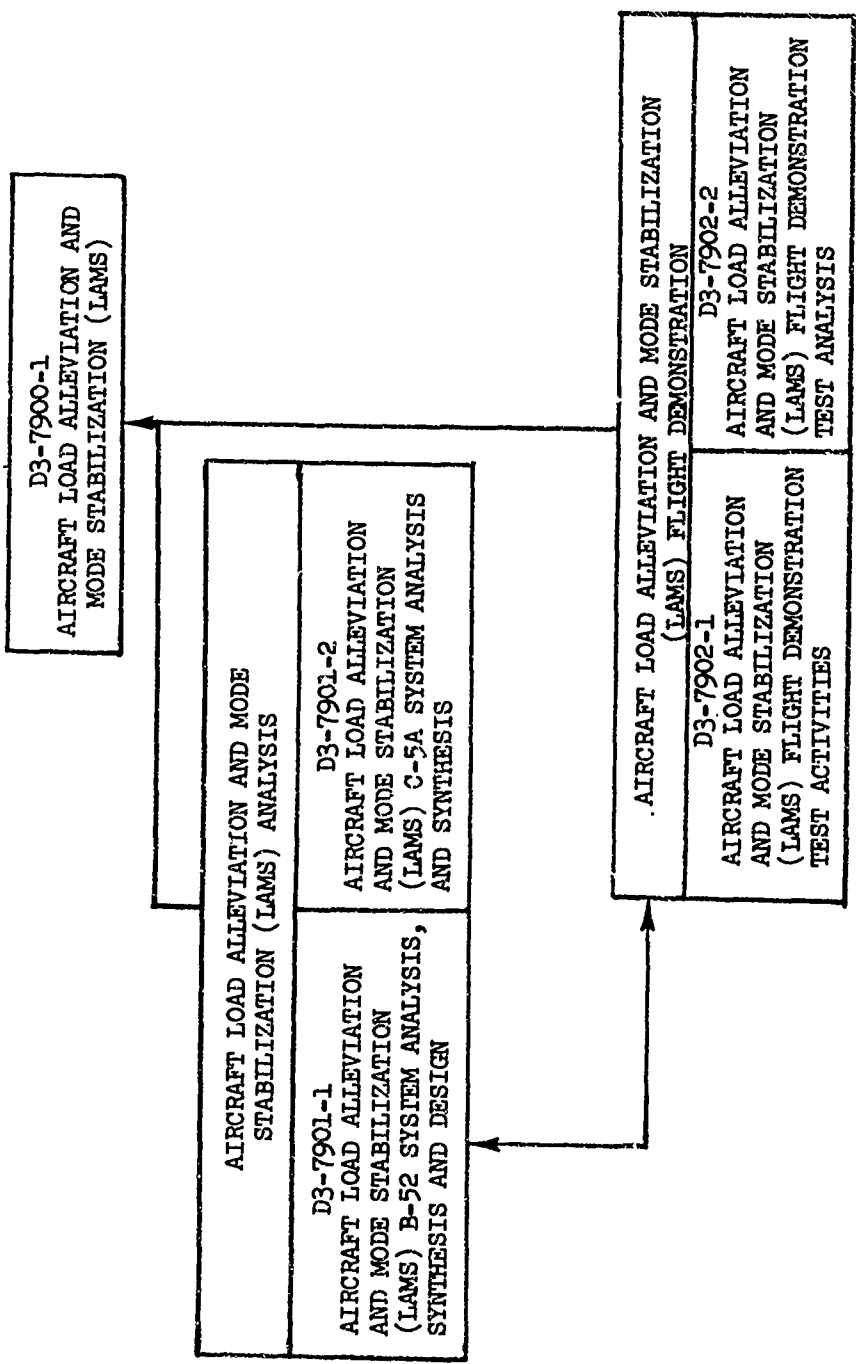
PSD	Power spectral density
PSI	Pounds per square inch
Rad.	Radians
RMS	Root mean square
RPM	Revolutions per minute
SAS	Stability augmentation system
SBL	Stabilizer buttock line
Sec	Second
Sta	Station
T.E.	Trailing edge
Vac	Volts alternating current
VBM	Vertical bending moment
WBL	Wing buttock line
WS	Wing station
WL	Water line
CG	Center of gravity
db	Decibel

## SYMBOLS

$g$	Acceleration	
$m$	Mach number	
$\alpha$	Angle of attack ( + nose up)	rad
$\beta$	Angle of sideslip ( + nose left)	rad
$\delta_c$	Column displacement	deg
$\delta_{RP}$	Rudder pedal displacement in	in
$\delta_{SP_{FBW}}$	Fly-by-wire spoiler deflection ( + up on right wing)	
$\delta_{SP_{LAMS}}$	LAMS spoiler deflection ( + up)	
$\delta_{WH}$	Wheel displacement	deg
$\delta_a$	Aileron deflection ( + Trailing edge down on right wing) (asymmetrical)	
$\delta_e$	Elevator deflection ( + Trailing edge down)	
$\delta_r$	Rudder deflection ( + Trailing edge left)	
$\delta_t$	Tab deflection	rad
$\zeta$	Damping ratio, fraction of critical damping	
$\zeta_{SP}$	Short period damping ratio	
$\theta$	Pitch attitude	rad
$\theta_x$	Roll angle ( + right wing down)	rad
$\theta_y$	Pitch angle ( + nose up)	rad
$\theta_z$	Heading angle ( + nose right)	rad
$\phi$	Roll angle ( + right wing down)	rad
$\psi$	Airplane heading ( + nose right)	rad
$\omega$	Frequency (radians/sec)	

SYMBOLS

$\Delta s$	Change in horizontal stabilizer position ( + leading edge up)	units
$\phi_Y(\omega)$	Power spectral density of $y(t)$	



LAMS DOCUMENT ORGANIZATION

FIGURE I

## 1.0 INTRODUCTION

This report presents the results of the ground testing accomplished prior to flight and the flight demonstration program conducted to evaluate the LAMS Flight Control System (FCS). Test results are compared with the performance predicted by theoretical analyses reported in Reference 4.

### 1.1 Background

The LAMS test vehicle NB-52E AF 56-632 includes all structural modifications through ECP 1128 which provides strength increases to the aft fuselage and vertical tail. To accomplish the LAMS program, the test vehicle was modified to include high response control surface hydraulic actuators for the elevators, rudder, ailerons, and LAMS spoilers (panels 1, 2, 13, and 14). In addition, new servo valves were installed to permit spoiler segments 3 through 12 to accept fly-by-wire electrical inputs. The pilot station was modified to a fly-by-wire (evaluation pilot) station. The co-pilot (monitor pilot) station retains the mechanical linkage connections to all control surface actuators. Rate gyros located throughout the aircraft provide control system sensing. The rate gyro signals are conditioned using the on-board analog computers for the Baseline SAS and the LAMS flight computer. Control system signals proceed to the control surface servos from either the Baseline SAS or LAMS-FCS. The computers and associated electronics are installed at the bombardier-navigator station. The test vehicle also includes the instrumentation required to provide quantitative data for system performance evaluation. Additional details of the test vehicle installations are presented in Reference .

The Baseline SAS and LAMS-FCS were designed for the following three flight conditions:

- (1) Flight Condition 1 (FC-1): 350,000 pound gross weight; 350 KIAS; 4000 feet altitude.
- (2) Flight Condition 2 (FC-2): 350,000 pound gross weight; 240 KIAS; 4000 feet altitude.
- (3) Flight Condition 3 (FC-3): 270,000 pound gross weight; .77 Mach; 32,700 feet altitude.

### 1.2 Purpose

The purpose of the ground and flight demonstration phase of the LAMS program was to produce experimental data for comparison with analytically predicted performance; thus demonstrating the system and validating the analytical techniques used in system design.

### 1.3 Objectives

Ground test objectives were:

- Ground vibration test (GVT) of the manual (i.e., monitor pilot) control system
- Determination of control surface actuator dynamic response characteristics
- Evaluation of the hydraulic power system
- Evaluation of the fly-by-wire control system characteristics
- Evaluation of the Baseline SAS and LAMS-FCS characteristics

Flight demonstration objectives were:

- Checkout of the basic aircraft with powered controls
- Stability demonstration of aircraft and control system
- Determination of aerodynamic control surface authority and effectivity and evaluation of handling qualities for the Baseline SAS and LAMS-FCS
- Evaluation of the Baseline SAS and LAMS-FCS dynamic response characteristics
- Demonstration of the LAMS system during flight through turbulence

### 1.4 Report Contents

- Section 2.0 summarizes the document
- Section 3.0 describes the aircraft modification and test system configurations
- Section 4.0 discusses and compares the performance of the test systems during flight with the analytically predicted performance
- Section 5.0 describes hardware performance as compared with specification or design requirements
- Section 6.0 presents the conclusions
- Section 7.0 contains references

## 2.0 SUMMARY

### 2.1 Introduction

The flight demonstration phase of the LAMS program was conducted to experimentally evaluate the basic aircraft with hydraulically powered controls, the Baseline SAS, and the LAMS-FCS.

### 2.2 Aircraft Configuration and Modification

The test vehicle was a loads demonstration test aircraft and included extensive instrumentation from that testing. LAMS testing was conducted with the 3000 gallon external tanks removed to permit airspeeds to 390 KIAS.

#### 2.2.1 Flight Control Systems

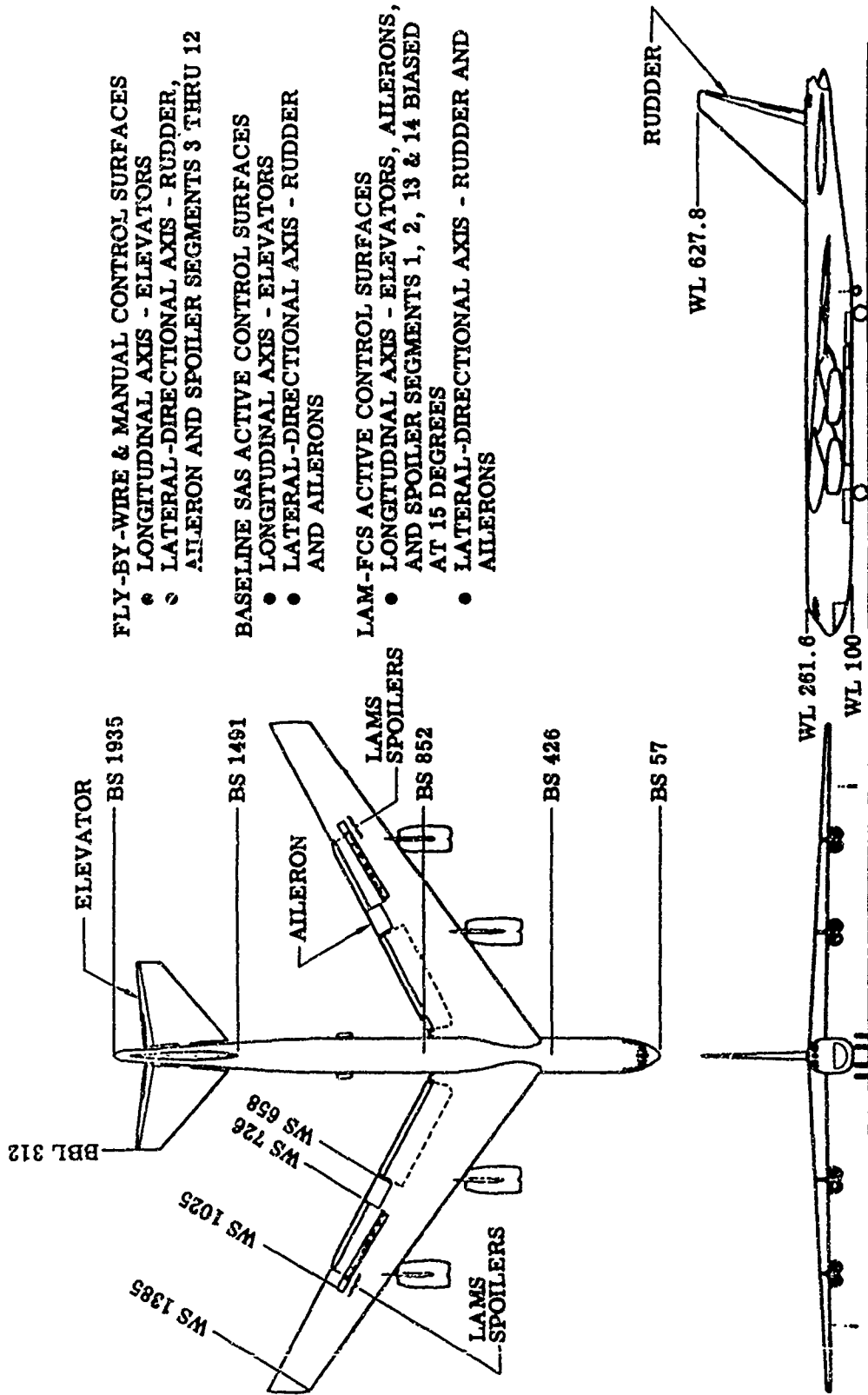
Test vehicle control system modifications consisted of hydraulically powered actuators on the rudder, elevators, and ailerons. The spoiler servo valves were modified to accept electrical signals and installed to actuate spoiler panels 3 through 12. The LAMS spoiler actuators (segments 1, 2, 13, and 14) were modified to include integral servo valves to accept SAS signals.

The cockpit arrangement included a monitor pilot station on the R.H. side and an evaluation or fly-by-wire pilot station on the L.H. side. The monitor pilot controls were connected to the mechanical pushrod, bellcrank, and cable system originally installed in the aircraft which directly command the surface actuators. The evaluation pilot controls were disconnected from the mechanical control system and connected to a feel system consisting of springs. The control column also included a viscous damper. The evaluation pilot input electrical signals were patched directly to the rudder, aileron, and spoiler servo valves for surface displacement. A parallel servo was used for elevator pitch commands providing displacement of the monitor pilot column proportional to the evaluation column. A three view of the test aircraft showing the control surface geometry and control functions is presented in Figure 2.

#### 2.2.2 Electronics and Instrumentation

The nucleus of the LAMS-FCS included electronic components such as sensors, the LAMS-FCS computer, two TR-48 computers, interface signal conditioning electronics, system engage controls, and system monitoring equipment. A pictorial of the installed electronic equipment is presented on Figure 3.

Extensive instrumentation was installed in the test aircraft to evaluate aircraft stability, handling qualities, and structural performance with the Baseline SAS and LAMS-FCS engaged. The instrumentation consisted of accelerometers, position indicators, rate gyro sensors, attitude gyros, strain gages for loads measurements, and hydraulic system temperature and pressure measurements. The detailed instrumentation requirements are contained in Section 3.4 of this report.



**FLY-BY-WIRE & MANUAL CONTROL SURFACES**

- LONGITUDINAL AXIS - ELEVATORS
- LATERAL-DIRECTIONAL AXIS - RUDDER, AILERON AND SPOILER SEGMENTS 3 THRU 12

**BASELINE SAS ACTIVE CONTROL SURFACES**

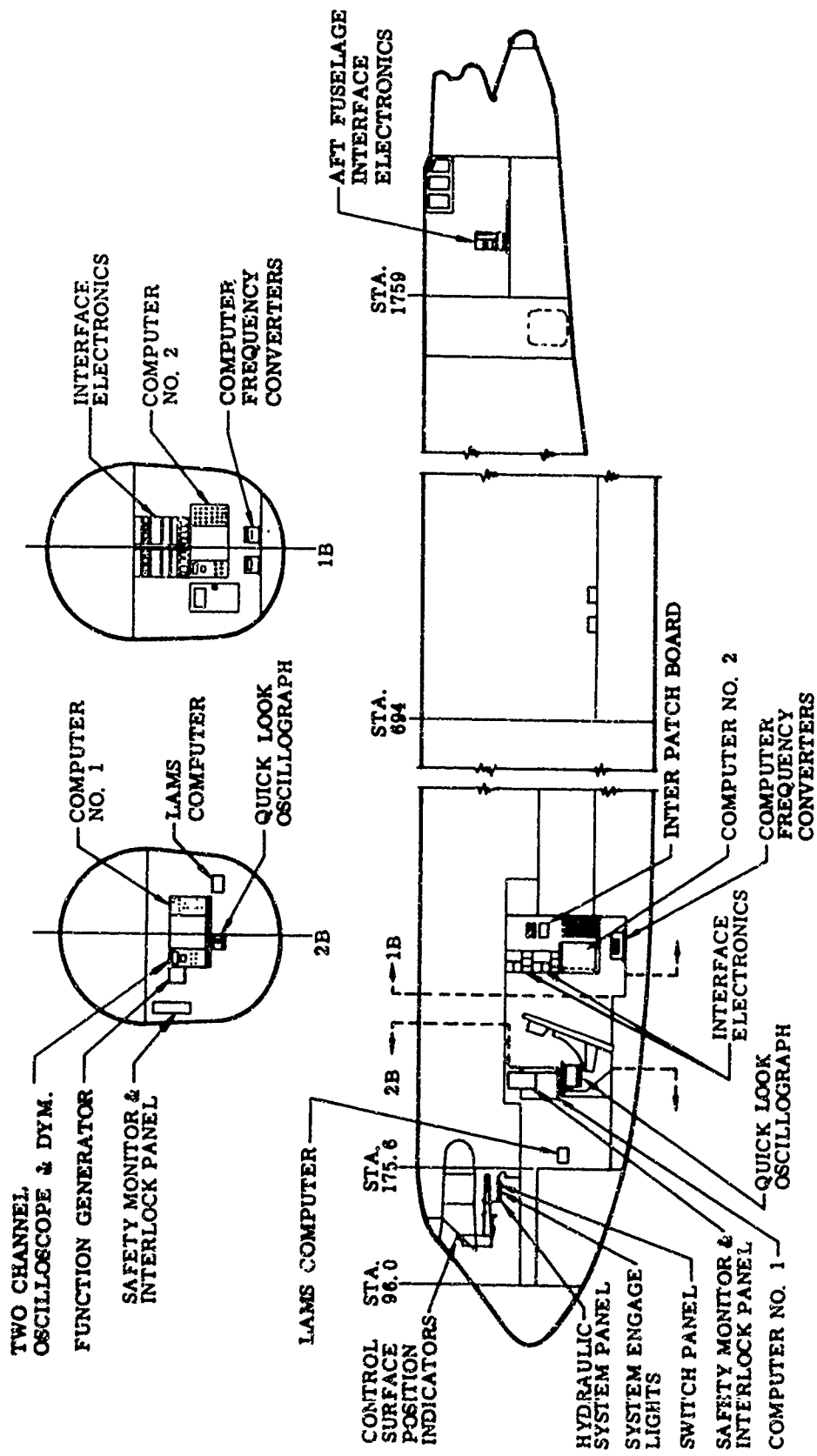
- LONGITUDINAL AXIS - ELEVATORS
- LATERAL-DIRECTIONAL AXIS - RUDDER AND AILERONS

**LAM-FCS ACTIVE CONTROL SURFACES**

- LONGITUDINAL AXIS - ELEVATORS, AILERONS, AND SPOILER SEGMENTS 1, 2, 13 & 14 BIASED AT 15 DEGREES
- LATERAL-DIRECTIONAL AXIS - RUDDER AND AILERONS

B-52E AIRCRAFT GEOMETRY

FIGURE 2



ELECTRONICS PROFILE

Figure 3

### 2.2.3 Baseline SAS

The Baseline SAS provides stability augmentation in the three rigid body axes. The system design accommodates operation of each axis independently or any combination of the three axes. The system was mechanized on the TR-48 computers located at the Flight Engineer's Station and is presented in more detail in Section 3.5. Engagement of the system was accomplished through the use of the pilot's aisle stand control panel.

### 2.2.4 LAMS-FCS

The LAMS-FCS was mechanized as separate electronics representative of contemporary flight control hardware and is described in more detail in Section 3.6. The system is a three axis Flight Controller and includes rigid body motion control in addition to control of selected structural modes to provide fatigue damage rate reduction due to flight through turbulence. LAMS system engagement was accomplished through the same control panel as the Baseline SAS. The flight control configuration was selected by insertion of a patch board in the interconnect panel. Each system has a unique patch board and only one controller could be engaged at any one time.

## 2.3 System Performance

The flight demonstration phase of the LAMS program was flown during a four month period ending 14 May 1968. The flight test plan and the test conduct detail is discussed in Reference 4.

### 2.3.1 Flutter Boundary and Dynamic Response Testing

Aeroelastic testing was required to establish the stability of the aircraft and SAS configurations and to permit aircraft operation at the design conditions for evaluation of the flight control systems. Airframe responses were evaluated following monitor pilot or function generator control transient inputs into the control surface actuators and by system excitation from multi-cycle sinusoidal inputs at discrete frequencies and amplitudes from the function generator at the Flight Engineer's Station.

#### 2.3.1.1 Basic Aircraft and Baseline SAS

The aircraft aeroelastic response was evaluated for the five fuel configurations presented in Table I which were selected from the proposed LAMS test vehicle fuel management sequence as critical fuel configurations based on past B-52 C-F flutter boundary testing. An altitude of 21,000 feet was used for the test and the airframe response was evaluated from 250 to 390 KIAS. An altitude of 21,000 feet was selected since this is the altitude at which the maximum straight and level airspeed and Mach number occur simultaneously and is the altitude which yields the lowest aircraft flutter boundaries for the B-52 aircraft.

Based on the results of this testing, the basic aircraft with hydraulic controls with and without the Baseline SAS has a satisfactory flutter boundary for all altitudes and airspeeds up to and including 390 KIAS and .90 Mach number for the fuel management sequence of the LAMS test vehicle.

TABLE I  
FLUTTER TEST CONFIGURATIONS

TEST CONFIGURATION NUMBER	FORWARD BODY NO. 1	CENTER WING	FORWARD BODY NO. 2	MID BODY	AFT BODY	MAINS & 3 1 & 4	OUTBOARD WING	EXTERNAL	1000 LBS.	GROSS WEIGHT	1000 LBS.	REPRESENTS SEQUENCE WEIGHT
1	↑	24.4	AR	32.6	AR	16.1	13.8	14.2	OFF	360.0 to 345.0		350.0
2		AR	0	32.6	AR	16.1	13.8	14.2	↓	345.0 to 315.0		325.0
3		AR	0	AR	0	16.1	13.8	14.2		320.0 to 270.0		270.0
4		AR	0	AR	0	8.9	13.8	7.1		309.0 to 241.0		241.0
5	↓	AR	0	AR	0	6.8	13.8	0		290.0 to 222.0		222.0

AR - Tank quantity as required to provide test range gross weight.

### 2.3.1.2 LAMS-FCS

The LAMS-FCS performance was evaluated for flight conditions 1 and 3 (FC-1 and 3) after accomplishing the aircraft and system stability at the following conditions:

- FC-1 flutter boundary evaluation at 10,000 feet altitude for safety from 225 to 365 KIAS for fuel configurations 1 and 2 of Table I
- FC-3 flutter boundary evaluation at 32,700 feet altitude from 200 to 290 KIAS for fuel configurations 3 and 4 of Table I

The initial LAMS-FCS gain configuration exhibited marginal aero-elastic damping in a symmetric 3 cps mode during fuel configuration 3. Reduction of the LAMS spoiler loop gain to 50 percent permitted completion of testing to 290 KIAS. Following discovery of the low damped oscillation, dynamic response testing was accomplished on the aircraft to evaluate response to spoiler excitation. Based on the results of the dynamic response testing and additional system analyses the longitudinal LAMS-FCS hardware was modified as presented in Reference 4.

The revised LAMS-FCS was then retested to determine aircraft and system stability in a manner similar to that outlined for the initial system testing. The results of this testing showed that the system had an adequate flutter boundary as shown in Figure 4. A problem encountered during the high speed testing of fuel configuration 4 did not result in additional modifications to the LAMS-FCS since this configuration is considerably below the design gross weight for FC-3 and outside the system design envelope.

### 2.3.2 Aerodynamic Testing

The aerodynamic testing included evaluating control surface authority and effectiveness and pilot handling qualities of each aircraft system configuration. The data was gathered at various design conditions to fulfill test requirements.

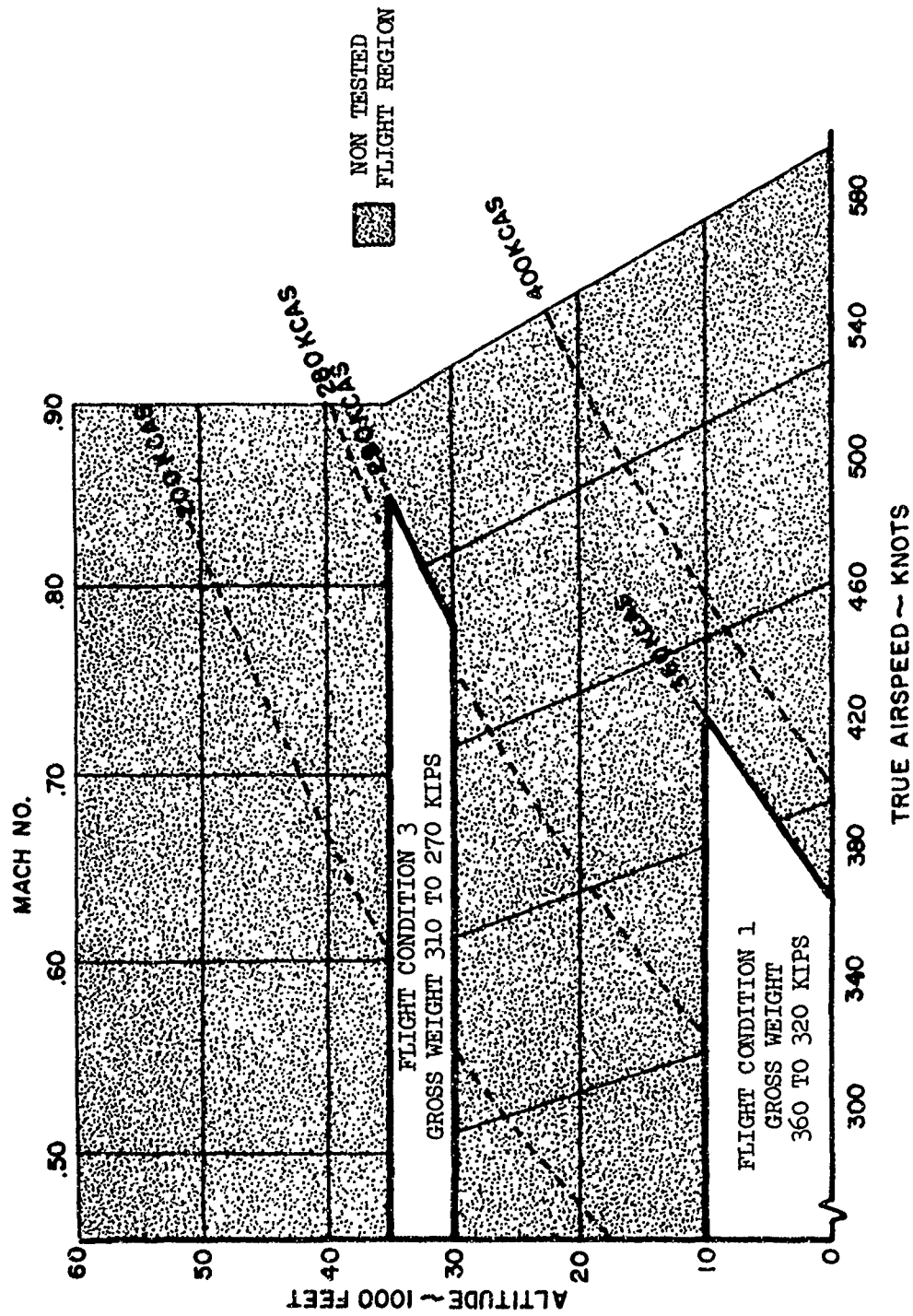
#### 2.3.2.1 Control Surface Authority and Effectiveness

The control surface authority and effectiveness testing was required to provide a comparison of predicted basic aircraft and experimental data to validate the theoretical analyses. Flight test data was obtained for the elevator, rudder, aileron (both symmetric and antisymmetric), and spoilers (both symmetric and antisymmetric), at 240, 300, and 350 KIAS and 10,000 feet and at .60, .77, and .85 Mach number and 32,700 feet. Section 4.2 presents a typical comparison (FC-1) of predicted versus flight test data.

#### 2.3.2.2 Handling Qualities

The LAMS design criteria stated that, in general, the aircraft handling qualities should not be degraded by the addition of the LAMS-FCS.

Significant improvement in Dutch roll stability was required to obtain the predicted structural performance, and the product of the Dutch roll frequency times the damping ratio was selected to be greater than



FLIGHT REGION FOR THE REVISED LAMS-FCS

FIGURE 4



.35 radians/second for flight through atmospheric turbulence. A comparison of predicted experimental Dutch roll handling qualities is presented in Figure 5. Dutch roll damping for the LAMS-FCS (FC-1) is slightly less than the above requirement but is still acceptable for normal flight operation.

The short period mode was highly damped on the basic aircraft and no significant change was noted with the addition of the Baseline SAS on LAMS-FCS. Also, the roll response time constant for all aircraft configurations was less than the required two seconds, and the spiral mode stability time constant was greater than the required twenty seconds.

### 2.3.3 Structural Response to Turbulence

The aircraft structural performance was evaluated during flight through atmospheric turbulence. Flight Condition 1 (low altitude and high speed) was the condition evaluated during the test to increase probability of turbulence encounter. The performance parameters evaluated were: fatigue damage rates, maximum expected stresses, and rms accelerations.

The gusts encountered during the two test flights selected for data reduction varied from 3.6 to 4.5 feet/second for the vertical component and from 3.0 to 3.8 feet/second for the lateral component.

A fictitious coherency loss at the Dutch roll peak for the basic aircraft is explained in some detail in Section 4.3.6. This coherency loss is due to the Dutch roll half-power bandwidth for the Basic Aircraft being equal to approximately .025 cps as defined from the handling qualities tests whereas the data reduction resolution used in the turbulence test data handling is .040 cps. This results in the computer coherency of the Dutch roll peak to lateral gusts to be approximately 60 percent of true value. All other responses were adequately defined. The performance of the Baseline SAS and LAMS-FCS in lateral turbulence across the total frequency spectrum evaluated was similar to that predicted. Also, the performance of the basic aircraft, the Baseline SAS, and LAMS-FCS in vertical turbulence was in good agreement to that predicted.

The structural performance is presented using the Baseline SAS as the reference since most present day large flexible aircraft have a yaw damper as a minimum stability augmentation system. The results of the test program with comparisons of the theoretical results are presented in Tables II, III, IV, and in Section 4.3. The inboard wing stress comparisons are good as noted in Tables II and III. Some benefit not predicted by the analyses was achieved by the LAMS-FCS along the fuselage and vertical tail. Increases noted in stabilizer damage rates are very small; fatigue damage rates for the Baseline SAS are approximately 1 percent of that experienced on the wing.

The fuselage accelerations as shown in Table IV show good agreement with the predicted results.

TABLE II

RELATIVE PEAK INCREMENTAL STRESSES  
(EXCEEDANCE LEVEL = .001/HOUR)

<u>STRESS LOCATION</u>	<u>LAMS FCS/BASELINE THEORETICAL</u>	<u>SAS TEST**</u>
W.S. 222 S-6	.79	.85
W.S. 820 S-5	.76	.81
W.S. 974 S-5	.84	.94
B.S. 805 U.L.*	.87	-
B.S. 1028 U.L.*	.97	-
B.S. 1222 U.L.	1.04	.97
B.S. 1412 U.L.	1.03	.97
S.B.L. 56 SPAR	1.10	1.13
F.S. 135 SPAR	1.02	1.00

\* Analysis Stations Only -- Not Instrumented

\*\* A & N<sub>0</sub> values used in the calculations were the average of values from tests 5415 and 5418.

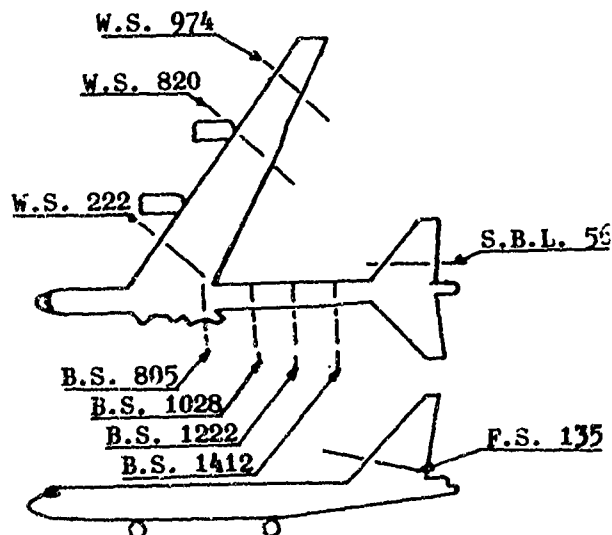


TABLE III  
RELATIVE FATIGUE DAMAGE RATES

<u>STRESS LOCATION</u>	<u>LAMS FCS/BASELINE THEORETICAL</u>	<u>SAS TEST**</u>
W.S. 222 S-6	.58	.64
W.S. 820 S-5	.55	.59
W.S. 974 S-5	.80	.95
B.S. 805 U.L.*	.54	-
B.S. 1028 U.L.*	.82	-
B.S. 1222 U.L.	1.15	.75
B.S. 1412 U.L.	1.11	.73
S.B.L. 56 SPAR	1.86	2.60
F.S. 135 SPAR	1.06	.95

\* Analysis Stations Only -- Not Instrumented

\*\* A & N<sub>0</sub> values used in the calculations were the average of values from tests 5415 and 5418.

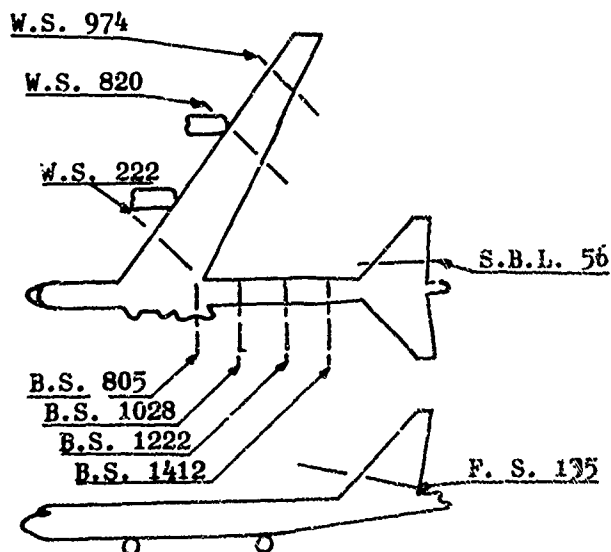
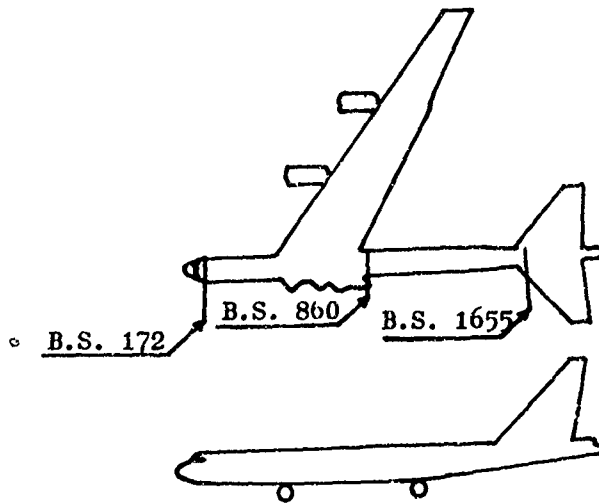


TABLE IV  
 RELATIVE RMS ACCELERATIONS  
 (Flight Condition 1)

<u>ACCELEROMETER LOCATION</u>	<u>LAMS FCS/BASELINE THEORETICAL</u>	<u>SAS TEST*</u>
B. S. 172 Vertical	.94	.98
B. S. 860 Vertical	1.01	1.02
B. S. 1655 Vertical	1.00	1.01
B. S. 172 Lateral	.91	.93
B. S. 860 Lateral	1.05	.99
B. S. 1655 Lateral	1.05	.96

\* Values tabulated are the average from tests 5415 and 5418.



## 2.4 Hardware Performance

The test vehicle and LAMS-FCS hardware performance was evaluated during ground tests prior to initiating the flight phase of the LAMS program. In general, the ground test results presented in Section 5.0 indicate that the hardware performed as theoretically predicted. Major areas of disagreement were the actuator frequency response characteristics of the aileron, rudder, and LAMS spoilers above 4 cps. The LAMS-FCS controlled structural modes up to 4 cps and the agreement in frequency response out to that frequency was adequate to attain the predicted structural performance.

The ground tests conducted prior to flight provided a high degree of confidence in the theoretical analyses and a good base on which to proceed into the flight phase of the program. It should be noted that after final hardware was installed in the LAMS test vehicle, all systems functioned with a minimum amount of maintenance throughout the flight demonstration program.

### 3.0 AIRCRAFT CONFIGURATION AND MODIFICATION

This section discusses the monitor and evaluation pilot control system modification as well as the electronic flight control equipment provided at the flight engineers station. In addition the Baseline SAS, LAMS-FCS, and the instrumentation required for system evaluation are described.

#### 3.1 Monitor Pilot Control System

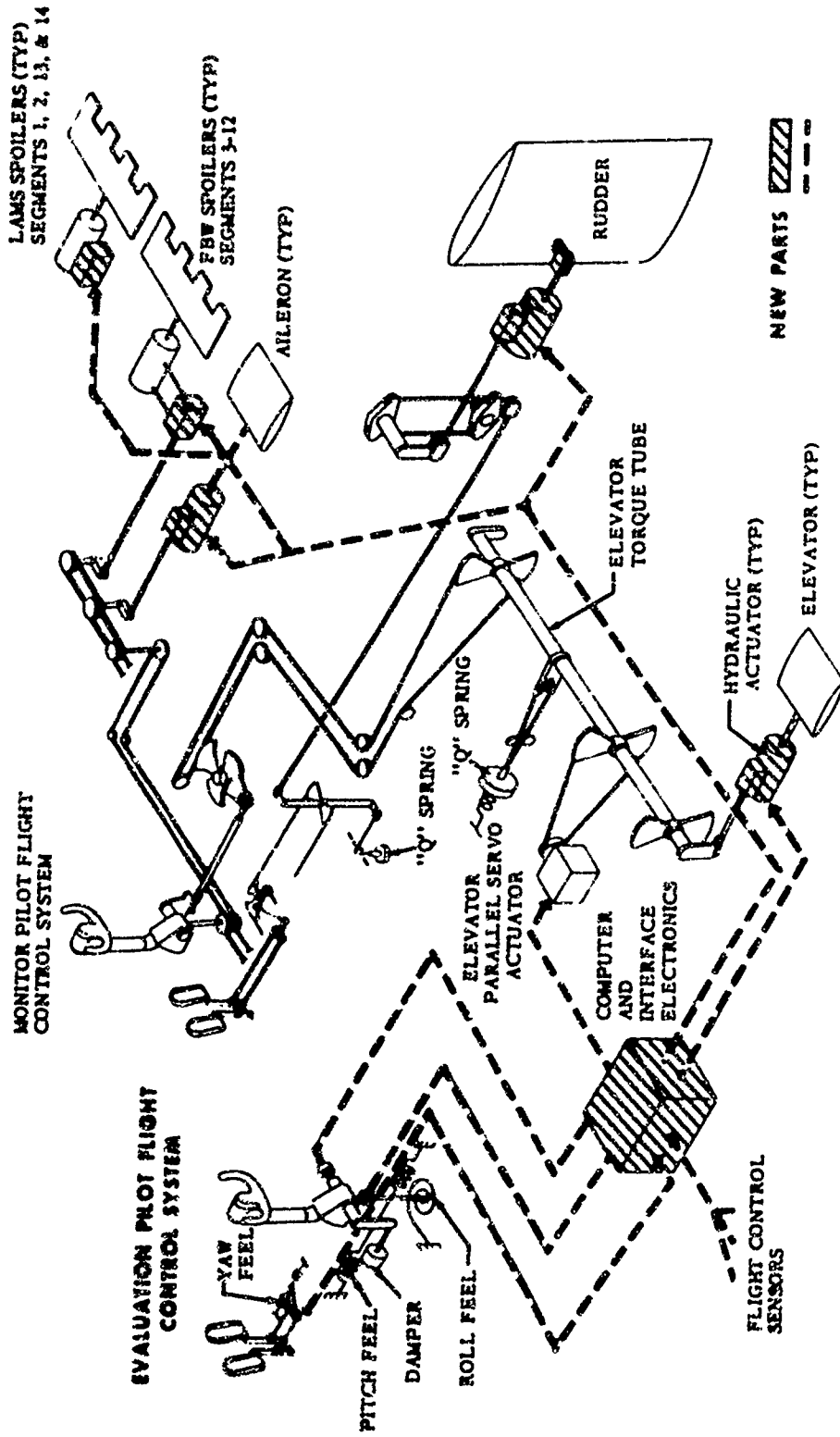
The monitor pilot's controls; the wheel, column and rudder pedals, are connected to the control cables as originally installed. With the LAMS modification, instead of driving tabs on the control surfaces, the cables provide mechanical input to hydraulic actuators which drive the control surfaces. The modified aircraft control system schematic is presented in Figure 6. The control wheel provides mechanical inputs to actuators which move the aileron and spoiler (the five inboard panels, 3-7 and 8-12, on each wing) surfaces antisymmetrically. The control column and rudder pedals provide mechanical inputs for elevator and rudder surface displacements respectively. In the roll and yaw axis the wheel and rudder pedal mechanical commands from the monitor pilot and the electrical commands from the evaluation pilot are summed in the actuator providing the monitor pilot the ability to override the evaluation pilot inputs. In the pitch axis any column input by the monitor pilot will disengage the fly-by-wire mode. This mechanization provides the monitor pilot full control in all three axes.

The monitor pilot has full authority in each axis with surface deflections as follows:

Aileron  $\pm$  17 degrees  
Spoiler + 60 degrees  
          - 0 degrees  
Rudder  $\pm$  19 degrees  
Elevator  $\pm$  19 degrees

#### 3.2 Evaluation Pilot Control System

The evaluation pilot control column, wheel and rudder pedals are disconnected from the original aircraft system control cables and connected to springs and dampers which provide the feel system as presented in Figure 6. Position potentiometers indicate electrically the position of the pilot's controls. These electrical signals are routed through the inter-patch panel to the analog computer where the gains can be adjusted as required. The control wheel signal then goes to the aileron and fly-by-wire (FBW) spoiler actuators which drive the control surfaces. The rudder pedal signal commands the rudder actuator driving the rudder surface. The control column signal is routed to the pitch parallel servo which mechanically drives the aft fuselage elevator torque tube and linkages to the elevator actuator to move the elevator surfaces. Since the aft fuselage elevator torque tube is driven by the pitch parallel servo the monitor pilot's column follows the evaluation pilot's column. The evaluation pilot has full authority in each axis the same as the monitor pilot.



PILOT CONTROL SYSTEM

FIGURE 6

The evaluation (fly-by-wire) pilot system and SAS control modes are engaged through a switch panel located between the pilots on the aisle stand. The control modes which can be selected are pitch FBW, pitch SAS, roll FBW, roll SAS, Yaw FBW, and Yaw SAS. Each may be selected independently of the other with the exception of the roll FBW which cannot be selected unless pitch FBW has already been selected. The engage switch is used to engage the control system after appropriate modes have been selected.

### 3.3 Flight Engineers Station

The interface electronics, safety monitoring and data monitoring equipment is located at the flight engineers station. See Figure 3 for the location of this equipment.

The interface electronics provide the nucleus of the electrical flight control system. All control signals pass through the interface electronics and signals are distributed, filtered and gain adjusted as required. An interpatch panel which is part of the interface electronics receives all flight control input and output signals. This panel provides a removable patch board containing 408 connections to a mating base panel. Since all signals pass through the interpatch base panel into the removable board and back out the base panel, any desired routing of signals may be wired on the removable board. Several interpatch boards are available to the flight engineer making it possible to select system configuration by changing interpatch boards.

Several signals are monitored in the safety monitor and interlock system. These signals are power supplies, accelerations at critical locations and input command signals to the control surface auxiliary actuators. The interlock system provides disengagement of the control system if a failure occurs or if the signal levels exceed a pre-set value. Each signal monitored has a warning light which indicates to the flight engineer the cause of system disengagement.

The two general purpose analog computers are slaved together and provide the linear and non-linear computer functions needed. The computer components are used for filtering and gain adjusting the signals for the Baseline SAS. The fly-by-wire signals are also gain adjusted on the analog computer and if the Baseline SAS and fly-by-wire are both engaged, the signals are summed on the computer. The computer digital voltmeter furnishes a means of signal monitoring.

Another method of signal monitoring is provided by the six channel oscillograph. A switch makes it possible to select 73 different combinations of signals or the flight engineer can program on the interpatch board any combination of signals he needs. The two channel oscilloscope is available and can be used to check the proper operation of the rate gyro motors and to monitor any signal available at the interpatch panel.

The flight engineer is provided instruments indicating aileron surface position, fly-by-wire spoiler surface position, and aft fuselage interface electronics rack temperature.

A function generator capable of generating sine, ramp, triangular, and square waves was installed for ground and inflight checkout and for inflight testing. The flight engineer can select the frequency and number of cycles ( $\frac{1}{2}$ , 1, 2, 3, 4, or free run operation) as well as the type function. The function generator output is routed through the analog computer to monitor and gain adjust the signal and directed to the appropriate control surface by the flight engineer.

### 3.4 Instrumentation

Narrow Band FM (NBFM) recording systems were used to record data to evaluate performance and handling qualities, to flutter clear the test flight envelope and to check system stability. Many of these signals are generated by sensors which are used in conjunction with the control systems on the LAMS aircraft. These signals are available at the interpatch panel and are routed from it to the recorders. A list of these signals is given in Table II and the sensor or pick-up locations are shown in Figure 7. Additional sensors were installed to make possible recording of all pertinent signals for system evaluation on the NBFM recording systems. These signals are not available at the interpatch panel but are routed directly to the tape recorder. These sensor signals are listed in Table II and locations are shown in Figures 7 and 8.

### 3.5 Longitudinal Axis

The primary function of the Baseline pitch SAS is to augment short period mode damping. The system employs pitch rate feedback to control the powered elevator. The signal is derived from a rate gyro located at Body Station 820, near the aircraft c.g. (see Figure 9). Electronic filters shape the feedback signal to increase short period damping and to obtain desired handling qualities without significantly disturbing or controlling structural modes. Figure 10 shows a block diagram of the Baseline Pitch SAS.

#### 3.5.2 Lateral-Directional Axis

The Baseline Roll SAS improves roll response of the aircraft to the pilot's wheel command without decreasing steady-state roll rate capability of the aircraft by more than 10 percent. Feedback decreases the roll time constant by sensing roll rate with a rate gyro located at Body Station 820, approximately at the c.g. (see Figure 9) and feeding it back to drive the aileron surface antisymmetrically. Since this signal is subtracted from the pilot's input, the evaluation pilot's wheel to aileron gain was increased over the unaugmented aircraft gain to retain similar steady state roll rate to wheel gain with the roll SAS engaged. Feedback loop electronic filters and a forward loop notch filter at 12 radians per second ensure system stability and desirable handling qualities.

The Baseline Yaw SAS augments Dutch roll damping with a yaw rate signal to the rudder, utilizing a rate gyro located at Body Station 616, forward of the c.g. (see Figure 9). The feedback signal is shaped to damp the Dutch roll mode without changing structural mode damping. Added Dutch roll damping obtains desirable handling qualities. A block diagram of the Baseline yaw and roll SAS design is presented in Figure 11.

TABLE V  
INSTRUMENTATION (AVAILABLE AT INTERPATCH PANEL)

INDEX NO.	MEASUREMENT
(Figure 7)	
<u>Accelerations</u>	
5	Lateral Acceleration - BS 1655
6	Lateral Acceleration - FS 354
8	Longitudinal Acceleration - Left WS 1359 and LWS 924
10	Vertical Acceleration - Left WS 1359 and LWS 924
12	Vertical Acceleration - BS 172, 860 and 1655
13	Vertical Acceleration - ISS 425
<u>Attitudes and Rates</u>	
14	Angle of Pitch - A/P C.G., BS 860
14	Angle of Roll - A/P C.G., BS 860
16	Rate of Pitch - BS 566, 860, and 1377
17	Rate of Roll - Left and Right WS 900
18	Rate of Roll - BS 805, 860, and 1655
19	Rate of Yaw - BS 425, 695, 860, 1028, and 1377
<u>Aileron and Spoiler Requirements</u>	
21	Control Wheel Position - Evaluation Pilot
22	Aileron Position - Left and Right
23	Aileron Auxiliary Actuator Position - Left and Right
23	Aileron Actuator Mechanical Input - Left and Right
24	Aileron Computer Command - Left and Right
25	Aileron Trim Command
26	Spoiler Position - Segments 3, 6, 9 and 12
27	Spoiler Auxiliary Actuator Position - Segments 3, 6, 9, and 12
28	Spoiler Computer Command - Segments 1 through 14
29	Spoiler Actuator Ram Position - Segments 1, 2, 13 and 14
<u>Elevator and Stabilizer Requirements</u>	
31	Control Column Position - Evaluation Pilot
32	Elevator Position - Left and Right (Bearing No. 4)
33	Elevator Auxiliary Actuator Positions 1 and 2 - Left and Right
33	Elevator Actuator Main Metering Valve Position - Left and Right
34	Elevator Servo No. 1 Computer Command - Left and Right
35	Pitch Parallel Servo Position
36	Pitch Parallel Servo Electric Input
37	Stabilizer Position - Hinge Line
<u>Rudder Requirements</u>	
39	Rudder Pedal Position - Evaluation Pilot
40	Rudder Position - Bearing No. 4
41	Rudder Auxiliary Actuator Positions 1 and 2
41	Rudder Actuator Main Metering Valve Position
42	Rudder Servo No. 1 Computer Command
<u>Miscellaneous</u>	
55	Copilot Override Signal
57	LAMS Engage Signal
57	Transient Generator Signal

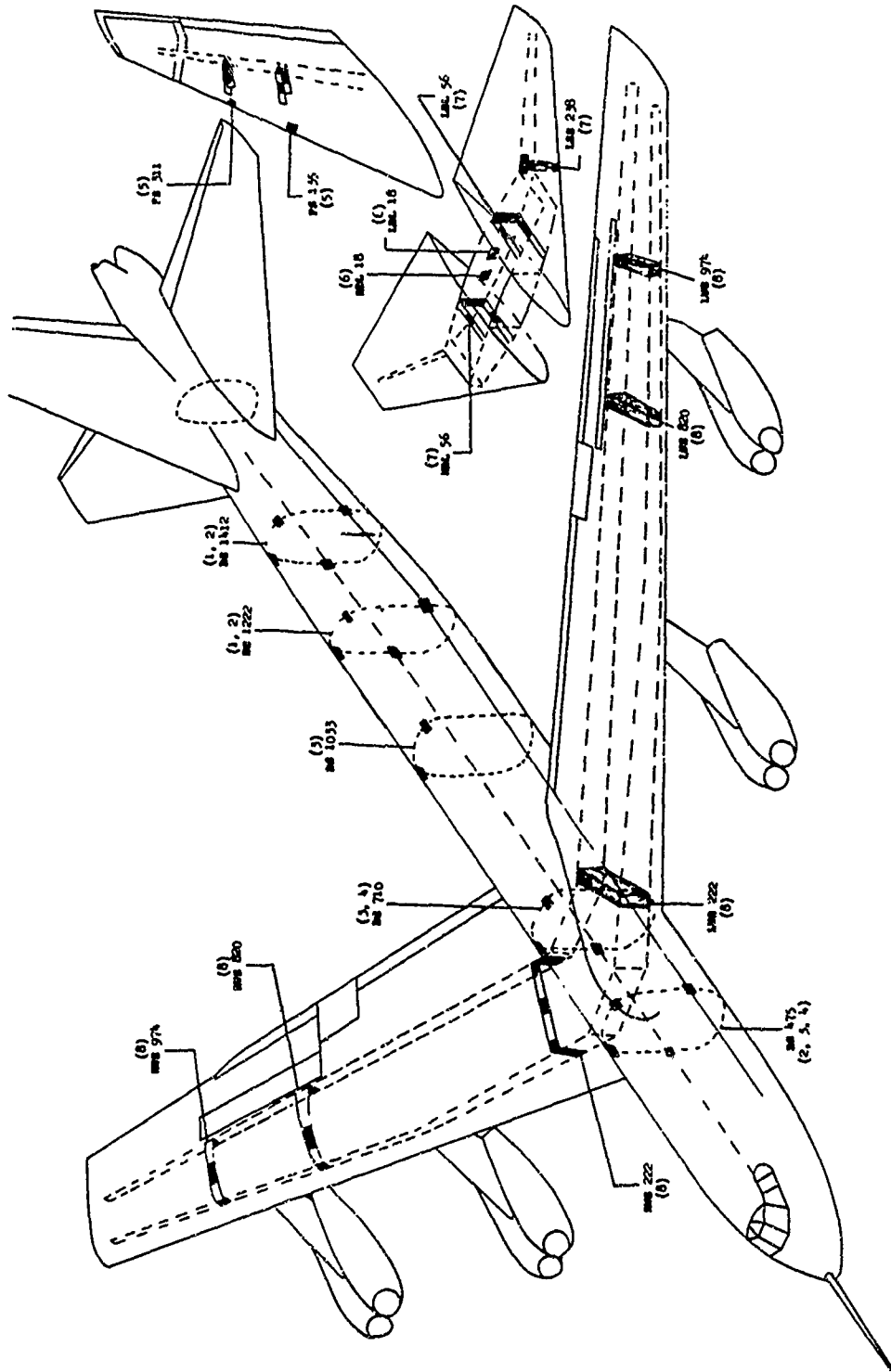


TABLE VI  
INSTRUMENTATION (NOT AVAILABLE AT INTERPATCH PANEL)

INDEX NO. (Figure 7)	MEASUREMENT
<u>Body Loads</u>	
1	Lateral Moment - BS 1222 and 1412
2	Vertical Moment - BS 475, 1222, and 1412
3	Left and Right Upper Longeron Axial Stress - BS 475, 710 and 1033
4	Left and Right Lower Longeron Axial Stress - (Lower Member) BS 475 and 710
<u>Fin Loads</u>	
5	Lateral Moment - FS 135 and 311
5	Shear - FS 135 and 311
5	Torsion - FS 135 and 311
<u>Stabilizer Loads</u>	
6	Rear Spar Shear Stress - Left and Right BL 18
7	Vertical Moment - Left and Right BL 56 and LSS 238
7	Shear - Left and Right BL 56 and LSS 238
7	Torsion - Left and Right BL 56 and LSS 238
<u>Wing Loads</u>	
8	Chordwise Moment - Left and Right WS 222, 820, and 974
8	Vertical Moment - Left and Right WS 222, 820, and 974
(Figure 8)	
<u>Gust Velocity</u>	
1	Angle of Pitch - Boom Base
1	Angle of Roll - Boom Base
1	Longitudinal Acceleration - Boom Base
2	Angle of Yaw - Probe
2	Angle of Attack Differential Pressure - Probe (Coarse and Fine)
2	Impact Pressure - Probe (Lateral and Vertical Static Reference)
2	Lateral Acceleration - Probe
2	Rate of Pitch - Probe
2	Rate of Roll - Probe
2	Rate of Yaw - Probe
2	Sideslip Differential Pressure - Probe (Coarse and Fine)
2	Static Pressure - Probe (Lateral and Vertical Ports)
2	Vertical Acceleration - Probe
<u>Accelerations</u>	
3	Angular Acceleration - Left and Right WS 1359 and LWS 540
4	Angular Acceleration - LSS 425
5	Lateral Acceleration - BS 172, 860, 1237
7	Lateral Acceleration - Nacelles No. 1 and 2
8	Longitudinal Acceleration - Left and Right WS 540 and LWS 924
9	Longitudinal Acceleration - BS 860
10	Vertical Acceleration - Right WS 1359 and LWS 924
11	Vertical Acceleration - Nacelles No. 1 and 2
12	Vertical Acceleration - BS 860 and 1237

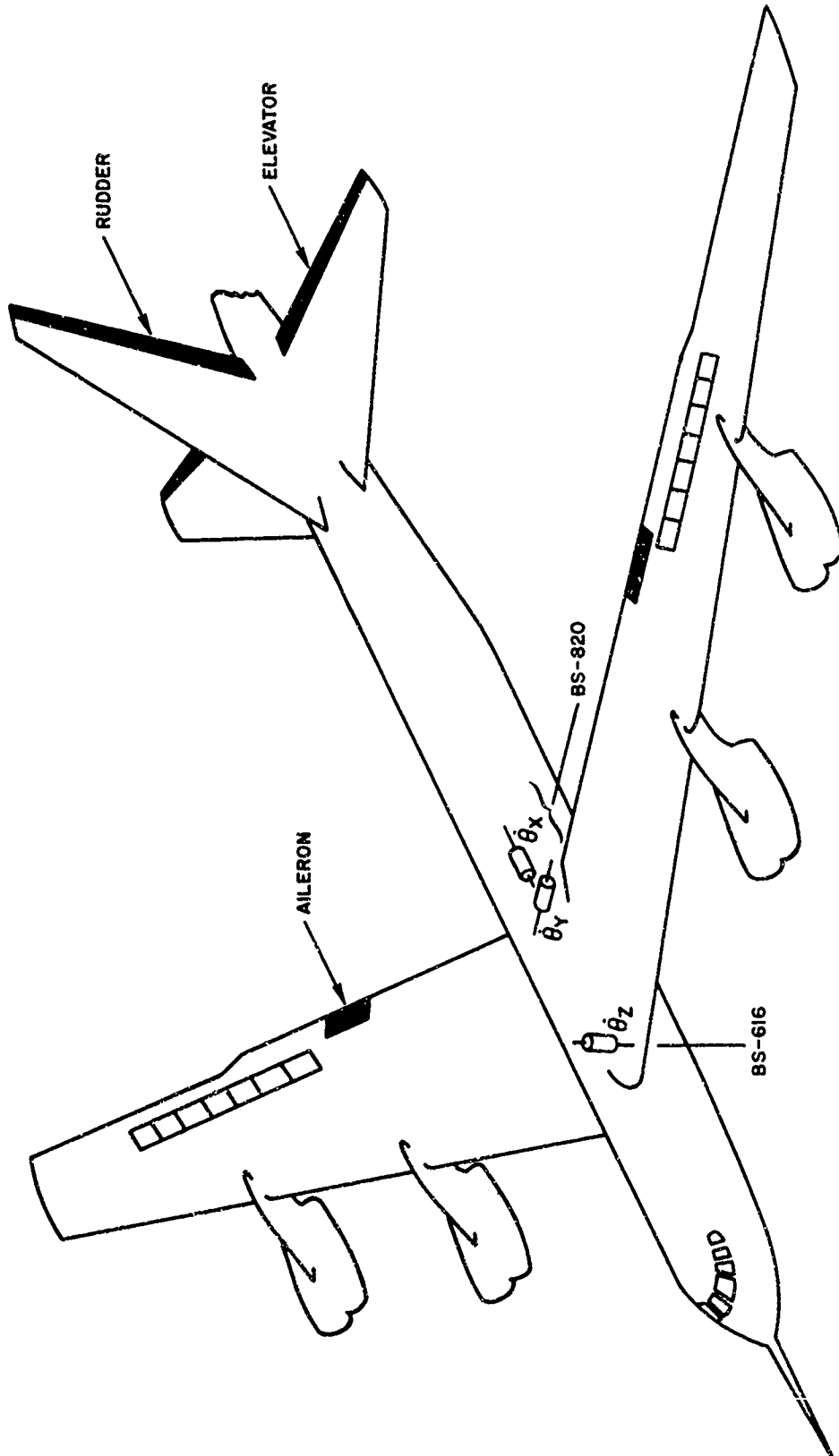
TABLE VI (Cont'd)

INDEX NO.	MEASUREMENT
<u>Aileron and Spoiler Requirements</u>	
20	Control Wheel Force - Monitor Pilot
20	Control Wheel Position - Monitor Pilot
23	Aileron Actuator Force - Left and Right
23	Aileron Actuator Mechanical Input - Left and Right
27	Spoiler Actuator Force - Segments 3, 6, 9 and 12
27	Spoiler Actuator Mechanical Input - Segments 3, 6, 9 and 12
<u>Elevator and Stabilizer Requirements</u>	
30	Control Column Force - Monitor Pilot
30	Control Column Position - Monitor Pilot
33	Elevator Actuator Force - Left and Right
33	Elevator Actuator Mechanical Input - Left and Right
37	Stabilizer Position - Jackscrew
<u>Rudder Requirements</u>	
38	Rudder Pedal Force - Monitor Pilot
38	Rudder Pedal Position - Monitor Pilot
41	Rudder Actuator Force
41	Rudder Actuator Mechanical Input
43	Rudder Trim Position
<u>Hydraulic Pressures and Temperatures</u>	
44	Hydraulic Pump Output Pressure - Engines 1, 3 and 4
44	Hydraulic Oil Temperature in Pump Bypass Line (Return) - Engines 1, 3, and 4
45	Left Outboard Spoiler System Hydraulic Oil Temperatures At Reservoir Inlet (Return Line)
46	Spoiler System Electric Motor Pump Output Pressure Left Inboard and Outboard
47	Spoiler System Control Valve Input and Return Pressure - Left Inboard and Outboard
48	Left Aileron Actuator Input and Output Pressure
49	Left Body System Electric Motor Pump Output Pressure
49	Left Body System Hydraulic Oil Temperature in Electric Motor Pump Bypass Line (Return)
50	Elevator and Rudder Forward Hydraulic Pump Output Pressure
50	Elevator and Rudder System Hydraulic Oil Temperature In Forward Electric Motor Pump Bypass Line (Return)
<u>Hydraulic Systems Electric Power Requirements</u>	
51	Spoiler Hydraulic System Electric Motor Pump Power Input - Left Inboard and Outboard
52	Left Body Hydraulic System Electric Motor Pump Power Input
53	Elevator and Rudder Forward Hydraulic System Electric Motor Pump Power Input
<u>Miscellaneous</u>	
15	Sideslip Differential Pressure - Aircraft System - BS 100
56	Indicated Outside Air Temperature



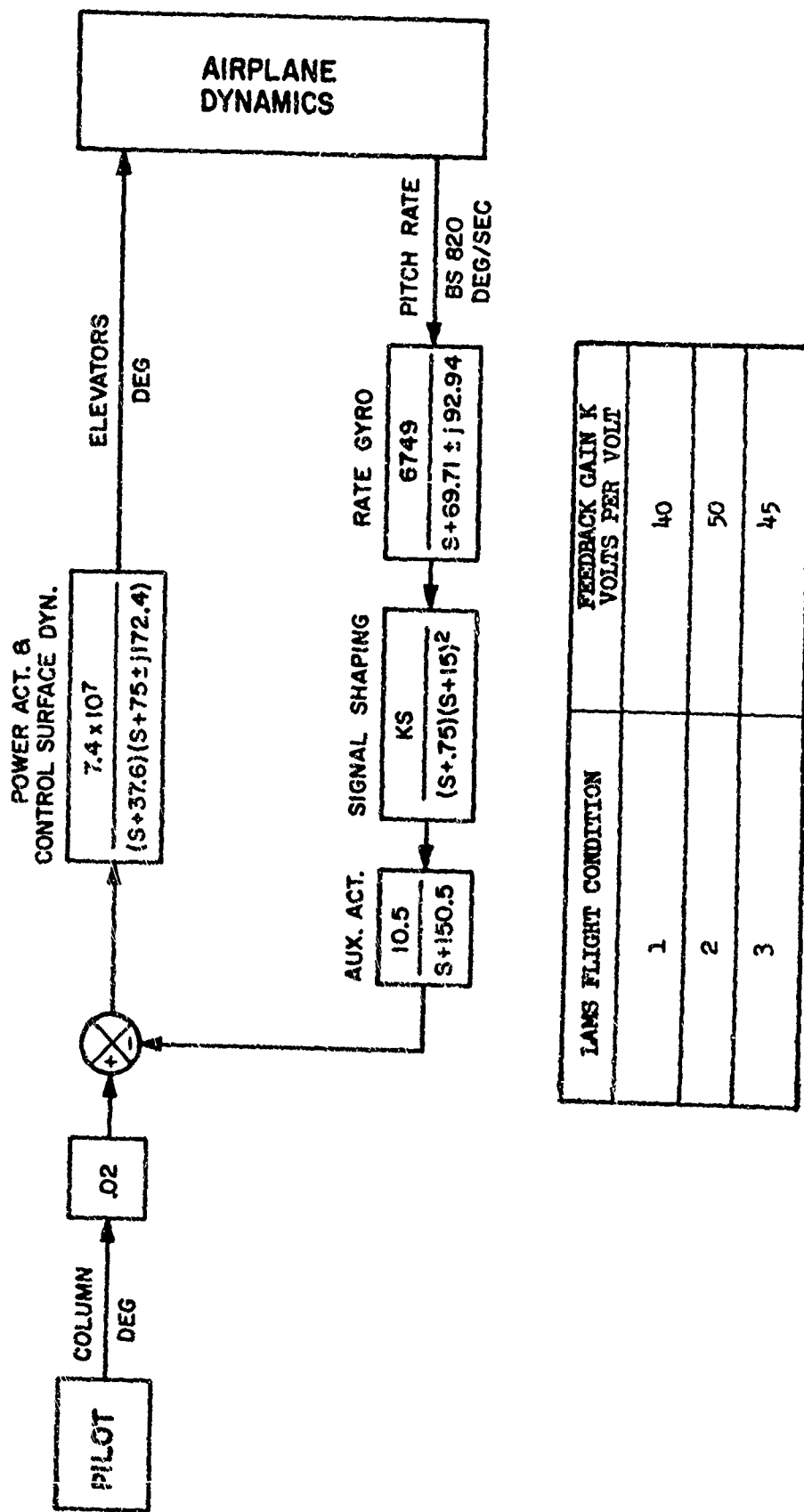
LOAD AND STRESS MEASUREMENT LOCATIONS

FIGURE 8



RATE GYRO LOCATIONS

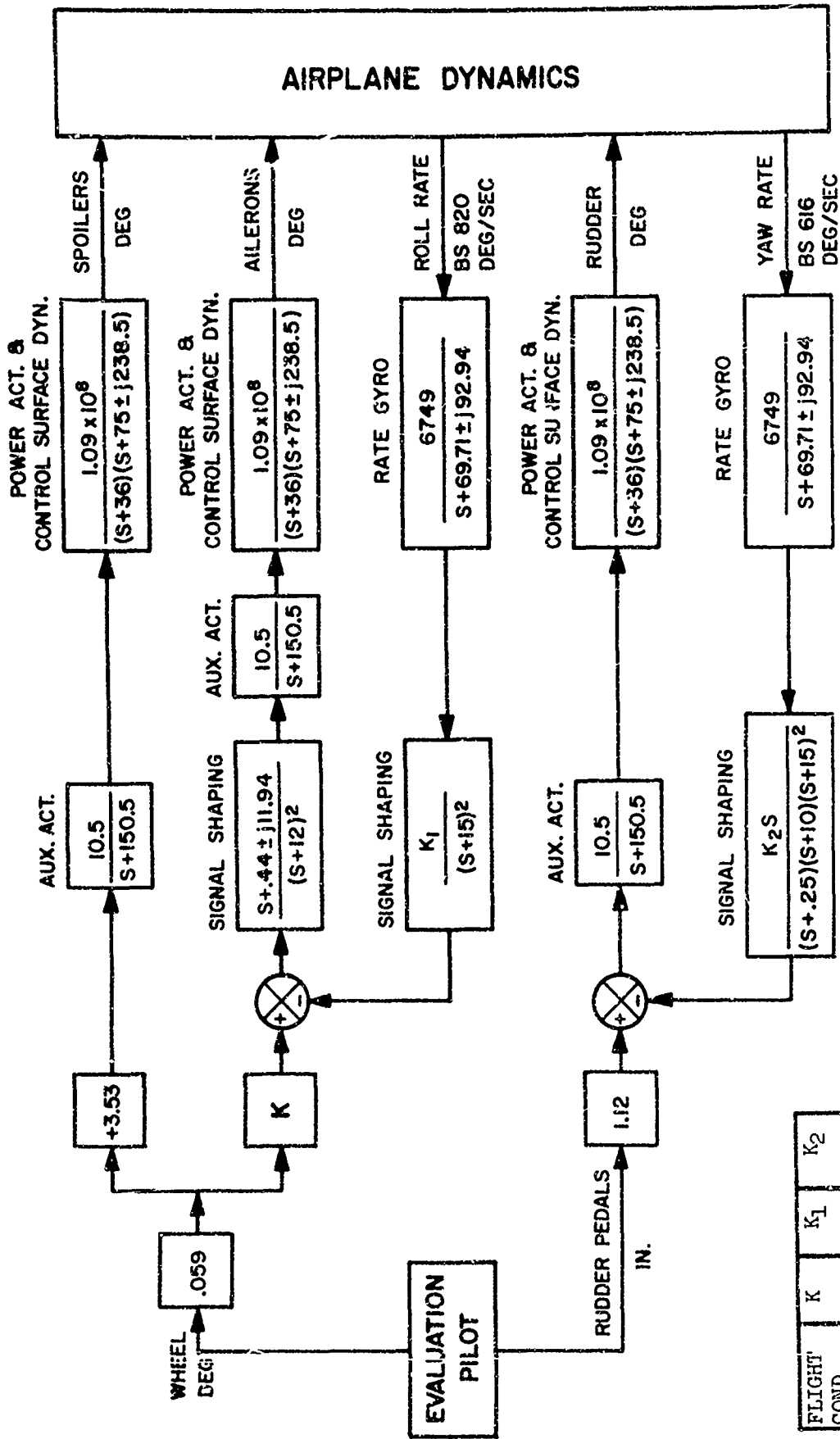
FIG. 9



LAMS FLIGHT CONDITION	FEEDBACK GAIN K VOLTS PER VOLT
1	40
2	50
3	45

BASELINE PITCH SAS BLOCK DIAGRAM

FIGURE 10



BASELINE ROLL AND YAW SAS BLOCK DIAGRAM

FIGURE 11

FLIGHT COND.	K	K <sub>1</sub>	K <sub>2</sub>
1	2	50	2000
2	2	50	2500
3	2	50	2500

### 3.6 LAMS-FCS

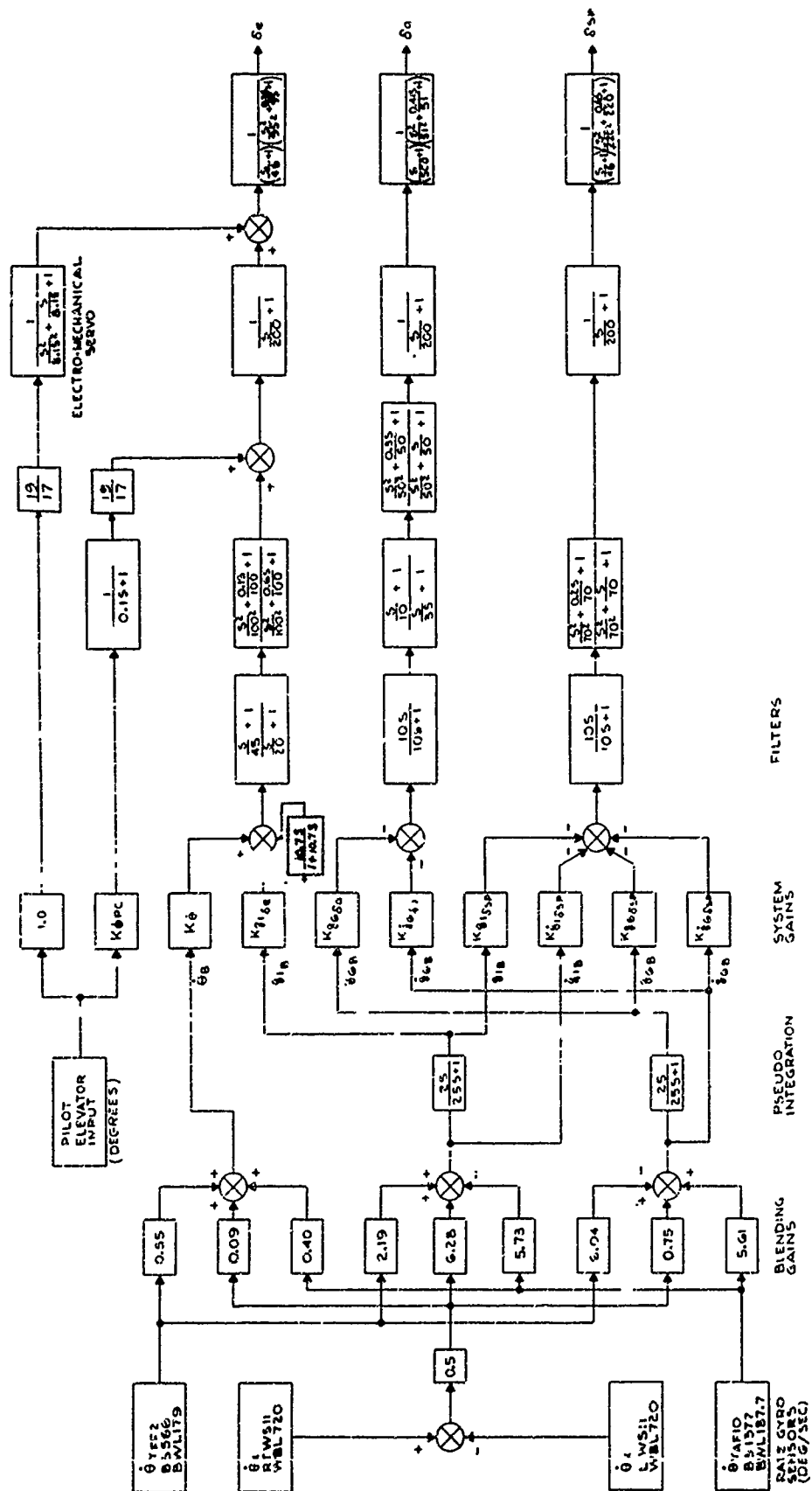
The LAMS-FCS is a three axis flight control system. For test purposes, each axis can operate independently or in combination with other axes, similar to the Baseline SAS.

#### 3.6.1 LAMS Longitudinal FCS

The LAMS Longitudinal FCS block diagram is shown in Figure 12. Feedback signals are derived from four rate gyros; one located in the forward fuselage, one in the aft fuselage, and one in each wing. The Longitudinal axis rate gyro locations are shown in Figure 13. These sensor signals are blended to produce three signals which are approximations of rigid body pitch rate, elastic mode one rate, and elastic mode six rate. Pseudo integration of the structural mode signals gives approximate mode displacement signals. The rate and displacement signals are then gain adjusted as a function of flight condition and shaped with electronic filters. The filters are primarily for stability compensation and the prevention of dc null offsets. System gains for each flight condition are tabulated in the Table on Figure 12. The system operates the elevators, ailerons and outboard spoiler panels (segments 1, 2, 13, and 14) on each wing symmetrically to provide control of the short period and the 1st and 6th symmetric structural modes. The spoiler panels operate in a 15 degree biased position to provide displacement in either direction. Desirable handling qualities are obtained by adding a column to elevator feedforward signal path parallel to the existing fly-by-wire path.

#### 3.6.2 LAMS Lateral-Directional FCS

Figure 14 is a block diagram of the LAMS Lateral-Directional FCS. There are two roll rate gyros and four yaw rate gyros mounted in the fuselage which are utilized to obtain the control signals. The Lateral-Directional FCS rate gyro locations are shown in Figure 13. The signal from the yaw rate gyro located at Body Station 695 is used to increase the damping of the Dutch roll mode using the rudder. The signal was filtered to maintain the required stability margins of the structural modes. The other five rate gyros were used to meet handling quality requirements and to increase antisymmetric structural mode 9 damping using the ailerons antisymmetrically. These signals were also filtered to maintain the required stability margins. Handling quality requirements necessitated adding an evaluation pilot wheel to aileron feedforward signal path parallel to the existing path. The gains changed with flight condition for both the roll and yaw axis and are given in the Table shown on Figure 14.

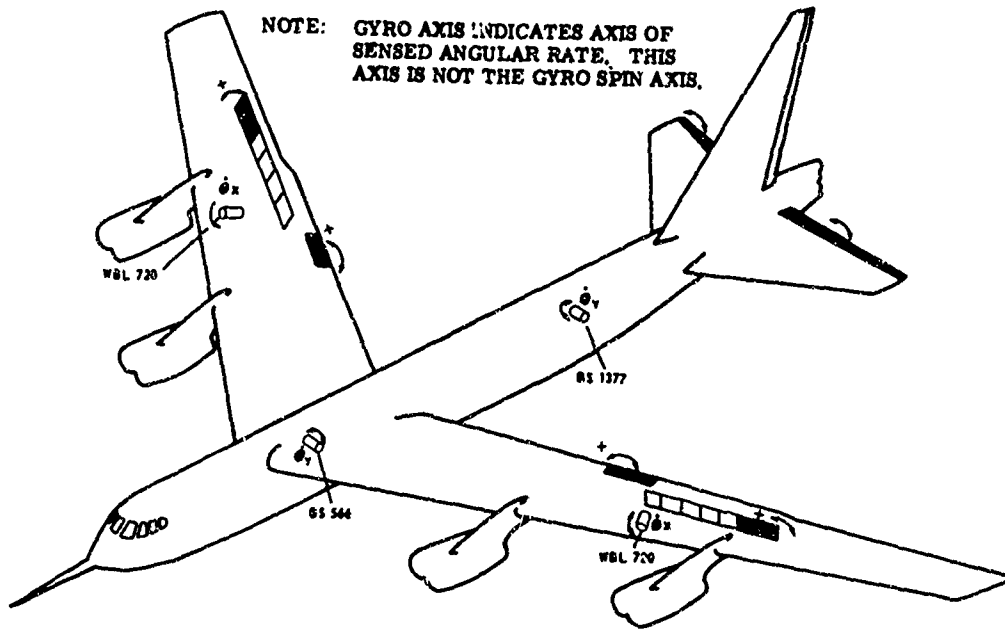


LONGITUDINAL FLIGHT CONTROL GAINS

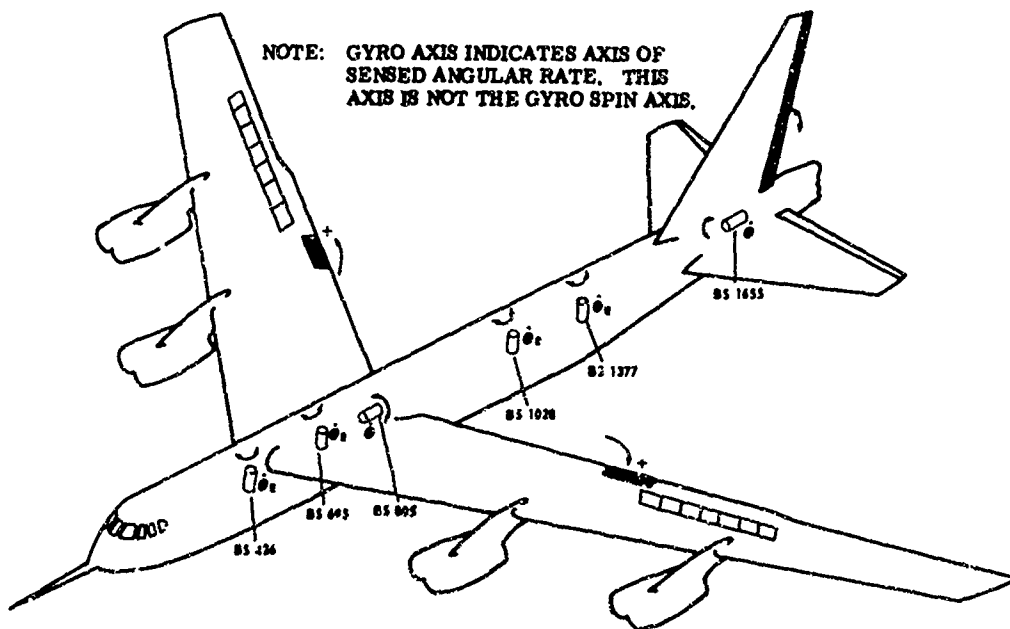
FLIGHT CONDITION	K $\delta$ pc	K $\delta$	K $\delta_1$	K $\delta_2$	K $\delta_3$	K $\delta_4$	K $\delta_5$	K $\delta_6$	K $\delta_7$	K $\delta_8$	K $\delta_9$
FC1	0.79	0.20	0.25	0.066	1.47	0.219	-1.02	0.34			
FC2	1.16	1.12	0.43	0.50	1.39	0.207	-1.10	0.38			
FC3	0.70	0.78	0.26	0.25	0.066	1.63	0.340	-1.57	0.53		

LAMS LONGITUDINAL FLIGHT CONTROL SYSTEM BLOCK DIAGRAM  
FIGURE 12

## LAMS LONGITUDINAL AXIS



## LAMS LATERAL - DIRECTIONAL



LAMS-FCS RATE GYRO LOCATIONS

FIGURE 13



#### 4.0 SYSTEM PERFORMANCE

This section contains the results of the flight demonstration phase of the LAMS program. The detailed test plan and testing accomplished are presented in Reference 5.

#### 4.1 Flutter Boundary and Dynamic Response Testing

The flutter boundary and dynamic response testing was conducted for the following:

- The basic aircraft with hydraulic controls
- Baseline SAS
- The initial LAMS-FCS
- The revised LAMS-FCS with different phasing for the LAMS spoilers than the initial LAMS-FCS.

##### 4.1.1 Basic Aircraft and Baseline SAS

The basic aircraft with hydraulic controls and the Baseline SAS configurations were required to be flutter free over the entire aircraft mission profile. Five fuel configurations presented in Table I were selected from the proposed fuel management sequence as significant test configurations based on past B-52 C-F aircraft testing. Testing was accomplished at 21,000 feet altitude (the altitude which yields the lowest flutter boundaries for the critical modes of the B-52 aircraft).

The aircraft response was obtained through manual control transient inputs to the column, wheel, and rudder pedals. The aeroelastic damping and frequency was evaluated from telemetered signals displayed in the ground station for approximately 10 airspeed points from 250 to 390 KIAS.

The test results indicated that the basic aircraft with hydraulic controls and Baseline SAS has a satisfactory flutter boundary for all altitudes and airspeeds up to and including 390 KIAS and .90 Mach number for the fuel management sequence of the LAMS test vehicle.

##### 4.1.2 Initial LAMS-FCS

The LAMS-FCS structural performance was evaluated at Flight Conditions 1 and 3 (FC-1 and FC-3) as outlined in Section 1.0. Aeroelastic testing of the LAMS-FCS was required to assure aircraft and system stability as follows:

- FC-1 was flutter tested at 10,000 feet altitude from 225 to 365 KIAS for fuel configurations 1 and 2 of Table I.
- FC-3 was tested at 32,700 feet altitude from 200 to 290 KIAS for fuel configurations 3 and 4 of Table I.

The aircraft aeroelastic response with the LAMS-FCS engaged was evaluated following manual control surface transients initiated by the evaluation pilot through the column, wheel, and rudder pedal controls. In addition, the flight test engineer initiated half cycle electrical control transients into the elevators, ailerons, and rudder at a frequency of approximately 4.5 cps from the function generator. The upper frequency limit of the controlled aircraft elastic modes is 4.0 cps and this vibration frequency is not adequately excited by the manual control inputs.

Initial flights with the LAMS spoilers at a fixed bias of 15° resulted in an erratic 25 cps oscillation at the wing tip. Investigation and analysis indicated that the oscillation was caused by the shedding vortices from the biased spoilers which excited a 25 cps wing tip torsion mode. The amplitude of the vibration was less than .025 inches double amplitude and would not result in structural damage. Therefore, the aircraft was cleared to fly with biased spoilers and the LAMS-FCS on.

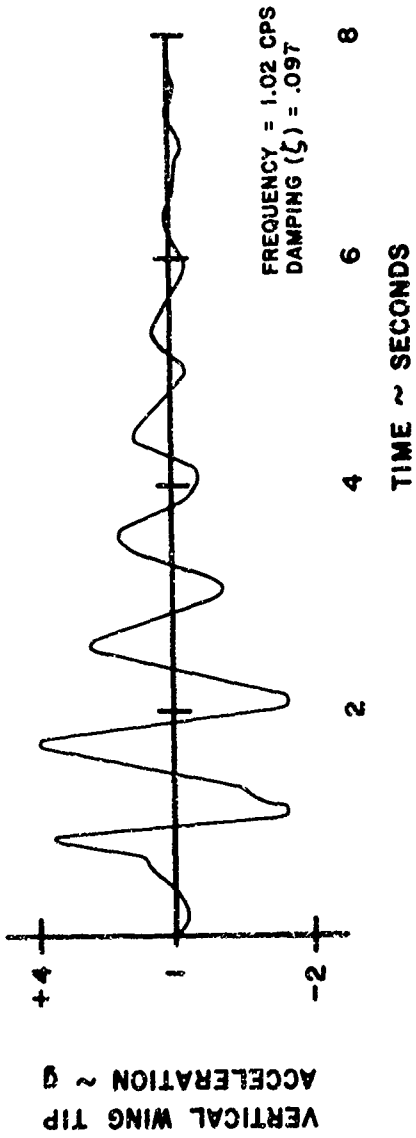
The initial aeroelastic tests of the LAMS-FCS encountered marginal stability for a 3cps symmetric body and wing bending mode while fuel configuration 3 was being evaluated. The problem occurred at 270 KIAS and required a 50 percent reduction in spoiler gain before testing could be completed to 290 KIAS. In addition, the first wing bending mode at 1 cps was degraded by the LAMS-FCS as shown in Figure 15.

To evaluate the problems noted above, dynamic response testing was accomplished using the function generator to excite the LAMS spoilers at various amplitudes and frequencies from 1 to 4 cps. The airframe response data resulting from the spoiler testing helped to define a phasing problem in the LAMS-FCS spoiler loop. With this information, additional analyses were conducted as described in Reference 4. The LAMS-FCS hardware was revised, based on the analytical results, to provide 25 degrees of lead for the first structural mode and 20 degrees of lead for the sixth structural mode in addition to that in the initial LAMS-FCS.

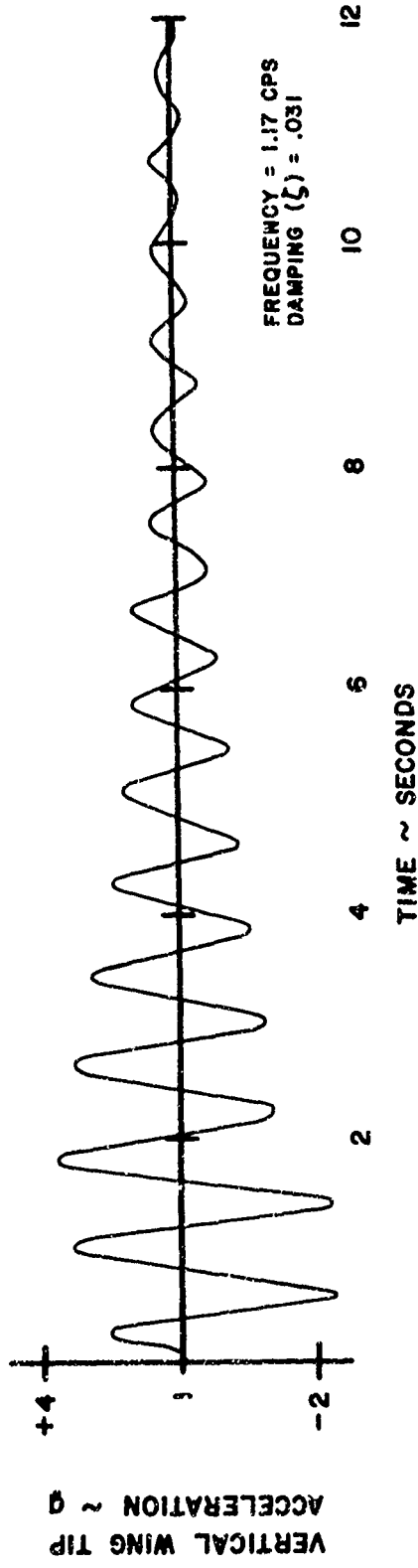
#### 4.1.3 Revised LAMS-FCS

The revised LAMS-FCS required flutter testing at the design conditions. Retesting consisted of the same testing outlined in paragraph 4.1.2. The test results showed that the aircraft had an adequate flutter boundary for fuel configurations 1 and 2 (FC-1) and fuel configuration 3 (FC-3). Also, dynamic response testing was accomplished to evaluate the revised LAMS-FCS performance. A typical response is shown for the first wing bending mode, Figure 16, and corroborates the analyses frequency and damping required to provide the predicted structural performance.

It should be noted that the revised LAMS-FCS stability was inadequate for fuel configuration 4 at 280 KIAS. However, the LAMS system was not further modified because fuel configuration 4 is considerably below the design condition gross weight, and based on the dynamic response test results noted above, the LAMS system was functioning correctly at the design flight conditions.



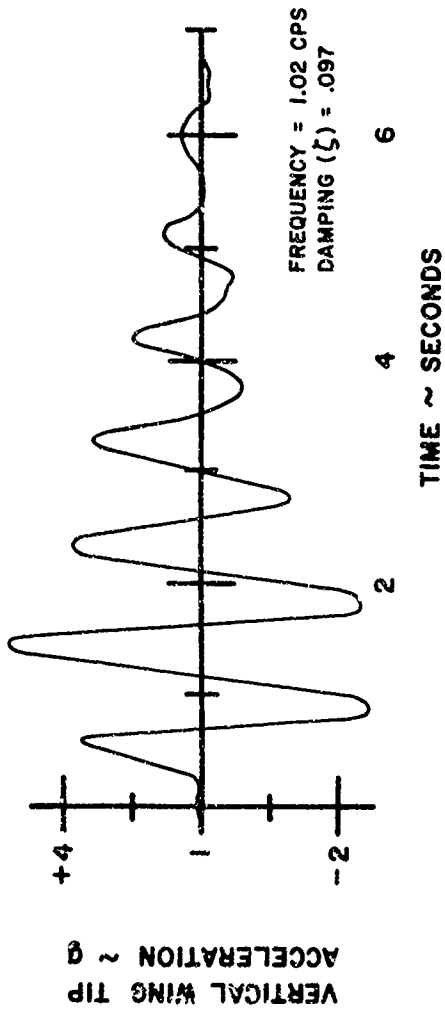
FREE AIRPLANE RESPONSE



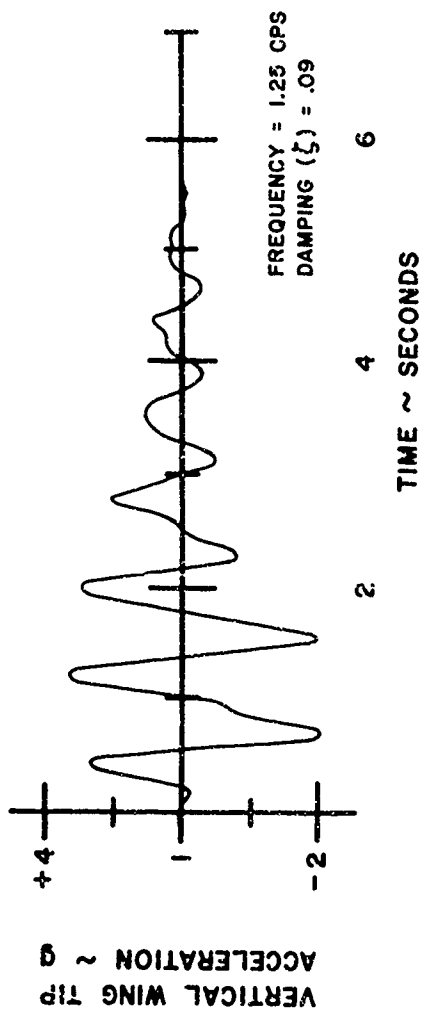
INITIAL LAMS FCS RESPONSE

DYNAMIC RESPONSE TESTING  
INITIAL LAMS-FCS  
WING TIP VERTICAL DISPLACEMENT

FIGURE 15



**FREE AIRPLANE RESPONSE**



**REVISED LAMS FCS RESPONSE**

DYNAMIC RESPONSE TESTING  
LAMS-FCS  
WING TIP VERTICAL DISPLACEMENT

FIGURE 16

Based on the results of the testing it is concluded that the revised LAMS-FCS has an adequate flutter boundary for the altitude, airspeeds, and gross weights presented in Figure 4.

## 4.2 Aerodynamic Evaluation

### 4.2.1 Handling Qualities Flight Test Results

The effect of the Baseline SAS and the LAMS-FCS on the aircraft handling qualities was evaluated by obtaining time history response data for the short period, Dutch roll, roll subsidence, and spiral modes. This section discusses this data and compares it to predicted analytical results where possible.

#### 4.2.1.1 Dutch Roll

Dutch roll frequency and damping values were obtained by exciting the aircraft with a three cycle sine wave rudder input from the function generator. Data was obtained for the basic aircraft, the Baseline SAS, and the LAMS flight control system. Flight test data is compared to the predicted values on the Dutch roll criterion plot in Figure 5.

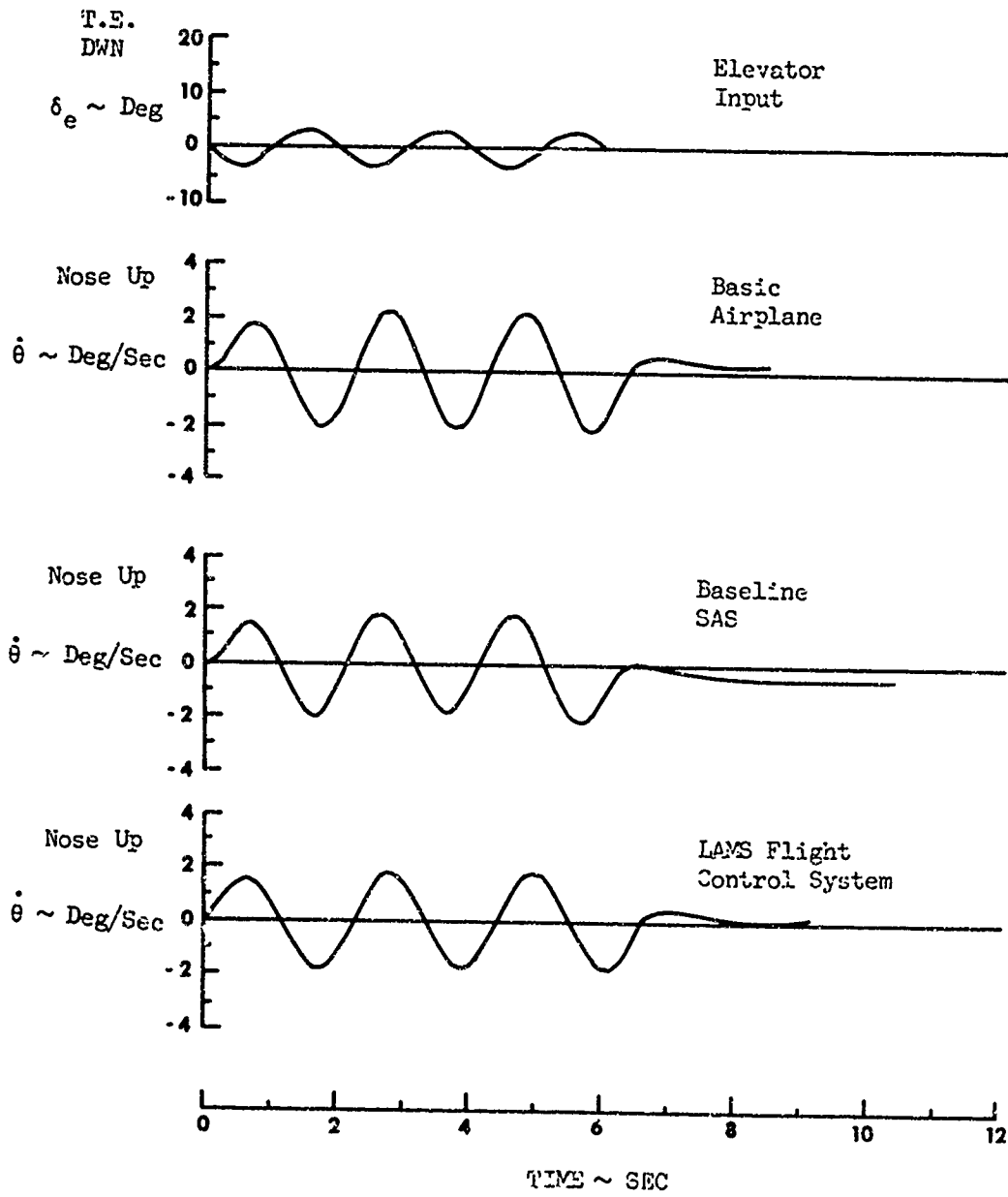
Satisfactory Dutch roll handling qualities were obtained with the Baseline SAS. Test results exceed the design requirement. The flight test Dutch roll damping ratio with LAMS was lower than analytical results by approximately .075 for both flight conditions tested. However, the Dutch roll frequency agreed well with the predicted value. It is noted that although the LAMS flight control system exceeded the handling qualities requirements for normal operation, it did not meet the turbulence boundary criterion for Flight Condition 1 and was only marginal for Flight Condition 3.

#### 4.2.1.2 Short Period

Short period response data was obtained in a manner similar to the Dutch roll data in that a sine wave elevator input was used to excite the aircraft. An attempt was made to obtain values for the short period frequency and damping from free aircraft flight test response data. Such methods as the maximum slope and others based on second order response were tried. However, the short period damping was very high with higher order effects present in the response, and reasonable values could not be obtained. The actual pitch rate responses are shown on Figures 17 through 19. The amplitude and frequency of the forced and unforced response for both the Baseline SAS and the LAMS-FCS did not change appreciably, and basic aircraft short period handling qualities were not degraded.

#### 4.2.1.3 Roll Response

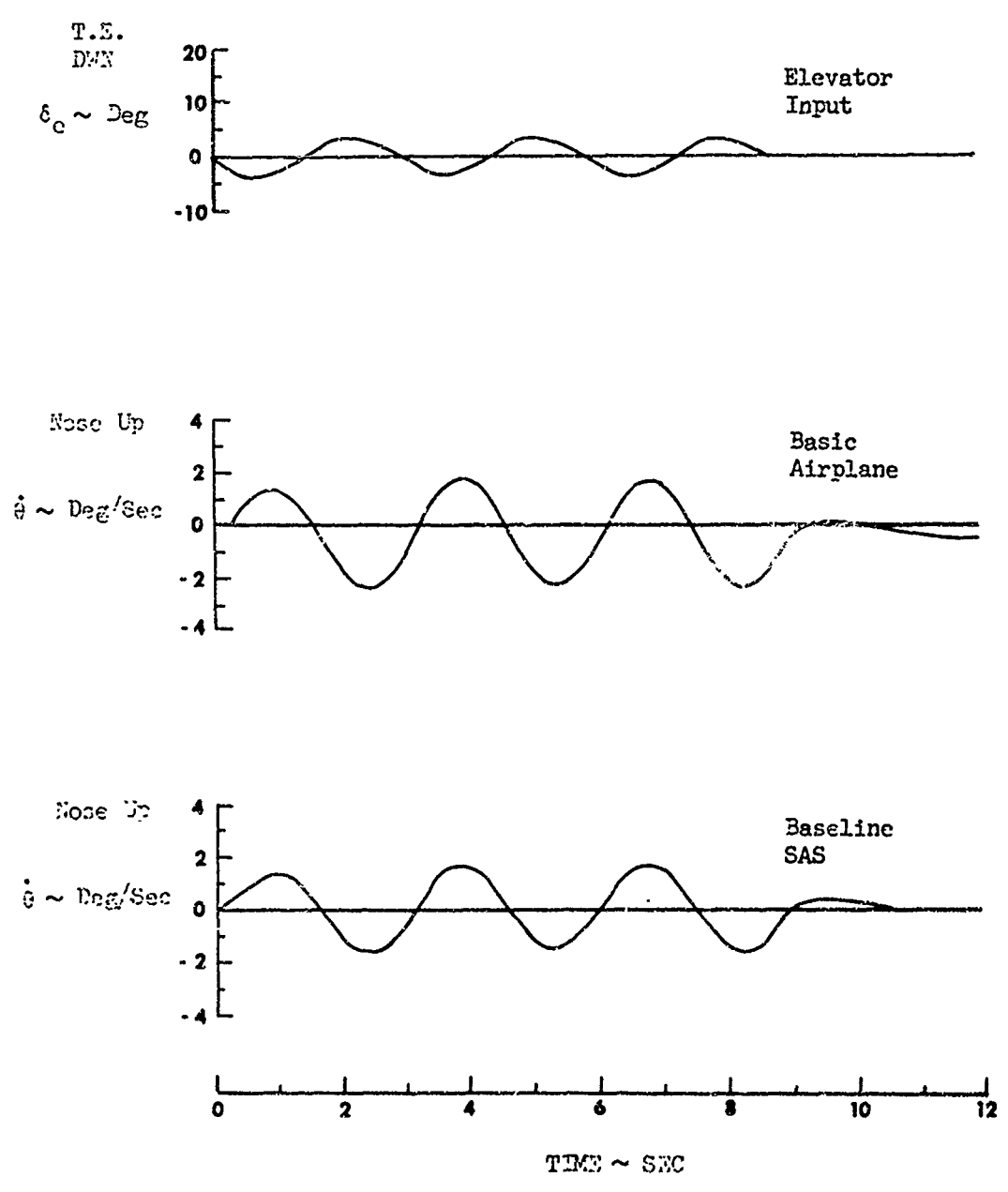
The roll axis handling qualities were specified such that the roll time constant should be less than two seconds. The table on page 56, presents the roll time constant data obtained from flight test as compared to predicted values for all three aircraft configurations, i.e., basic aircraft, Baseline SAS, and the LAMS flight control system. Agreement is good for all test conditions and all time constants are well within the specified



SHORT PERIOD RESPONSE FLIGHT TEST DATA

FLIGHT CONDITION 1

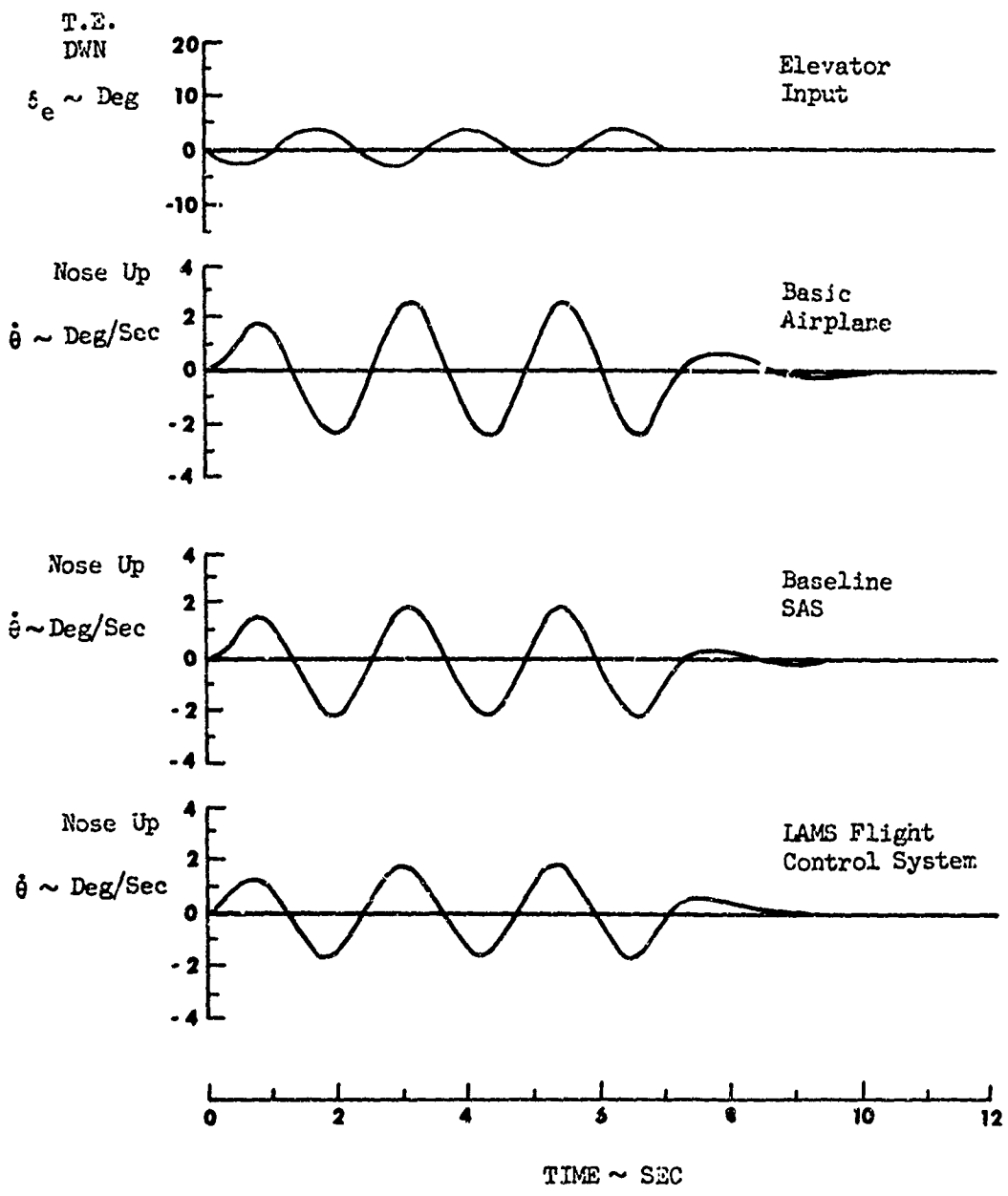
FIGURE 17



SHORT PERIOD RESPONSE FLIGHT TEST DATA

FLIGHT CONDITION 2

FIGURE 16



SHORT PERIOD RESPONSE FLIGHT TEST DATA

FLIGHT CONDITION 3

FIGURE 19

two seconds. Flight test data was not obtained for Flight Condition 2 with the LAMS flight control system operating.

FLIGHT CONDITION	BASIC AIRPLANE		BASELINE SAS		LAMS FLIGHT CONTROL SYSTEM	
	ANALYSIS	FLIGHT TEST	ANALYSIS	FLIGHT TEST	ANALYSIS	FLIGHT TEST
1	1.05	1.0	1.07	.99	1.16	1.13
2	1.05	.99	1.05	.92	1.70	----
3	1.05	1.22	1.33	1.06	1.50	1.34

#### 4.2.1.4 Spiral Mode Stability

The design requirement for the spiral mode stability was that, in the cruise configuration, the roll amplitude shall not double in less than 20 seconds. Spiral mode testing indicated that the aircraft was well within the requirement in that it exhibited essentially neutral stability.

#### 4.2.2 Control Surface Effectiveness Results

To evaluate the effectiveness of the control surfaces on the LAMS aircraft, control effectiveness data was obtained during the flight test. This section discusses this data and compares it to predicted analytical results. Data for Flight Condition 1 is shown as typical; however, similar and additional data can be found in Reference 6.

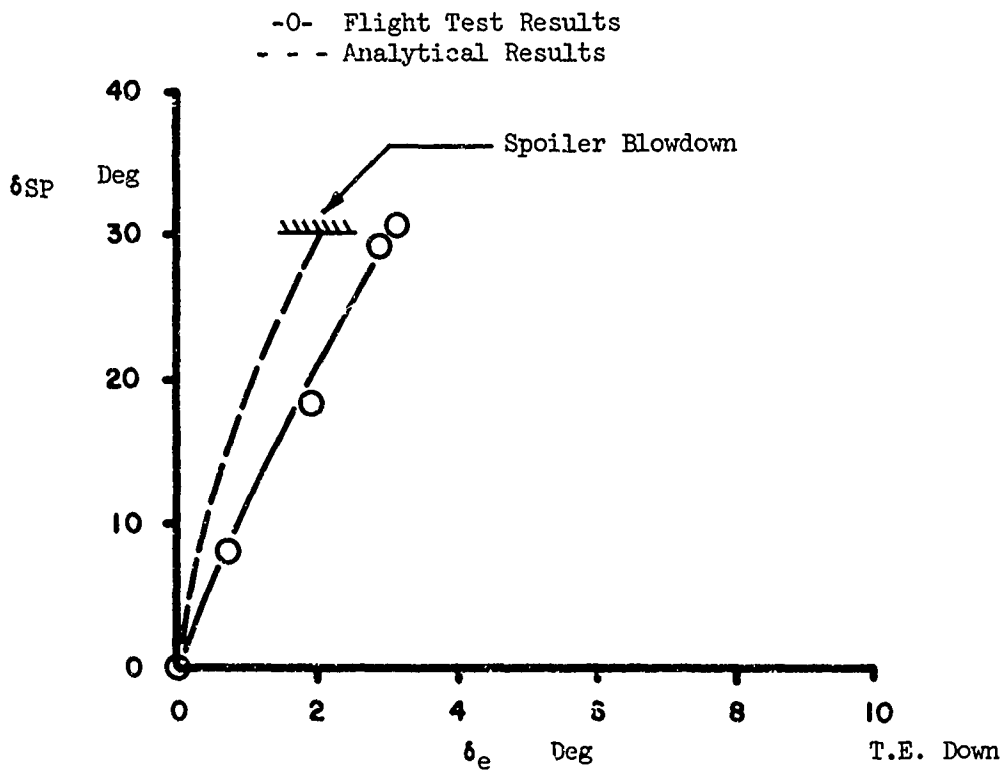
##### 4.2.2.1 Symmetrical Spoiler Effectiveness

Longitudinal effectiveness data for the LAMS-FCS spoilers was obtained by trimming the pitching moment produced by symmetrical spoiler deflection with elevator. Flight test data as well as a comparison with analytical results is shown in Figure 20.

There was no wind tunnel data available for the two outboard spoiler segments and their effectiveness was difficult to estimate. However, the comparison indicates that the predicted pitching moment produced by the LAMS-FCS spoiler was conservative, i.e. the flight test data shows that it takes more elevator than predicted to trim spoiler pitching moment.

##### 4.2.2.2 Symmetrical Aileron Effectiveness

The LAMS-FCS requires symmetrical aileron operation and through electrical command, the LAMS test bed has this unique capability. To help assess symmetrical aileron effectivity, aileron-elevator trades were conducted. Data obtained from test is plotted in Figure 21. A comparison with the predicted analytical result shows the predicted to be conservative.

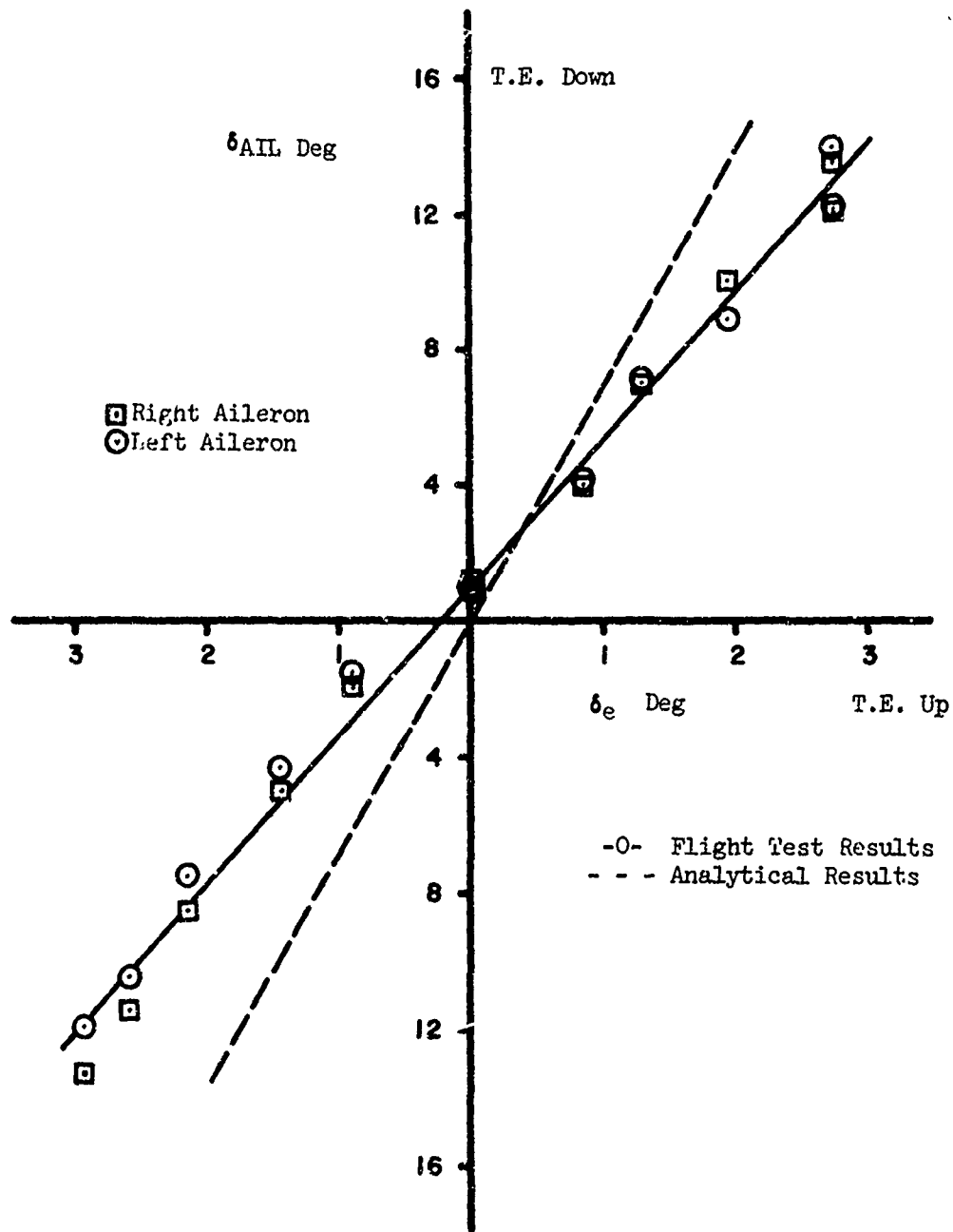


SYMMETRICAL SPOILER EFFECTIVENESS

LAMS-FCS SPOILERS

FLIGHT CONDITION 1

FIGURE 20



SYMMETRICAL AILERON EFFECTIVENESS

FLIGHT CONDITION 1

FIGURE 21

Like the symmetrical spoiler trades, the flight test data shows that it requires more elevator than predicted to trim aileron deflections.

#### 4.2.2.3 Spoiler Roll Response

Spoiler roll response data was obtained for the roll control provided by the five inboard spoiler panels. The two outboard LAMS spoilers were retracted in the wing and the ailerons were deactivated.

Typical data is plotted in Figure 22 for LAMS Flight Condition 1. Steady state roll rate is plotted as a function of wheel deflection.

Predicted Flight Condition 1 data is compared to the flight test data. The predicted steady state roll rate was calculated using the average inboard and outboard spoiler positions.

#### 4.2.2.4 Aileron Roll Response

Aileron roll response data is shown plotted in Figure 23. Steady state roll rate is plotted as a function of wheel deflection. The predicted aileron roll rate was obtained by calculating the maximum steady state roll rate and assuming the steady state roll rate to be linear with aileron deflection.

#### 4.2.2.5 Elevator Effectiveness

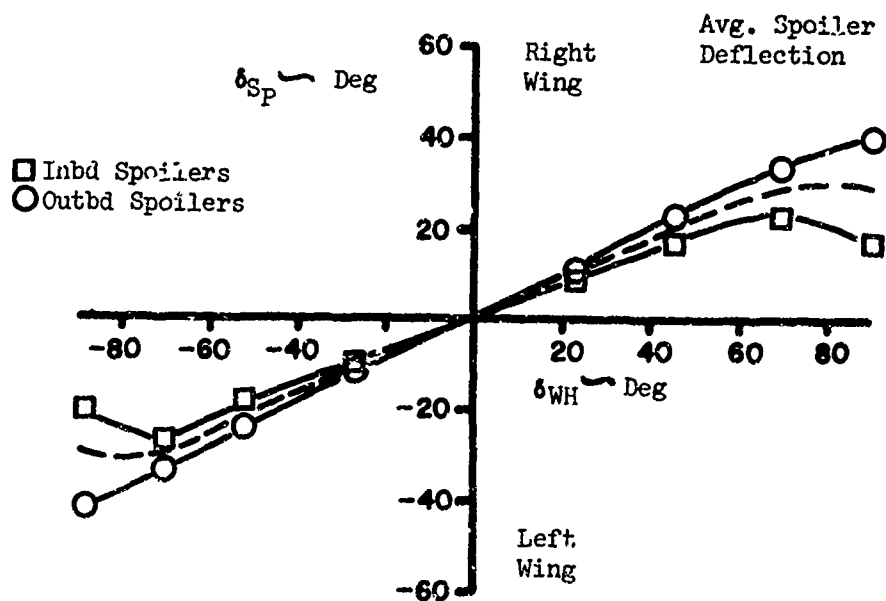
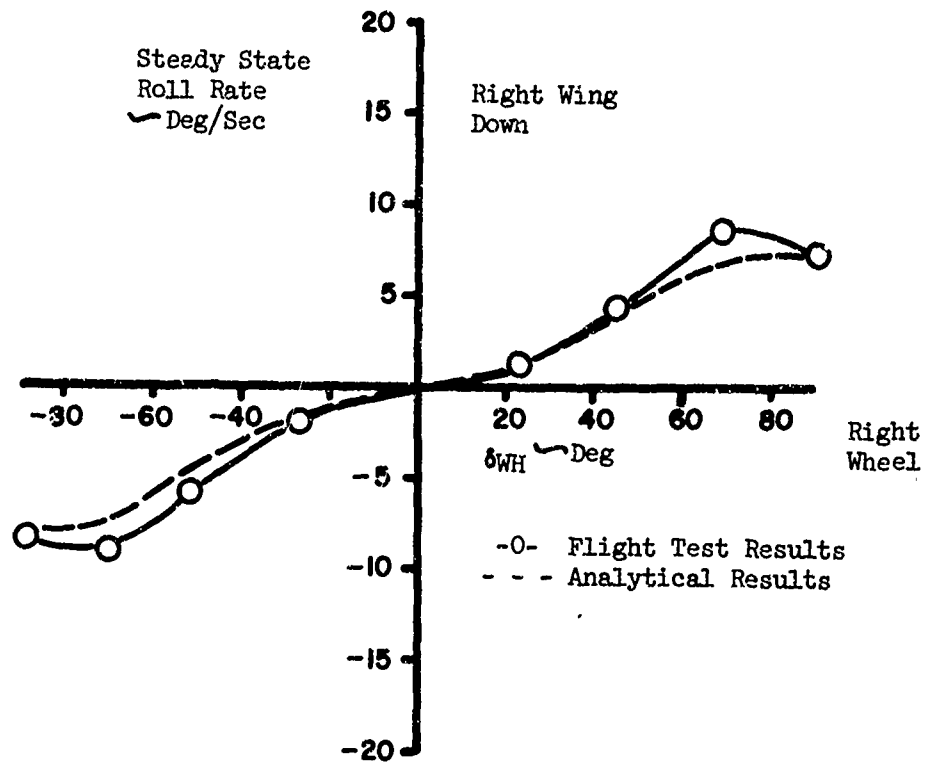
Elevator effectiveness data was obtained by trading stabilizer for elevator in increments of elevator from full forward and full aft column. This data is plotted in Figure 24. A comparison of flight data with the predicted linear derivative ( $dS/d\delta_e$ ) for Flight Condition 1 is also shown.

Comparing the slopes of the linear portion of each curve ( $dS/d\delta_e$ ), the analytical slope is slightly higher than flight data. The analytical data relates equivalent elevator deflection including elastic effects, whereas the test data is for elevator deflection adjacent to the elevator actuator.

#### 4.2.2.6 Rudder Effectiveness

Rudder effectiveness data was obtained by establishing steady state sideslip angles using the rudder. Ailerons were used to counteract roll due to rudder or sideslip. This data ( $\beta$  vs  $\delta_r$ ) is plotted on Figure 25.

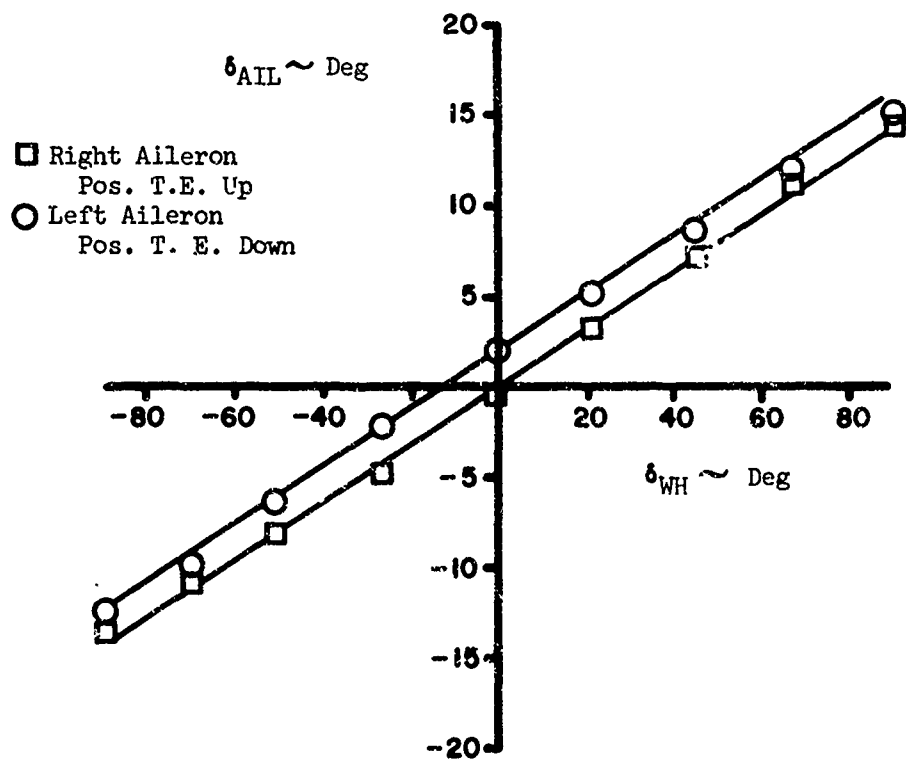
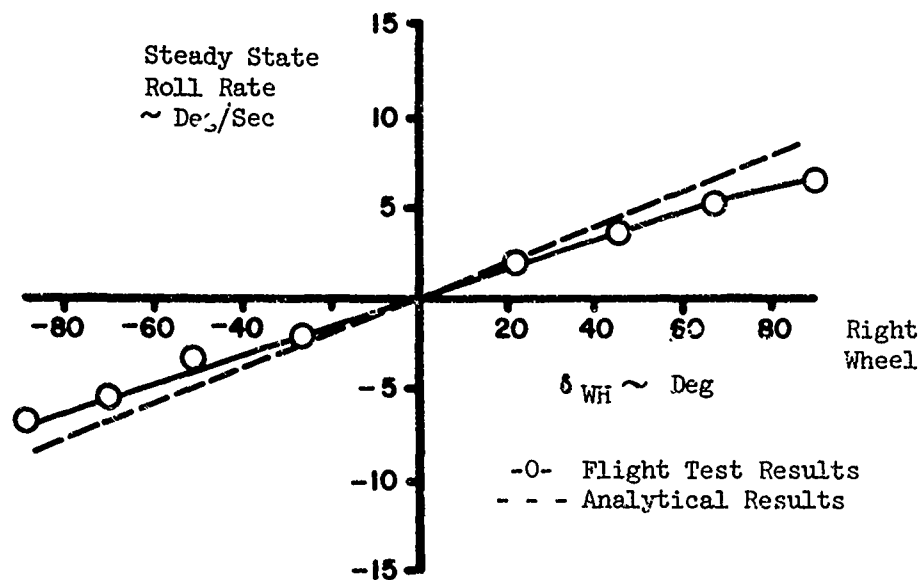
The predicted linear slope, obtained from the yawing moment stability derivatives  $C_{n\dot{\beta}}$  and  $C_{n\dot{\delta}_r}$ , is lower than the flight data. The predicted slope was calculated assuming that all the roll due to rudder or sideslip had been trimmed. Also, the predicted data relates equivalent rudder deflection, whereas the test data is for rudder deflection adjacent to the rudder actuator.



SPOILER ROLL RESPONSE

FLIGHT CONDITION 1

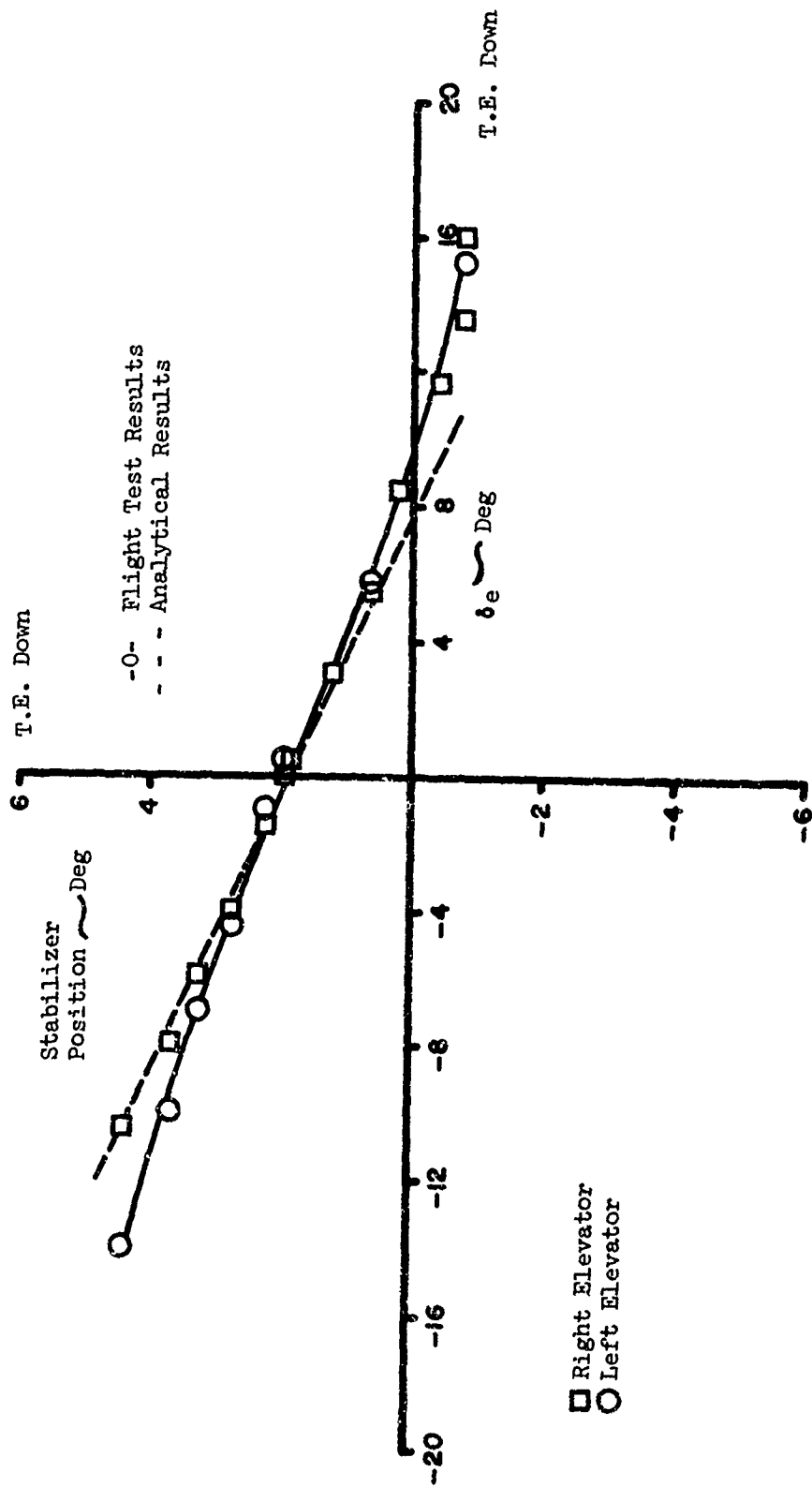
FIGURE 22



AILERON ROLL RESPONSE

FLIGHT CONDITION 1

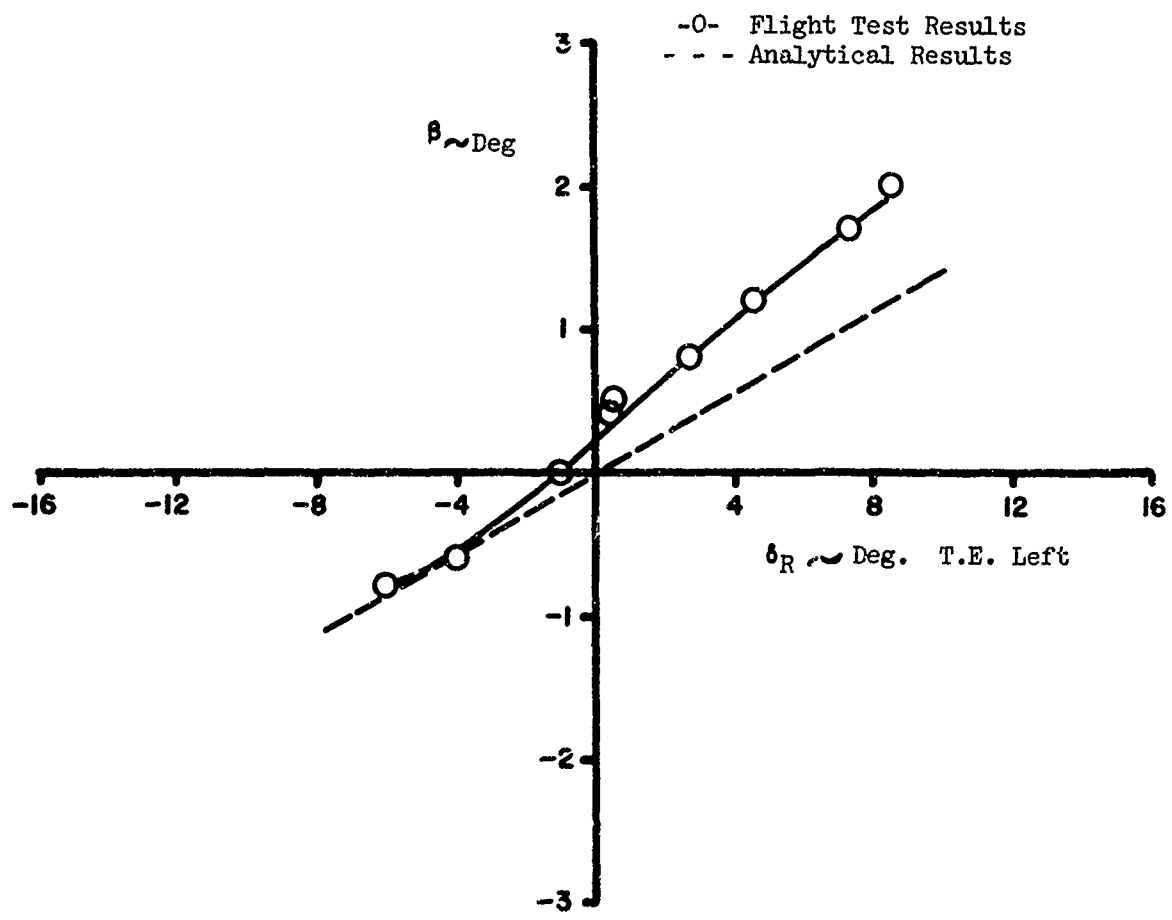
FIGURE 23



ELEVATOR EFFECTIVENESS

FLIGHT CONDITION 1

FIGURE 24



RUDDER EFFECTIVENESS

FLIGHT CONDITION 1

FIGURE 25

### 4.3 Structural Response to Turbulence

The LAMS B-52 flight test was designed to evaluate control system performance during flight through random atmospheric turbulence. Performance parameters considered were fatigue damage rates, maximum expected stresses and rms accelerations. The random nature of atmospheric turbulence required analysis and experimental data to be derived by statistical techniques. Data is presented in a form which permits direct comparison of flight test data with analytical results.

#### 4.3.1 Data Collection and Reduction

The test data presented in this section is from two flight tests, #54-15 and #54-18. Both tests included ten-minute data collection runs in each of the following configurations:

- Basic aircraft
- Baseline SAS on, all axes
- LAMS flight control system on, all axes

The raw data was processed by ground equipment yielding sampled time-histories (50 samples per second, each channel synchronized with the others) of vertical and lateral gust components, accelerations, bending moments, and control surface motions.

The responses (accelerations, bending moments, and control surface motions) were then reduced to frequency response functions. Frequency response functions are independent of the input spectrum, and can be compared for various flight segments even though gust environments of individual samples were not identical. The frequency responses were computed using the cross-spectral approach.

$$T_{r/g}(i\omega) = \frac{\hat{\Phi}_{r,g}(i\omega)}{\hat{\Phi}_{g,g}(i\omega)}$$

where:  $T_{r/g}(i\omega)$  is the complex frequency response of "r" with respect to the input "g"

$\hat{\Phi}_{r,g}(i\omega)$  is the complex cross-spectral density of "r" and "g"

$\hat{\Phi}_{g,g}(i\omega)$  is the auto-spectral density of the input "g"

The cross spectral method of data reduction eliminates all response information not statistically coherent with the selected gust component as measured at the probe.

Assumptions inherent in the turbulence response testing are that:

- The airframe, aerodynamics, actuators, recorders, etc. are within their linear ranges
- All gust measurements have an adequate signal-to-noise ratio
- Pilot inputs are incoherent with gust inputs
- Vertical and lateral turbulence components are statistically independent
- The gust components everywhere on the aircraft are perfectly coherent with the respective gust components at the probe

The linearity assumption is considered valid in the range of gust intensities investigated. Signal-to-noise ratios for the gust components were estimated by comparing power spectral density calculations in still air to those in turbulence and is presented in Section 4.3.2. Coherencies between gust components and between pilot and gust were calculated and are presented in Sections 4.3.3 and 4.3.4. Spanwise and time coherencies of the turbulence components cannot be measured with a single gust probe. Less than perfect coherence would result in lowered frequency response amplitudes as computed from the single-input cross-spectral equation, and the apparent coherency between gusts at the probe and response would decrease as the wave length of turbulence decreased. Such an effect is present in all test data, probably indicating the spanwise and timewise variation in the turbulence field.

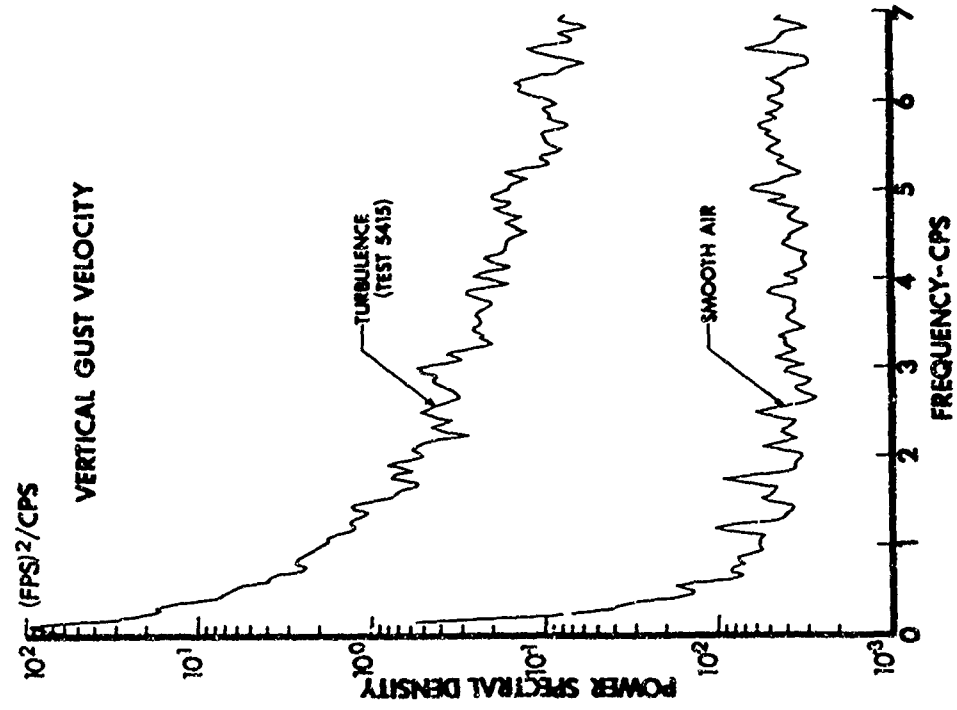
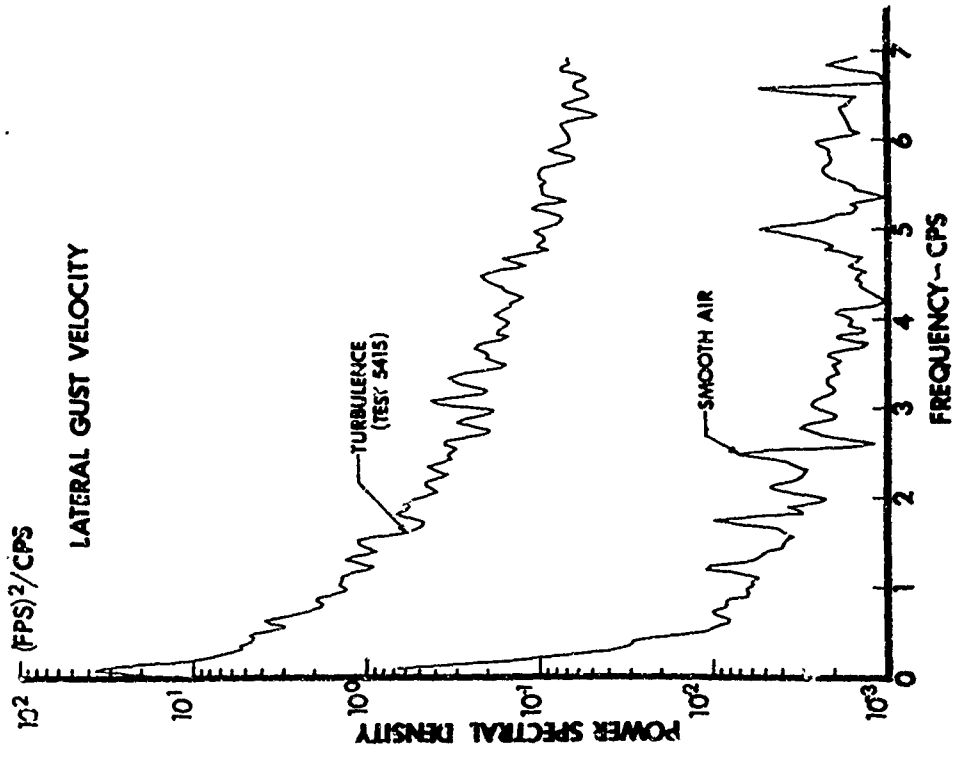
Test and theoretical frequency response function comparisons are presented in Sections 4.3.5 and 4.3.6. Response spectrum parameters  $A$  and  $N_0$  (rms response per unit rms turbulence, and characteristic frequency) were computed for the various configurations and are presented in Section 4.3.7. Structural fatigue damage rates and peak stress calculations based on these  $A$ 's and  $N_0$ 's are presented in Section 4.3.8 as a performance measure. Crew compartment acceleration spectra for the three configurations are presented in Section 4.3.9.

#### 4.3.2 Gust Signal to Noise Comparisons

Gust component power spectral densities were computed from gust probe data for flight in turbulence and for flight in still air. The comparison of results gives an estimate of signal-to-noise ratio for the gust measurement which is the input to the flight test frequency response calculations.

Figure 26 presents the results for test #54-15. Both vertical gust and lateral gust measurements were larger than the still air measurements by at least a factor of ten between 0.2 cps and 7.0 cps. The turbulence measurements were at least a factor of ten between 0.2 cps and 7.0 cps. The turbulence measurements were 100 times greater than the still air measurements between 0.2 cps and 2.0 cps.

This level of signal to noise ratio was considered adequate for definition of the gust environment.



SIGNAL TO NOISE COMPARISON

FIGURE 26

#### 4.3.3 Coherency of Pilot Inputs vs. Gusts

The control surface rms motions during the basic aircraft tests were in some cases as large as the rms control surfaces motions during the LAMS-FCS and Baseline SAS runs. The raw time-history response data was therefore contaminated by pilot inputs. The cross-spectral analysis of the data performed for this report removes the pilot effects, leaving only the time correlated gust response data, provided that the pilot inputs are incoherent with the gust components.

Figure 27 presents the computed coherencies between gust velocity and control surface displacement for the basic aircraft configuration from flight test #54-15. The coherencies were considered low enough to assure isolation of the gust-response data.

#### 4.3.4 Gust Spectra and Coherency

Gust spectral density results are presented in Figure 28 for the six turbulence tests--two conditions each for basic aircraft, Baseline SAS, and LAMS-FCS. The plotted data are normalized to 1 ft/sec rms. The actual rms gust component velocities for the six flights are tabulated below. Vertical gusts were somewhat more severe than lateral gusts, as is typical of moderate turbulence during low altitude flight over the plains.

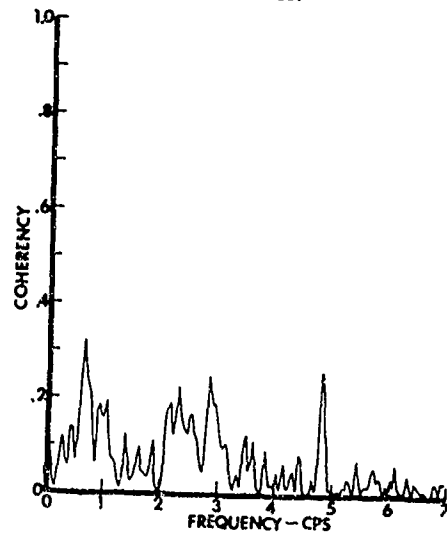
	MEASURED GUST 's - FT/SEC					
	TEST 54-15			TEST 54-18		
	Basic	Baseline	LAMS	Basic	Baseline	LAMS
Vertical Gust	4.453	4.501	4.245	3.604	4.003	4.205
Lateral Gust	3.012	2.967	3.328	3.248	3.286	3.846

Both the analysis and the test planning assumed that the vertical and lateral gust components would be incoherent with each other. Figure 29 shows the test coherencies were indeed very low.

#### 4.3.5 Frequency Responses to Vertical Gusts

This section contains frequency response amplitude plots due to vertical gusts obtained from the two turbulence flight tests. The plots are arranged to provide visual comparisons of the three aircraft configurations: the LAMS-FCS, Baseline SAS and Basic aircraft. Similar plots of theoretical responses are included.

ELEVATOR DISPLACEMENT  
AND  
VERTICAL GUST

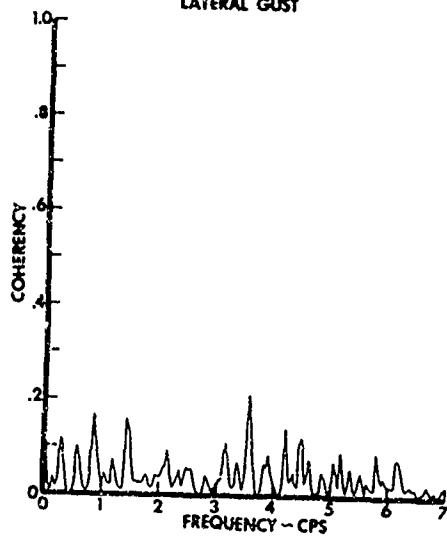


COHERENCY FUNCTION BETWEEN  
PILOT AND GUST INPUTS

BASIC - NO SAS CONFIGURATION

TEST 5415

ANTI-SYMMETRIC  
AILERON DISPLACEMENT  
AND  
LATERAL GUST



RUDDER DISPLACEMENT  
AND  
LATERAL GUST

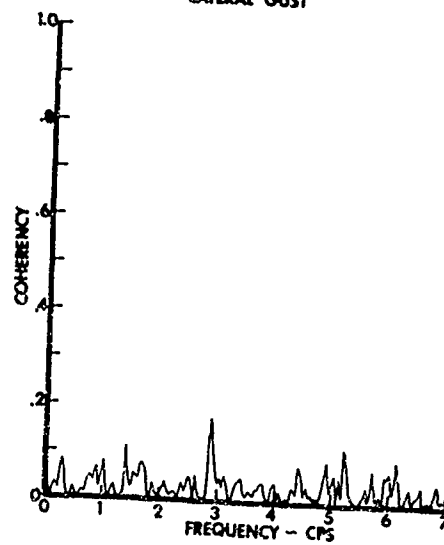
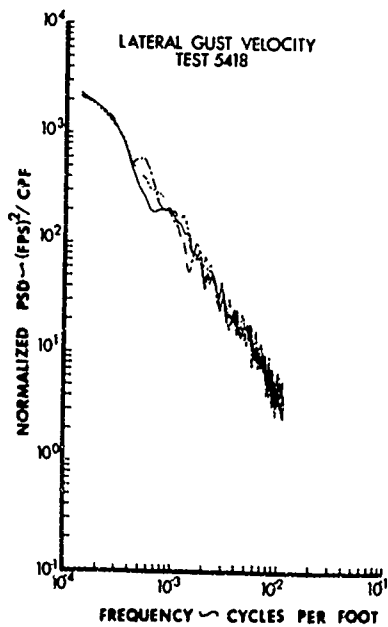
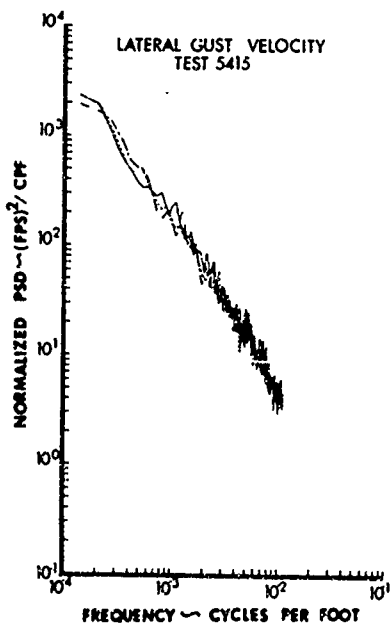
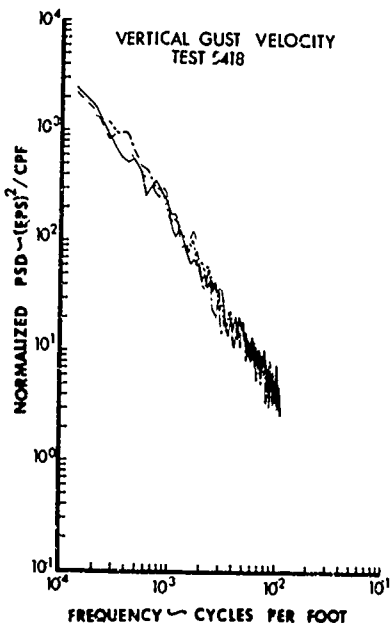
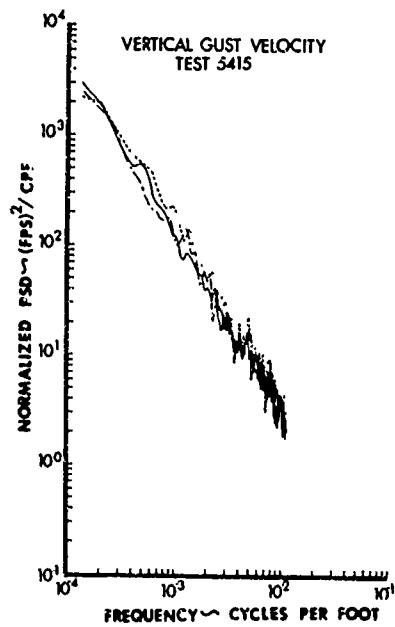


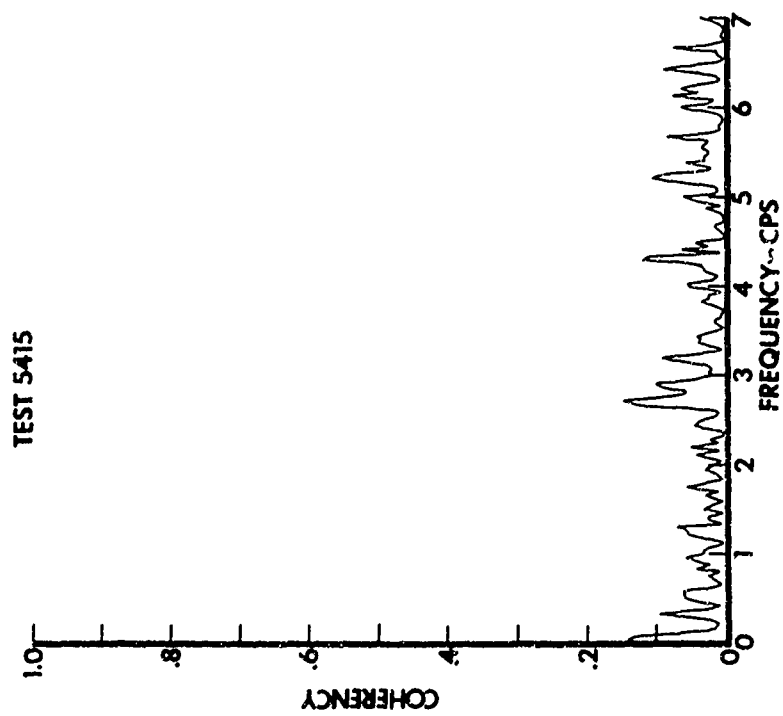
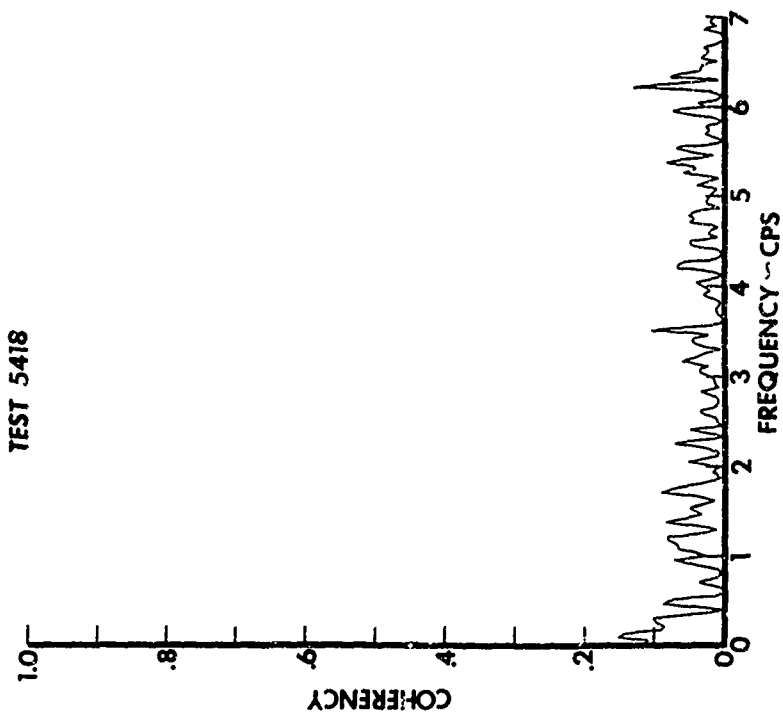
FIGURE 27



— NO SAS  
 - - - BASELINE SAS  
 ····· LAMS FLIGHT CONTROL SYSTEM

NORMALIZED GUST SPECTRA

FIGURE 28



COHERENCY FUNCTION BETWEEN VERTICAL AND LATERAL COMPONENTS  
(NO SAS CONFIGURATION)

FIGURE 29

Figures 30 through 44 contain responses of body and stabilizer vertical bending moment, wing vertical and chordwise bending moments, body vertical accelerations, and control surface motions. These contain only the test data which was statistically coherent with the vertical gust.

Without referring to specific figures, some general conclusions can be drawn:

- Consistency of results between the two tests is remarkably good
- Relative performance of the LAMS-FCS, Baseline SAS, and basic aircraft is similar to that predicted theoretically
- The important features of the responses are similar to the theoretical predictions throughout the frequency range tested

All of the test frequency response functions showed a roll-off of amplitude vs. frequency. An example of this is evident in Figure 32. This was a direct result of a reduced coherency with increasing frequency. The most likely cause is a reduced coherency between vertical gust components at various locations across the span of the aircraft wing.

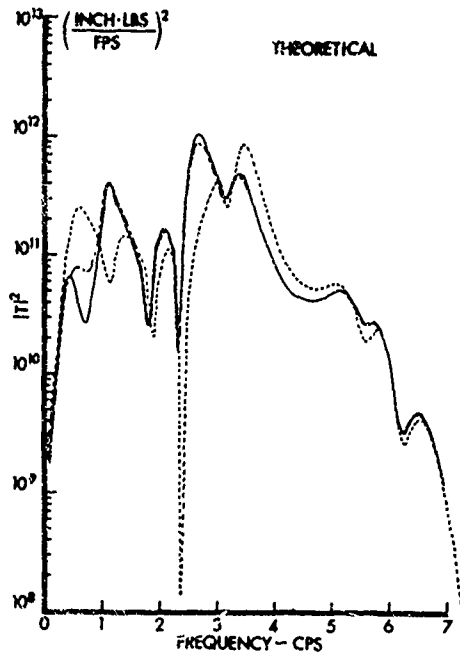
An important contribution of the LAMS-FCS is reduced wing vertical bending moment. The effect is clearly shown at the short period and 1st bending frequencies, Figures 33, 35, and 37. The control surface activity required to attain the structural performance is presented in Figures 42, 43, and 44.

#### 4.3.6 Frequency Responses to Lateral Gusts

This section contains plots of frequency response amplitude due to the lateral component of the measured turbulence. Data is presented from two turbulence flight tests and theoretical calculations. As in Section 4.3.5 (response to vertical gusts) the plots are arranged to provide comparison of the LAMS-FCS, Baseline SAS and basic aircraft.

Figures 45 through 59 contain responses of vertical tail and fuselage side bending moments, stabilizer vertical bending moment (antisymmetric) wing vertical, and fore and aft bending moments, body side acceleration, and control surface motions. These were obtained from cross-spectral analysis of the test data so that only the responses coherent with the lateral gust component remain.

The general conclusions noted in Section 4.3.5 apply in this section. All of the basic aircraft responses include an apparent coherency loss at the Dutch roll peak. The half-power bandwidth of Dutch roll for the basic aircraft is about .025 cps (estimated from Dutch roll damping measured in handling qualities tests). The frequency resolution of the data reduction system was .040 cps and the computed coherency of Dutch roll to lateral gust was reduced by  $.025/.040$ , or about 60 percent. The true frequency response peaks for the basic aircraft Dutch roll frequency are greater than the peaks shown by a factor of approximately 2.5. Responses at all other frequencies (with the LAMS-FCS or Baseline SAS, at all frequencies, including Dutch roll) were adequately defined by the cross-spectral analysis.



**FREQUENCY RESPONSE FUNCTION  
(AMPLITUDE - SQUARED)**

Body Station 1222

Vertical Bending Moment

DUE TO VERTICAL GUST

- NO SAS
- - - BASELINE SAS
- - - LAMS FLIGHT CONTROL SYSTEM

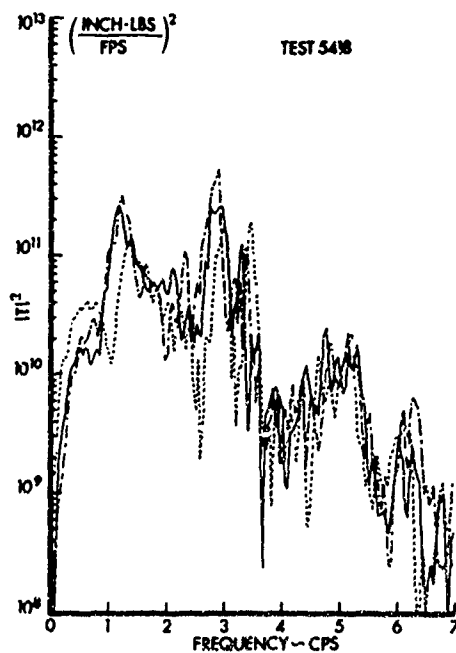
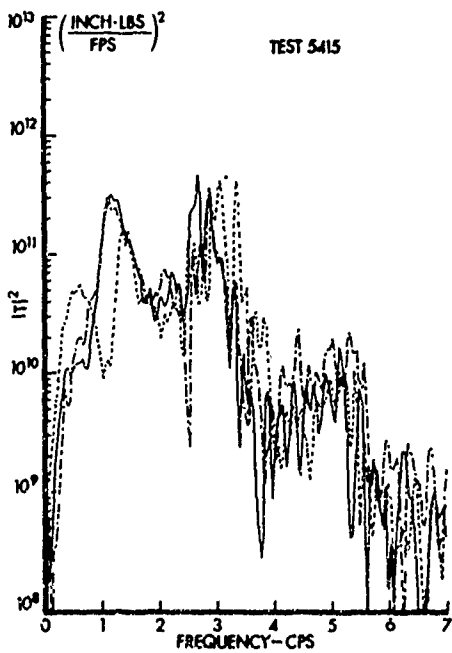
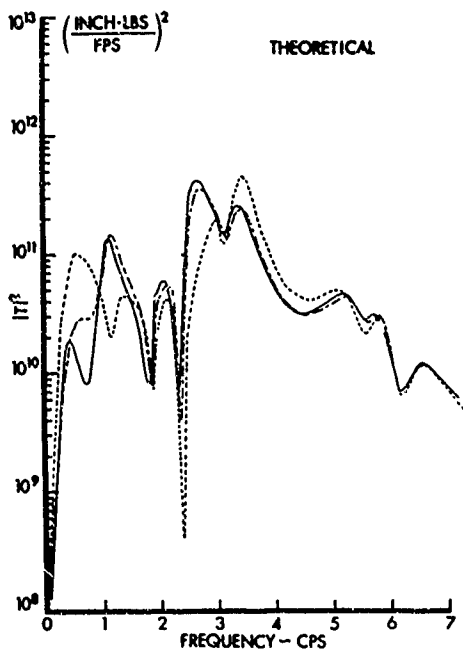


FIGURE 30



FREQUENCY RESPONSE FUNCTION  
(AMPLITUDE - SQUARED)

Body Station 1412  
Vertical Bending Moment

DUE TO VERTICAL GUST

- NO SAS
- - - BASELINE SAS
- - - LAMS FLIGHT CONTROL SYSTEM

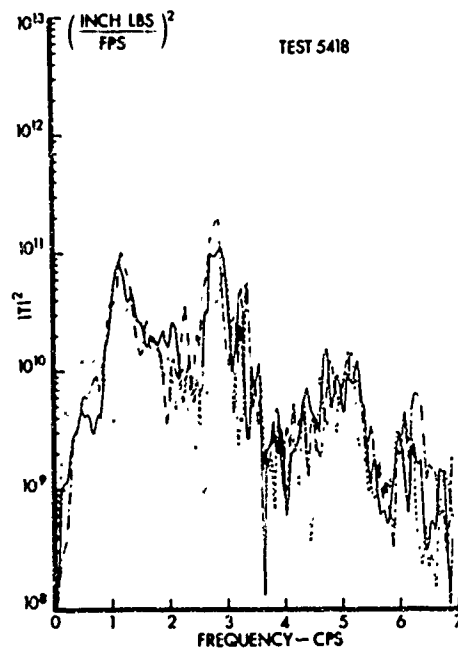
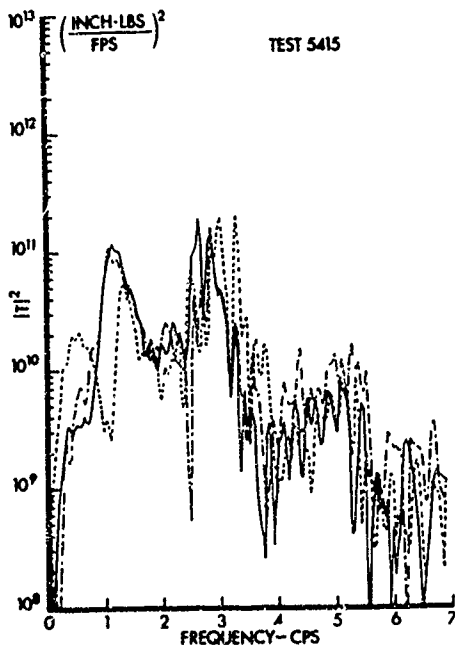
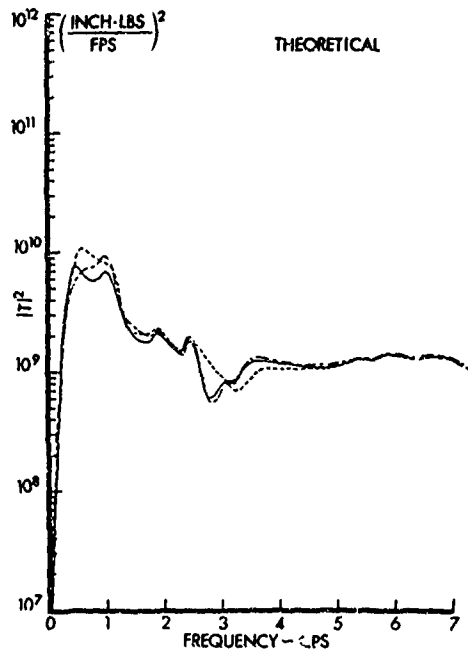


FIGURE 31



FREQUENCY RESPONSE FUNCTION  
(AMPLITUDE - SQUARED)  
Stabilizer Buttock Line 56  
Vertical Bending Moment  
DUE TO VERTICAL GUST

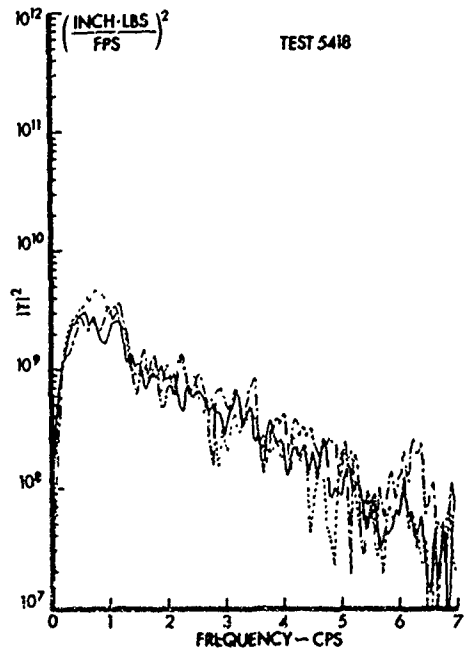
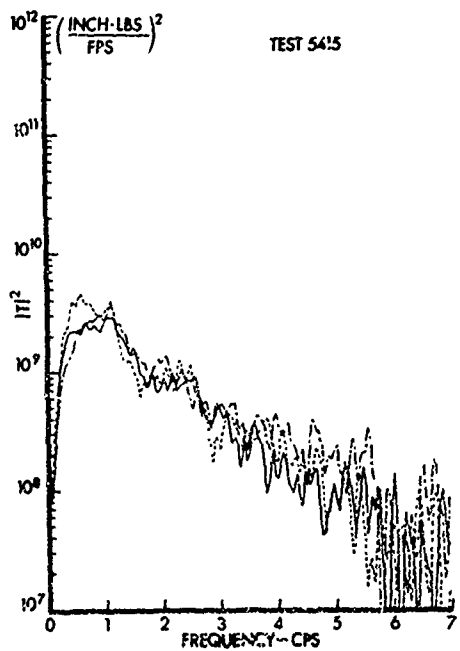
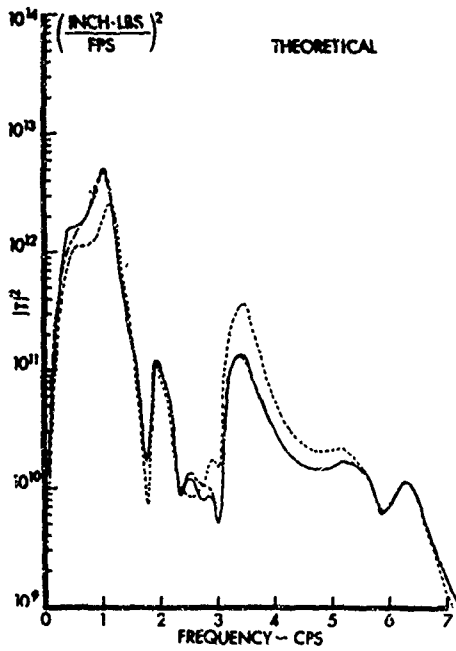


FIGURE 32



FREQUENCY RESPONSE FUNCTION  
(AMPLITUDE - SQUARED)

Wing Station 222  
Vertical Bending Moment

DUE TO VERTICAL GUST

- NO SAS
- - - BASELINE SAS
- · - LAMS FLIGHT CONTROL SYSTEM

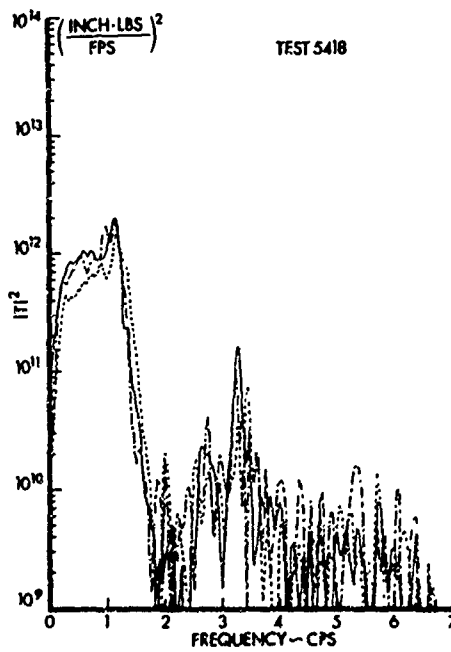
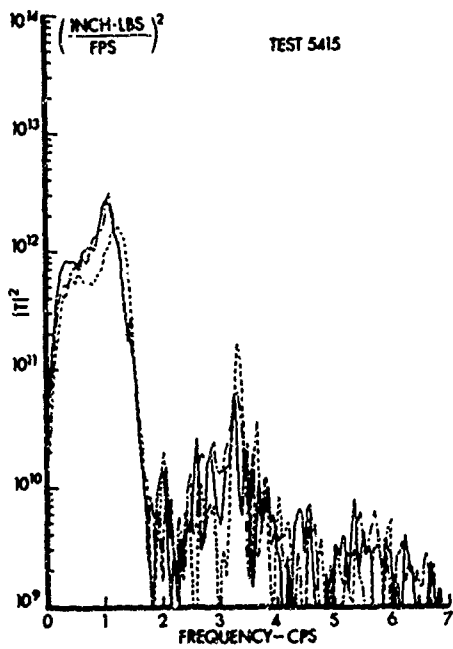
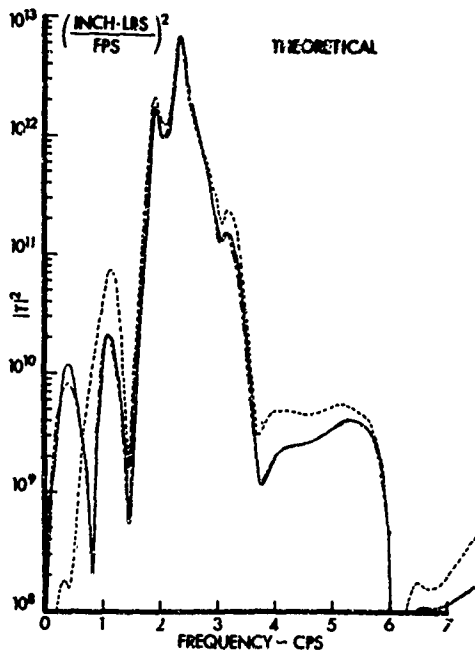


FIGURE 33



**FREQUENCY RESPONSE FUNCTION  
(AMPLITUDE - SQUARED)**

Wing Station 222  
Chordwise Bending Moment  
DUE TO VERTICAL GUST

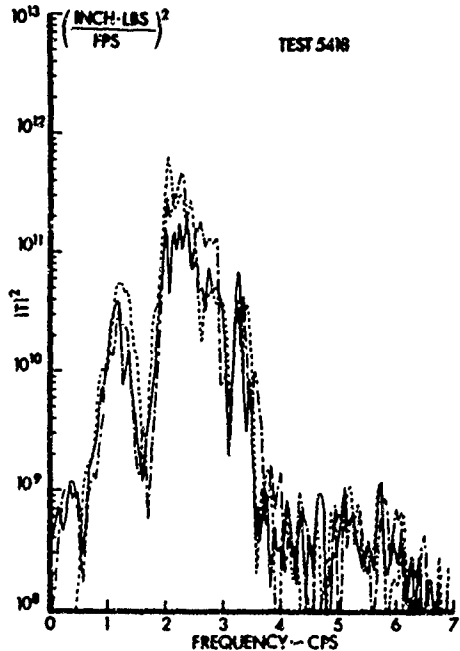
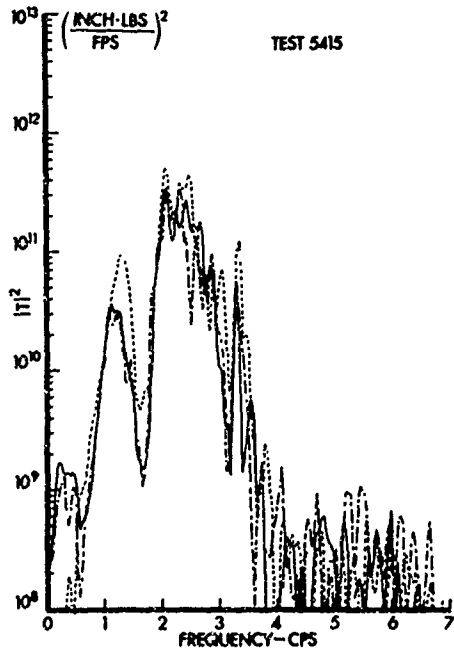
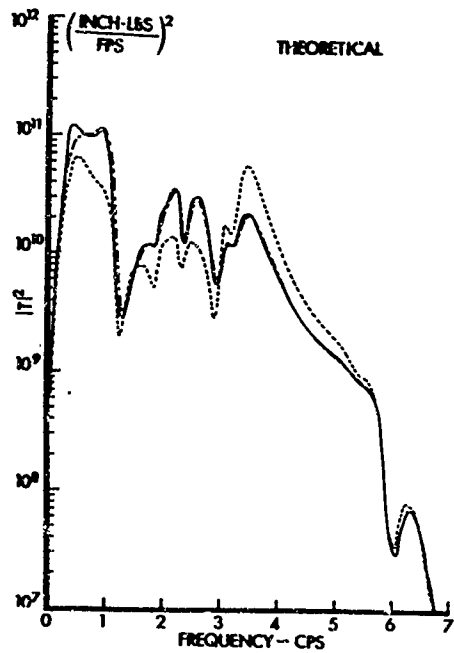


FIGURE 34



FREQUENCY RESPONSE FUNCTION  
(AMPLITUDE - SQUARED)

Wing Station 820

Vertical Bending Moment

DUE TO VERTICAL GUST

- NO SAS
- - - BASELINE SAS
- - - LAMS FLIGHT CONTROL SYSTEM

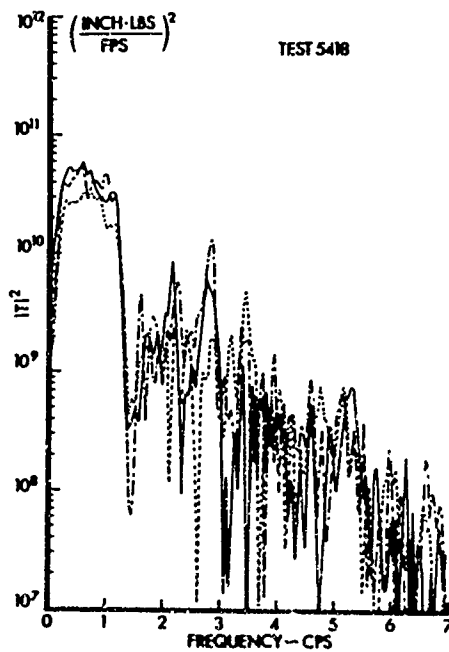
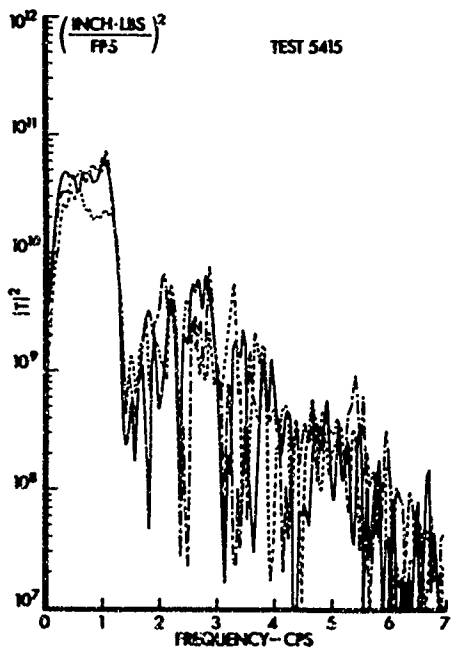
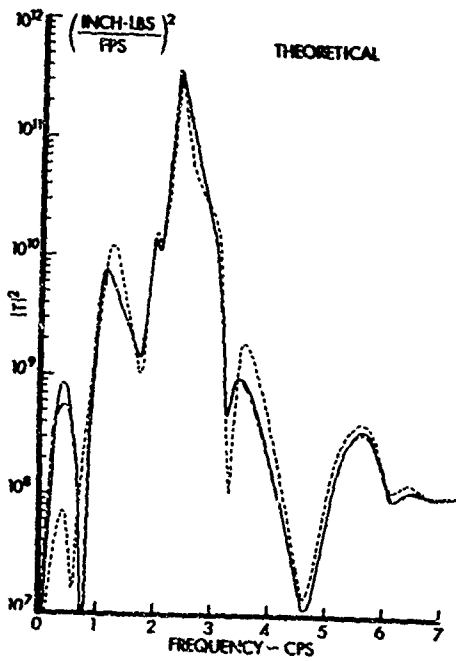


FIGURE 35



**FREQUENCY RESPONSE FUNCTION  
(AMPLITUDE - SQUARED)**

Wing Station 820  
Chordwise Bending Moment

DUE TO VERTICAL GUST

- NO SAS
- - - BASELINE SAS
- · - LAMS FLIGHT CONTROL SYSTEM

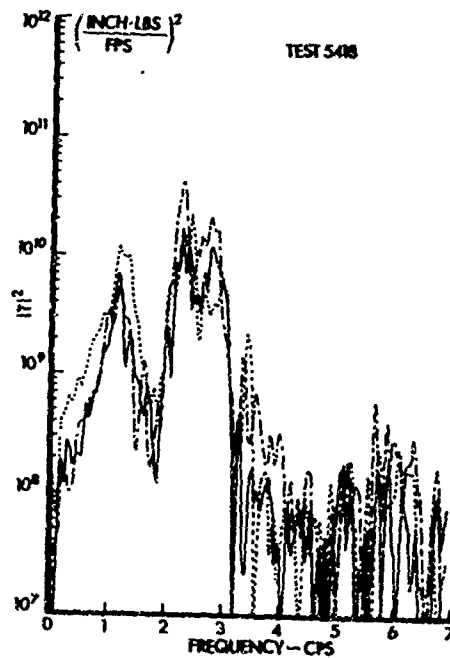
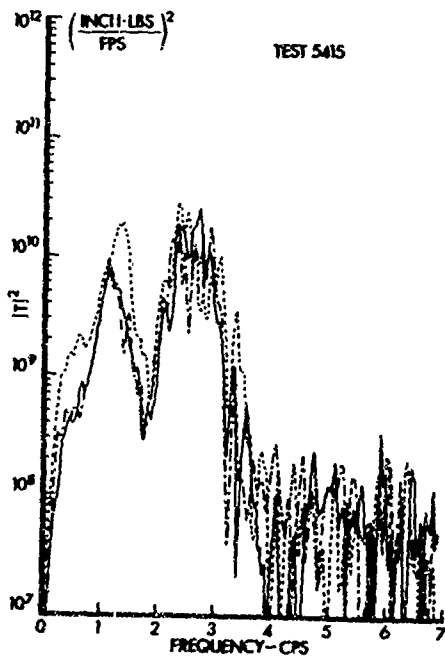
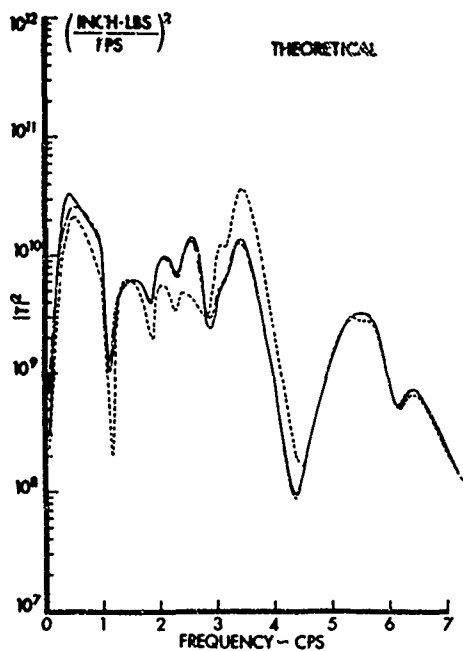


FIGURE 36



FREQUENCY RESPONSE FUNCTION  
(AMPLITUDE - SQUARED)

Wing Station 974  
Vertical Bending Moment  
DUE TO VERTICAL GUST

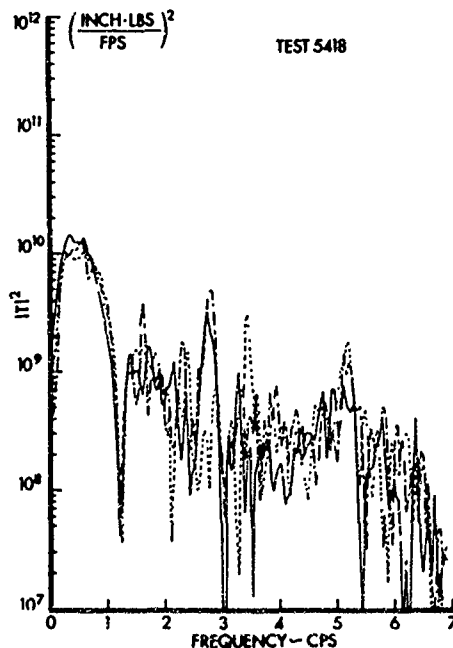
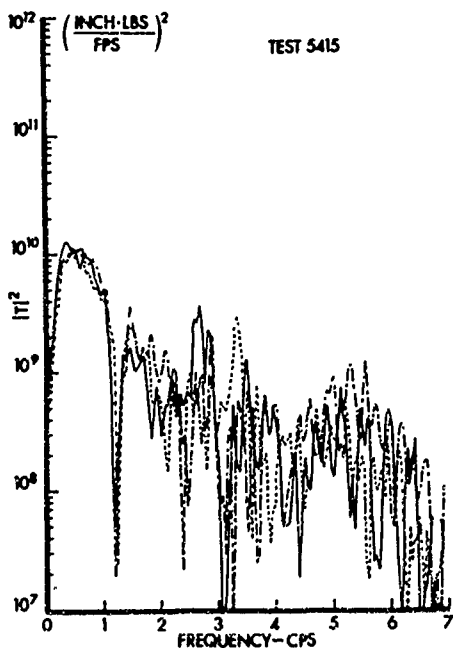
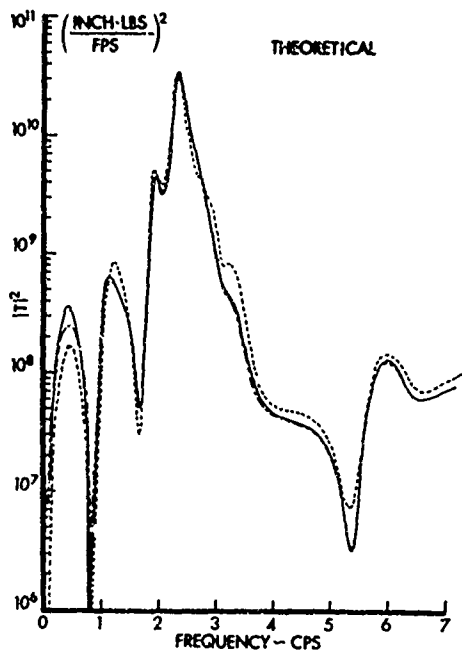


FIGURE 37



**FREQUENCY RESPONSE FUNCTION  
(AMPLITUDE - SQUARED)**

Wing Station 974

Chordwise Bending Moment

DUE TO VERTICAL GUST

- NO SAS
- - - BASELINE SAS
- · - LAMS FLIGHT CONTROL SYSTEM

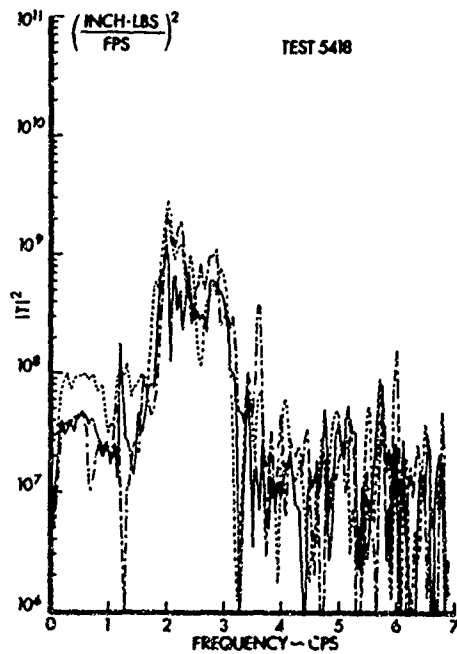
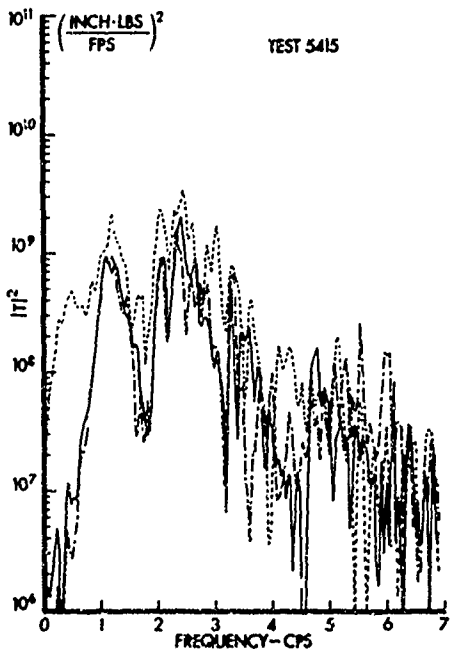
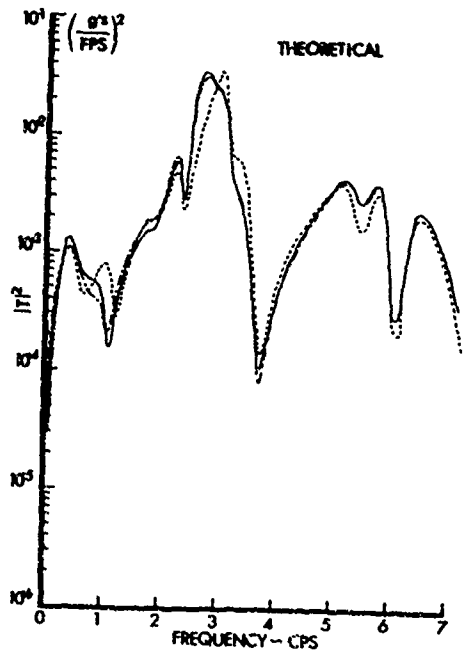


FIGURE 38



**FREQUENCY RESPONSE FUNCTION  
(AMPLITUDE - SQUARED)**

Body Station 172  
Vertical Acceleration  
DUE TO VERTICAL GUST

- NO SAS
- - - BASELINE SAS
- - - LAMS FLIGHT CONTROL SYSTEM

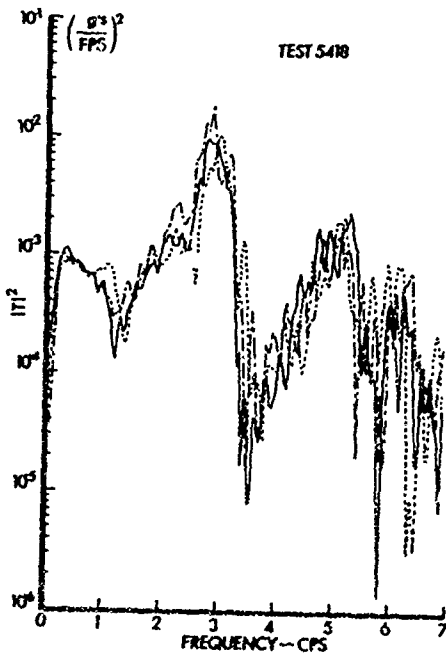
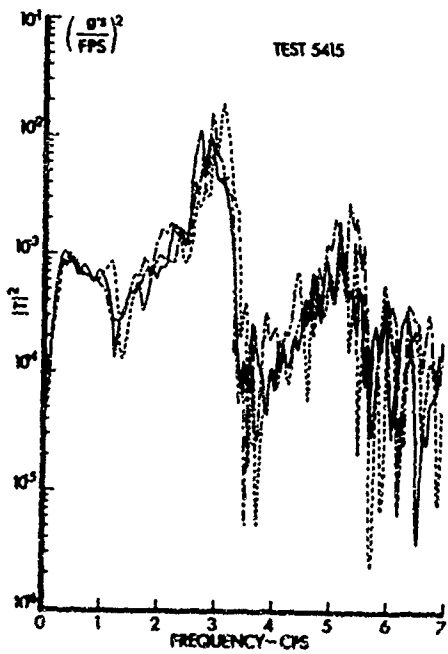
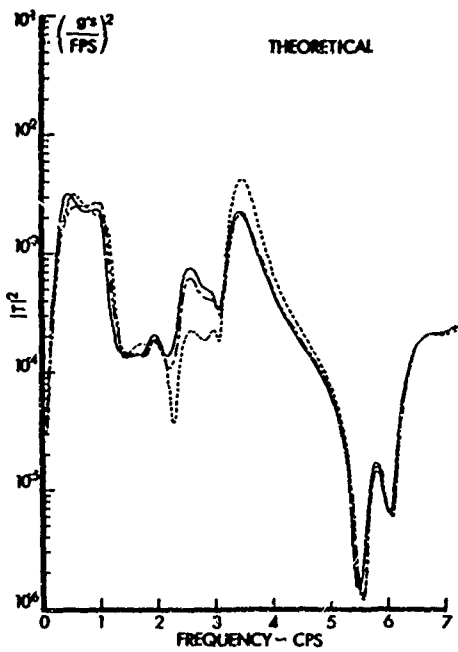


FIGURE 39



**FREQUENCY RESPONSE FUNCTION  
(AMPLITUDE - SQUARED)**

Body Station 860  
Vertical Acceleration

**DUE TO VERTICAL GUST**

- NO SAS
- - - - BASELINE SAS
- - - - LAMS FLIGHT CONTROL SYSTEM

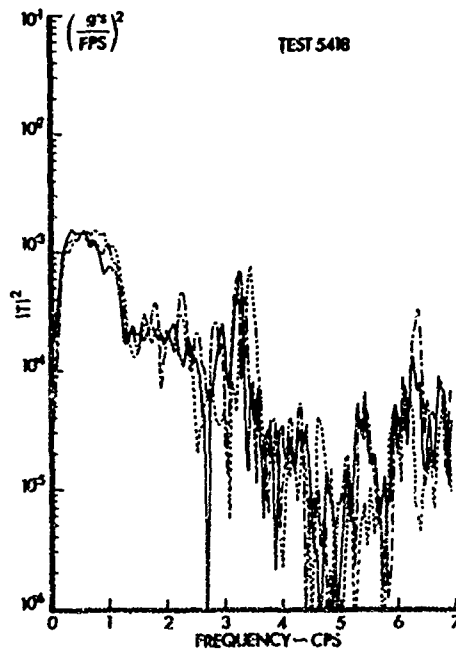
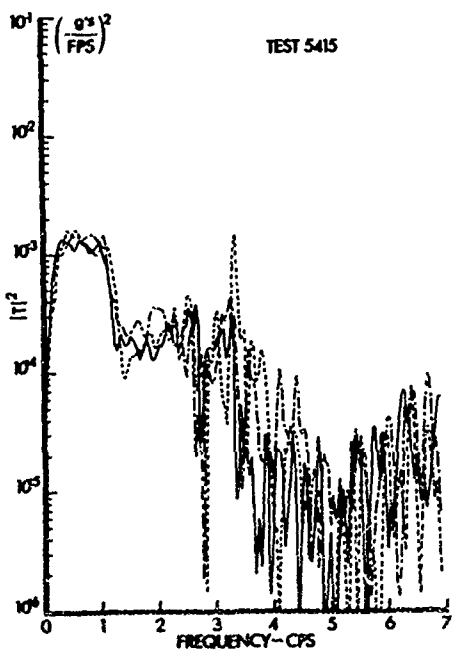
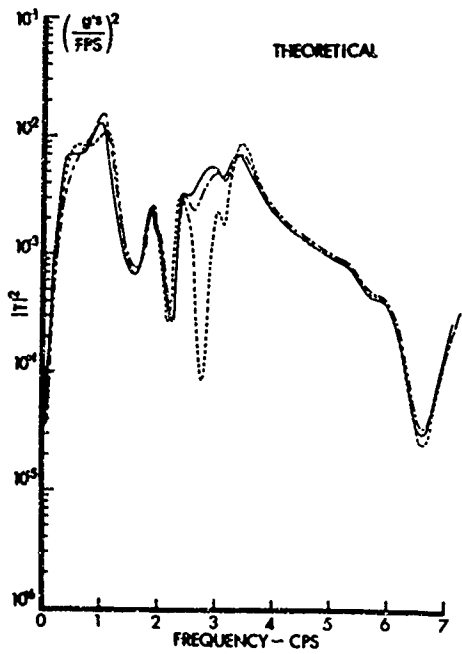


FIGURE 40



**FREQUENCY RESPONSE FUNCTION  
(AMPLITUDE - SQUARED)**

Body Station 1655

Vertical Acceleration

DUE TO VERTICAL GUST

- NO SAS
- - - - BASELINE SAS
- · · · LAMS FLIGHT CONTROL SYSTEM

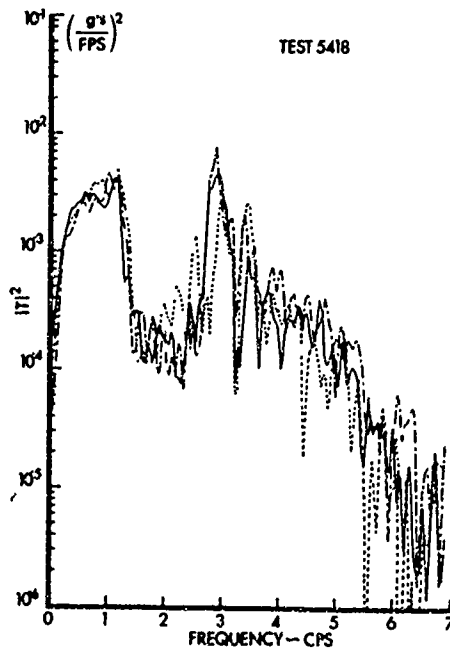
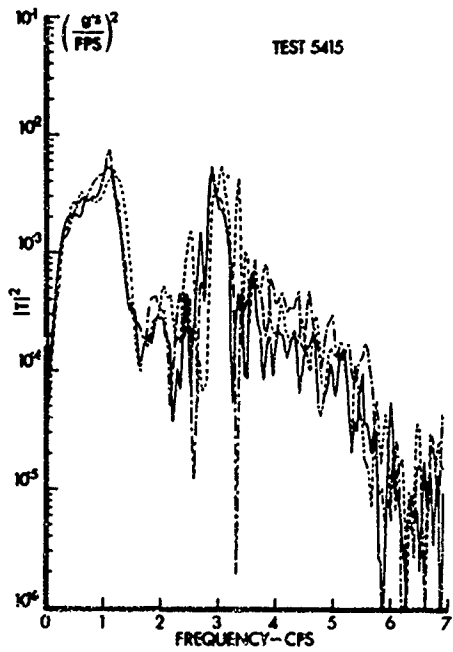
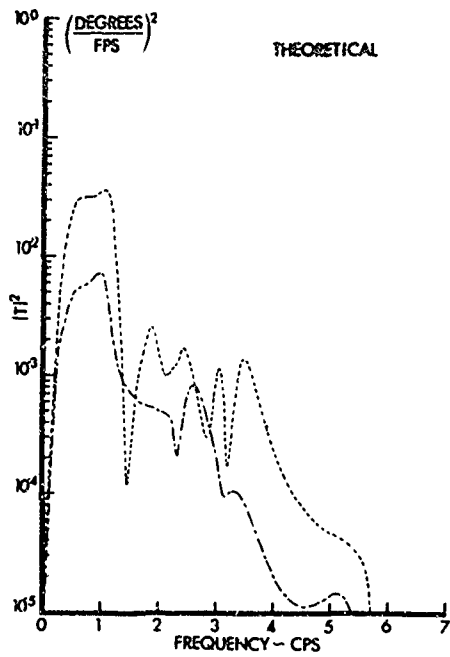


FIGURE 41



**FREQUENCY RESPONSE FUNCTION  
(AMPLITUDE - SQUARED)**

**Elevator Angular Displacement**

**DUE TO VERTICAL GUST**

- NO SAS
- - - - BASELINE SAS
- · - · LAMS FLIGHT CONTROL SYSTEM

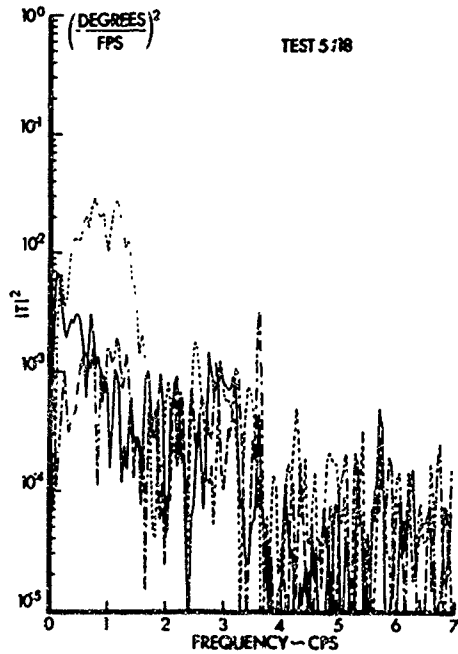
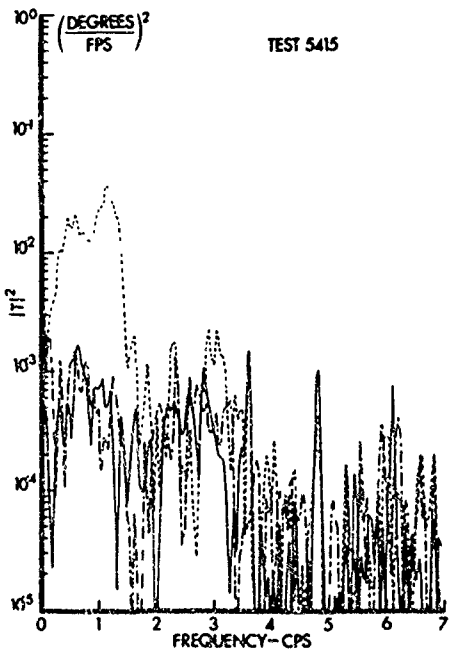
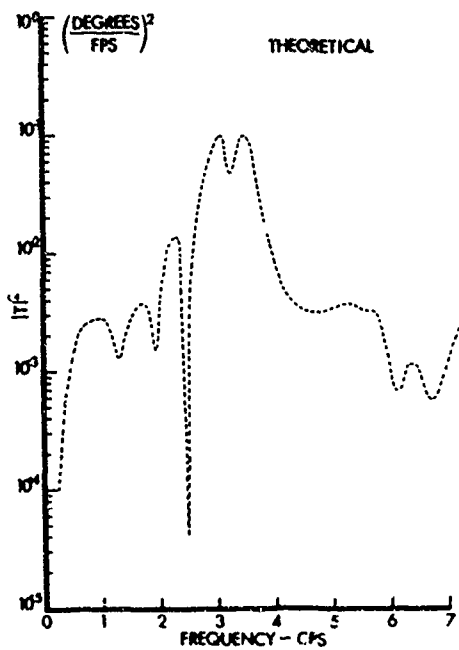


FIGURE 42



FREQUENCY RESPONSE FUNCTION  
(AMPLITUDE - SQUARED)

Aileron Angular Displacement

DUE TO VERTICAL GUST

- NO SAS
- - - - BASELINE SAS
- - - - LAMS FLIGHT CONTROL SYSTEM

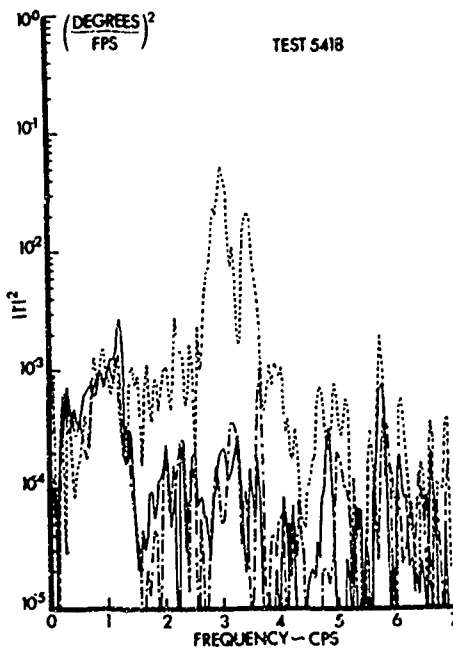
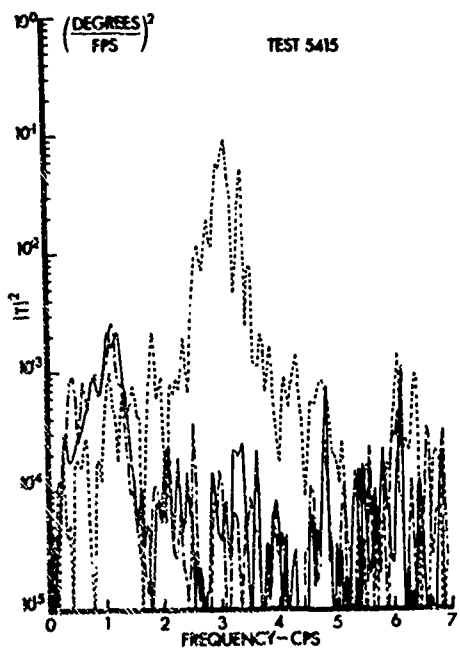
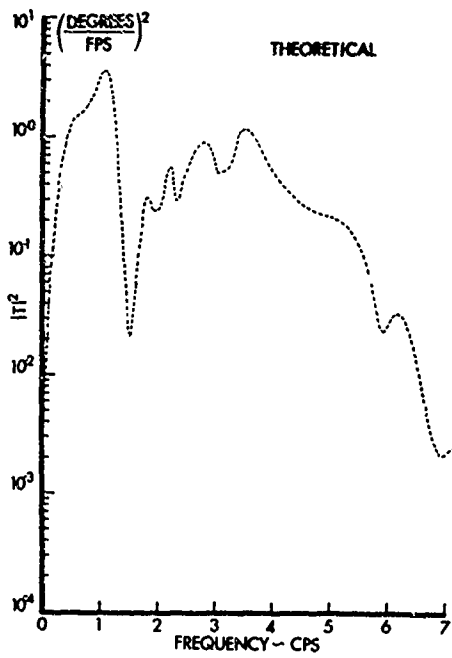


FIGURE 43



FREQUENCY RESPONSE FUNCTION  
(AMPLITUDE - SQUARED)

Spoiler Angular Displacement

DUE TO VERTICAL GUST

- NO SAS
- - - BASELINE SAS
- - - LAMS FLIGHT CONTROL SYSTEM

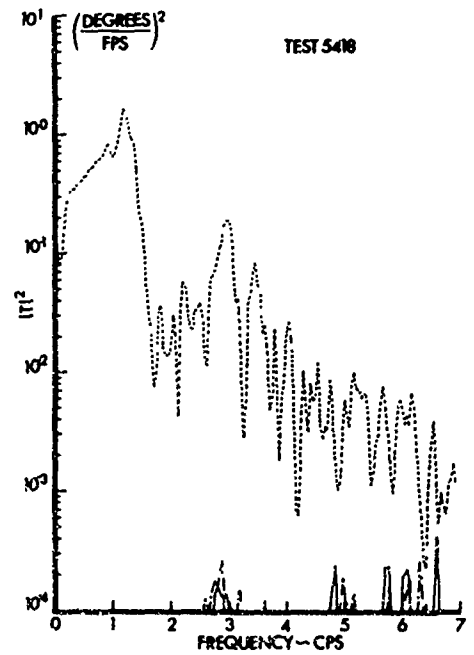
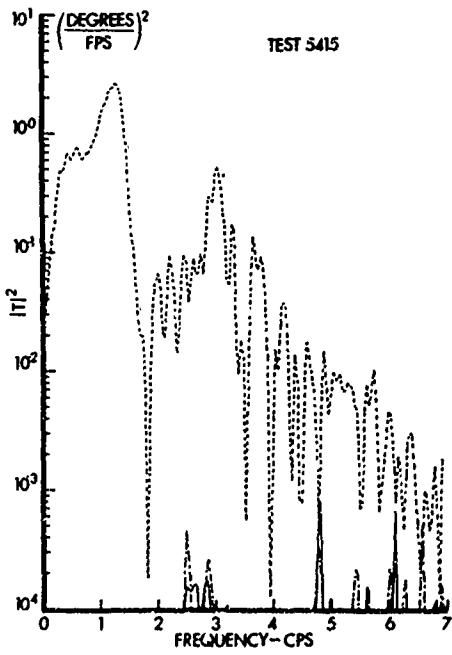
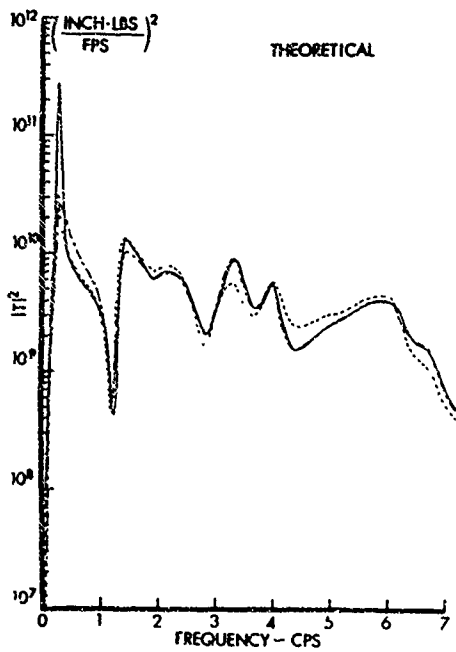


FIGURE 44



FREQUENCY RESPONSE FUNCTION  
 (AMPLITUDE - SQUARED)

Fin Station 135

Side Bending Moment

DUE TO LATERAL GUST

- NO SAS
- - - BASELINE SAS
- - - - LAMS FLIGHT CONTROL SYSTEM

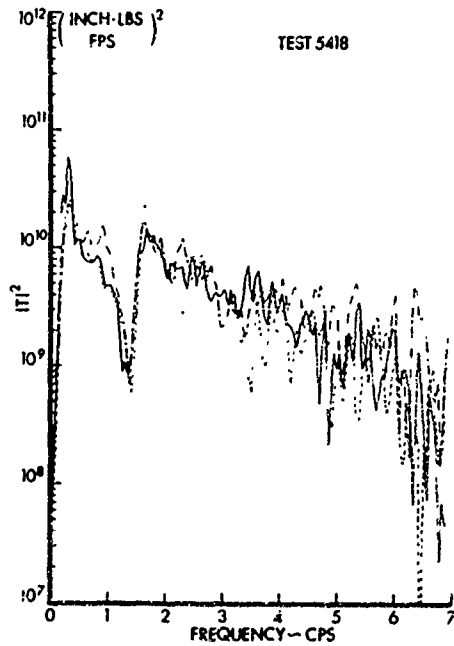
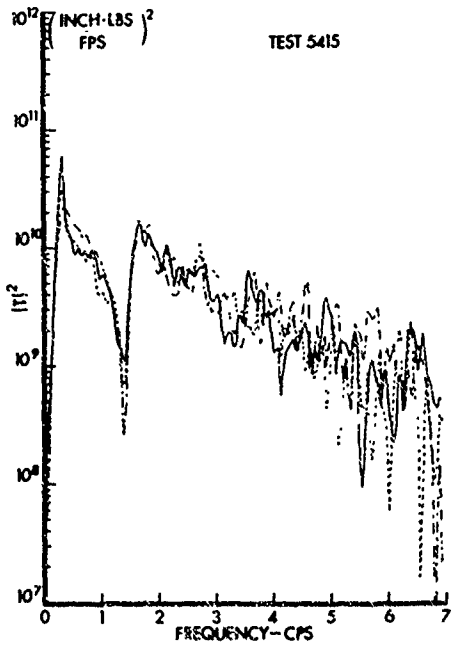
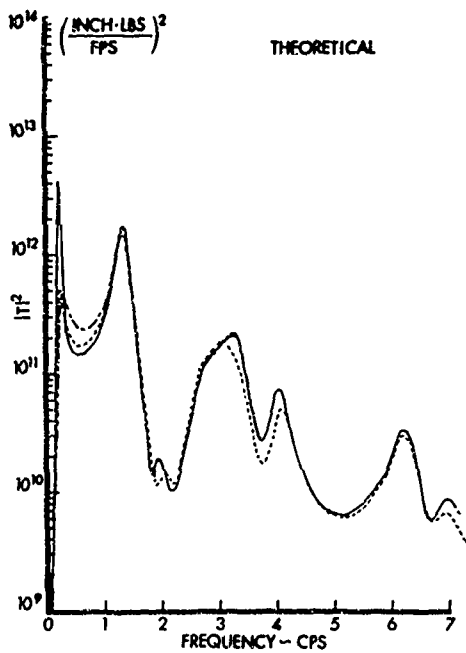


FIGURE 45



FREQUENCY RESPONSE FUNCTION  
(AMPLITUDE - SQUARED)

Body Station 1222  
Side Bending Moment

DUE TO LATERAL GUST

- NO SAS
- - - BASELINE SAS
- - - LAMS FLIGHT CONTROL SYSTEM

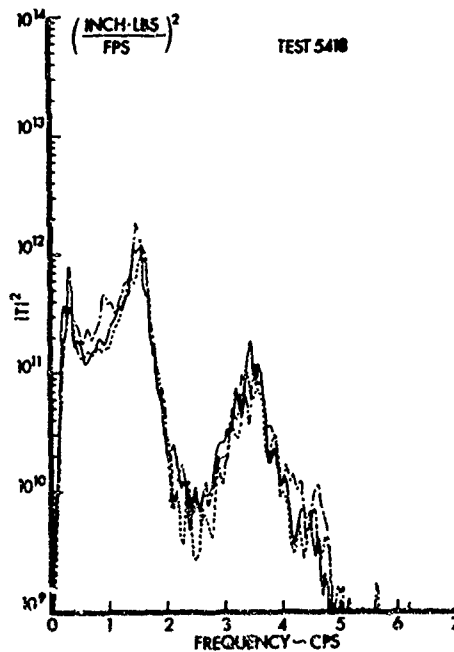
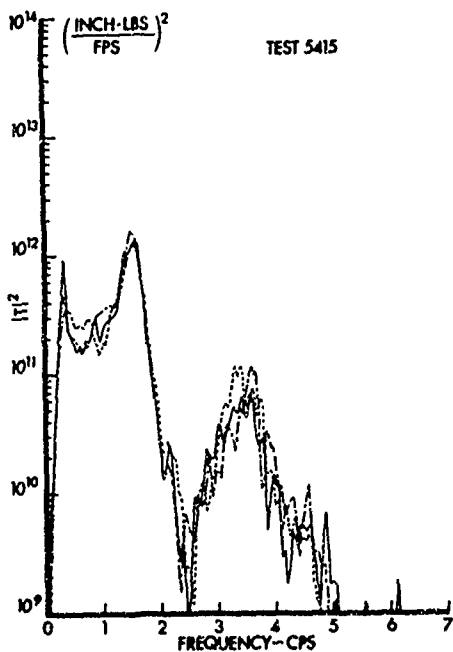


FIGURE 46

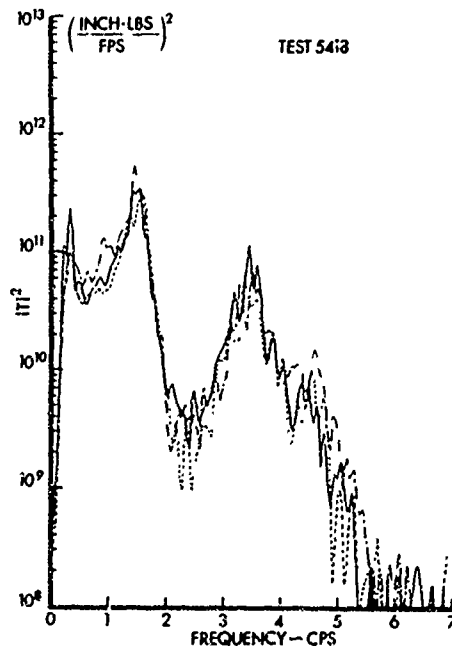
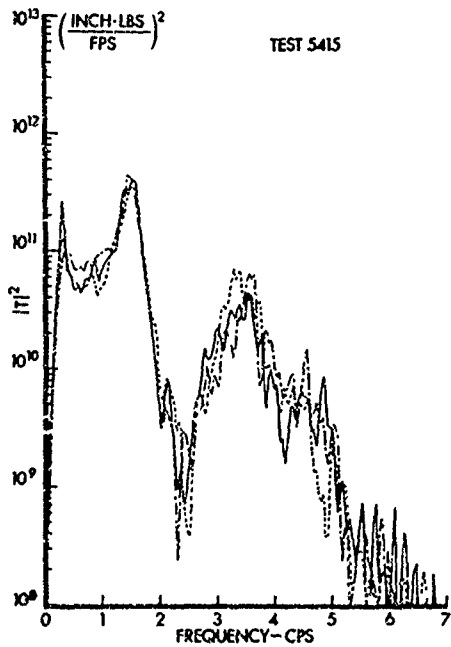
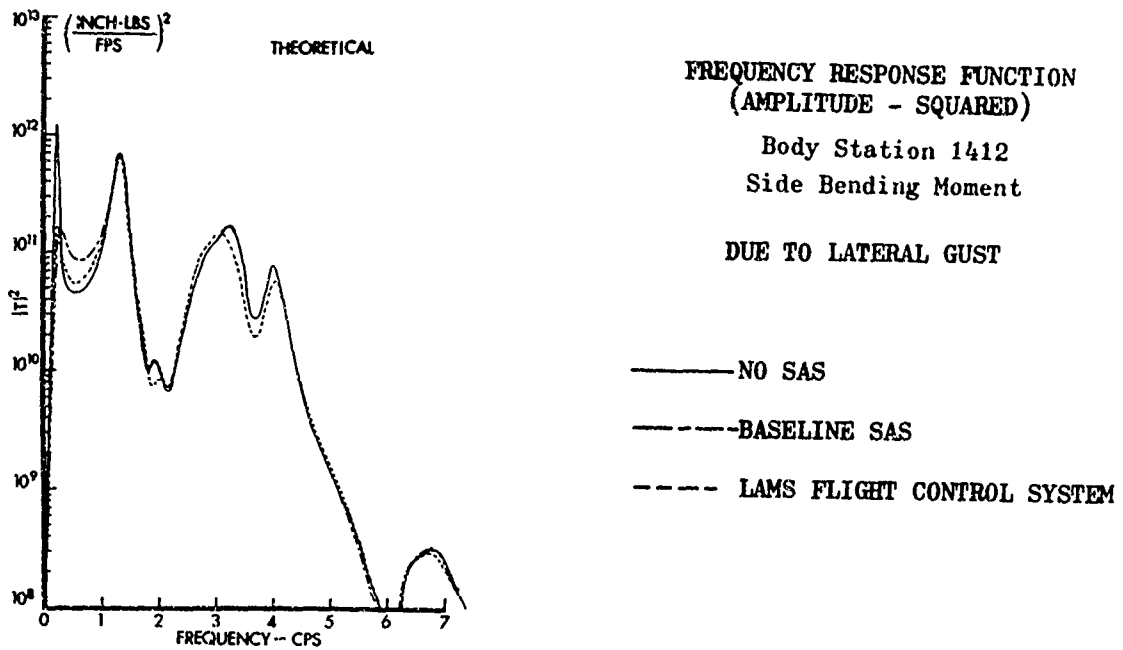
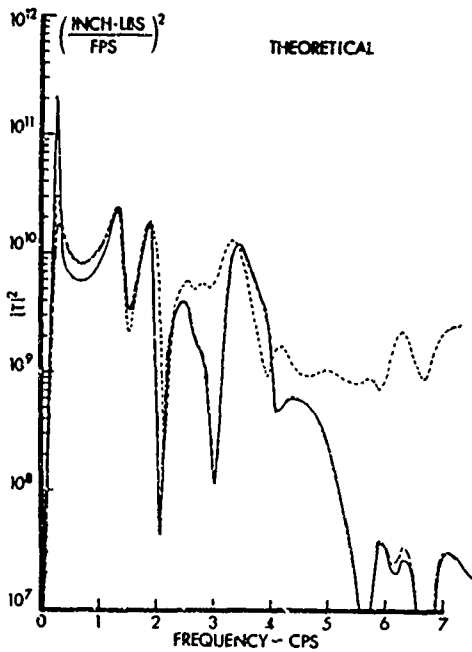


FIGURE 47



**FREQUENCY RESPONSE FUNCTION  
(AMPLITUDE - SQUARED)**

Wing Station 222

Vertical Bending Moment

DUE TO LATERAL GUST

- NO SAS
- - - BASELINE SAS
- · - LAMS FLIGHT CONTROL SYSTEM

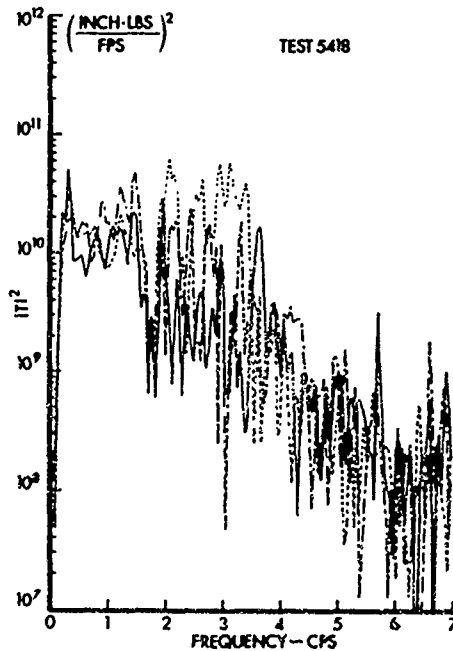
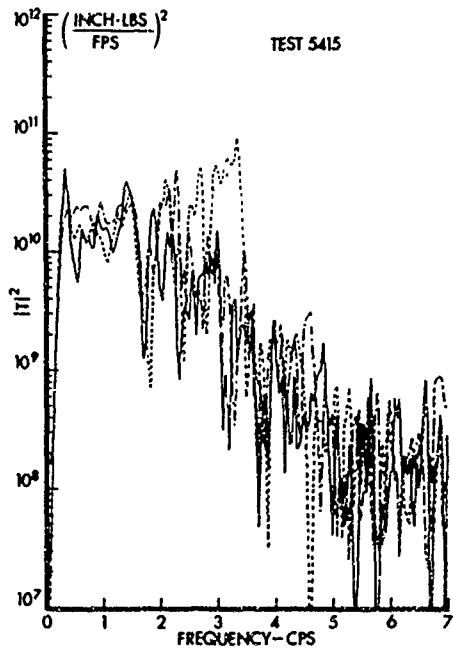
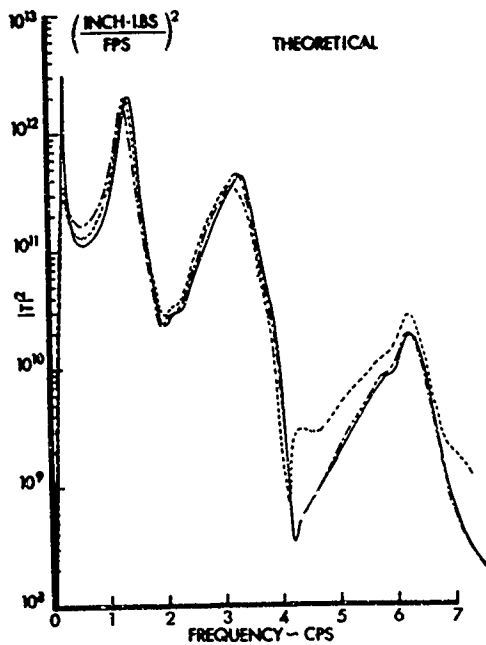


FIGURE 48



FREQUENCY RESPONSE FUNCTION  
(AMPLITUDE - SQUARED)

Wing Station 222

Chordwise Bending Moment

DUE TO LATERAL GUST

- NO SAS
- - - - BASELINE SAS
- · - · LAMS FLIGHT CONTROL SYSTEM

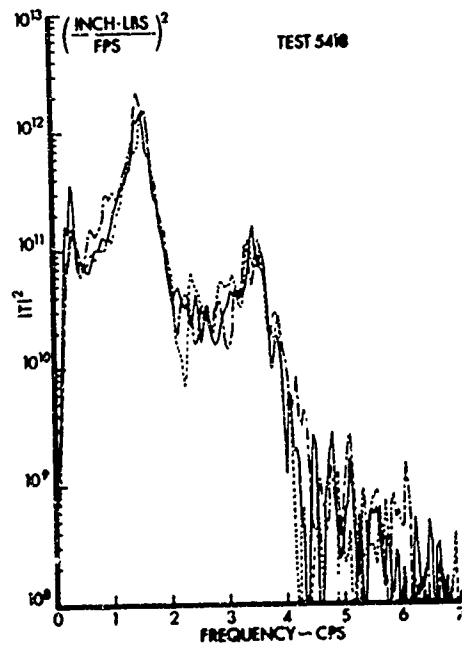
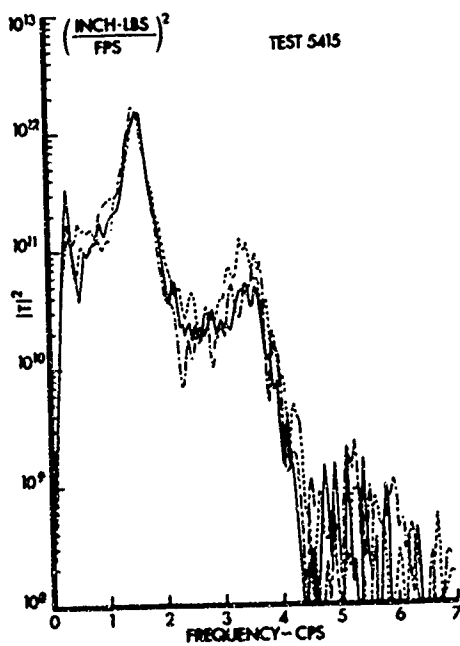
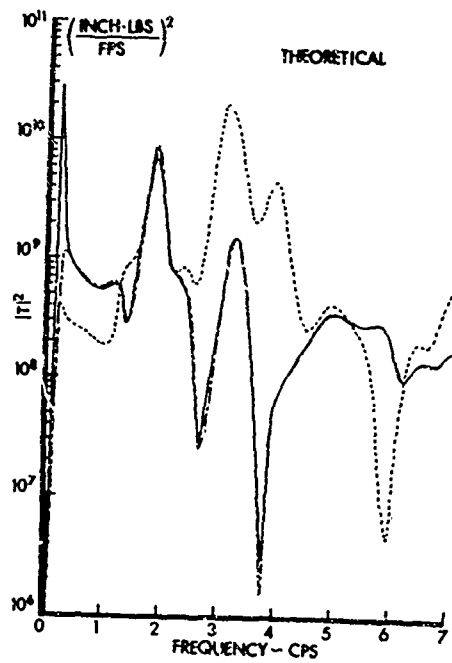


FIGURE 49



FREQUENCY RESPONSE FUNCTION  
(AMPLITUDE - SQUARED)

Wing Station 820  
Vertical Bending Moment

DUE TO LATERAL GUST

- NO SAS
- - - BASELINE SAS
- · · LAMS FLIGHT CONTROL SYSTEM

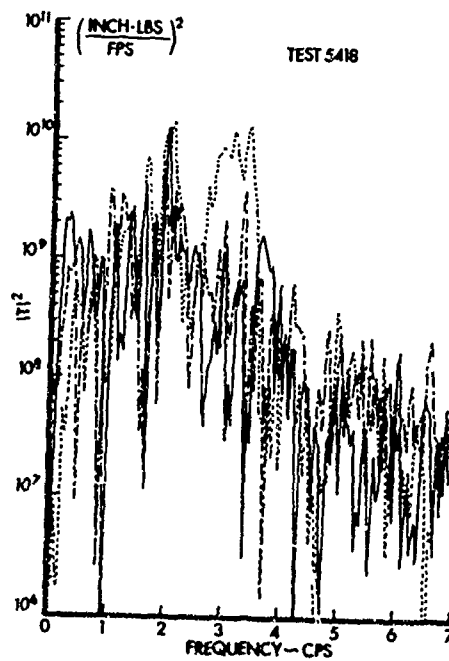
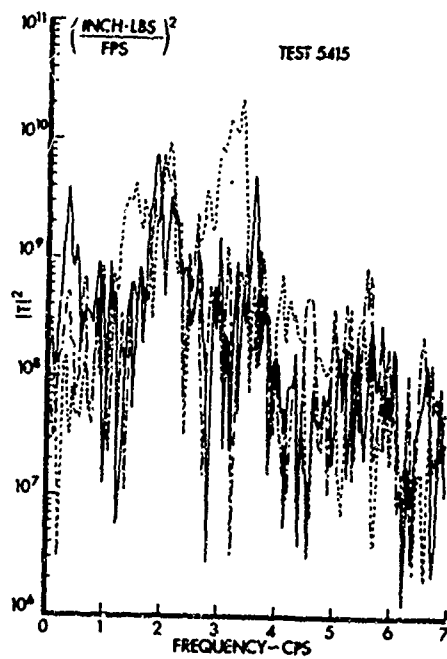
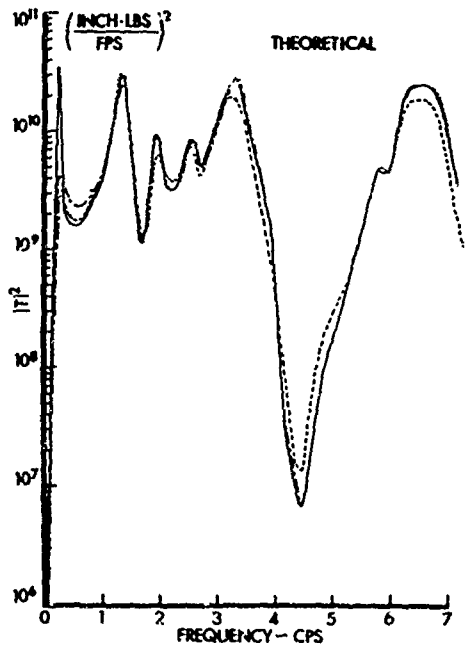


FIGURE 50



**FREQUENCY RESPONSE FUNCTION  
(AMPLITUDE - SQUARED)**

Wing Station 820  
Chordwise Bending Moment  
DUE TO LATERAL GUST

- NO SAS
- - - BASELINE SAS
- · · LAMS FLIGHT CONTROL SYSTEM

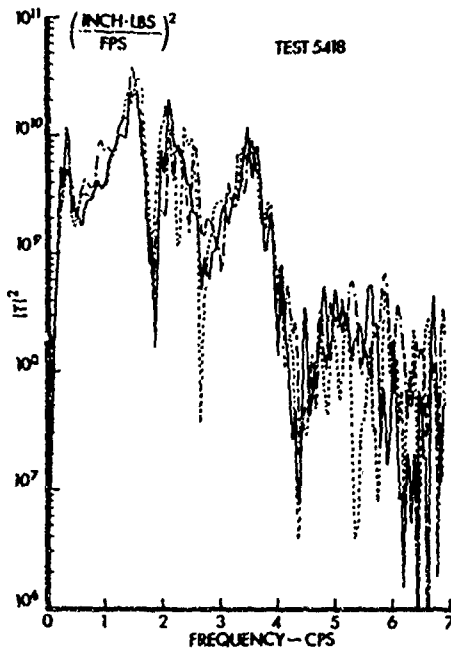
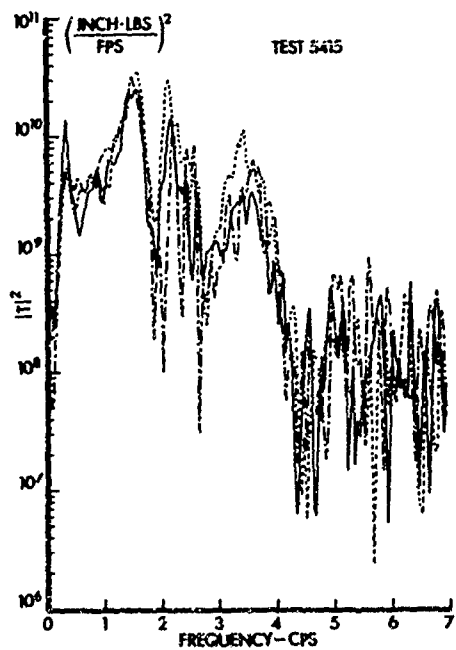
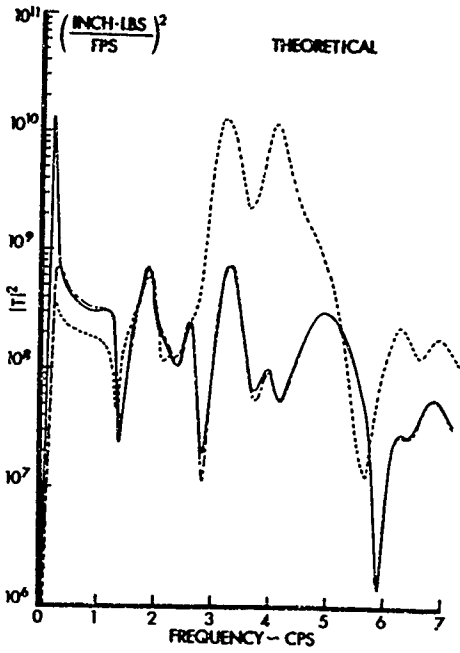


FIGURE 51



**FREQUENCY RESPONSE FUNCTION  
(AMPLITUDE - SQUARED)**

Wing Station 974

Vertical Bending Moment

DUE TO LATERAL GUST

- NO SAS
- - - BASELINE SAS
- · - LAMS FLIGHT CONTROL SYSTEM

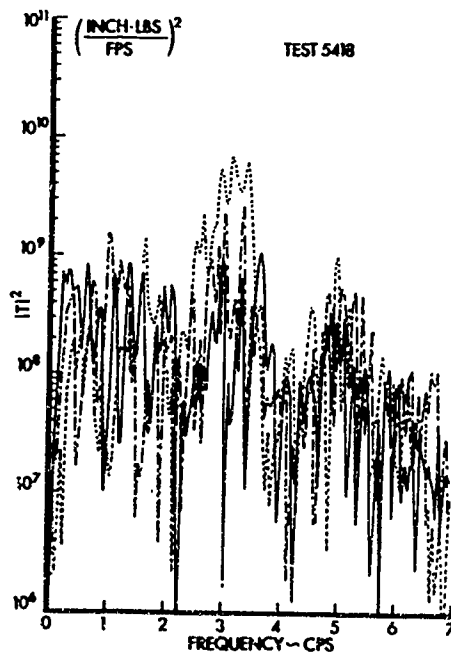
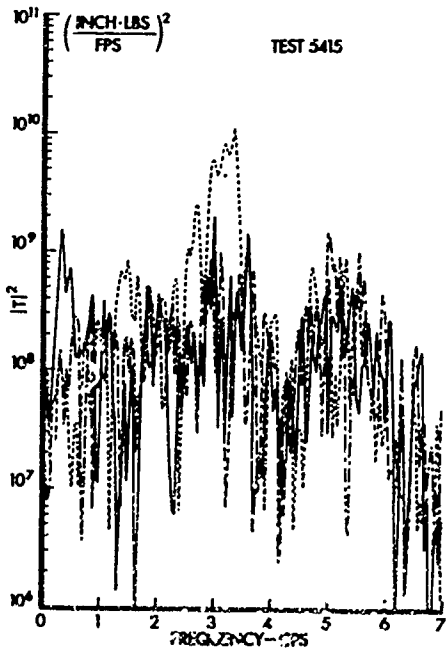
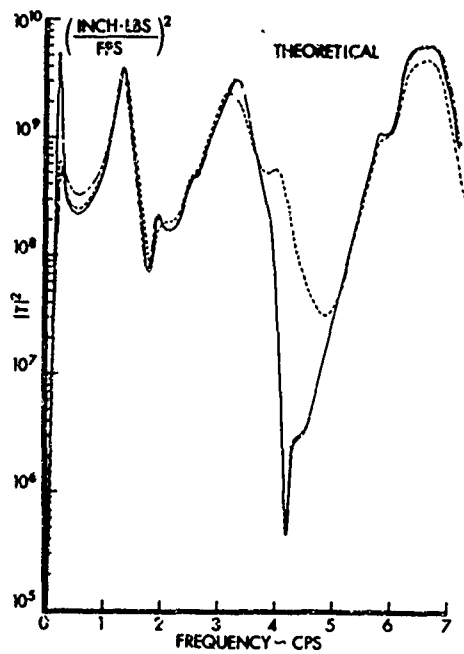


FIGURE 52



FREQUENCY RESPONSE FUNCTION  
(AMPLITUDE - SQUARED)

Wing Station 974  
Chordwise Bending Moment  
DUE TO LATERAL GUST

- NO SAS
- - - BASELINE SAS
- · - LAMS FLIGHT CONTROL SYSTEM

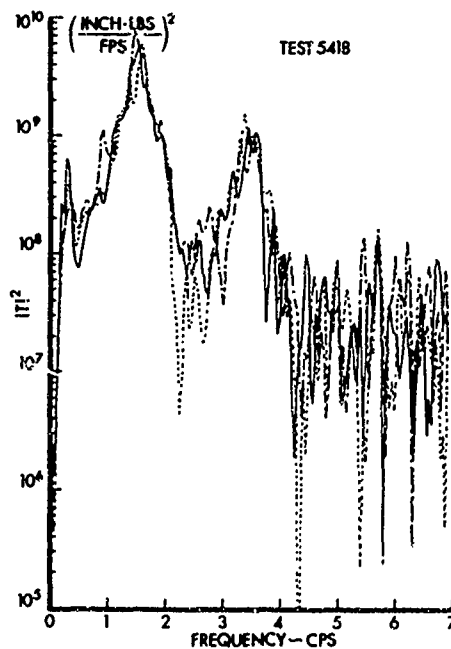
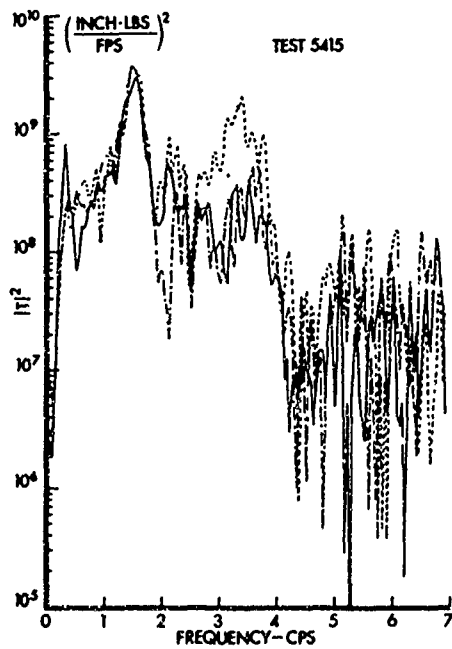
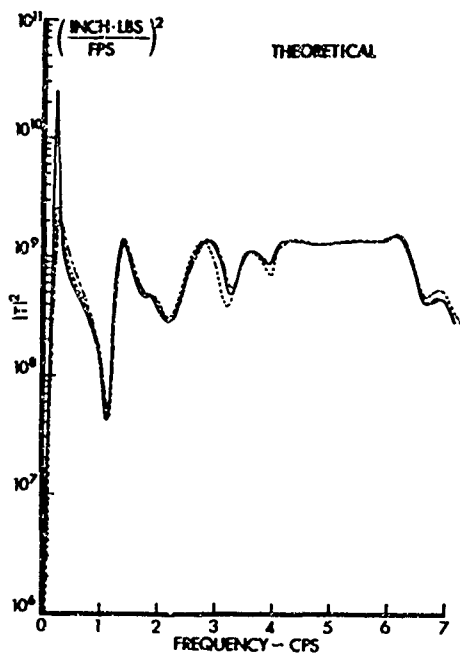


FIGURE 53



FREQUENCY RESPONSE FUNCTION  
(AMPLITUDE - SQUARED)

Stabilizer Buttock Line 56  
Vertical Bending Moment

DUE TO LATERAL GUST

- NO SAS
- - - - BASELINE SAS
- - - - LAMS FLIGHT CONTROL SYSTEM

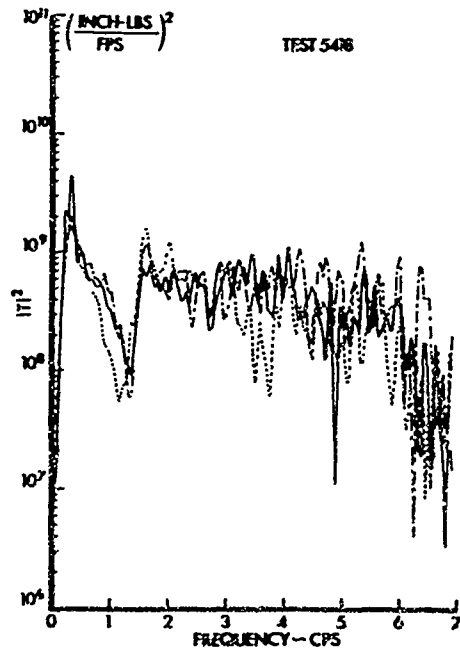
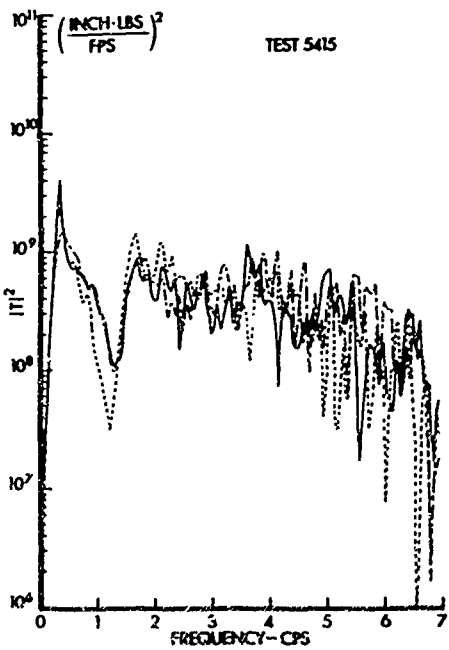
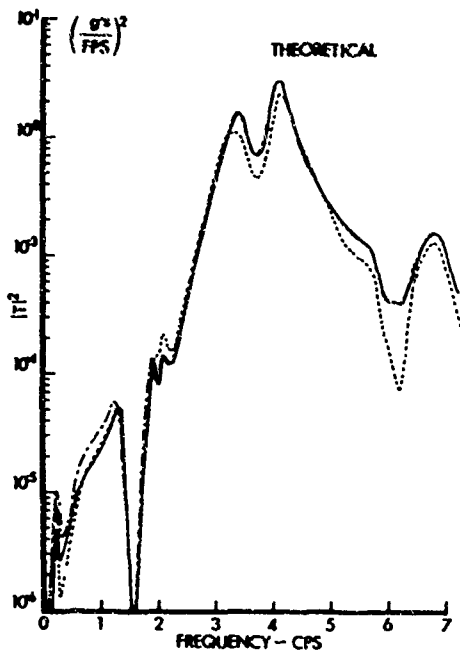


FIGURE 54



**FREQUENCY RESPONSE FUNCTION  
(AMPLITUDE - SQUARED)**

Body Station 172  
Side Acceleration

DUE TO LATERAL GUST

- NO SAS
- - - BASELINE SAS
- · · LAMS FLIGHT CONTROL SYSTEM

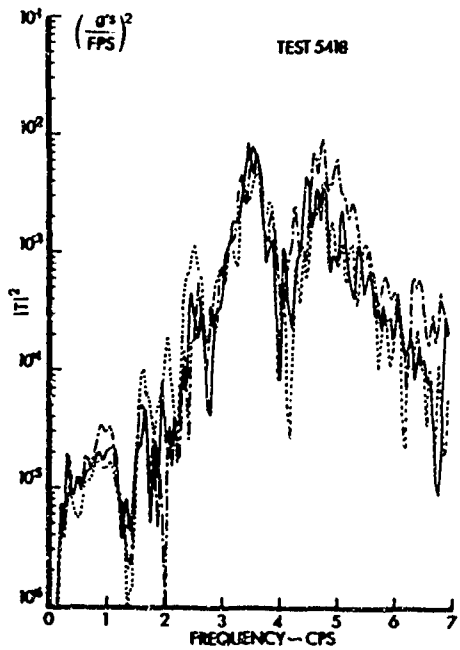
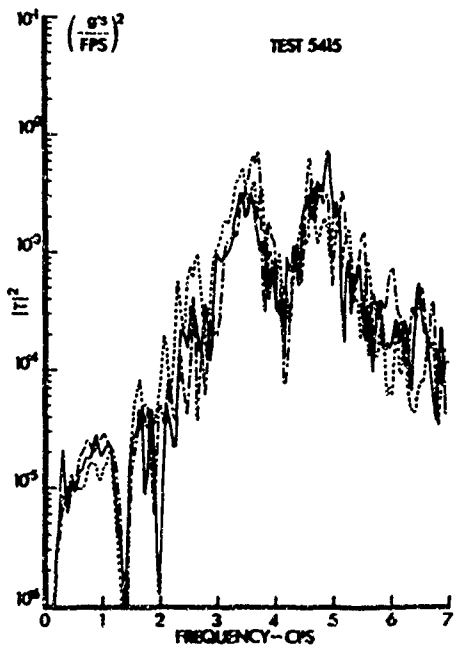
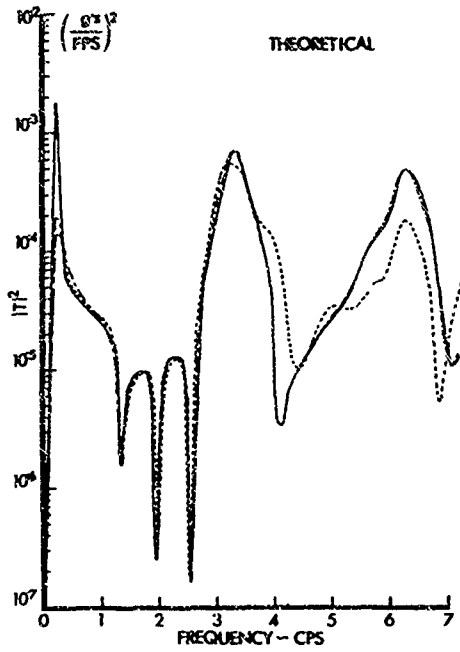


FIGURE 55



**FREQUENCY RESPONSE FUNCTION  
(AMPLITUDE - SQUARED)**

**Body Station 860  
Side Acceleration**

**DUE TO LATERAL GUST**

- NO SAS
- - - BASELINE SAS
- · - LAMS FLIGHT CONTROL SYSTEM

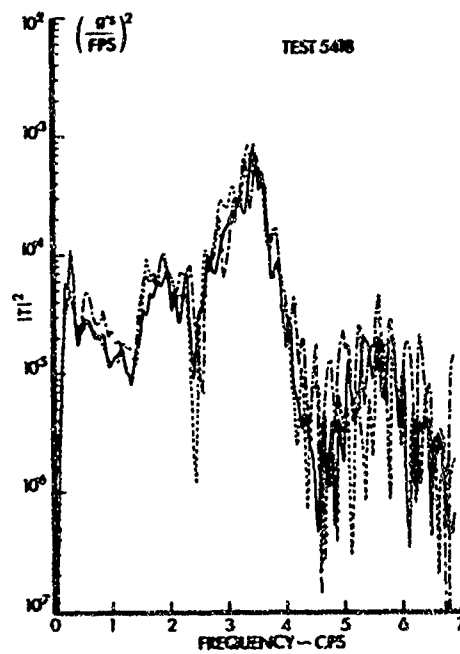
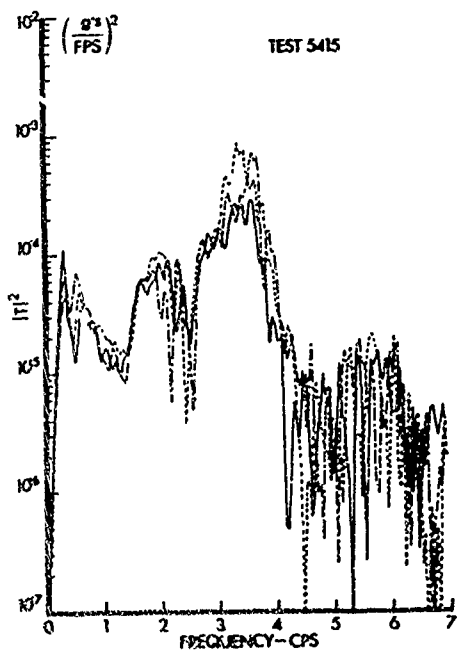
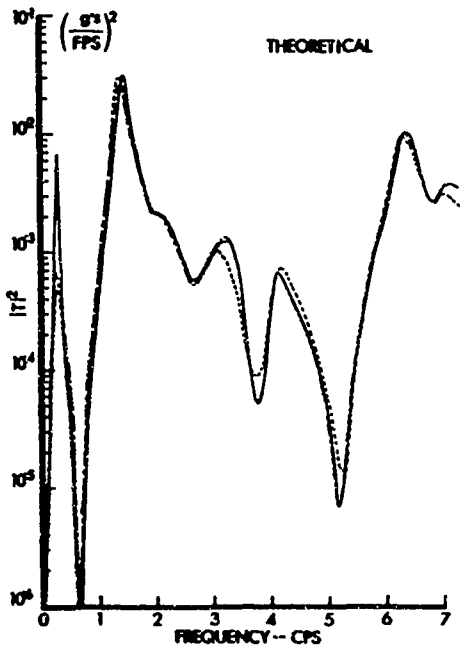


FIGURE 56



FREQUENCY RESPONSE FUNCTION  
(AMPLITUDE - SQUARED)

Body Station 1655  
Side Acceleration

DUE TO LATERAL GUST

- NO SAS
- - - - BASELINE SAS
- · - · LANS FLIGHT CONTROL SYSTEM

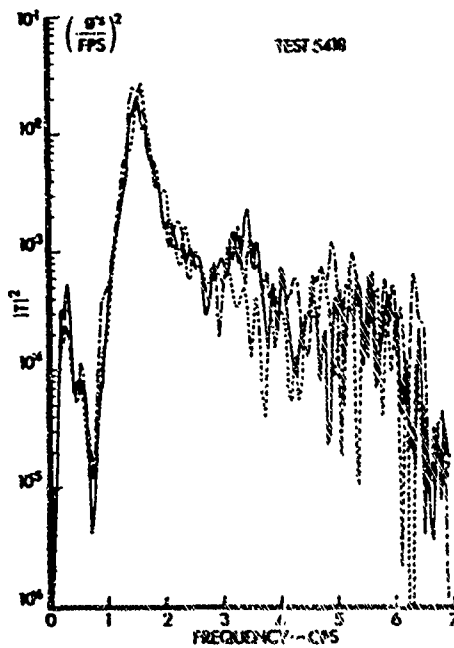
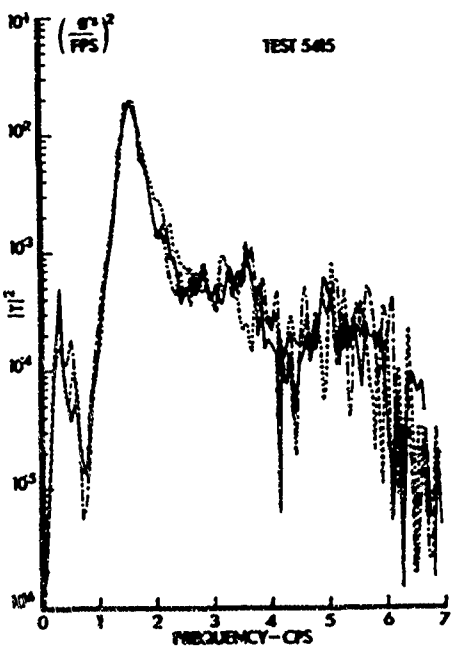
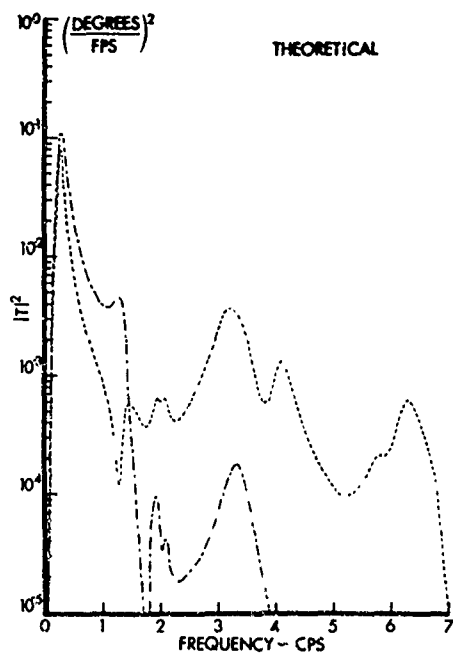


FIGURE 57



FREQUENCY RESPONSE FUNCTION  
(AMPLITUDE - SQUARED)

Rudder Angular Displacement

DUE TO LATERAL GUST

- NO SAS
- - - - BASELINE SAS
- · - · LAMS FLIGHT CONTROL SYSTEM

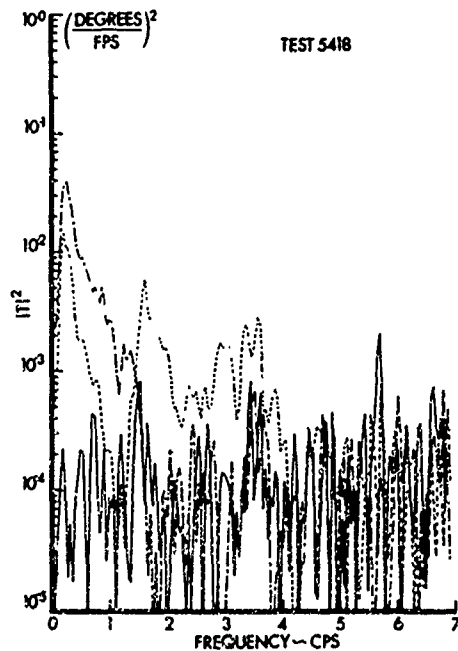
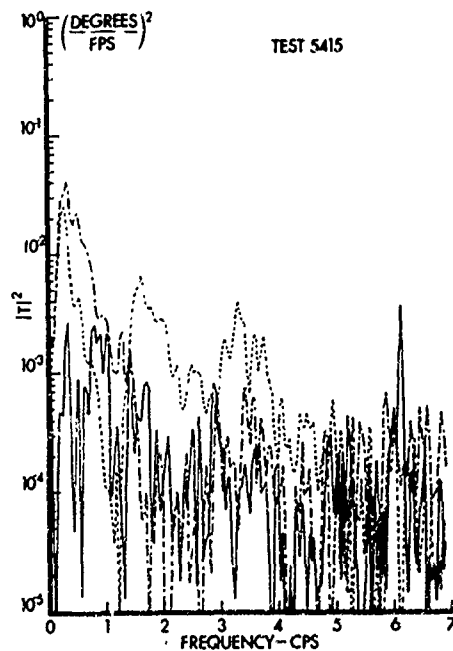
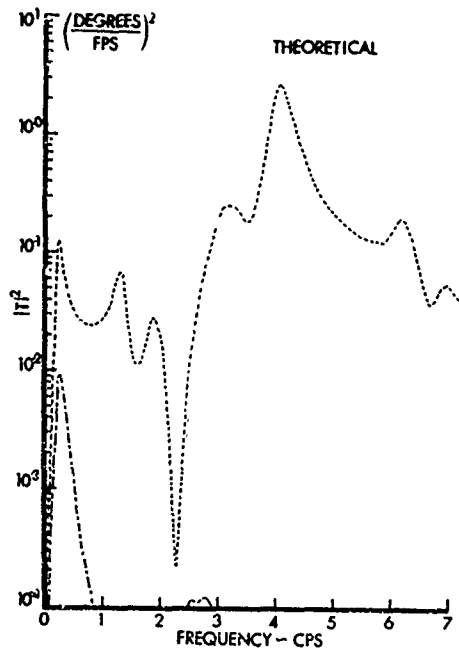


FIGURE 58



FREQUENCY RESPONSE FUNCTION  
(AMPLITUDE - SQUARED)

Aileron Angular Displacement

DUE TO LATERAL GUST

- NO SAS
- - - BASELINE SAS
- - - LAMS FLIGHT CONTROL SYSTEM

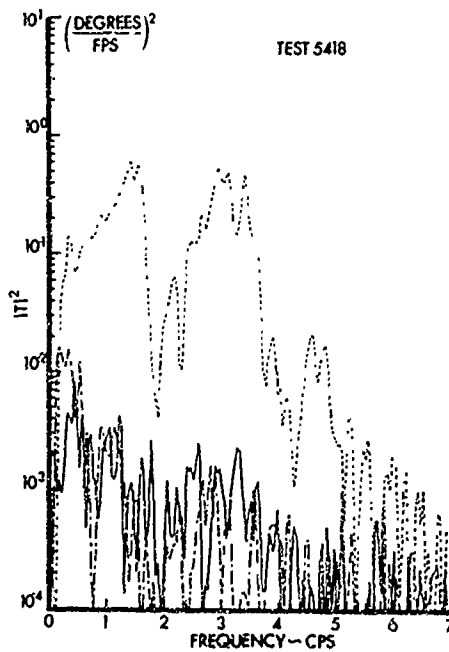
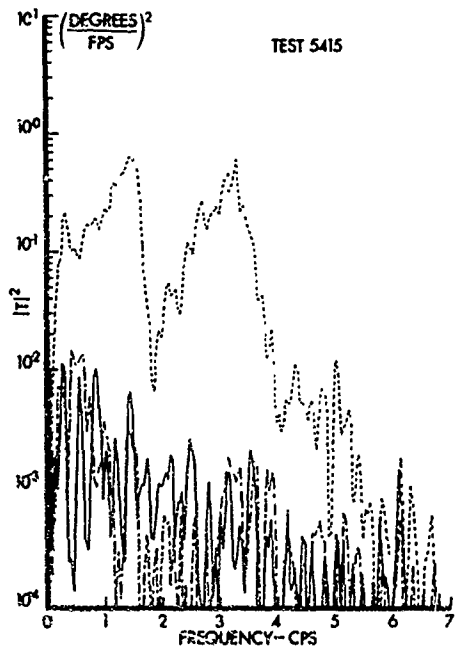


FIGURE 59

The general performance of the Baseline SAS and LAMS-FCS in lateral turbulence was similar to that predicted as verified by the following figures. The control surface activity required to obtain the structural performance is presented in Figures 58 and 59.

#### 4.3.7 Spectral Parameters "A" and "N<sub>0</sub>"

This section presents the gust response parameters "A" and "N<sub>0</sub>" (normalized rms response and characteristic frequency) from the two turbulence flight tests, 54-15 and 54-18. The data is arranged to show the relative performance of the three aircraft configurations: LAMS-FCS, Baseline SAS, and basic aircraft.

In Figures 60 through 65, test "A" values are plotted on graphs of theoretical "A" values for the wing and body. The figures show "A" values computed from the raw time-history data, coherent (with gust) values based on test frequency response functions, and the theoretical gust spectral density. The following observations can be made:

- "A"-values obtained by the two methods (raw data, cross-spectral analysis) generally bracket the predicted response
- Comparing tests 54-15 and 54-18, the cross-spectral "A"- values are in better agreement than are the raw data "A" values

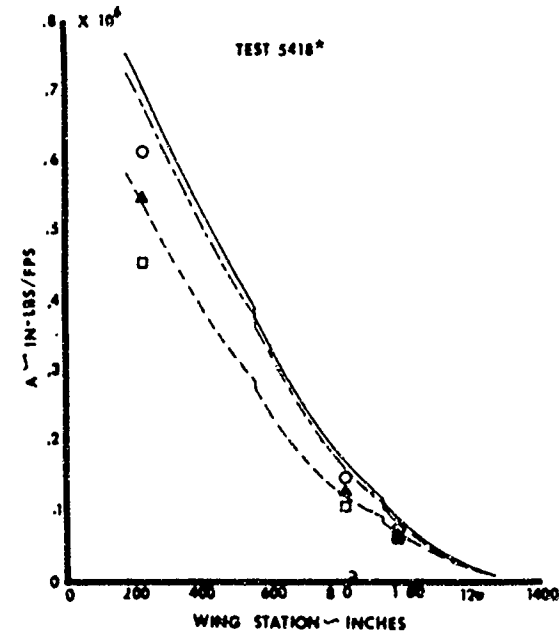
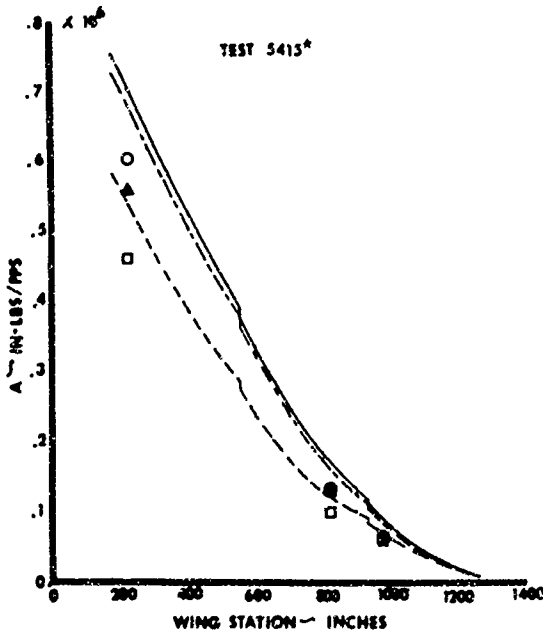
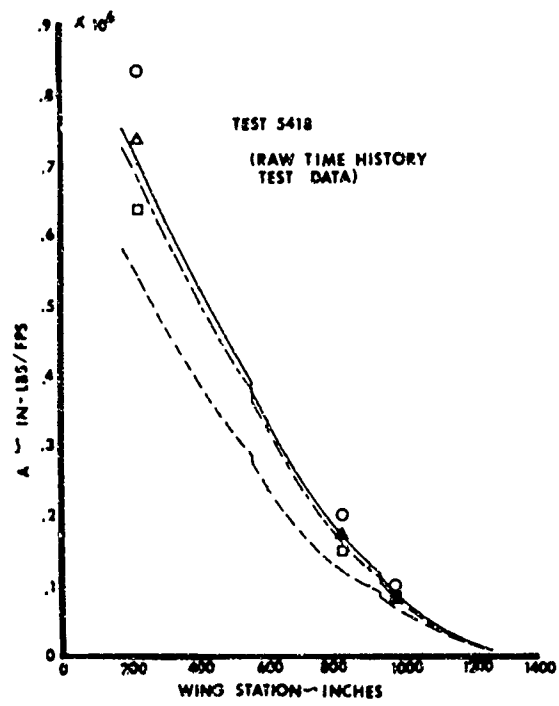
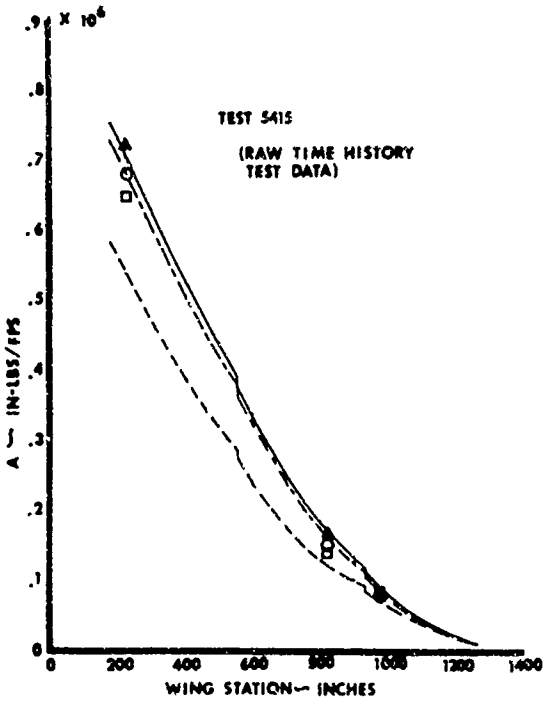
The cross spectral "A" values are lower than the predicted as a result of the following. The coherent data reduction method reduces the response due to pilot inputs (the primary reason for requiring coherent data reduction). In addition, there is a lack of coherency between gust components at the gust probe and various points on the aircraft for the higher frequencies further reducing the response functions. The summation of these two effects results in responses below that predicted. Also, for the basic aircraft configuration only about 60 percent of the Dutch roll contribution to rms load was lost because of the bandwidth of the data reduction process (see the discussion in Section 4.3.6).

Additional normalized rms response ("A") values are presented in Tables VII through XII. Tables XIII through XVI contain test and theoretical characteristic frequency ("N<sub>0</sub>") values for all of the flight test responses.

#### 4.3.8 Extrapolated Peak Load and Fatigue Damage Comparisons

The aircraft with Baseline SAS is representative of current designs. Comparisons in this section are between the performance of the LAMS-FCS and Baseline SAS. Computations are based on combined vertical and lateral gusts.

Estimates of structural performance of the LAMS B-52 with LAMS-FCS and Baseline SAS were made using flight test "A" and "N<sub>0</sub>" parameters. The "A" and "N<sub>0</sub>" values used were the average of those obtained from Tests 54-15 and 54-18 using cross-spectrum frequency response data with a theoretical gust spectrum.

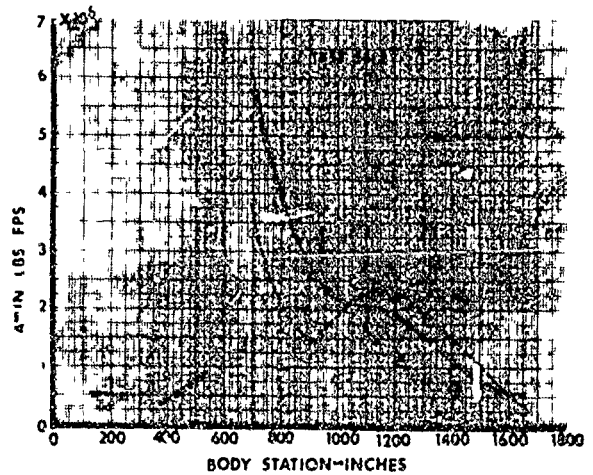
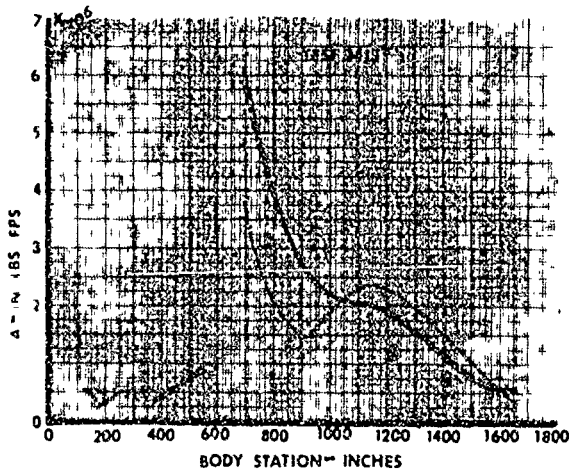
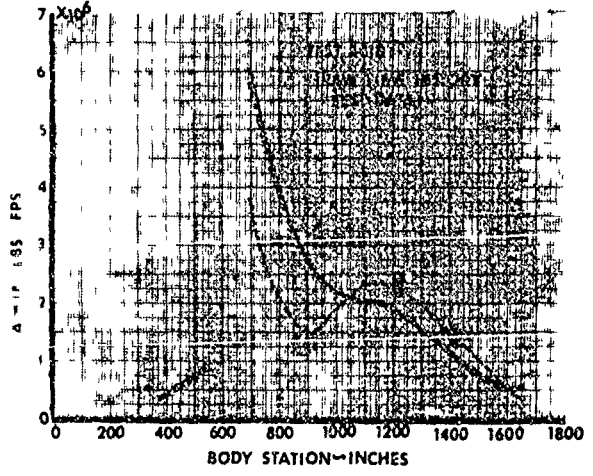
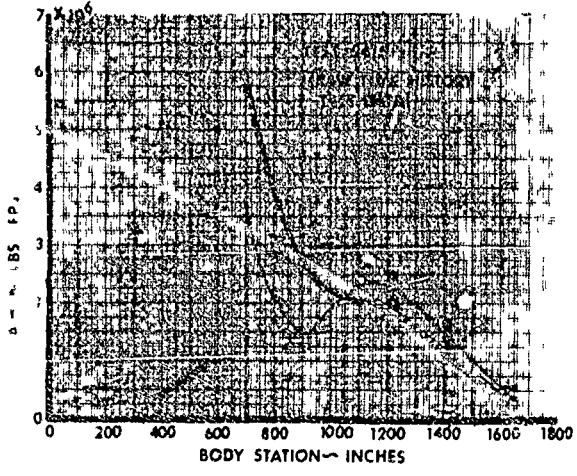


\* TEST DATA CALCULATED USING:

- CROSS SPECTRUM DERIVED  
FREQUENCY RESPONSE FUNCTION
- THEORETICAL GUST SPECTRUM

THEORETICAL		TEST
—————	NO SAS	○
- - - - -	BASELINE SAS	△
· · · · ·	LAMS FLIGHT CONTROL SYSTEM	□

WING RMS VERTICAL BENDING MOMENT DUE TO VERTICAL GUST  
FIGURE 60



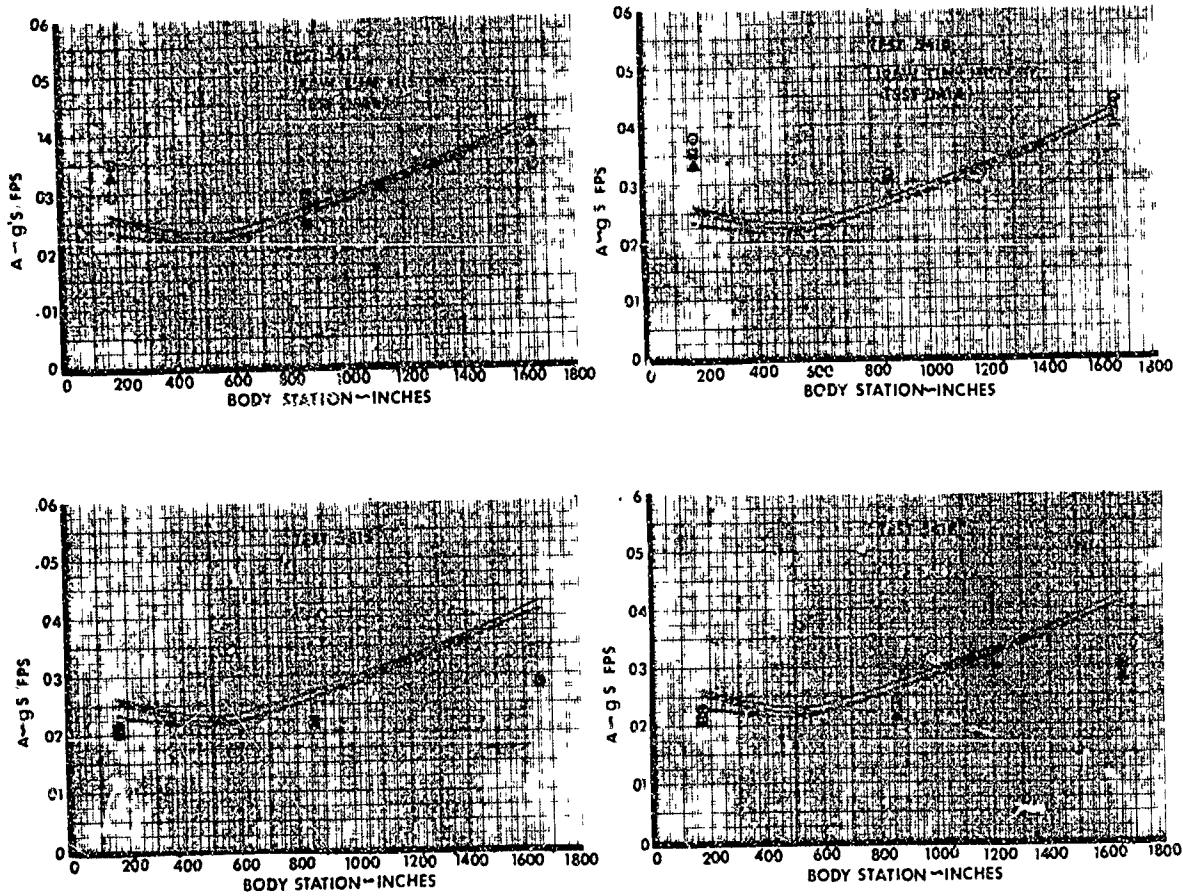
\*TEST DATA CALCULATED USING

- CROSS-SPECTRUM DERIVED FREQUENCY RESPONSE FUNCTION
- THEORETICAL GUST SPECTRUM

THEORETICAL		TEST
—————	NO SAS	○
- - - - -	BASELINE SAS	△
- · - · -	LAMS FLIGHT CONTROL SYSTEM	□

FUSELAGE RMS VERTICAL BENDING MOMENT DUE TO VERTICAL GUST

FIGURE 61

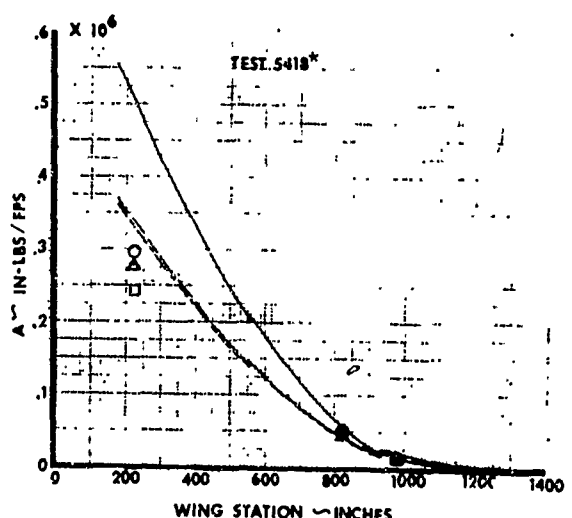
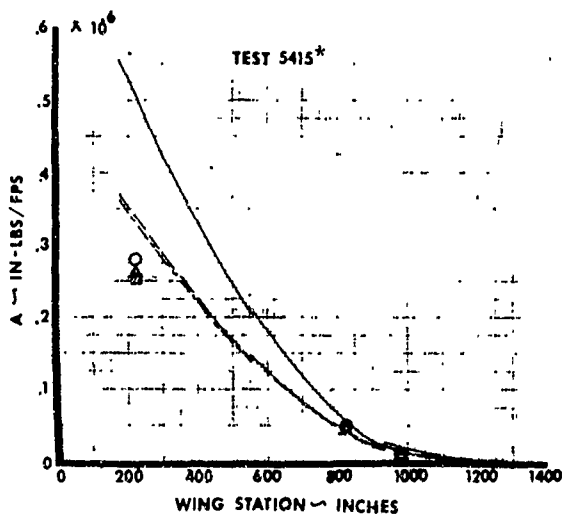
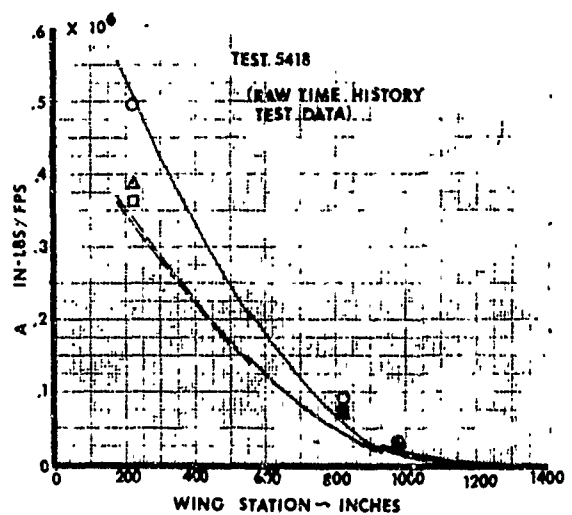
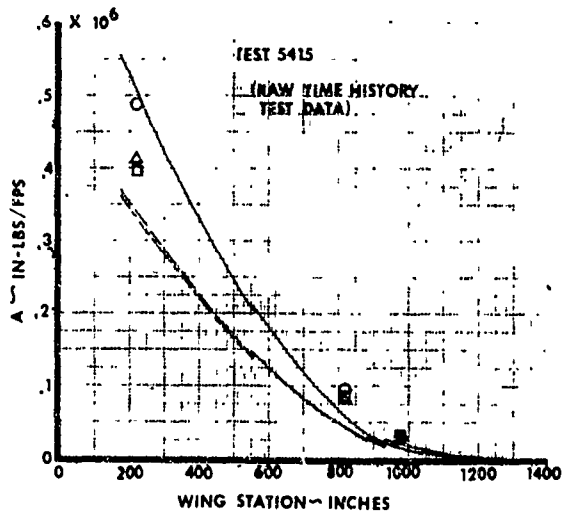


\*TEST DATA CALCULATED USING  
 • CROSS-SPECTRUM DERIVED  
 FREQUENCY RESPONSE FUNCTION  
 • THEORETICAL GUST SPECTRUM

THEORETICAL		TEST
—————	NO SAS	○
-----	BASELINE SAS	△
- - - - -	LAMS FLIGHT CONTROL SYSTEM	□

FUSELAGE RMS VERTICAL ACCELERATION DUE TO VERTICAL GUST

FIGURE 62



\*TEST DATA CALCULATED USING:

- CROSS SPECTRUM DERIVED  
FREQUENCY RESPONSE FUNCTION
- THEORETICAL GUST SPECTRUM

THEORETICAL

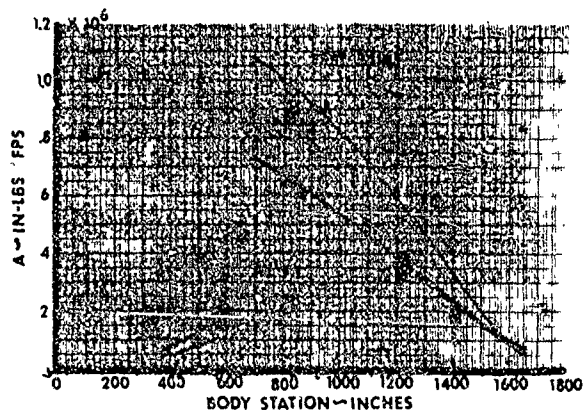
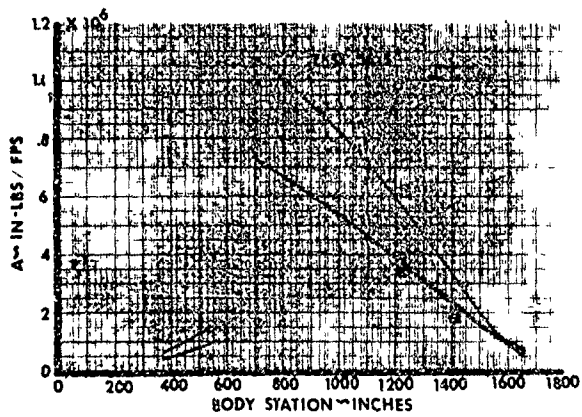
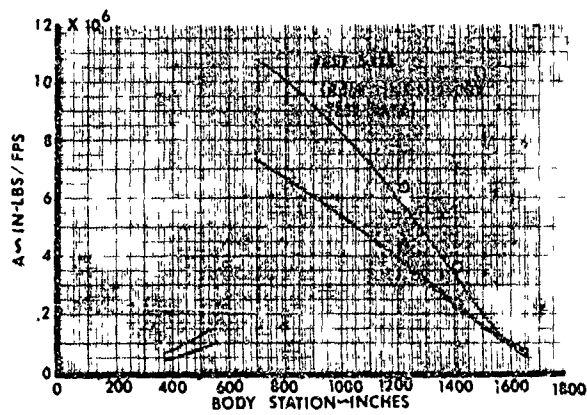
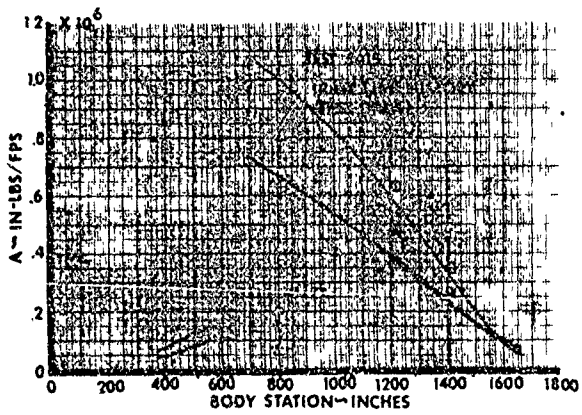
- NO SAS
- - - BASELINE SAS
- - - LAMS FLIGHT CONTROL SYSTEM

TEST

- 
- △
- 

WING RMS CHORDWISE BENDING MOMENT DUE TO LATERAL GUST

FIGURE 63

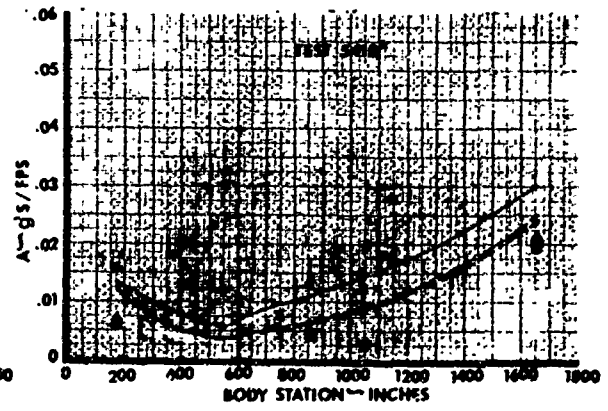
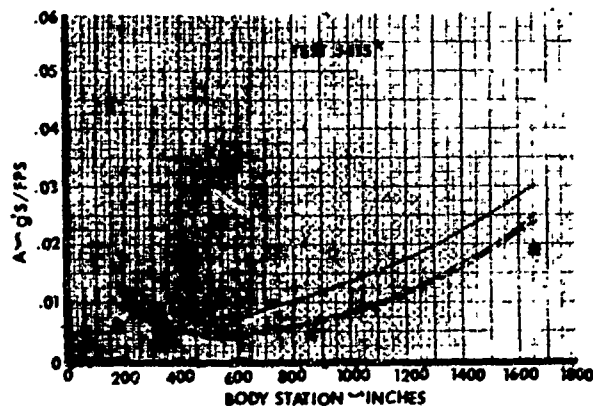
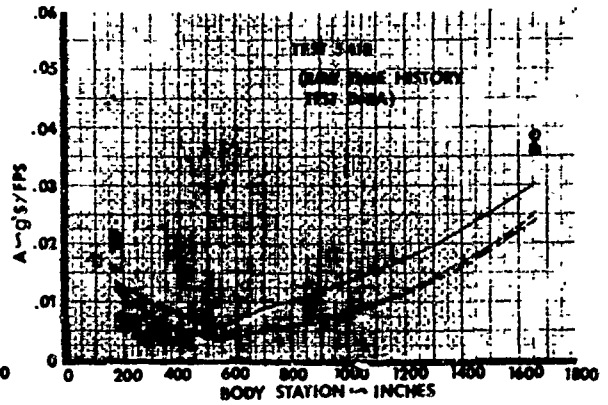
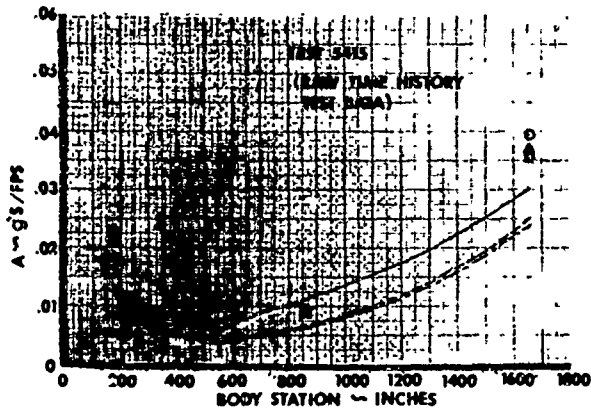


\*TEST DATA CALCULATED USING  
 • CROSS-SPECTRUM DERIVED  
 FREQUENCY RESPONSE FUNCTION  
 • THEORETICAL GUST SPECTRUM

THEORETICAL		TEST
————	NO SAS	○
-----	BASELINE SAS	△
-----	LAMS FLIGHT CONTROL SYSTEM	□

FUSELAGE RMS SIDE BENDING MOMENT DUE TO LATERAL GUST

FIGURE 64



\*TEST DATA CALCULATED USING:

- CROSS-SPECTRUM DERIVED FREQUENCY RESPONSE FUNCTION
- THEORETICAL GUST SPECTRUM

THEORETICAL

- NO SAS
- - - - - BASELINE SAS
- - - - - 2 AMS FLIGHT CONTROL SYSTEM

TEST

- 
- △
- 

FUSELAGE RMS SIDE ACCELERATION DUE TO LATERAL GUST

FIGURE 65

TABLE VII  
VERTICAL GUST A'S

RAW-TIME HISTORY DATA

RESPONSE	UNITS	TEST 5415			TEST 5418		
		BASIC	BASELINE	LAMS	BASIC	BASELINE	LAMS
Vert. Accel. B.S. 172	$\frac{g's}{FPS}$	.0296	.0325	.0349	.0380	.0332	.0354
Vert. Accel. B.S. 860	$\frac{g's}{FPS}$	.0243	.0275	.0294	.0312	.0277	.0306
Vert. Accel. B.S. 1655	$\frac{g's}{FPS}$	.0339	.0377	.0417	.0439	.0395	.0433
Aileron Displacement	$\frac{DEG.}{FPS}$	.0328	.0426	.0989	.0436	.0404	.105
Spoiler Displacement	$\frac{DEG.}{FPS}$	.0147	.0154	.833	.0157	.0141	.704
Elevator Displacement	$\frac{DEG.}{FPS}$	.0706	.112	.140	.156	.0863	.147
VBM W.S. 222	$\frac{10^6 IN-LB}{FPS}$	.679	.717	.645	.833	.735	.636
CBM W.S. 222	$\frac{10^6 IN-LB}{FPS}$	.140	.155	.201	.182	.169	.195
VBM W.S. 820	$\frac{10^6 IN-LB}{FPS}$	.149	.164	.138	.198	.170	.147
CBM W.S. 820	$\frac{10^6 IN-LB}{FPS}$	.0471	.0516	.0686	.0586	.0538	.0604
VBM W.S. 974	$\frac{10^6 IN-LB}{FPS}$	.0746	.0824	.0806	.0993	.0836	.0844
CBM W.S. 974	$\frac{10^6 IN-LB}{FPS}$	.0168	.0174	.0311	.0254	.0167	.0197
VBM B.S. 1222	$\frac{10^6 IN-LB}{FPS}$	.196	.207	.247	.245	.219	.232
VBM B.S. 1412	$\frac{10^6 IN-LB}{FPS}$	.127	.135	.164	.152	.132	.145
VBM S.B.L. 56	$\frac{10^6 IN-LB}{FPS}$	.0302	.0325	.0433	.0396	.0362	.0442

TABLE VIII  
VERTICAL GUST A'S

A's calculated using:

- Cross-spectrum derived frequency response functions
- Theoretical gust spectrum

RESPONSE	UNITS	TEST 5415			TEST 5418		
		BASIC	BASELINE	IAMS	BASIC	BASELINE	IAMS
Vert. Accel. B.S. 172	$\frac{g's}{FPS}$	.0212	.0207	.0201	.0227	.0213	.0211
Vert. Accel. B.S. 860	$\frac{g's}{FPS}$	.0221	.0219	.0215	.0242	.0216	.0230
Vert. Accel. B.S. 1655	$\frac{g's}{FPS}$	.0286	.0288	.0284	.0308	.0280	.0299
Aileron Displacement	$\frac{DEG.}{FPS}$	.0125	.0151	.0198	.0156	.0148	.0200
Spoiler Displacement	$\frac{DEG.}{FPS}$	.0017	.0019	.509	.0017	.0018	.453
Elevator Displacement	$\frac{DEG.}{FPS}$	.0171	.0281	.0725	.0516	.0199	.0684
VEM W.S. 222	$\frac{10^6 IN-LB}{FPS}$	.602	.556	.459	.611	.545	.452
CEM W.S. 222	$\frac{10^6 IN-LB}{FPS}$	.0683	.0655	.0813	.0552	.0688	.0735
VEM W.S. 820	$\frac{10^6 IN-LB}{FPS}$	.132	.127	.0982	.147	.128	.105
CEM W.S. 820	$\frac{10^6 IN-LB}{FPS}$	.0222	.0227	.0327	.0190	.0220	.0265
VEM W.S. 974	$\frac{10^6 IN-LB}{FPS}$	.0654	.0629	.0576	.0737	.0636	.0608
CEM W.S. 974	$\frac{10^6 IN-LB}{FPS}$	.0066	.0062	.0142	.0057	.0060	.0081
VEM B.S. 1222	$\frac{10^6 IN-LB}{FPS}$	.118	.115	.125	.111	.115	.116
VEM B.S. 1412	$\frac{10^6 IN-LB}{FPS}$	.0712	.0695	.0778	.0626	.0651	.0669
VEM S.B.L. 56	$\frac{10^6 IN-LB}{FPS}$	.0280	.0269	.0322	.0306	.0276	.0335

TABLE IX  
VERTICAL GUST A'S

THEORETICAL

LAMS FLIGHT CONDITION 1  
 (350000 LBS, 350 KTS EAS, 4000 FT)

<u>RESPONSE</u>	<u>UNITS</u>	<u>BASIC</u>	<u>BASELINE</u>	<u>LAMS</u>
Vert. Accel. B.S. 172	$\frac{g's}{FPS}$	.0259	.0252	.0236
Vert. Accel. B.S. 860	$\frac{g's}{FPS}$	.0273	.0260	.0263
Vert. Accel. B.S. 1655	$\frac{g's}{FPS}$	.0426	.0411	.0411
Aileron Displacement	$\frac{DEG.}{FPS}$	.000	.000	.039
Spoiler Displacement	$\frac{DEG.}{FPS}$	.000	.000	.616
Elevator Displacement	$\frac{DEG.}{FPS}$	.000	.033	.072
VEM W.S. 222	$\frac{10^6 \text{ IN-LB}}{FPS}$	.702	.677	.537
CBM W.S. 222	$\frac{10^6 \text{ IN-LB}}{FPS}$	.212	.215	.216
VEM W.S. 820	$\frac{10^6 \text{ IN-LB}}{FPS}$	.170	.161	.119
CBM W.S. 820	$\frac{10^6 \text{ IN-LB}}{FPS}$	.0481	.0482	.0427
VEM W.S. 974	$\frac{10^6 \text{ IN-LB}}{FPS}$	.0895	.0840	.0684
CBM W.S. 974	$\frac{10^6 \text{ IN-LB}}{FPS}$	.0167	.0166	.0154
VEM B.S. 1222	$\frac{10^6 \text{ IN-LB}}{FPS}$	.182	.186	.226
VEM B.S. 1412	$\frac{10^6 \text{ IN-LB}}{FPS}$	.111	.116	.147
VEM S.B.L. 56	$\frac{10^6 \text{ IN-LB}}{FPS}$	.0427	.0411	.0463

TABLE X  
LATERAL GUST A'S

RAW-TIME HISTORY DATA

RESPONSE	UNITS	TEST 5415			TEST 5418		
		BASIC	BASELINE	LAMS	BASIC	BASELINE	LAMS
Side Accel. B.S. 172	$\frac{g's}{FPS}$	.0213	.0224	.0224	.0212	.0205	.0199
Side Accel. B.S. 860	$\frac{g's}{FPS}$	.0092	.0088	.0090	.0097	.0078	.0081
Side Accel. B.S. 1655	$\frac{g's}{FPS}$	.0395	.0371	.0354	.0384	.0362	.0356
Aileron Displacement	$\frac{DEG.}{FPS}$	.273	.486	.532	.296	.292	.444
Rudder Displacement	$\frac{DEG.}{FPS}$	.128	.147	.114	.114	.132	.0826
VBM W.S. 222	$\frac{10^6 IN-LB}{FPS}$	.185	.168	.180	.182	.142	.155
CBM W.S. 222	$\frac{10^6 IN-LB}{FPS}$	.487	.413	.396	.496	.387	.362
VBM W.S. 820	$\frac{10^6 IN-LB}{FPS}$	.0751	.0790	.0787	.0765	.0682	.0668
CBM W.S. 820	$\frac{10^6 IN-LB}{FPS}$	.0933	.0798	.0851	.0908	.0698	.0722
VBM W.S. 974	$\frac{10^6 IN-LB}{FPS}$	.0430	.0452	.0462	.0438	.0383	.0386
CBM W.S. 974	$\frac{10^6 IN-LB}{FPS}$	.0270	.0253	.0321	.0292	.0251	.0234
SEM B.S. 1222	$\frac{10^6 IN-LB}{FPS}$	.631	.484	.475	.636	.441	.418
SEM B.S. 1412	$\frac{10^6 IN-LB}{FPS}$	.349	.261	.260	.361	.243	.227
VBM S.B.L. 56	$\frac{10^6 IN-LB}{FPS}$	.0411	.0292	.0322	.0448	.0282	.0289
SEM F.S. 135	$\frac{10^6 IN-LB}{FPS}$	.149	.104	.110	.162	.101	.0993

TABLE XI  
LATERAL GUST A'S

A's calculated using:

- Cross-spectrum derived frequency response functions
- Theoretical gust spectrum

RESPONSE	UNITS	TEST 5415			TEST 5418		
		BASIC	BASELINE	LAMS	BASIC	BASELINE	LAMS
Side Accel. B.S. 172	$\frac{g's}{FPS}$	.0055	.0061	.0063	.0064	.0070	.0059
Side Accel. B.S. 860	$\frac{g's}{FPS}$	.0046	.0043	.0045	.0049	.0044	.0043
Side Accel. B.S. 1655	$\frac{g's}{FPS}$	.0191	.0188	.0188	.0200	.0213	.0196
Aileron Displacement	$\frac{DEG.}{FPS}$	.0429	.0602	.261	.0400	.0861	.239
Rudder Displacement	$\frac{DEG.}{FPS}$	.0199	.102	.0744	.0086	.104	.0607
VBM W.S. 222	$\frac{10^6 \text{ IN-LB}}{FPS}$	.0921	.0860	.0949	.0937	.0848	.0926
CBM W.S. 222	$\frac{10^6 \text{ IN-LB}}{FPS}$	.281	.262	.256	.296	.277	.243
VBM W.S. 820	$\frac{10^6 \text{ IN-LB}}{FPS}$	.0248	.0139	.0159	.0271	.0188	.0168
CBM W.S. 820	$\frac{10^6 \text{ IN-LB}}{FPS}$	.0504	.0448	.0461	.0494	.0456	.0434
VBM W.S. 974	$\frac{10^6 \text{ IN-LB}}{FPS}$	.0153	.0077	.0097	.0156	.0116	.0091
CBM W.S. 974	$\frac{10^6 \text{ IN-LB}}{FPS}$	.0131	.0119	.0122	.0143	.0143	.0132
SBM B.S. 1222	$\frac{10^6 \text{ IN-LB}}{FPS}$	.389	.340	.341	.390	.346	.315
SBM B.S. 1412	$\frac{10^6 \text{ IN-LB}}{FPS}$	.214	.180	.183	.217	.188	.168
VBM S.B.L. 56	$\frac{10^6 \text{ IN-LB}}{FPS}$	.0254	.0207	.0229	.0275	.0225	.0224
SBM F.S. 135	$\frac{10^6 \text{ IN-LB}}{FPS}$	.0932	.0769	.0812	.0996	.0821	.0778

TABLE XII  
LATERAL GUST A'S

THEORETICAL

LAMS FLIGHT CONDITION 1  
(350000 LBS, 350 KTS EAS, 4000 FT)

<u>RESPONSE</u>	<u>UNITS</u>	<u>BASIC</u>	<u>BASELINE</u>	<u>LAMS</u>
Side Accel. B.S. 172	$\frac{g's}{FPS}$	.0135	.0136	.0123
Side Accel. B.S. 860	$\frac{g's}{FPS}$	.0111	.0063	.0066
Side Accel. B.S. 1655	$\frac{g's}{FPS}$	.0302	.0239	.0252
Aileron Displacement	$\frac{DEG.}{FPS}$	.000	.0439	.191
Rudder Displacement	$\frac{DEG.}{FPS}$	.000	.159	.1231
VBM W.S. 222	$\frac{10^6 \text{ IN-LB}}{FPS}$	.123	.0721	.0843
CBM W.S. 222	$\frac{10^6 \text{ IN-LB}}{FPS}$	.509	.331	.339
VBM W.S. 820	$\frac{10^6 \text{ IN-LB}}{FPS}$	.0457	.0197	.0168
CBM W.S. 820	$\frac{10^6 \text{ IN-LB}}{FPS}$	.0587	.0420	.0419
VBM W.S. 974	$\frac{10^6 \text{ IN-LB}}{FPS}$	.0312	.0140	.0138
CBM W.S. 974	$\frac{10^6 \text{ IN-LB}}{FPS}$	.0218	.0151	.0153
SBM B.S. 1222	$\frac{10^6 \text{ IN-LB}}{FPS}$	.569	.378	.372
SBM B.S. 1412	$\frac{10^6 \text{ IN-LB}}{FPS}$	.318	.232	.221
VBM S.B.L. 56	$\frac{10^6 \text{ IN-LB}}{FPS}$	.0418	.0226	.0239
SBM F.S. 135	$\frac{10^6 \text{ IN-LB}}{FPS}$	.119	.0789	.0798

TABLE XIII  
VERTICAL GUST N<sub>0</sub>'s ~ CPS

N<sub>0</sub>'s calculated using:

- Cross-spectrum derived frequency response functions
- Theoretical gust spectrum

RESPONSE	TEST 5415			TEST 5418		
	BASIC	BASELINE	LAMS	BASIC	BASELINE	LAMS
Vert. Accel. B.S. 172	1.242	1.360	1.368	1.188	1.416	1.201
Vert. Accel. B.S. 860	.552	.595	.607	.504	.588	.554
Vert. Accel. B.S. 1655	.767	.810	.841	.716	.845	.751
Aileron Displacement	.943	.755	2.756	.754	.718	2.117
Spoiler Displacement	3.113	3.017	.780	3.078	2.977	.671
Elevator Displacement	.744	.480	.649	.331	.749	.645
VBM W.S. 222	.619	.655	.686	.542	.598	.628
CBM W.S. 222	1.980	1.988	2.043	1.928	2.098	2.009
VBM W.S. 820	.507	.534	.529	.447	.509	.496
CBM W.S. 820	1.697	1.611	1.373	1.648	1.909	1.355
VBM W.S. 974	.473	.503	.513	.419	.492	.489
CIM W.S. 974	1.721	1.751	1.235	1.472	1.803	1.364
VBM B.S. 1222	1.483	1.419	1.298	1.441	1.513	1.139
VBM B.S. 1412	1.577	1.511	1.364	1.571	1.629	1.211
VBM S.B.L. 56	.725	.819	.693	.665	.790	.671

TABLE XIV  
VERTICAL GUST  $N_0$ 's ~ CPS

THEORETICAL

LAMS FLIGHT CONDITION 1  
 (350000 LBS, 350 KTS EAS, 4000 FT)

<u>RESPONSE</u>	<u>BASIC</u>	<u>BASELINE</u>	<u>LAMS</u>
Vert. Accel. B.S. 172	2.364	2.380	2.487
Vert. Accel. B.S. 860	.891	.925	.988
Vert. Accel. B.S. 1655	1.356	1.406	1.458
Aileron Displacement	—	—	3.383
Spoiler Displacement	—	—	.993
Elevator Displacement	—	.702	.724
VBM W.S. 222	.709	.731	.772
CBM W.S. 222	2.261	2.268	2.289
VBM W.S. 820	.656	.681	.782
CBM W.S. 820	2.252	2.260	2.297
VBM W.S. 974	.709	.737	.913
CBM W.S. 974	2.035	2.077	2.273
VBM B.S. 1222	1.781	1.708	1.334
VBM B.S. 1412	2.066	1.936	1.502
VBM S.B.L. 56	.895	.956	.880

TABLE XV  
LATERAL GUST NO'S ~ CPS

No's calculated using:

- Cross-spectrum derived frequency response functions
- Theoretical gust spectrum

RESPONSE	TEST 5415			TEST 5418		
	BASIC	BASELINE	LAMS	BASIC	BASELINE	LAMS
Side Accel. B.S. 172	3.734	3.798	3.514	3.630	3.937	3.531
Side Accel. B.S. 860	1.190	1.501	1.587	1.292	1.538	1.595
Side Accel. B.S. 1655	1.504	1.570	1.565	1.496	1.579	1.564
Aileron Displacement	.573	.455	1.001	.582	.295	1.095
Rudder Displacement	.711	.344	.407	1.247	.310	.412
VBM W.S. 222	.651	.796	.870	.581	.786	.876
CBM W.S. 222	.936	1.029	1.031	.869	1.040	1.047
VBM W.S. 820	.784	1.367	2.064	.738	1.073	1.989
CBM W.S. 820	.847	.976	1.128	.895	1.018	1.107
VBM W.S. 974	.744	1.483	2.313	.713	1.100	2.205
CBM W.S. 974	.994	1.155	1.399	1.173	1.267	1.243
SBM B.S. 1222	.694	.821	.761	.652	.811	.753
SBM B.S. 1412	.718	.859	.804	.689	.849	.810
VBM S.B.L. 56	.656	.831	.723	.621	.812	.709
SBM F.S. 135	.583	.703	.669	.548	.710	.673

TABLE XVI  
LATERAL GUST  $N_0$ 's ~ CPS

THEORETICAL

LAMS FLIGHT CONDITION 1  
 (350000 LBS, 350 KTS EAS, 4000 FT)

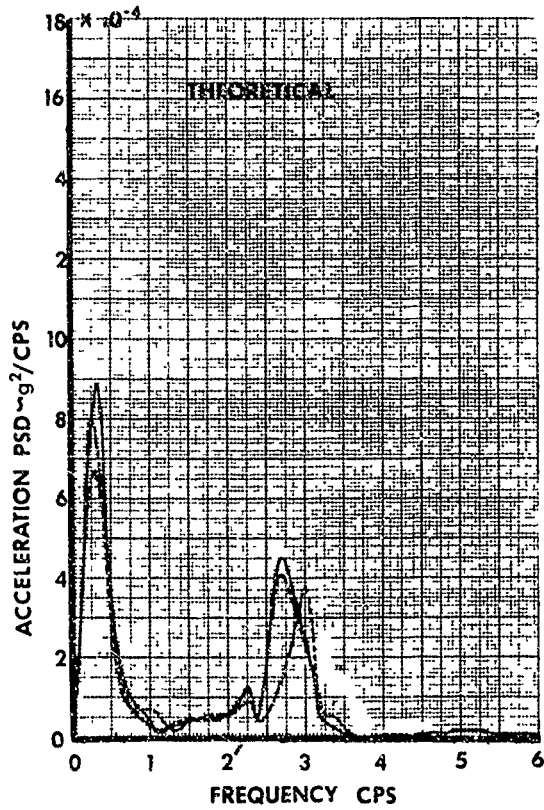
<u>RESPONSE</u>	<u>BASIC</u>	<u>BASELINE</u>	<u>LAMS</u>
Side Accel. B.S. 172	3.859	3.833	3.839
Side Accel. B.S. 860	.830	1.424	1.313
Side Accel. B.S. 1655	1.529	1.895	1.822
Aileron Displacement	--	.286	2.269
Rudder Displacement	--	.291	.304
VBM W.S. 222	.447	.713	.728
CBM W.S. 222	.636	.941	.934
VBM W.S. 820	.520	1.108	2.296
CBM W.S. 820	1.261	1.752	1.593
VBM W.S. 974	.432	.841	2.589
CBM W.S. 974	1.368	1.960	1.794
SBM B.S. 1222	.530	.780	.770
SBM B.S. 1412	.644	.884	.893
VBM S.B.L. 56	.636	1.124	1.070
SBM F.S. 135	.448	.719	.707

Table II shows peak incremental stress ratios, LAMS-FCS to Baseline SAS, for an exceedance expectation of once per 1000 hours of contour low-level flying. Agreement of the test results with theoretical predictions is considered very good.

Table III presents fatigue damage rates computed from the test "A" and " $N_0$ " values. Data compares the LAMS-FCS to the Baseline SAS. Agreement with predicted values is excellent for the wing. Test data shows that the LAMS-FCS performance was somewhat better than predicted for the fuselage and fin. Stabilizer damage rate was greater than predicted, but is still acceptable at only about 1 percent of the inboard wing damage rates.

#### 4.3.9 Crew Compartment Acceleration Spectral Density

The crew compartment acceleration transfer functions presented in 4.3.5 have been multiplied by the theoretical vertical gust spectral density to obtain the graphs in Figure 66 . It is apparent that the amplitude of the rigid body response at .25 cps was diminished by the Baseline SAS and even more by the LAMS-FCS. The predicted increase in frequency of the body mode from 2.7 cps to 3.0 cps) due to the LAMS-FCS is also shown by the test data.



**BODY STATION 172**  
**VERTICAL ACCELERATION PSD**

TEST DATA CALCULATED USING

- CROSS SPECTRUM DERIVED FREQUENCY RESPONSE FUNCTION
- THEORETICAL GUST SPECTRUM

— NO SAS  
 - - - BASELINE SAS  
 - · - LAMS FLIGHT CONTROL SYSTEM

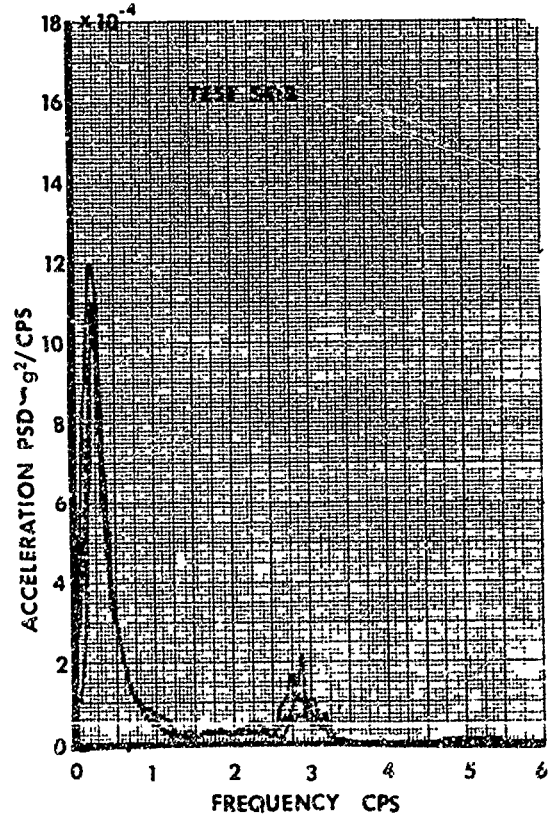
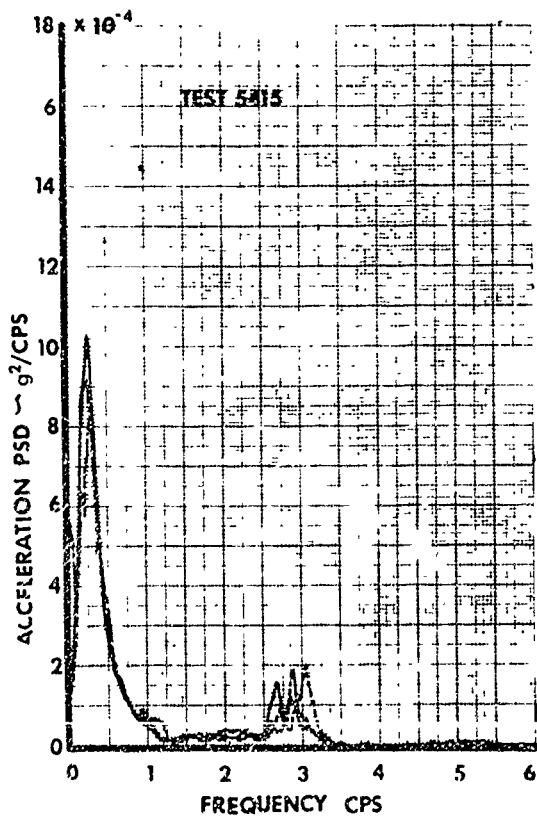


FIGURE 66

## 5.0 HARDWARE PERFORMANCE

This section of the report contains the results of the hardware performance evaluated during ground tests and compares the test data to that of the design requirements.

The hardware was evaluated during the following activities:

- Aircraft control system ground vibration test
- Control surface actuator dynamic response testing
- Hydraulic power system tests
- Evaluation (Fly-By-Wire) pilot system characteristics
- Stability augmentation system tests of the Baseline SAS and LAMS-FCS

### 5.1 Aircraft Control System Ground Vibration Test

Major modifications to the flight control systems were accomplished during the LAMS program. A ground vibration test of the manual control systems was required to obtain experimental data for comparison with that used in the theoretical analyses to verify the accuracy of the analytical results.

#### 5.1.1 Directional and Longitudinal Control Systems

Test data obtained from a similarly configured test vehicle, the ECP 1195 aircraft, was used for the rudder and elevator manual control systems; consequently, no ground testing was accomplished for these systems on the LAMS vehicle. The data for these systems was obtained during the ground vibration tests of References 1 and 2.

Figures 67 and 68 present the control system dynamic response versus "Q" spring pressure for the rudder and elevator control systems respectively. Results of the control systems, with the evaluation pilot (L.H.) controls removed from the system and values of the system dynamics used in the theoretical analyses are indicated on the two figures.

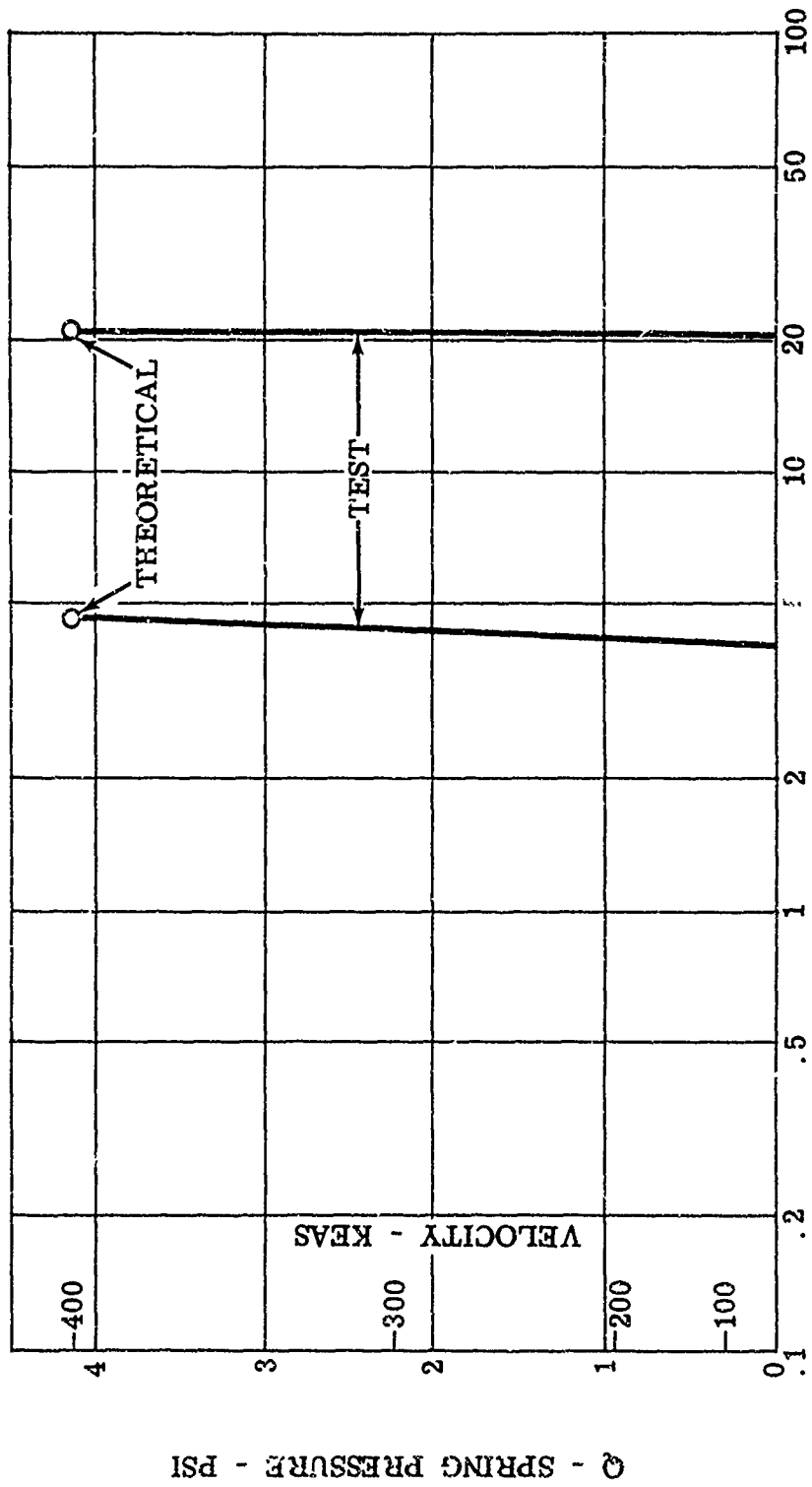
The control surface modes of vibration versus the theoretical analyses results are as follows:

- Rudder Torsion Mode (Test = 21.4 cps vs. Theory = 21.1 cps)
- Elevator Torsion Mode (Test = 29.8 cps vs. Theory = 29.7 cps)

#### 5.1.2 Lateral Control System

Ground vibration testing of the powered control systems on the wings was conducted to establish the manual aileron-spoiler system dynamic characteristics.

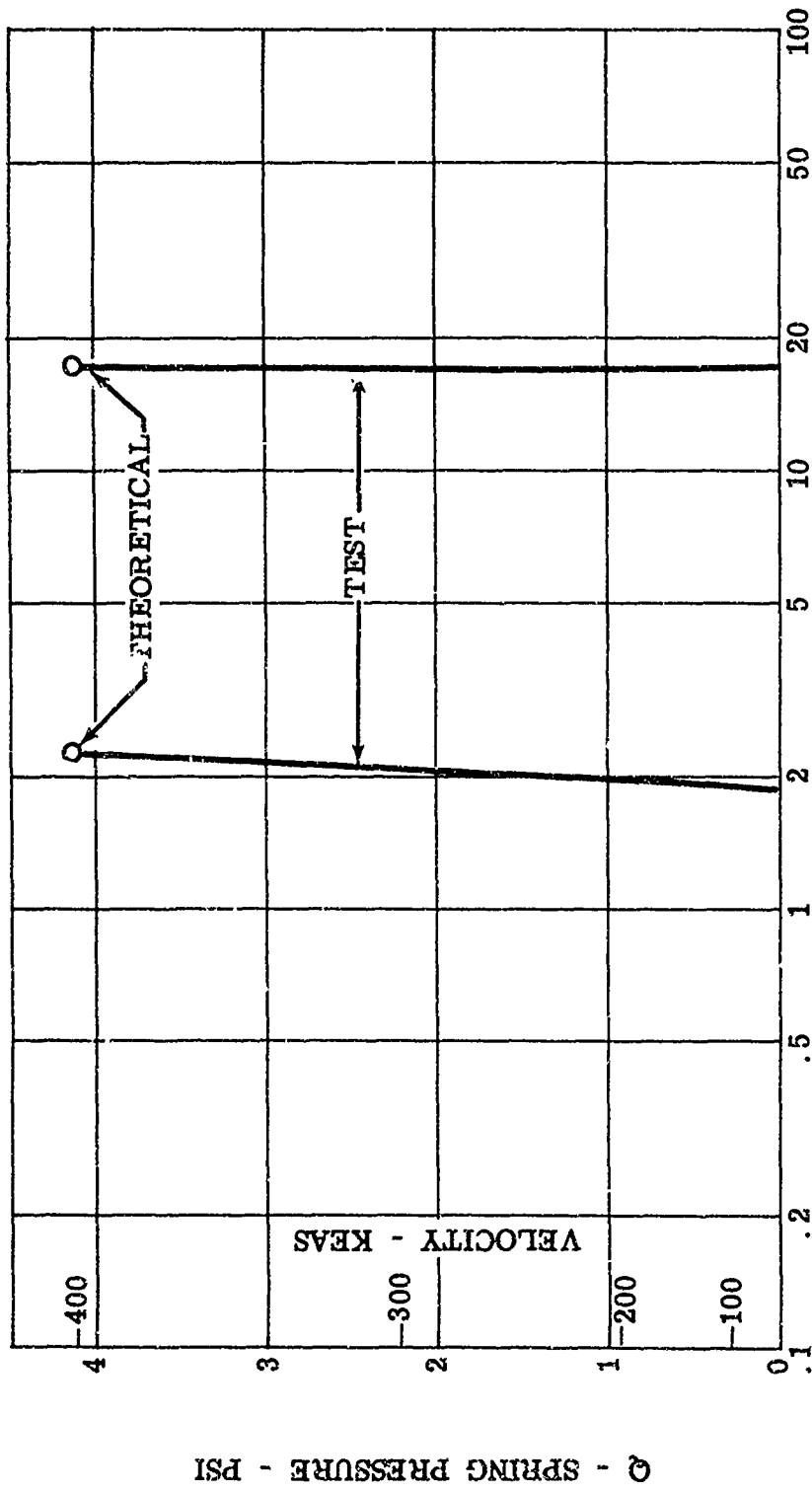
The aircraft was restrained to minimize the coupling between the aircraft elastic modes and the control system. Instrumentation consisted of



FREQUENCY - HZ  
 RUDDER TORSION MODE = 21.7 Hz (THEORETICAL = 20.8 Hz)

DIRECTIONAL MANUAL (MONITOR PILOT)  
 CONTROL SYSTEM DYNAMICS

FIGURE 67



FREQUENCY - Hz  
 ELEVATOR TORSION MODE = 38.0 Hz (THEORETICAL = 37.0 Hz)

LONGITUDINAL MANUAL (MONITOR PILOT)  
 CONTROL SYSTEM DYNAMICS

FIGURE 68

position indicators and accelerometers installed at appropriate locations throughout the system.

Testing was accomplished in four parts:

- Vibration of the aileron against the powered actuator
- Actuation of the aileron through the mechanical input lever
- Oscillation of the monitor pilot control wheel
- Oscillation of the monitor pilot control wheel with the spoiler valve mechanical input disconnected

The results of the above testing are described in the following paragraphs.

#### 5.1.2.1 Vibration of the Aileron Against the Powered Actuator

An electrodynamic shaker was attached to the L.H. aileron approximately 27.5 inches aft of the hinge line. The test was conducted with the shaker on either the inboard or outboard edges of the aileron with no appreciable change in the dynamic characteristics noted for either shaker location. The results are presented in the impedance plot of Figure 69 and summarized below:

- Coupled actuator, structure, and aileron resonance at 11.6 cps with a viscous damping coefficient equal to .12
- Aileron Torsion Mode (Test = 38.5 cps vs. Theory = 39.0 cps)

#### 5.1.2.2 Actuation of the Aileron Through the Mechanical Input Arm (AMVIA)

The actuator and aileron systems were oscillated sinusoidally by an electrodynamic shaker attached to the mechanical input arm (AMVIA) on the aileron actuator. The results of this test are presented in Figure 70.

The plot compares the experimental data with two different theoretical transfer functions used in the flutter analyses. The analyses with either theoretical transfer function provided a satisfactory aircraft flutter boundary and would be stable using the experimental transfer function.

#### 5.1.2.3 Oscillation of the Monitor Pilot Control Wheel

The lateral control system was tested by attaching an electrodynamic shaker to a bellcrank which replaced the control wheel. Figure 71 presents the results of this test. The manual lateral system exhibited only one resonance at approximately 5 cps which is associated with the aileron actuator feel spring. The actuator feel spring is a preloaded spring and exhibits non-linear characteristics dependent on amplitude. The theoretical analyses predicted the system frequency at this amplitude of oscillation ( $\pm 7.5$  degrees of wheel displacement). Also noted during this portion of the test was a spoiler panel-actuator resonance at approximately 18 cps as verified from previous vibration tests.

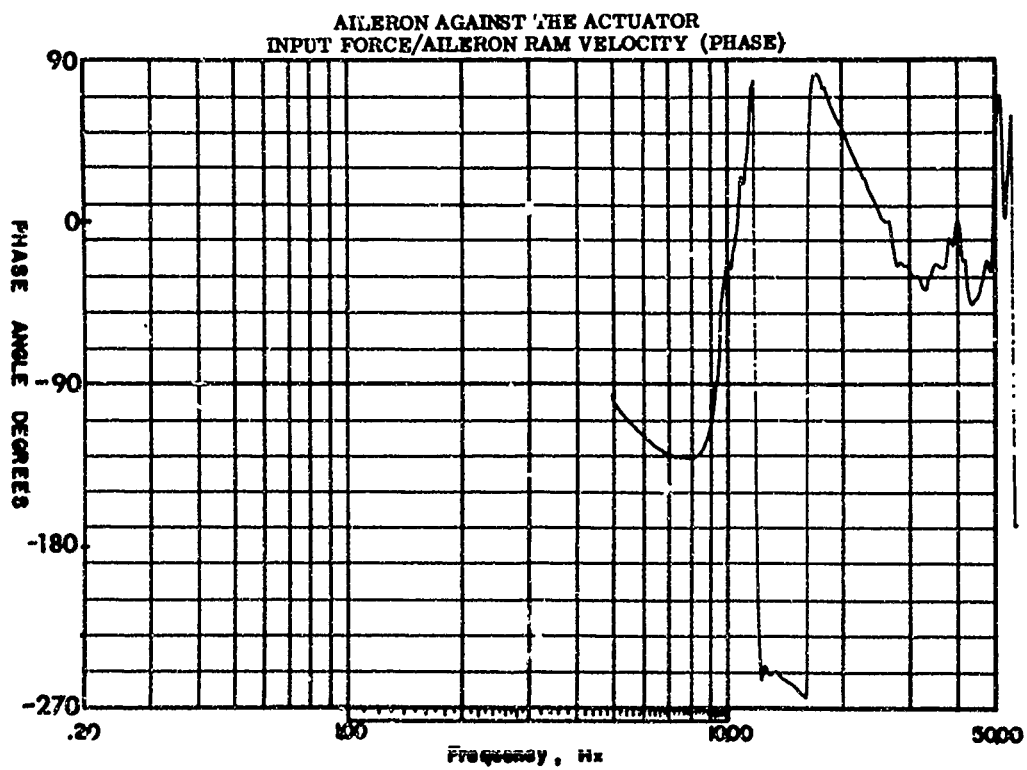
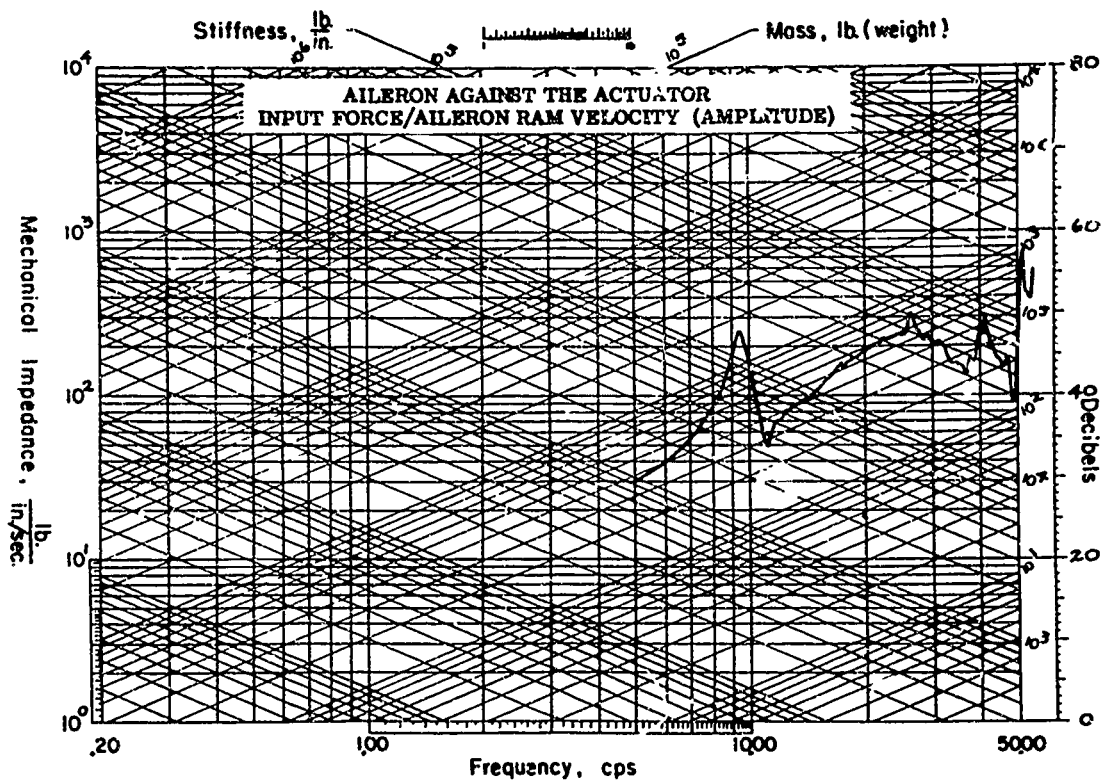


FIGURE 69

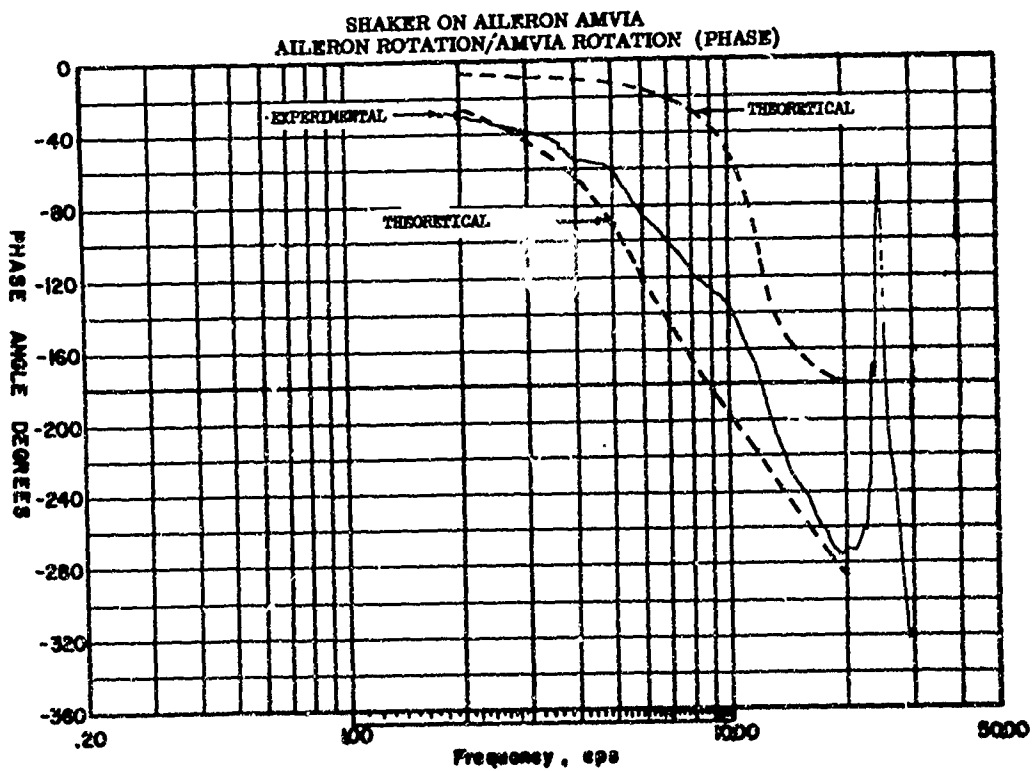
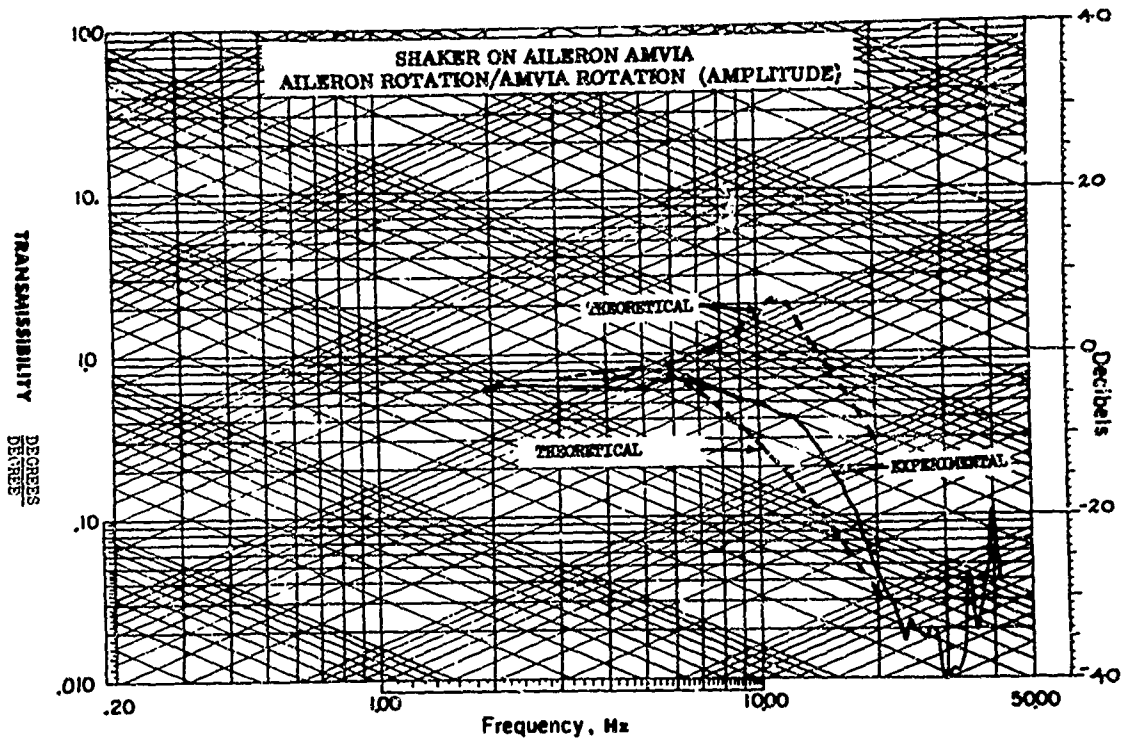


FIGURE 70

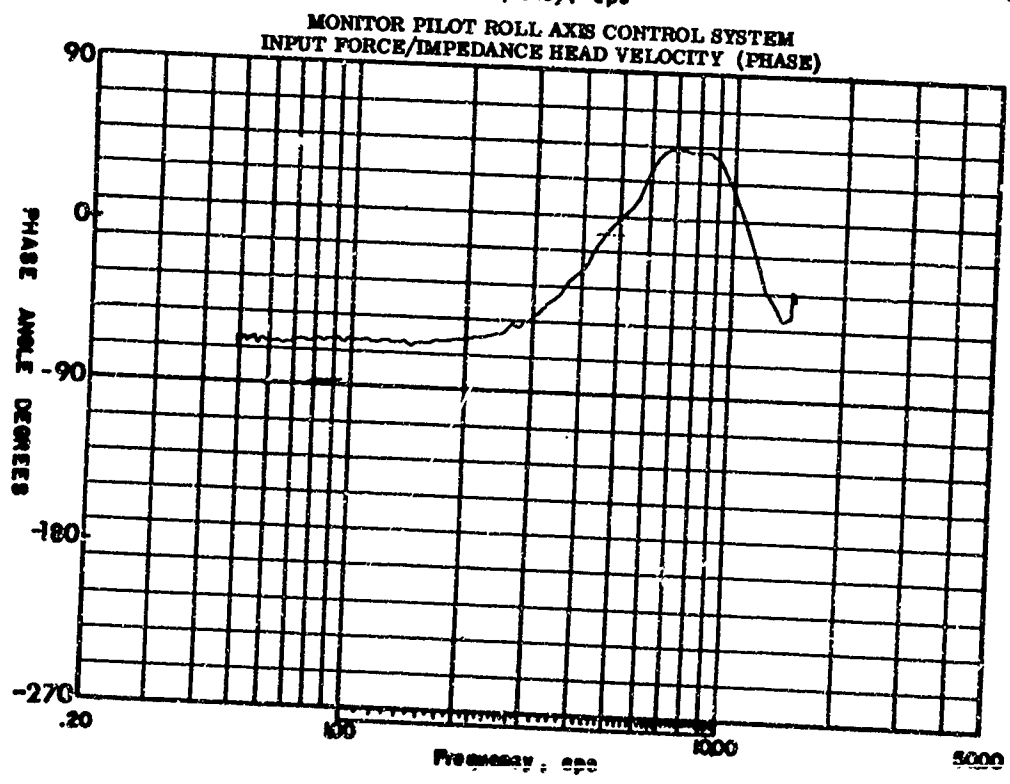
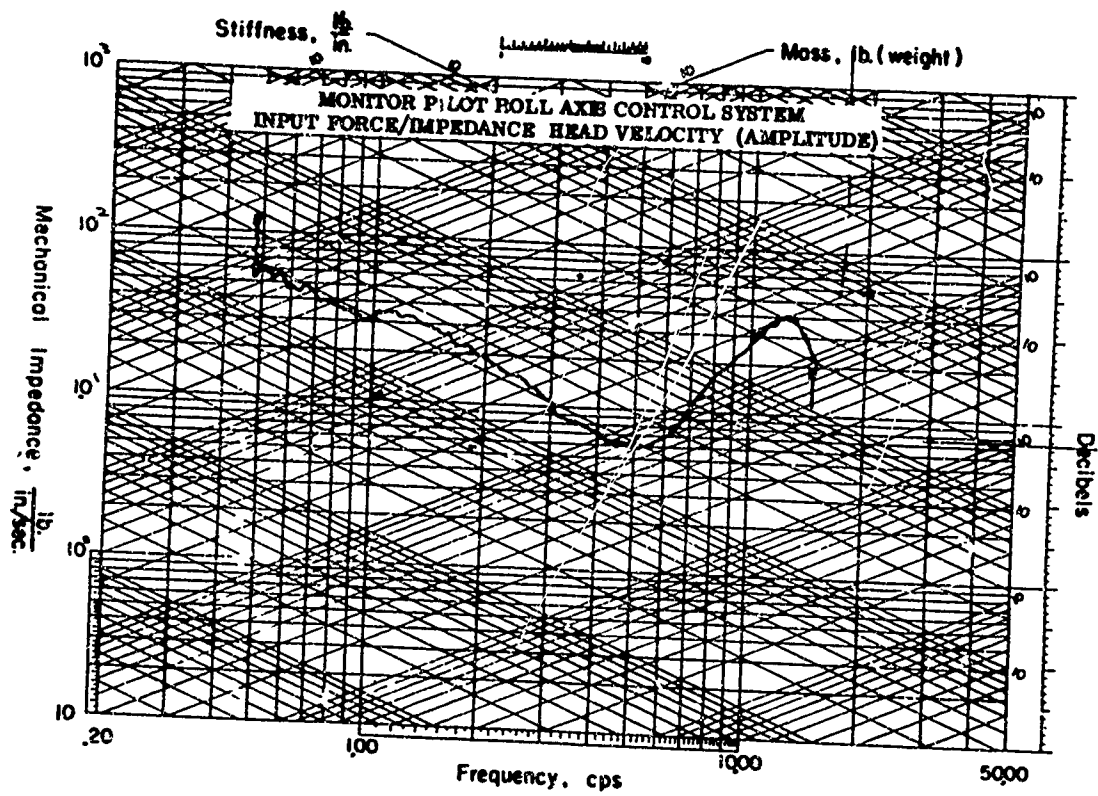


FIGURE 71

#### 5.1.2.4 Oscillation of the Monitor Pilot Control Wheel With the Spoilers Disconnected

This test was conducted in the same manner as the test in paragraph 5.1.2.3 and allowed sweeping a broader frequency spectrum with larger input amplitudes because of the elimination of the wing support and spoiler resonances in the 20 to 30 cps frequency spectrum. Figure 72 presents the results of this test and shows that the R.H. aileron actuator had a damping coefficient ( $\zeta$ ) equal to approximately .12 which was less than the design requirements. The actuator frequency response characteristics were noted to be very sensitive to amplitude. Consequently the aileron actuators were subsequently modified to provide a higher damping coefficient ( $\zeta = .5$ ). The results of the final actuator tests are presented in Section 5.2.

### 5.2 Hydraulic Actuators

The electrical authority and maximum rates of the ailerons, elevators, rudder and the LAMS spoiler hydraulic actuators are presented in Figure 73. Good agreement is noted between the predicted and experimental data for frequencies below 5 cps. The experimental response rate above 5 cps is less than predicted because of the actuator characteristics presented in the following sections.

#### 5.2.1 Aileron Actuator

The aileron actuators were manufactured by Cadillac Gage Company to Boeing specifications. The vendor accomplished the specified flight-worthiness testing. Major elements of this testing included performance, vibration and endurance tests. The test specimen completed all required testing satisfactorily without major incident.

In addition to the acceptance tests performed at the vendor's facility, the flight hardware was subjected to rigorous performance tests while installed on the test vehicle. Figure 74 is a plot of the closed loop frequency response. The actuator response was not within the design band for gain at frequencies above 3.5 cps and phase at frequencies above 4.5 cps.

The design limits were theoretically established considering, among other factors, structural stiffness of the attach point and the bulk modulus of the hydraulic fluid. It was determined on the mock-up that the structural stiffness of the attach point and the bulk modulus were less than predicted. Both factors tend to reduce both the natural frequency of the actuator system and damping ratio. To counteract the reduction in damping ratio, it was necessary to increase the force feedback gain; this change further reduced the natural frequency. Thus, the natural frequency of the final system installation was approximately 5 cps instead of the desired 20 cps. This reduced natural frequency was judged acceptable for LAMS usage because the highest frequency mode which the aileron controls is approximately 4 cps.

Figure 75 indicates that the open loop frequency response for the auxiliary actuator was within the design limits. The aileron surface response to a one degree step input is shown in Figure 76. Figure 77 is a hysteresis plot and shows a maximum dead zone of approximately .10 degree which provides adequate small input actuator response characteristics.

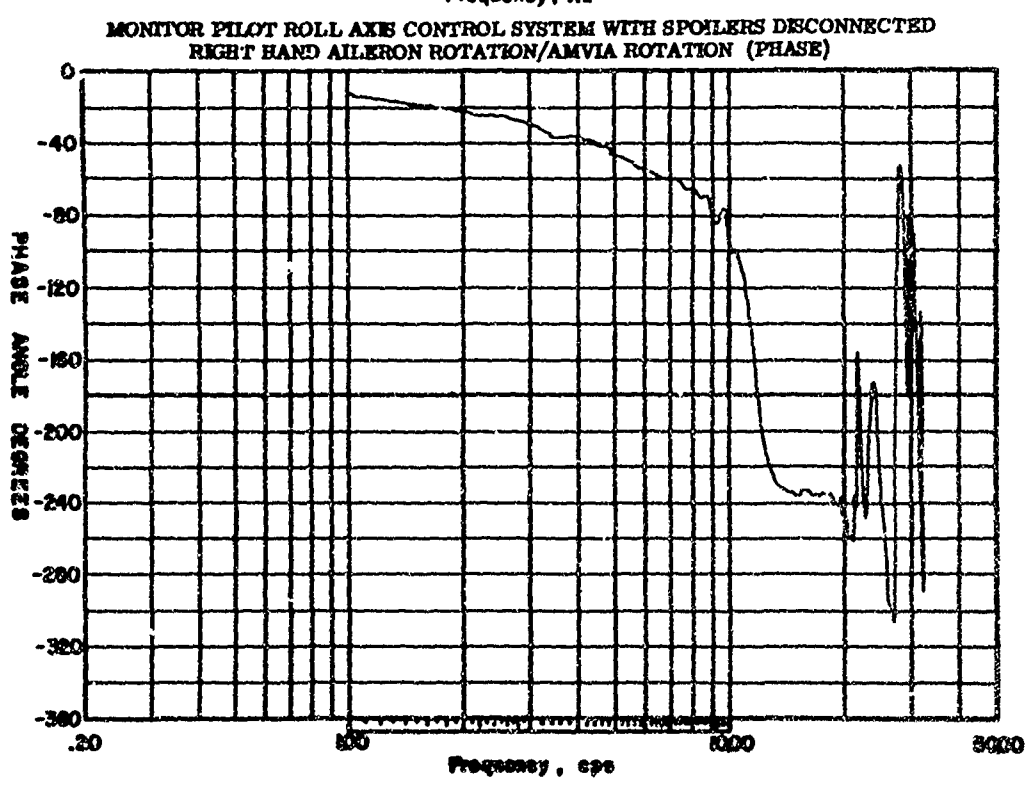
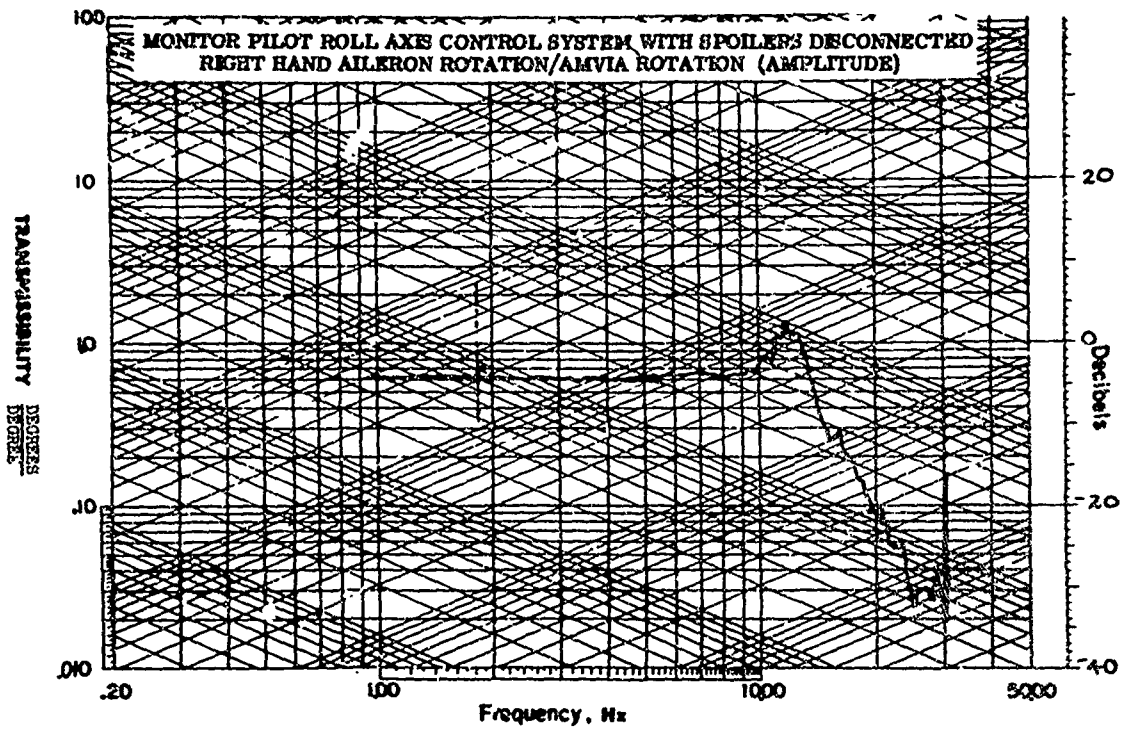
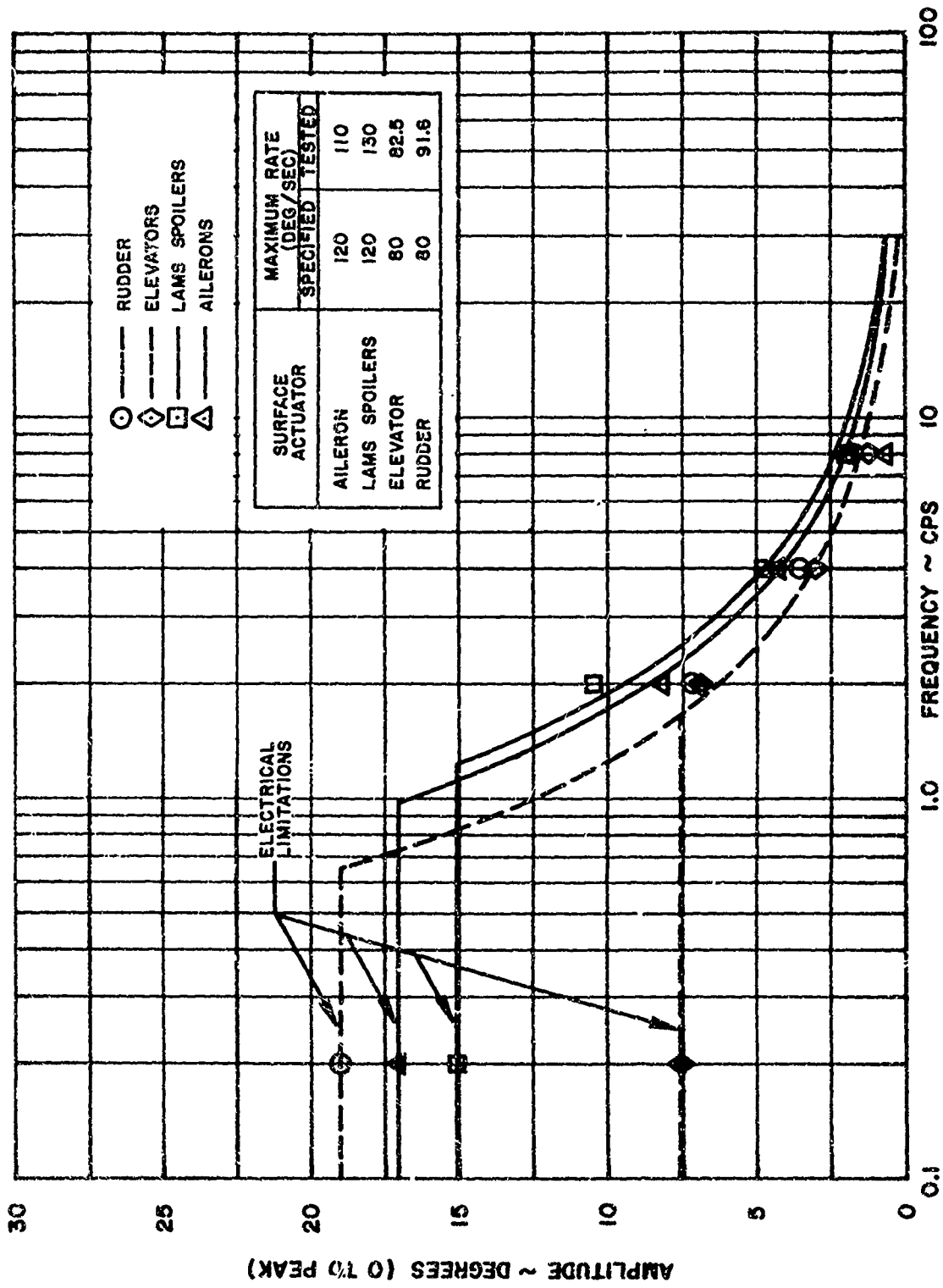
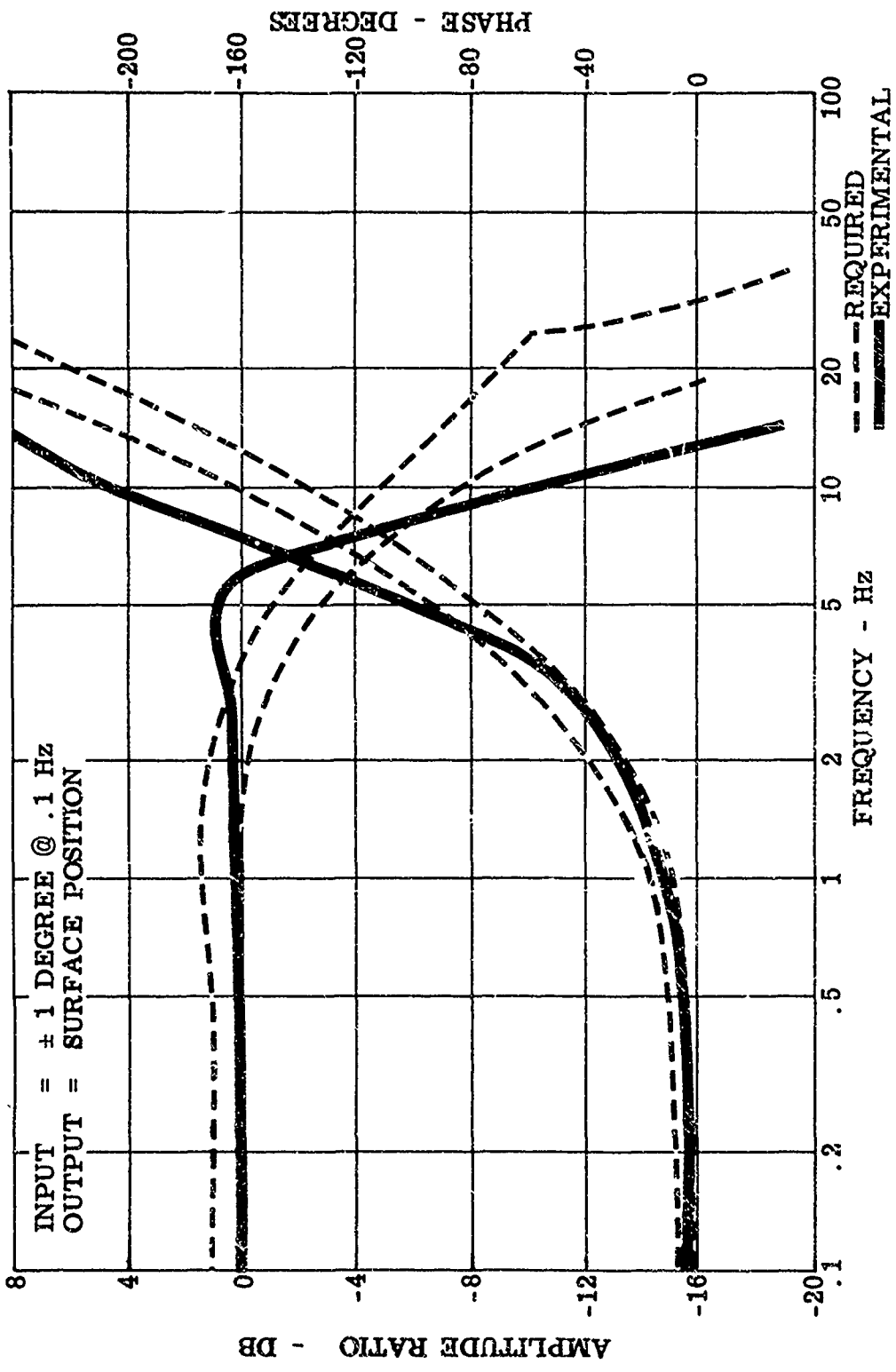


FIGURE 72



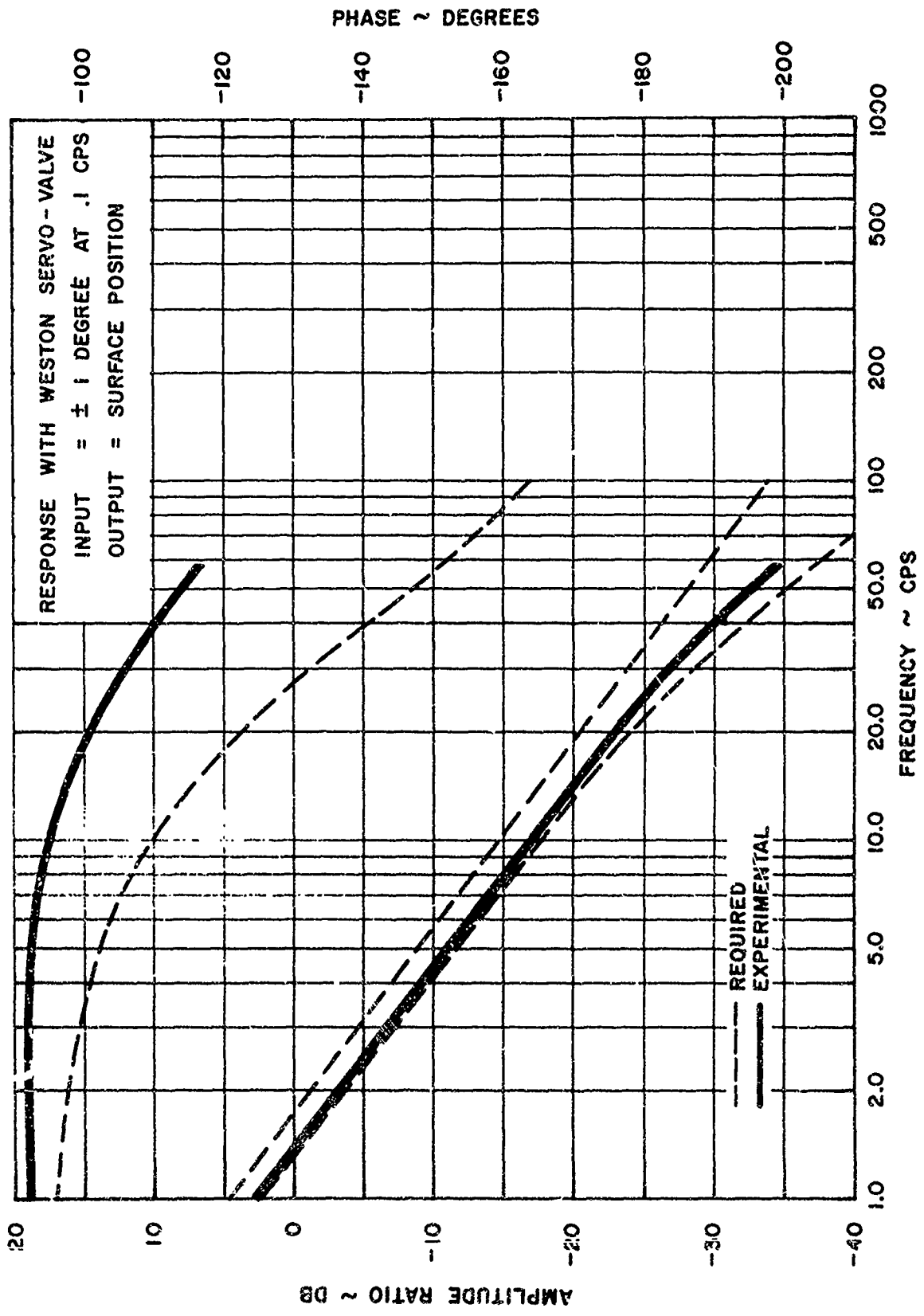
ACTUATOR MAXIMUM SURFACE AMPLITUDE LIMITS FOR LINEAR RESPONSE TO SINUSOIDAL INPUTS

FIGURE 73



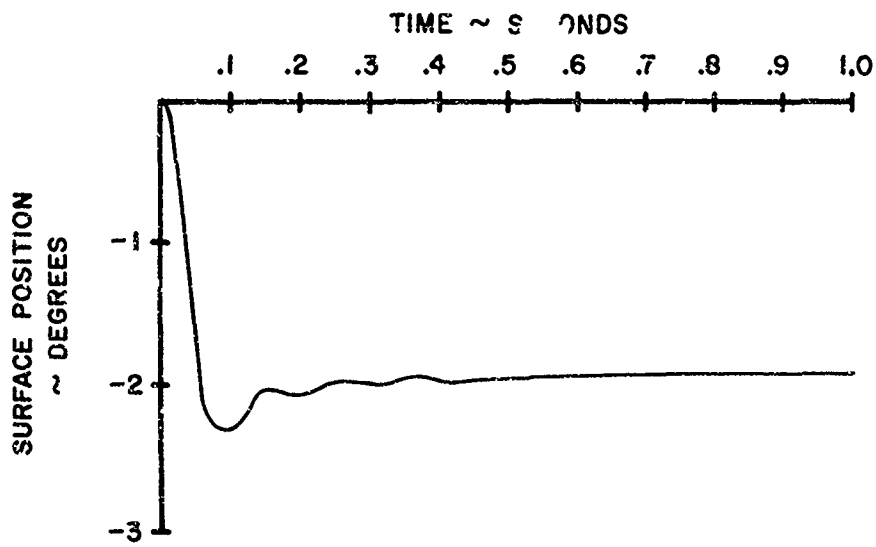
AILERON ACTUATOR FREQUENCY RESPONSE

FIGURE 74



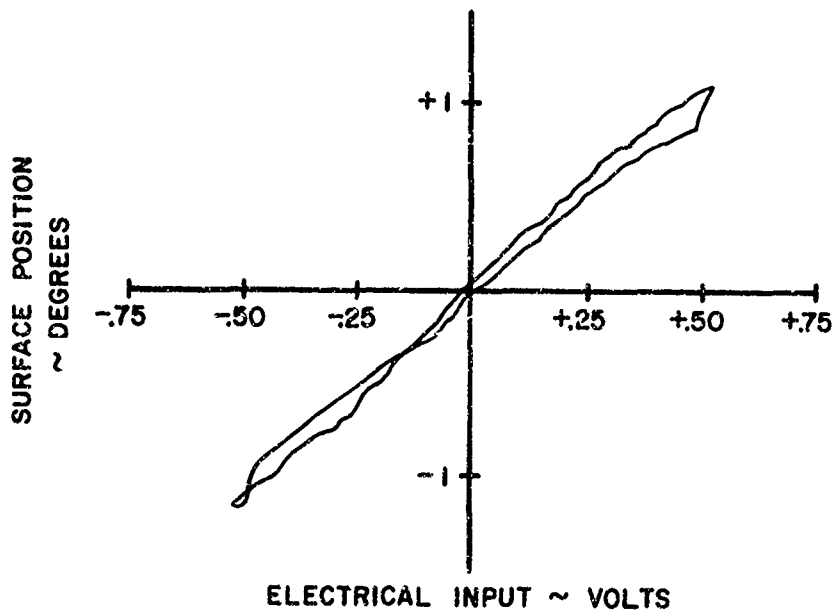
AILERON AUXILIARY ACTUATOR OPEN LOOP FREQUENCY RESPONSE

FIGURE 75



AILERON ACTUATOR STEP RESPONSE

FIGURE 76



AILERON ACTUATOR HYSTERESIS

FIGURE 77

### 5.2.2 LAMS-FCS Spoiler Actuator

The LAMS-FCS spoiler actuators were assembled by The Boeing Company. The assembly includes a hydraulic actuator, hydraulic manifold, Moog servo-valve, and position feedback potentiometer. The hydraulic actuators used were the original spoiler system components. Extensive performance tests of the assembly were performed in the laboratory on an operational mockup and with the actuator installed on the test vehicle.

The performance of the actuator at panel number 1 is considered representative of the LAMS spoiler system. Figure 78 shows the closed loop frequency response of the actuator installed on the aircraft. Figure 79 shows the LAMS spoiler actuator ram position in response to a one degree step input signal and Figure 80 shows that the unit has virtually zero hysteresis.

### 5.2.3 Spoiler Actuator (Integrated Spoiler Servo Valve)

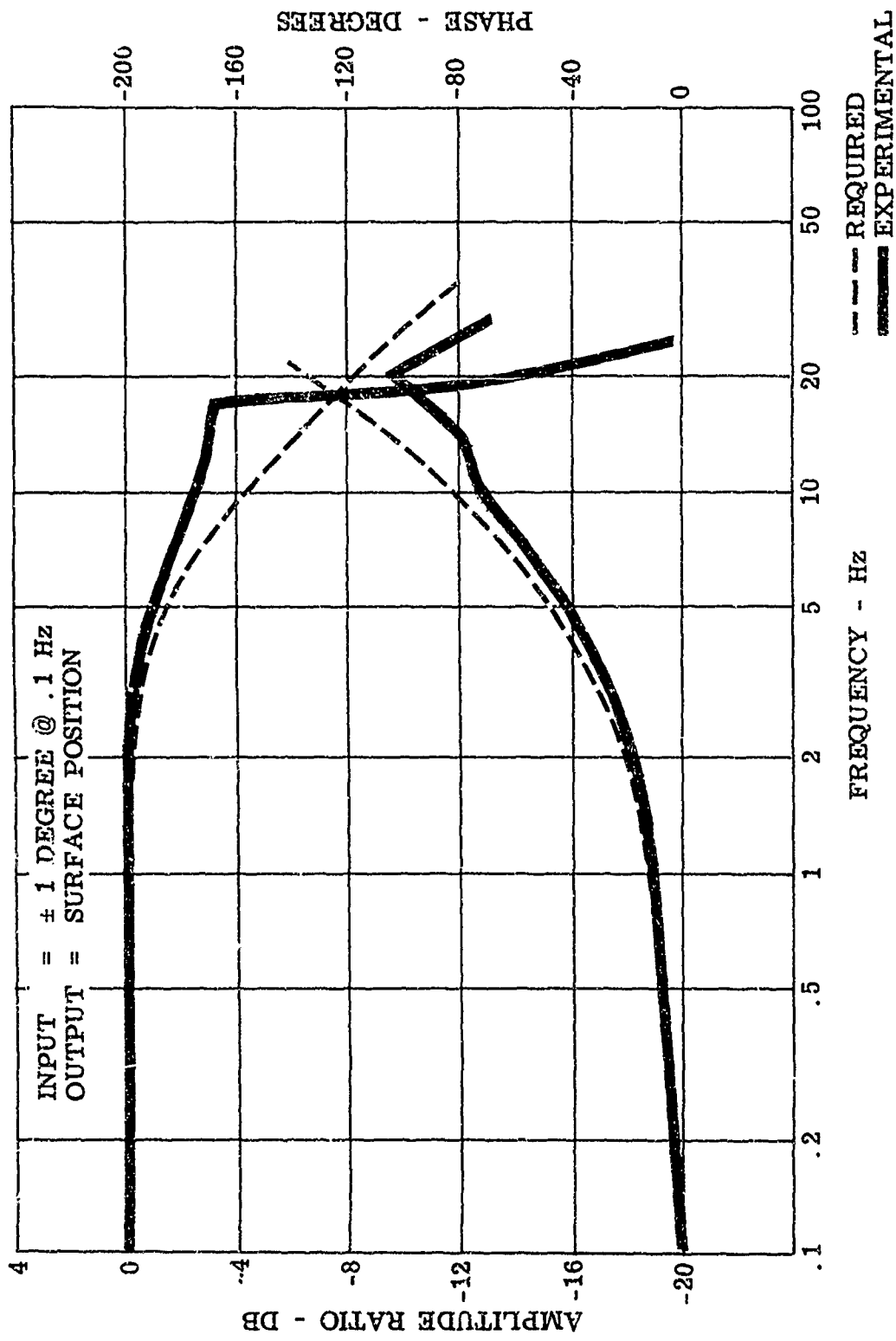
The integrated spoiler servo valves were manufactured by the Cadillac Gage Company to Boeing specifications. As in the case of the aileron actuators, the vendor accomplished the required flight-worthiness testing. The test specimen completed all required testing satisfactorily without major incident.

In addition to the acceptance tests accomplished by the vendor, limited performance tests were also accomplished. Figure 81 is representative of the open loop frequency response of the auxiliary actuator. It is important to note that when the system concept was revised (that is using only the two outboard spoiler panels for LAMS-FCS signals), the requirement for high frequency response from the integrated spoiler valves was relaxed. These servo valves were required to accept only fly-by-wire pilot commands and airbrake commands.

### 5.2.4 Rudder Actuator

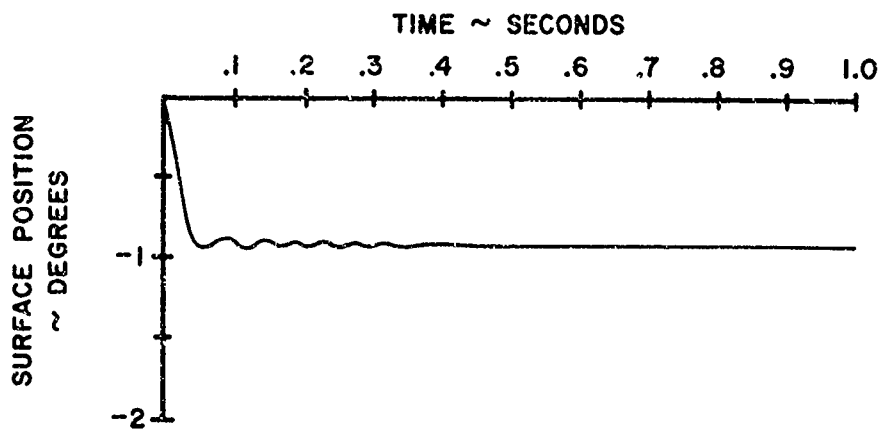
The rudder actuator was manufactured by Weston Hydraulics to Boeing specification. Since this unit, with the exception of minor mechanical details, was mechanically and functionally identical to previously flight qualified units, duplication of flight worthiness testing was not required. The unit was subjected to acceptance tests by the vendor and comprehensive performance testing after installation on the aircraft.

Figure 82 is typical of the closed loop frequency response of the unit. The gain of the actuator was within desired limits at frequencies above 3 cps and phase at frequencies above 10 cps. The gain outside the required envelope at frequencies over 3 cps was due to both channels of the servo actuator being used during flight operation. Combined dynamic effects of the servo actuators and demodulators resulted in more actuator authority than was initially required at frequencies over 1 cps. Figure 82 shows that the natural frequency of the system was approximately 15 cps rather than 20 cps predicted. This was due to a lower stiffness than predicted at the actuator attach point and a lower than predicted hydraulic oil bulk modulus. The SAS rudder controls elastic modes below 1 cps and response is attenuated electrically at higher frequencies. Therefore, system performance was not



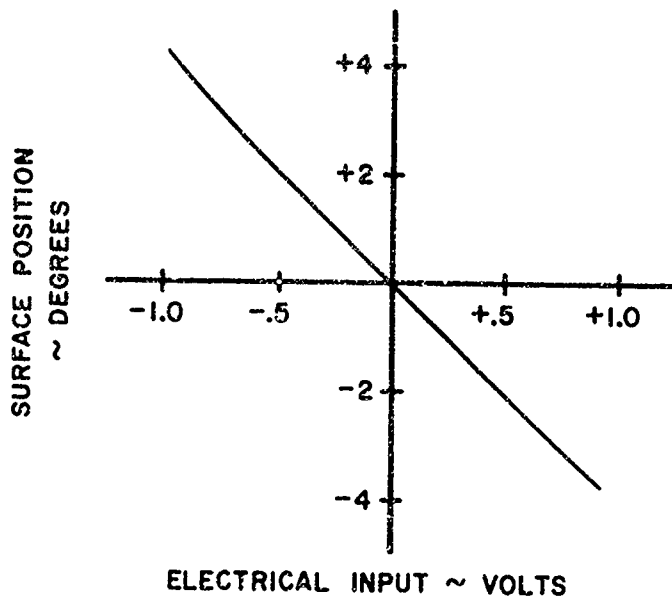
LAMS SPOILER ACTUATOR FREQUENCY RESPONSE

FIGURE 78



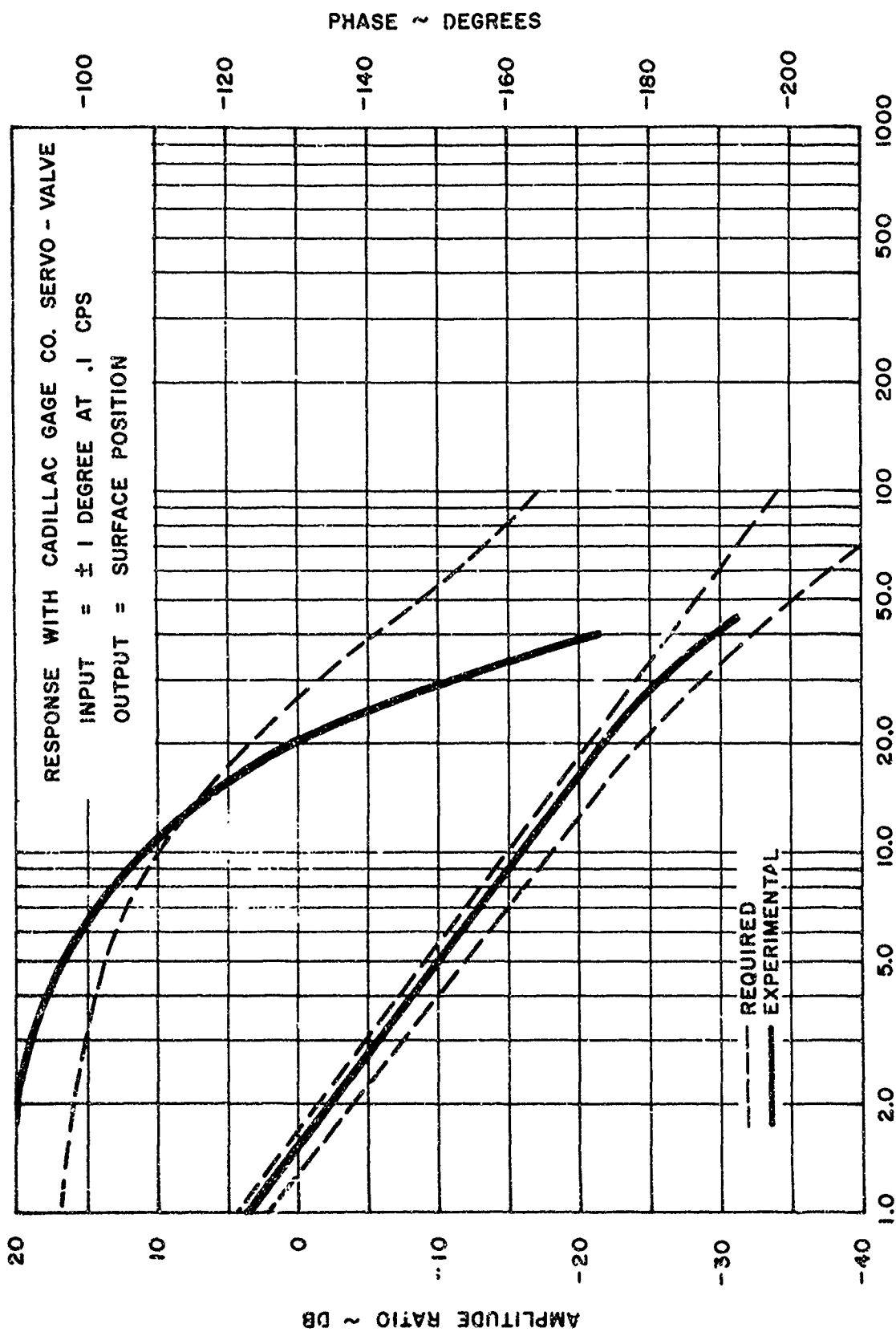
IAMS SPOILER ACTUATOR STEP RESPONSE

FIGURE 79

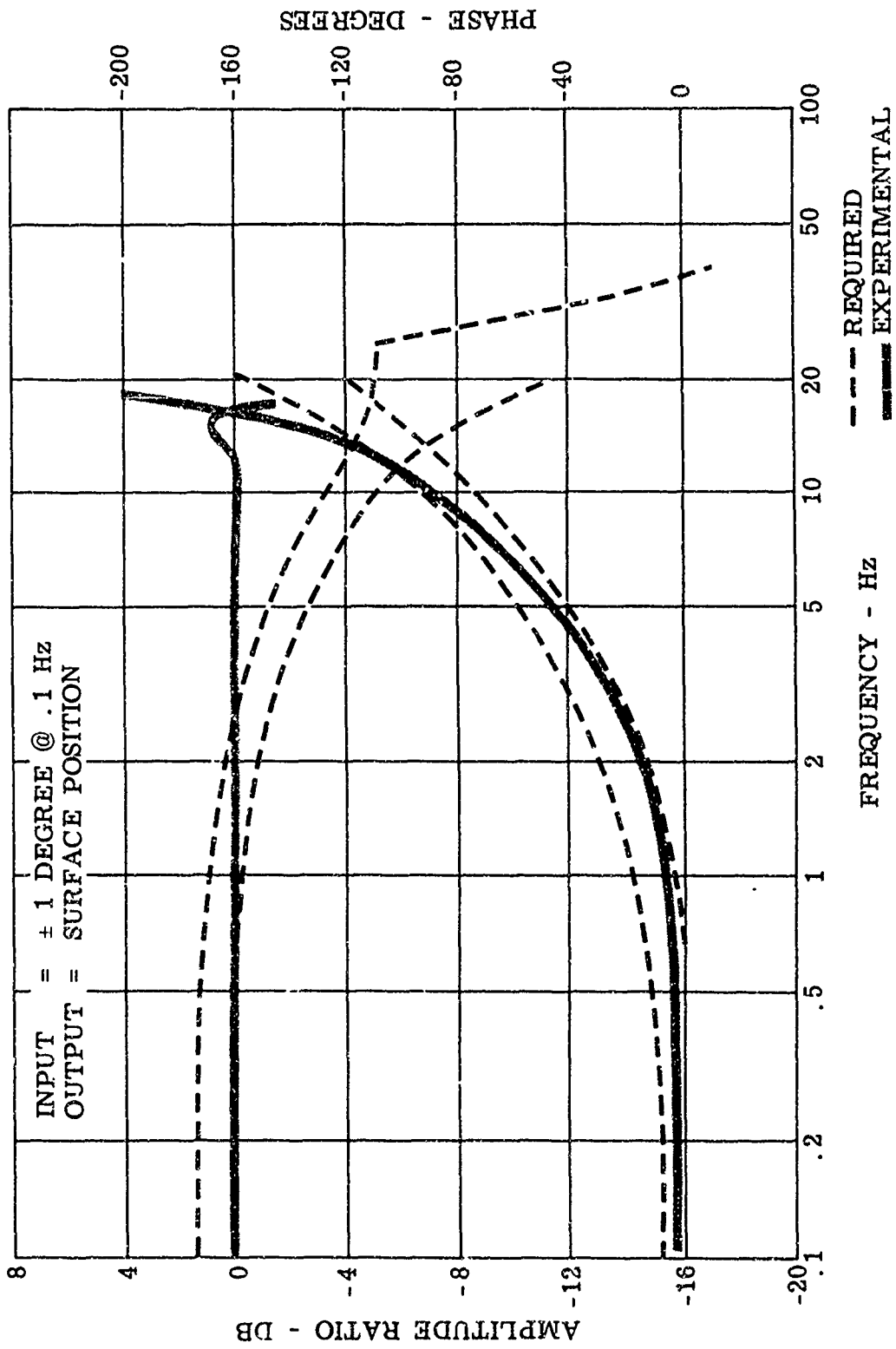


IAMS SPOILER ACTUATOR HYSTERESIS

FIGURE 80



FBW SPOILER ACTUATOR OPEN LOOP FREQUENCY RESPONSE  
 FIGURE 81



RUDDER ACTUATOR FREQUENCY RESPONSE

FIGURE 82

affected by the higher bandwidth and performance proved adequate for the LAMS program.

Figure 83 shows response of the surface to a one degree electrical step input and Figure 84 that the unit has approximately .125 degrees of hysteresis for small inputs. The data for the preceding figures were recorded with the actuator installed in the aircraft at the conclusion of the flight program.

#### 5.2.5 Elevator Actuator

The elevator actuators were manufactured by Weston Hydraulics to Boeing specification. As was the case of the rudder actuator, the units were essentially identical to previously qualified flight units.

Figure 85 shows the closed loop frequency response of the elevator actuator while installed in the aircraft. Gain and phase for the elevator actuator were within design limits over its operating range. Figure 86 shows the response of the surface to a one degree electrical step input and Figure 87 shows that actuator has less than .10 degrees of hysteresis for small inputs.

#### 5. Hydraulic Power System Performance

An analysis of the existing hydraulic power systems revealed that available power of each hydraulic system would have to be increased for peak demands and that two new systems would be required in the aft body of the aircraft to provide power to the new powered actuation systems.

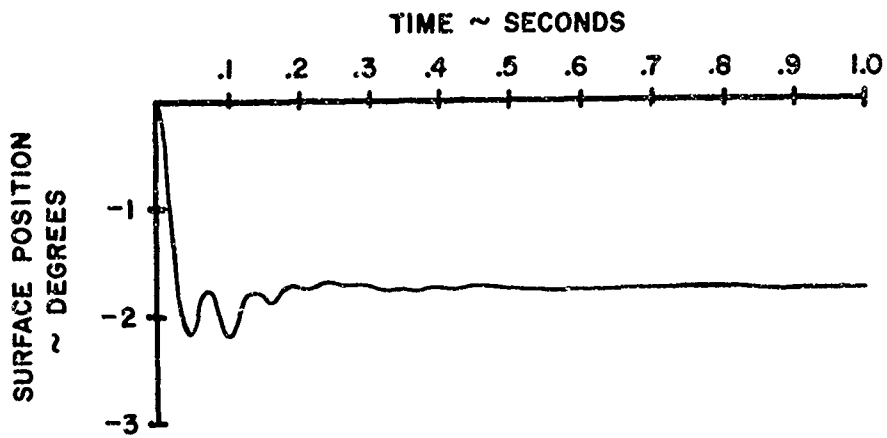
##### 5.3.1 Roll Axis Hydraulic Power Systems

Hydraulic power for actuating the spoilers and ailerons is provided by six separate, existing hydraulic systems. The primary source of power for each system is an engine driven pump. Increasing flow in these systems was accomplished by replacing the existing stand-by pumps with larger auxiliary motor-pump assemblies.

The spoiler system motor-pumps are "off the shelf" assemblies from the ABEX Company. Each pump has a 3.8 GPM flow rating and is the rotating cylinder barrel and piston type, driven through a pivoting hanger with an inclined camface. The pump is driven by a Westinghouse (7.5 H.P.), 400 cps electric motor rotating at 12,000 RPM. The aileron system pump assemblies were manufactured to a Boeing Specification by New York Airbrake Company. Each pump has a 6 GPM flow rating and is a variable delivery, axial piston type with integral pressure regulation and flow control. Pistons reciprocate within a fixed block and fluid is discharged through individual check valves with pumping action being accomplished by a "wobble plate". A General Electric (12 H.P.) 400 cps electric motor rotating at 7750 RMP provides pump power.

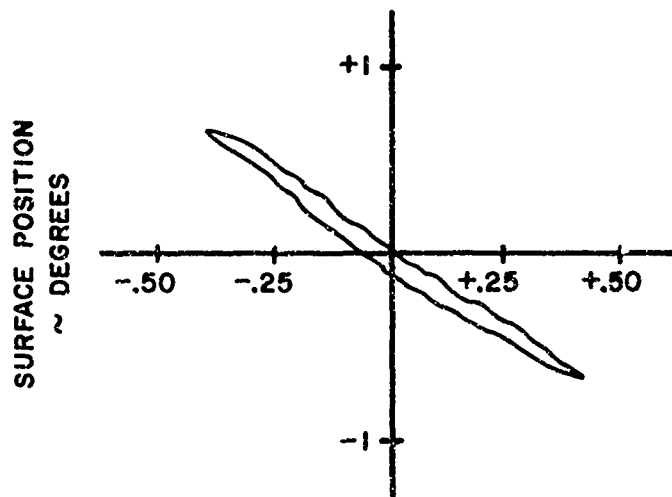
##### 5.3.2 Rudder-Elevator Hydraulic Power System

Hydraulic power for actuating the rudder-elevator system is provided by a dual hydraulic system. Each system provides half the power to operate



RUDDER ACTUATOR STEP RESPONSE

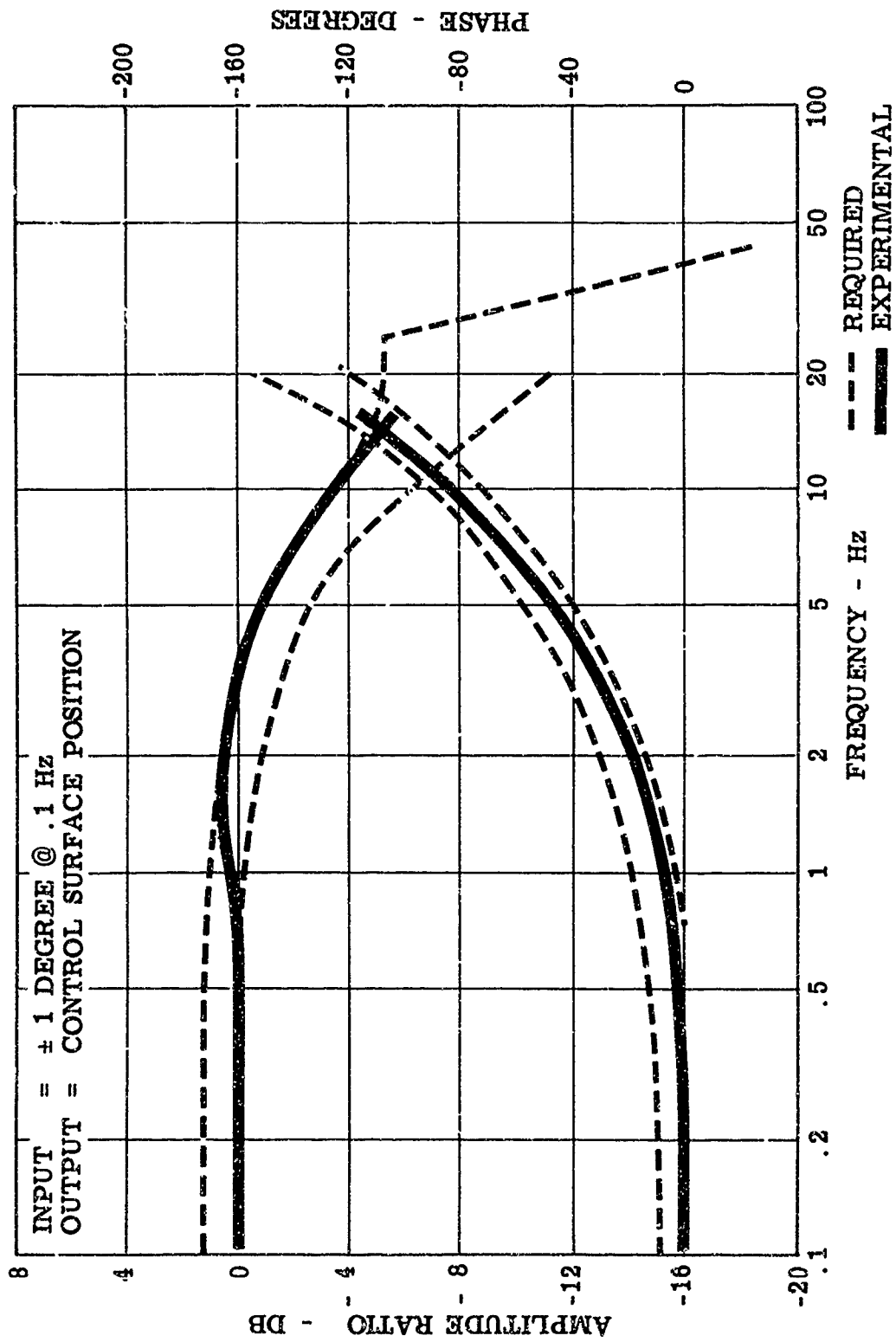
FIGURE 83



ELECTRICAL INPUT ~ VOLTS

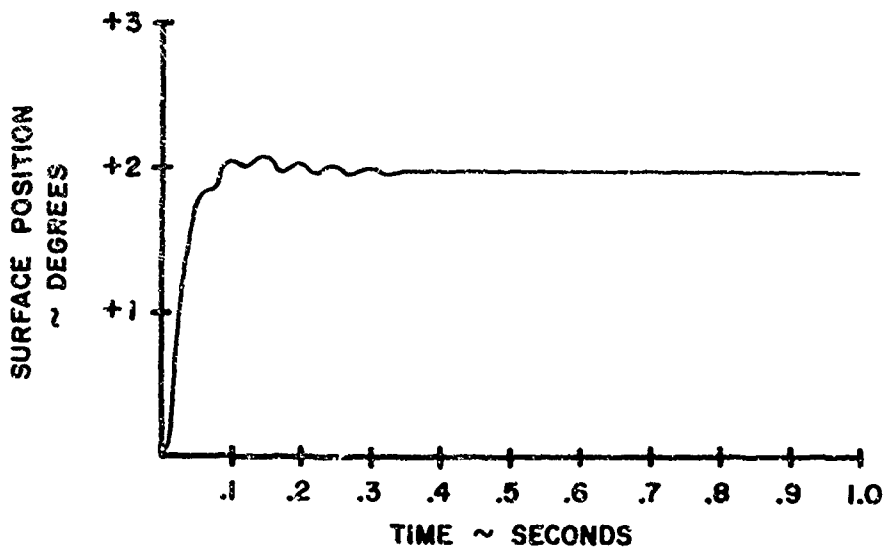
RUDDER ACTUATOR HYSTERESIS

FIGURE 84



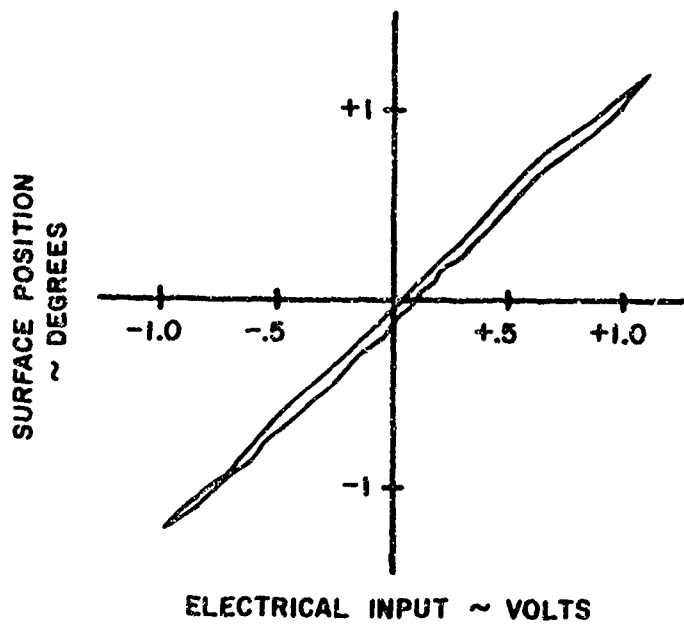
ELEVATOR ACTUATOR FREQUENCY RESPONSE

FIGURE 85



ELEVATOR ACTUATOR STEP RESPONSE

FIGURE 86



ELEVATOR ACTUATOR HYSTERESIS

FIGURE 87

each of the actuators in the rudder-elevator system.

The pump assemblies are manufactured to a Boeing Specification by The New York Airbrake Company. Each pump has a 6 GPM flow rating and is variable delivery axial piston type with integral pressure regulation and flow control. Pistons reciprocate within a fixed block and fluid is discharged through individual check valves. Piston pumping action is accomplished by a "wobble plate". A General Electric (12 H.P.) 400 cps electric motor rotating at 7750 RMP nominal provides pump power.

Each system has a self pressurizing, air-less reservoir and an integral manifold containing filters, relief valves, pressure switches, and attach ports.

A standby source of hydraulic power is provided by a hydraulic motor driven pump (transformer). The transformer assemblies are manufactured by the ABEX Company to a Boeing Specification. Each pump has a 2 GPM flow rating and consists of a hydraulic motor mechanically driving a hydraulic pump. The motor and pump are of the same type, a rotating cylinder barrel and piston, driven through a pivoting hanger with an inclined camface. The hydraulic motor receives power from the R.H. body-aileron system and mechanically transmits this energy to one empennage system. Transformer power is transmitted only if low pressure is sensed in the empennage system, either through system failure or transient peak demands from the elevator-rudder system.

### 5.3.3 LAMS Hydraulic Power System Testing

New components of the modified hydraulic systems received and passed the flight-worthiness qualification tests outlined in the Boeing Specifications. In the case of "off the shelf hardware", existing qualification data was reviewed and acceptance was granted through test data similarity to the B-52 requirements.

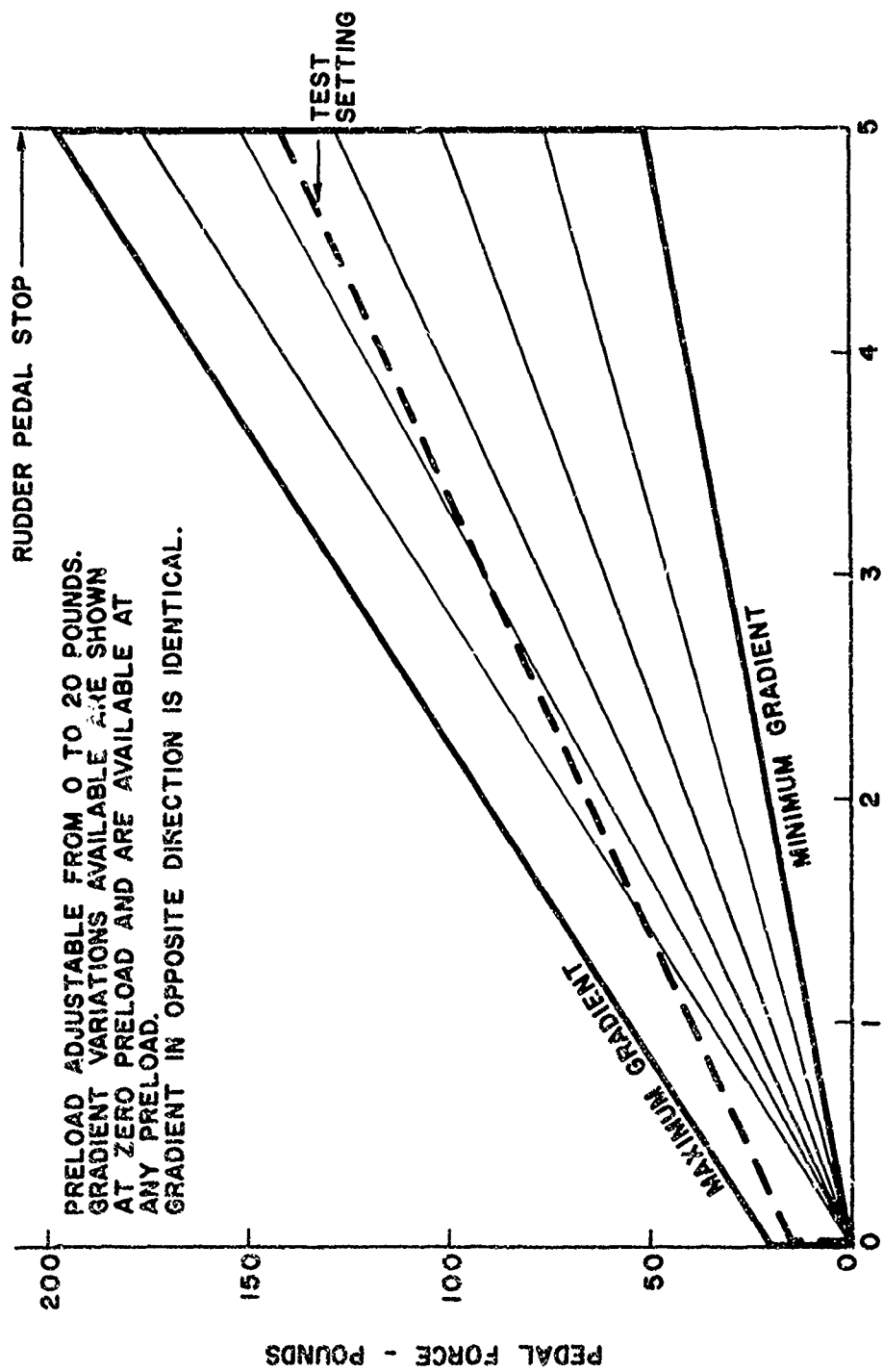
All hydraulic components successfully passed acceptance tests prior to installation on the aircraft. Each hydraulic system was ground tested and satisfactorily fulfilled the requirements.

Instrumentation was installed at selected points in the modified and new hydraulic systems to sense pressure, temperature, and flow. The system performed satisfactorily during the flight test program.

### 5.4 Evaluation Pilot Feel System

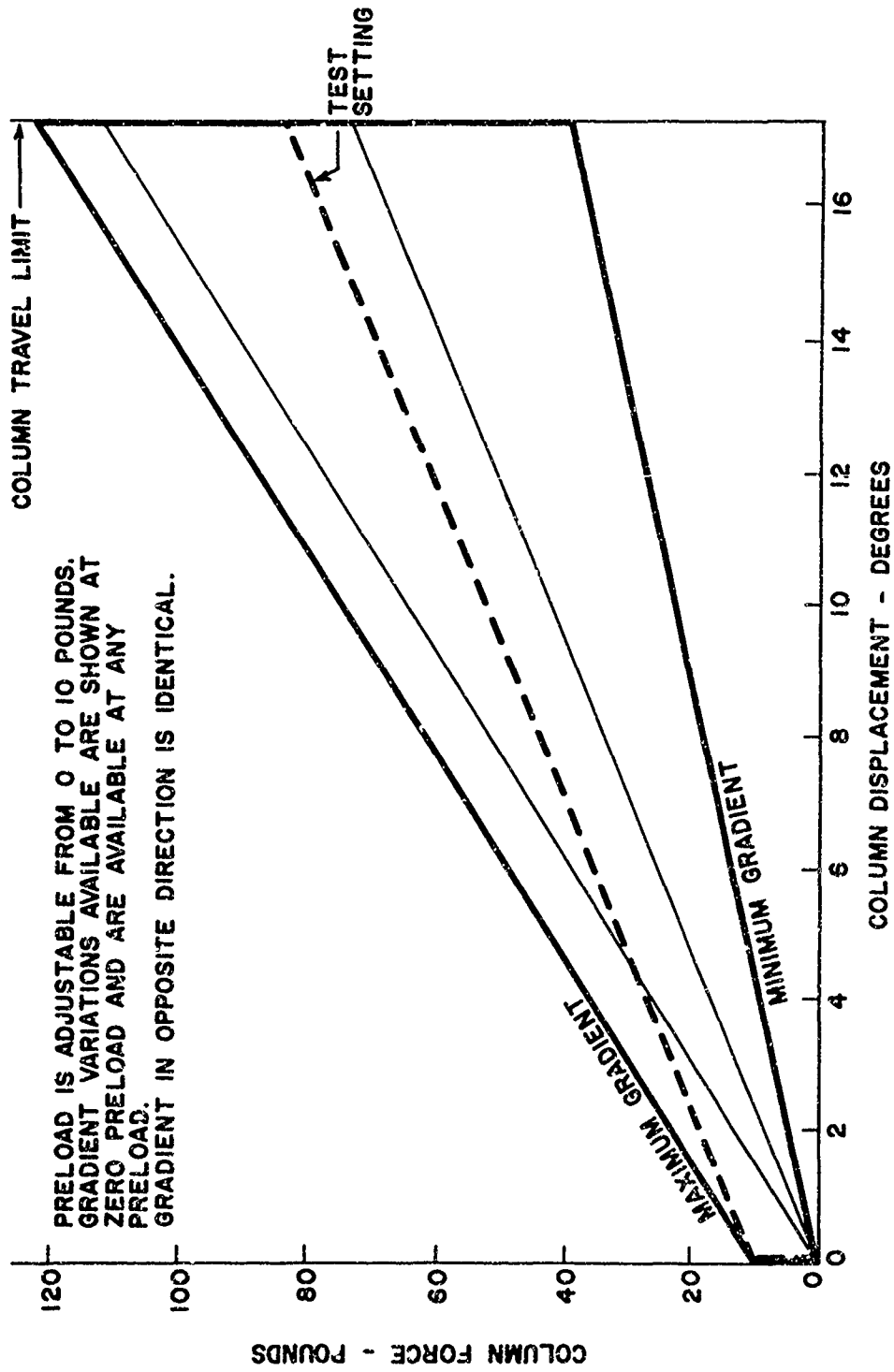
The evaluation pilot controls (the left seat of the LAMS test vehicle) are not connected to the normal aircraft control cable and feel system, but are connected to springs for centering and force gradient. Position potentiometers provide electrical indication of the position of the controls to command the aircraft through fly-by-wire means.

The centering and force gradients of the controls in each axis were adjusted to simulate the actual values of existing aircraft cable control systems at the test flight condition. Figures 85, 86, and 87 reflect the test vehicles gradients and the force adjustment envelope available on the



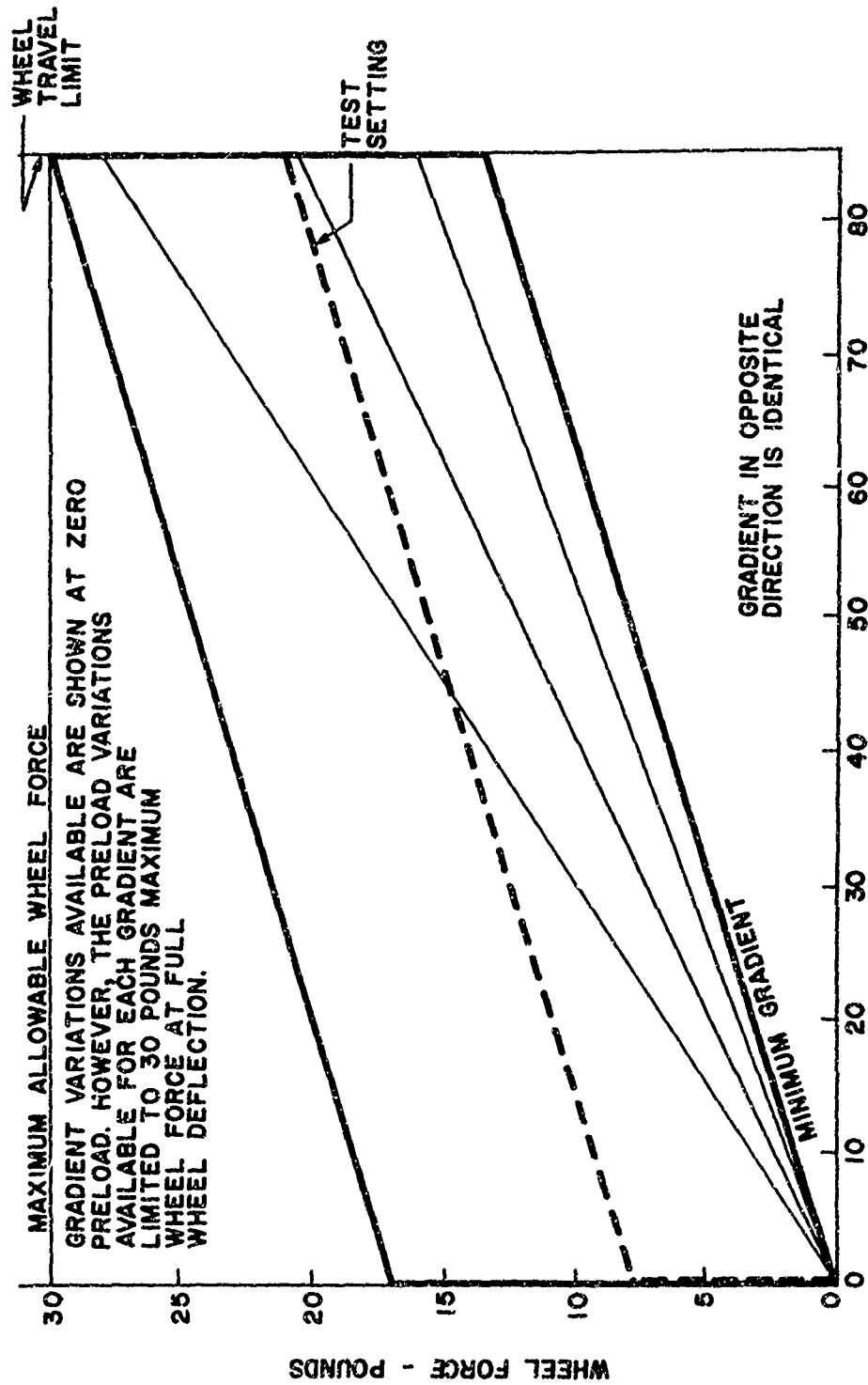
EVALUATION PILOT RUDDER PEDAL FEEL SYSTEM PRELOAD AND SPRING GRADIENT

FIGURE 88



EVALUATION PILOT CONTROL COLUMN FEEL SYSTEM PRELOAD AND SPRING GRADIENT

FIGURE 89



EVALUATION PILOT CONTROL WHEEL FEEL SYSTEM PRELOAD AND SPRING GRADIENT

FIGURE 90

test vehicle. The inherent cable system friction was not duplicated and consequently an oscillation is apparent in the wheel and pedal movement around center. The column was provided an eddy current damper which provides dynamic damping.

The dynamic cycling apparent on the wheel and rudder pedals would cause a deteriorous effect on the test vehicle through electrical input signals to the wide band actuation systems. To prevent wheel and pedal induced oscillations, first order electrical filters have been added to the roll and yaw fly-by-wire signals on the analog computer which attenuate the signal 12 db at 6.3 cps.

## 5.5 Electrical Equipment

The electrical equipment includes the monitor system, analog computers, and the function generator. The monitor system consists of the safety monitor and data monitoring equipment, the indicators, oscilloscope, oscillograph, and digital voltmeter.

### 5.5.1 Monitor System

The safety monitor system presented no apparent problems during ground testing; however, during the first flight the system was subjected to numerous nuisance disengagements. These disengagements were attributed to two factors: low signal limits on several structural acceleration monitors, and high frequency electrical transients. Subsequently, gain changes were made in the structural acceleration monitor modules and a first order low pass filter was added to all safety monitor modules to reduce nuisance disengagements.

Seven special indicators were installed at the pilot station. The column and rudder pedal force indicators and aileron and rudder position indicators operated satisfactorily. The indicators initially chosen for elevator position, normal acceleration at the aircraft c.g., and sideslip were so heavily damped that they proved unsatisfactory in flight and were replaced by instruments with less damping.

The aft fuselage electronics rack temperature indicator was calibrated to 120° F and for certain transient speed conditions this temperature was exceeded during an early flight. Since the equipment can operate at temperatures in excess of 120° F for short periods of time without damage, two additional temperature sensors which actuate warning lights at the flight engineers station were installed. These temperature switches were set at 150° F and were located on the upper and lower corners of the electronics rack. The 150° F temperature level provided the required indication to identify an electronic rack overheat condition.

Three items of equipment for inflight and ground checkout data monitoring were provided for the flight engineer: a two channel oscilloscope, the computer digital voltmeter with selectable signal inputs, and the "quick look" oscillograph. The dual trace oscilloscope and digital voltmeter signal selection and readout capability provided on-line data to evaluate the control system status. All signals available at the interpatch panel were accessible for display on the oscilloscope and/or digital voltmeter through

the switching panel provided. The oscillograph had an adequate signal selection since 73 combinations of signals were available using the switch panel. However, the signal gain scaling restricted usefulness of the oscillograph. Only two gain scaling switch selections were available; 10 volts/inch and 5 volts/inch.

#### 5.5.2 Analog Computers

One of the EAI TR-48 analog computers was vibration tested at the EAI testing laboratory to verify that the computer would perform satisfactorily in the B-52 environment. The computer was mounted in an isolation frame and sinusoidally vibrated at frequencies of 5 cps to 13 cps at 0.20 inch peak to peak and at 0.5 g's from 13 cps to 300 cps. A 15 minute frequency sweep through the frequency envelope was accomplished in each of the three computer axes. As resonant frequencies occurred, these frequencies were held so that affected computer components could be located and observed to verify that no damage would result. Foam material and padding were installed as required to reduce component acoustic excitation. During the entire test the computer was operating. A program was "patched" on the computer so that operation of all modules could be observed. The computer operated satisfactorily during vibration and no major discrepancies were noted.

During the flight test no major problems occurred in the computer component modules. However, several unpotted computer potentiometer wires located on the computer right door panel failed during the flight test program. These broken wires were easily detected and repaired as required. No simple method of support was found to prevent such failures.

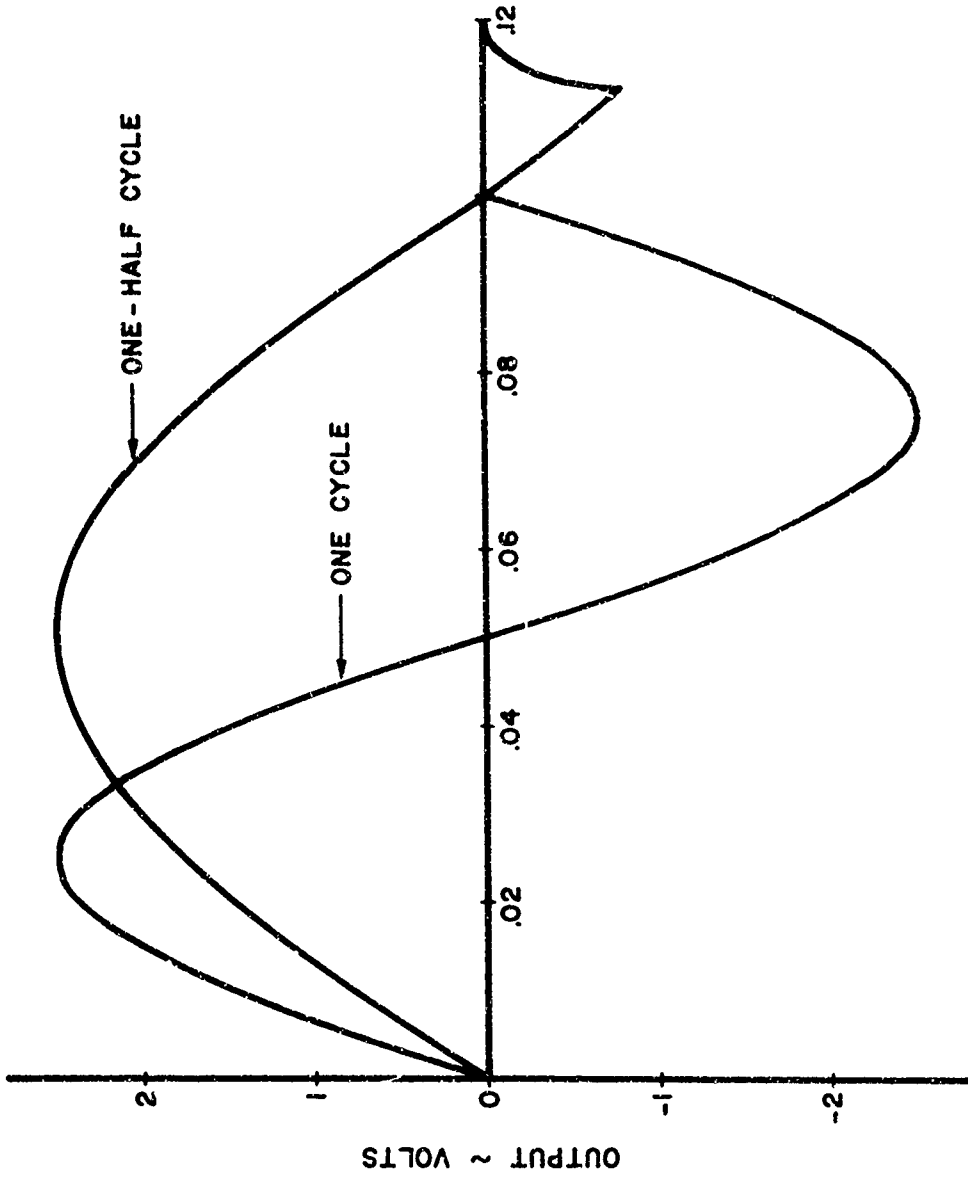
#### 5.5.3 Function Generator

The function generator supplies sine, ramp, triangular, and square wave output signals over a range of 0.005 cps to one megacycle and allows selection of  $\frac{1}{2}$ , 1, 2, 3, 4, cycles or free run operation. Figure 91 shows a  $\frac{1}{2}$  cycle and a 1 cycle sine wave function generator output. The  $\frac{1}{2}$  cycle sine wave output signal exhibited a peak overshoot of 32 percent at signal cutoff due to low voltage diode characteristics. The short time duration prevented the overshoot from causing any problem in use.

#### 5.6 Baseline SAS

The Baseline SAS was synthesized in accordance with the block diagrams presented in Section 3.5 using the forward computer patch board at the Flight Engineer's Station. The ground test functional checkout consisted of applying a simulated rate gyro signal into each SAS channel (pitch, roll and yaw). The sinusoidal rate gyro output was simulated by a Weston, Boonshaft and Fuchs Transfer Function Analyzer and the system output response (control surface position) was fed back to the analyzer for gain and phase measurements.

The functional test was run for all three flight conditions. Since electrical filtering does not change and only a gain change occurs between flight conditions, data for flight condition two (the maximum gain condition) is shown and is typical of all conditions.



TIME ~ SECONDS

FUNCTION GENERATOR SINE WAVE OUTPUT

FIGURE 91

### 5.6.1 Longitudinal Axis

The longitudinal axis was tested simulating the pitch rate gyro response at B.S. 820. The results of the elevator deflection response with respect to the pitch rate signal are presented on Figure 92, and show good agreement with the theoretical requirements in the frequency band below 3 cps. The gain disagreement above 3 cps is not significant because the system response at these frequencies is well attenuated.

### 5.6.2 Lateral-Directional Axis

The lateral axis was tested simulating the roll rate gyro response at B.S. 820. The results of the aileron position response with respect to the roll rate signal are presented on Figure 93, and show good agreement at frequencies below 3 cps. The disagreement between experiment and theory is not significant above 3 cps because the system response amplitude is well attenuated for higher frequencies.

The directional axis was tested simulating the yaw rate gyro response at B.S. 616. The results of the rudder deflection response with respect to the yaw rate signal are presented on Figure 94, and show excellent agreement with the theoretical requirement throughout the frequency spectrum tested.

## 5.7 LAMS-FCS Hardware

### 5.7.1 LAMS Computer Performance

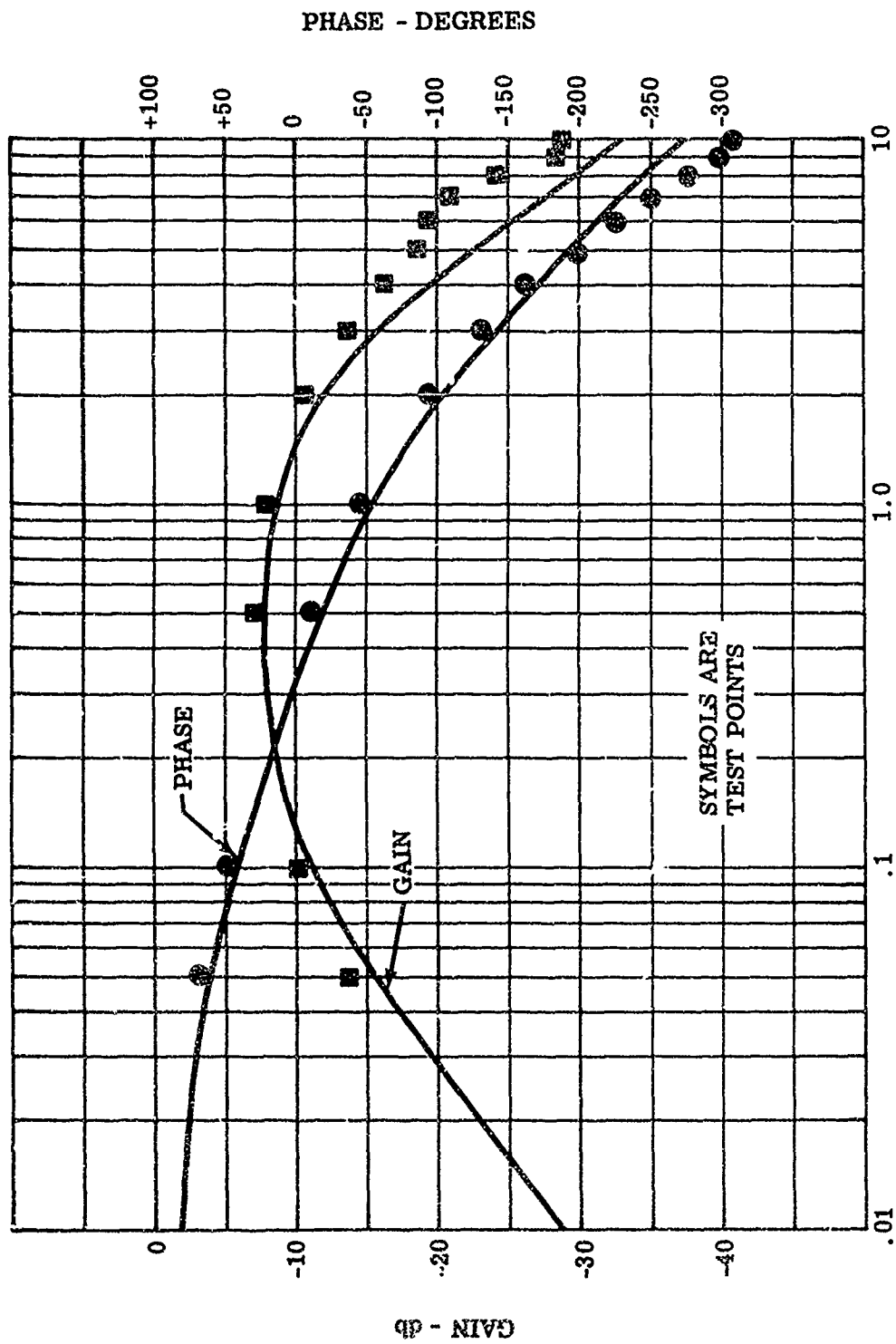
To check the functional performance of the LAMS-FCS computer, end-to-end frequency responses for the 13 independent signal paths were run. Since the functional testing of the LAMS computer was performed before the equipment was installed in the aircraft the resulting frequency responses do not include the actuator or control surface dynamics. A sinusoidal rate gyro output was simulated by a Weston, Boonshaft and Fuchs Transfer Function Analyzer and the output of the computer (command signal to servo amplifier) was fed back into the analyzer for gain and phase measurement.

The functional test was run for all three flight conditions. However, since electrical filtering is constant and only gain changes from one flight condition to another, data for only one flight condition is presented and is typical of all.

Figures 95 through 107, show the results of this functional testing. The theoretical values are shown plotted in a solid line and the test values as points. The LAMS computer design specification states that all gains shall be within  $\pm 1\%$  percent of nominal and all phases within  $\pm 7$  degrees of nominal except where specified otherwise. These exceptions are at the various channel notch frequencies in the system. The tests were within all stated specifications.

### 5.7.2 Longitudinal Axis

Locations of the four rate gyros used in the pitch axis are shown in Figure 13. There are two roll rate gyros, one located in each wing. These



SYMBOLS ARE TEST POINTS

PHASE

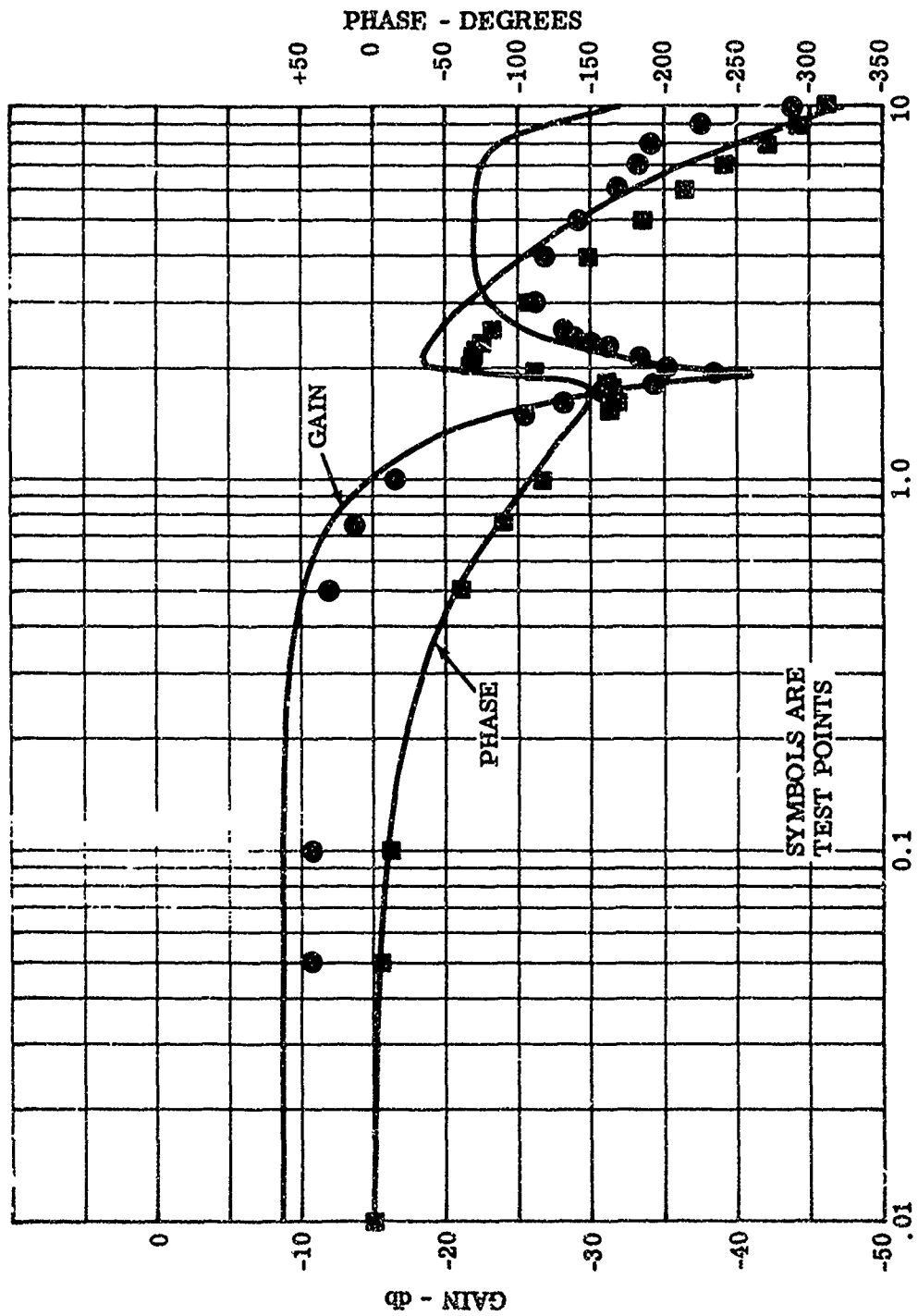
GAIN

FREQUENCY - Hz

OPEN LOOP FREQUENCY RESPONSE

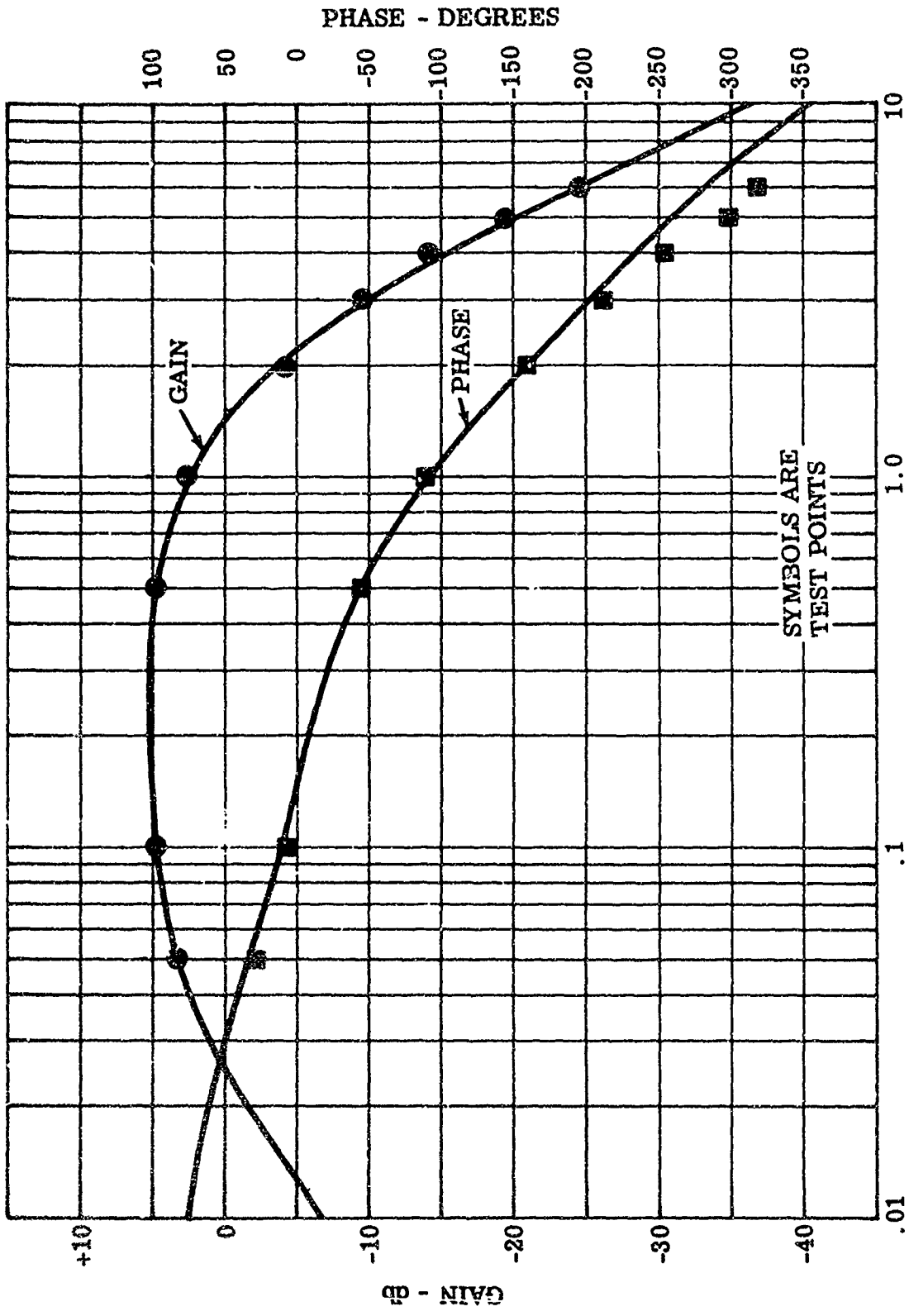
BASELINE PITCH SAS FC-2

FIGURE 92



OPEN LOOP FREQUENCY RESPONSE  
 BASELINE ROLL SAS FC-2

FIGURE 93



OPEN LOOP FREQUENCY RESPONSE  
 BASELINE YAW SAS FC-2  
 FIGURE 94

two gyro signals were gain adjusted and summed into a single signal. However, three independent channels were evaluated since this single gyro signal is routed to the elevators, ailerons, and spoilers, operating symmetrically. The forward and aft body rate gyro signals also go to all three control surfaces requiring three independent channels to be evaluated for each gyro. The evaluation pilot column to elevator channel has a first order roll off to filter high frequency inputs and is tested as a separate channel. Figures 95 through 104 present the functional test results for the pitch axis channels.

### 5.7.3 Lateral-Directional Axis

The six yaw and roll rate gyro locations for the lateral-directional axis are shown in Figure 13. The yaw axis has one channel from the yaw rate gyro located at B.S. 695 to the rudder. The results of the yaw axis testing are plotted in Figure 102. The roll axis has two roll rate gyros, one near the c.g. and one in the aft body, and three yaw rate gyros, one in the forward fuselage and two in the aft fuselage. The five roll axis rate gyro signals are gain adjusted and summed into a single channel to drive the ailerons antisymmetrically. An evaluation pilot wheel to aileron signal is filtered similar to the evaluation pilot column signal and is tested as a separate channel. The roll axis results are shown in Figures 103 and 104.

### 5.8 System Checkout

When the aircraft modification was complete and the aircraft was ready for flight, extensive functional testing was performed to assure the proper operation of the electrical and hydraulic equipment. Additional, between flight testing was accomplished to insure that any random or flight produced system deterioration or failures would be discovered and repaired before subsequent flights. Two system checkouts were performed before each flight. Preflight checkouts were accomplished the day before each flight and thoroughly checked the LAMS equipment. Prior to flight checkout was done immediately prior to take-off and rechecked all system components on an end-to-end basis. A detailed procedure for preflight and prior to flight checkout is documented in Reference 3.

In preflight checkout the LAMS suitcase tester was used for checking the LAMS-FCS. The tester made it possible to monitor output signals from the LAMS computer and many intermediate signals in each channel and to check and adjust power supplies. Loop isolation switches provided isolation of each channel for trouble shooting. Data from the preflight checkouts was recorded for each flight.

#### 5.8.1 Preflight Checkout

Several interpatch boards and analog computer boards were aboard the aircraft. Therefore, each board was numbered and a check made to insure that the proper boards were installed for flight and/or ground testing. The procedure followed to accomplish the preflight checks is presented in the following paragraphs.

The interface electronics modules located above the analog computer and in the aft fuselage were inspected to insure proper installation.

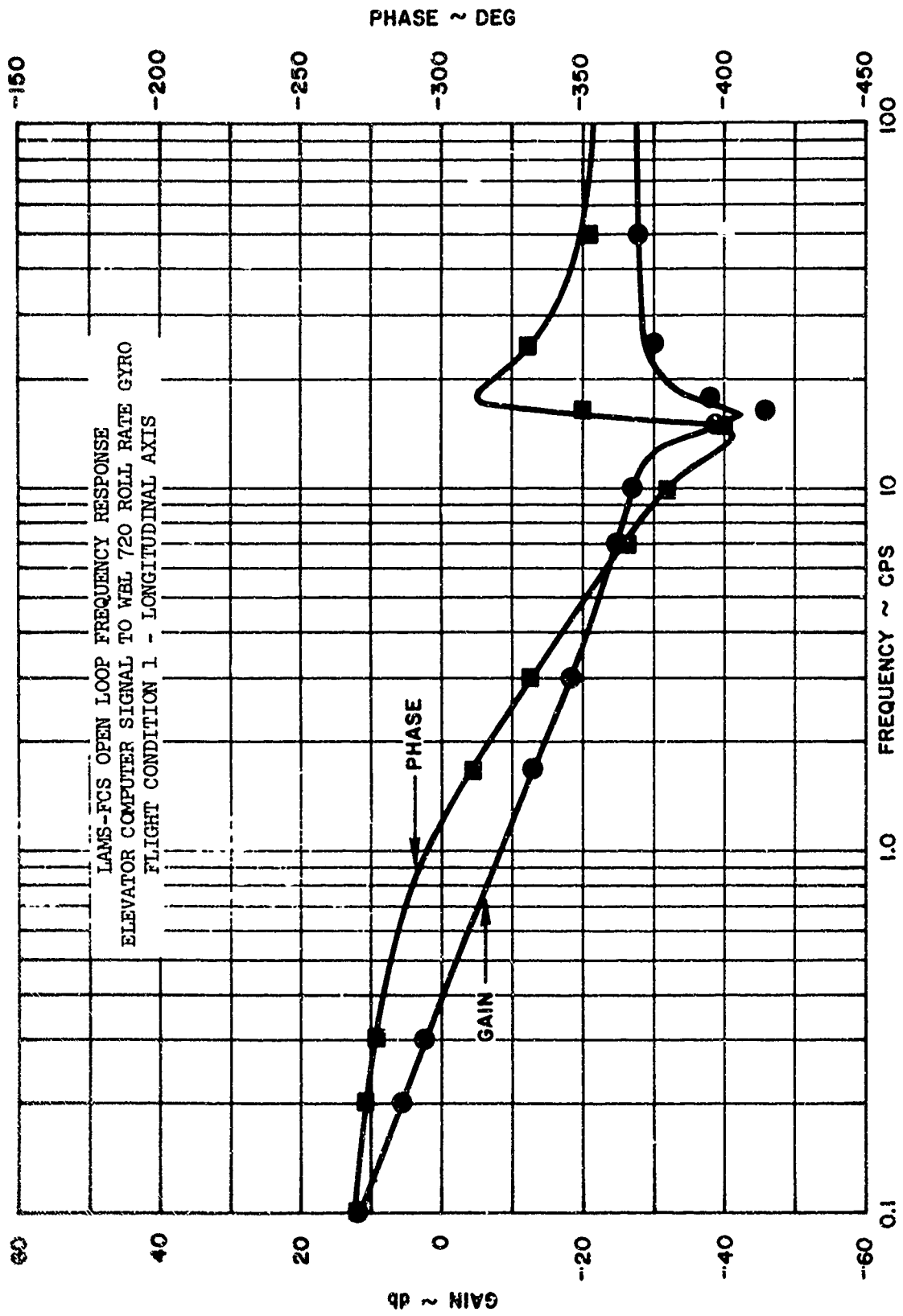


FIGURE 95

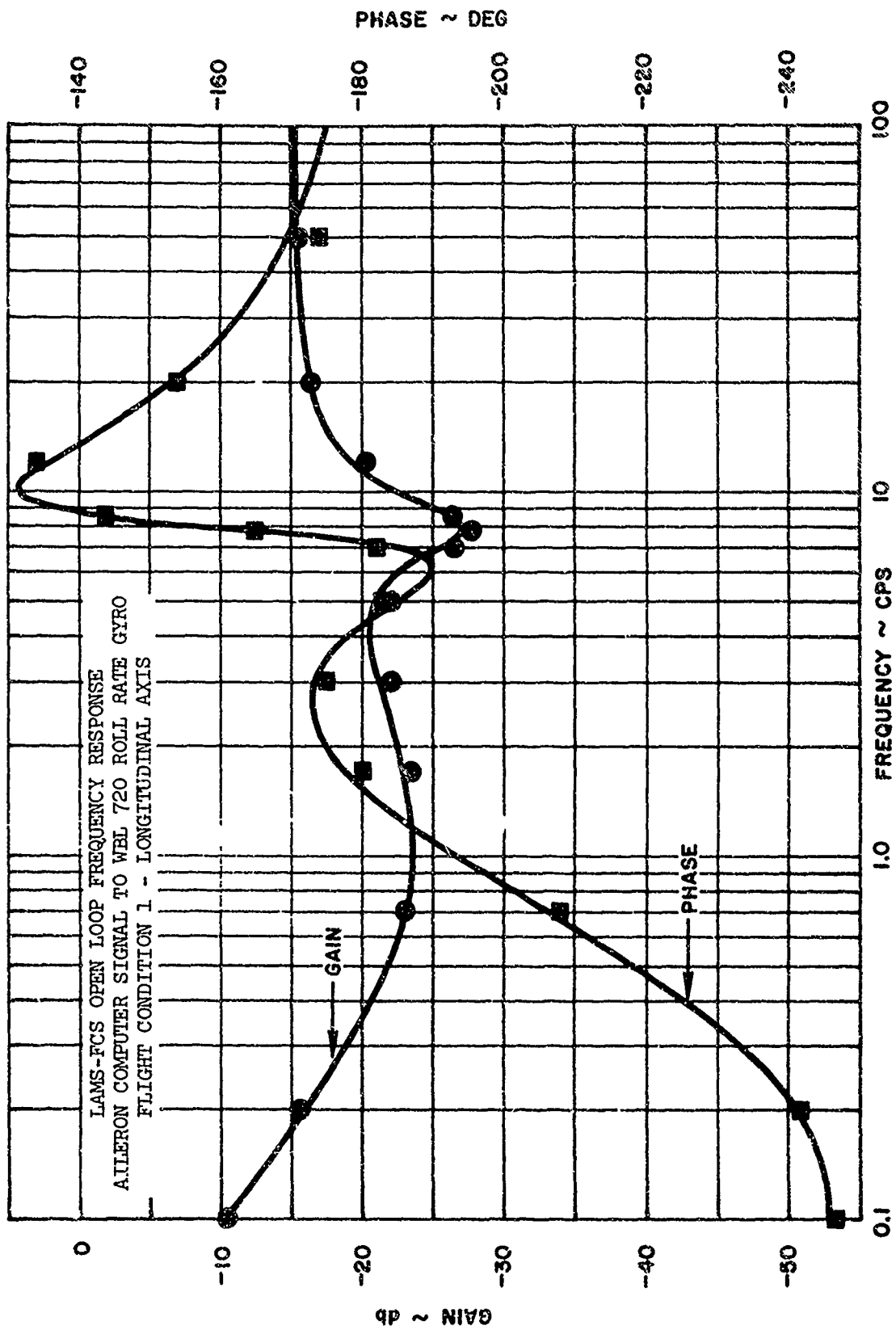


FIGURE 96

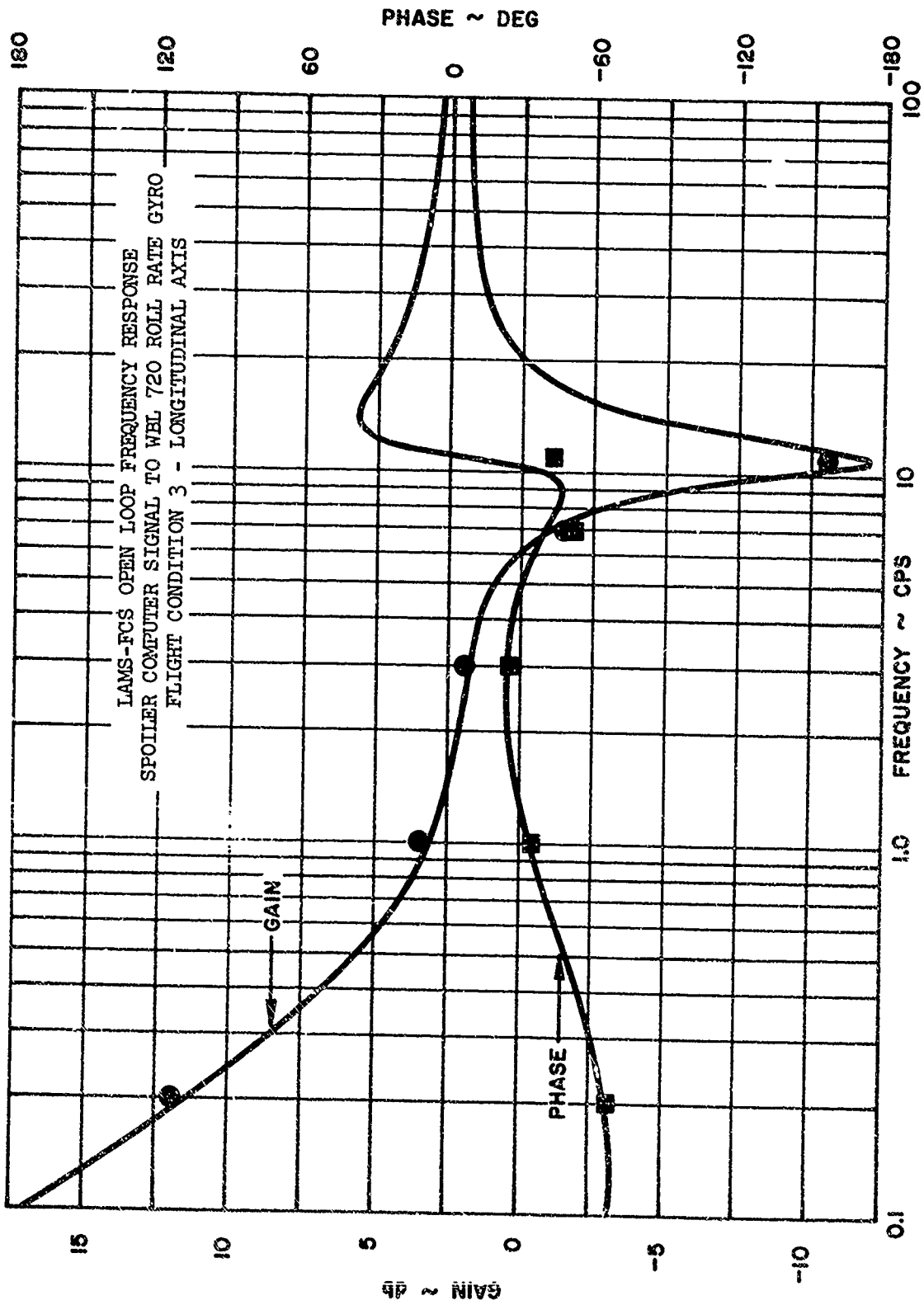


FIGURE 97

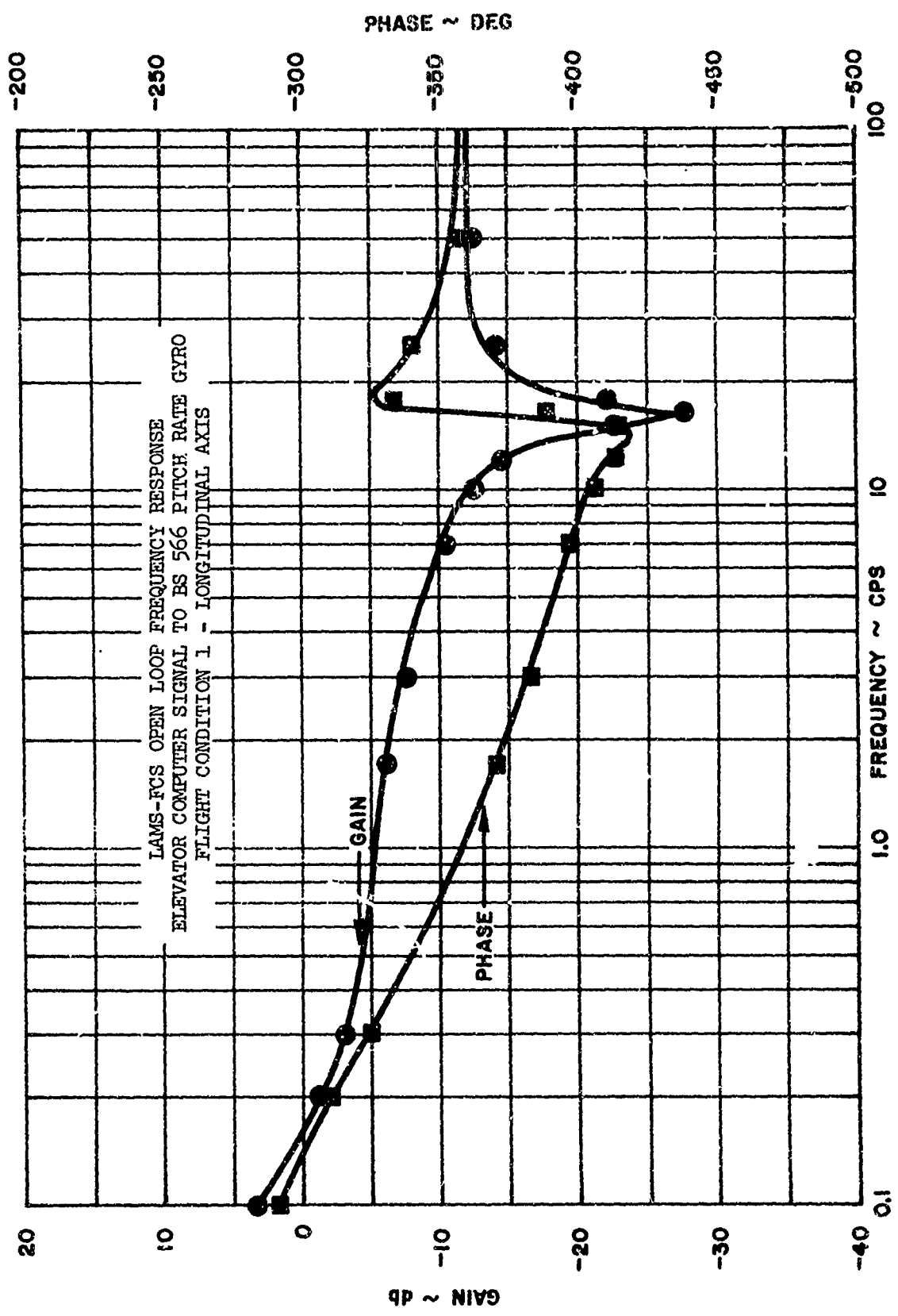


FIGURE 98

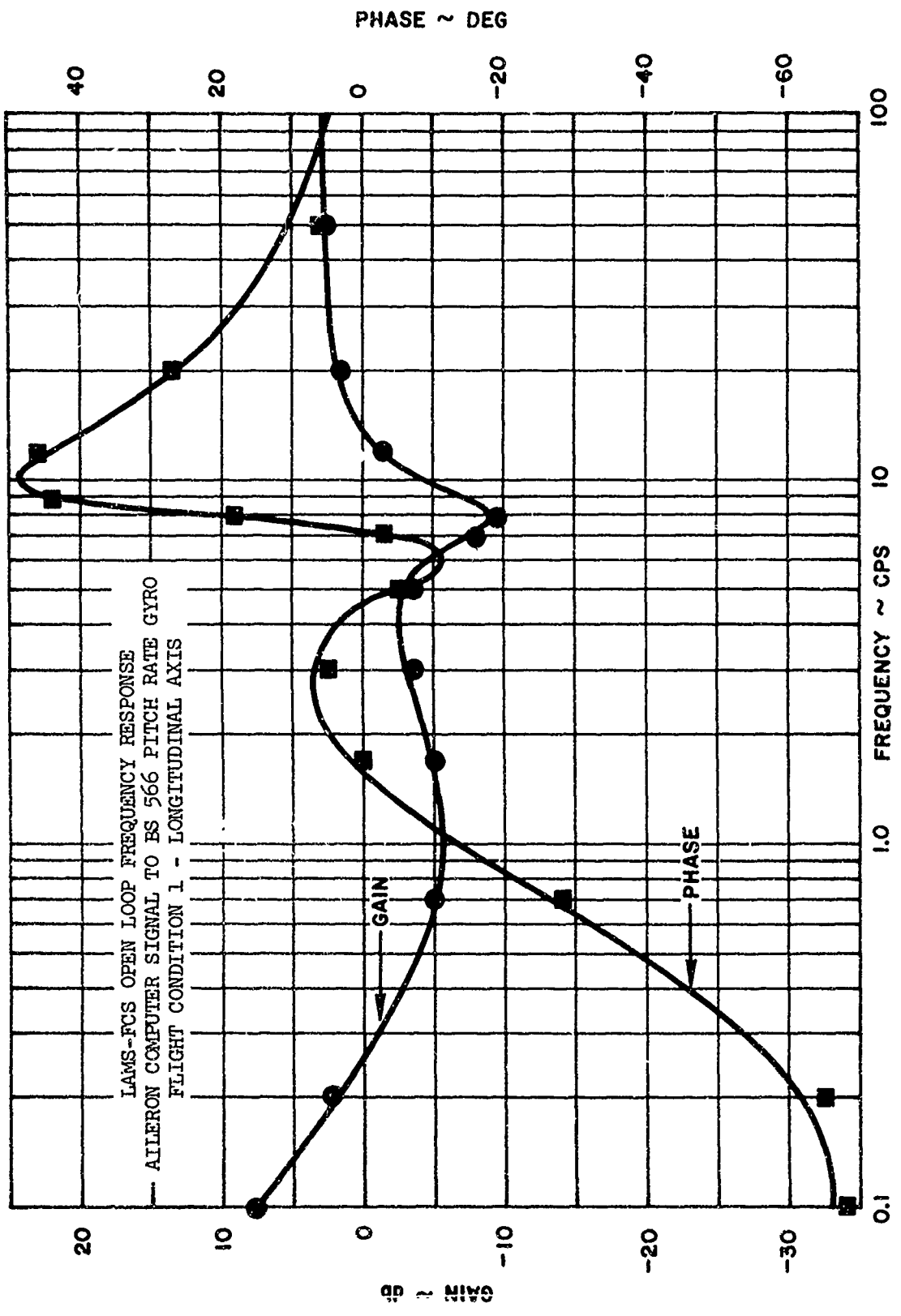


FIGURE 99

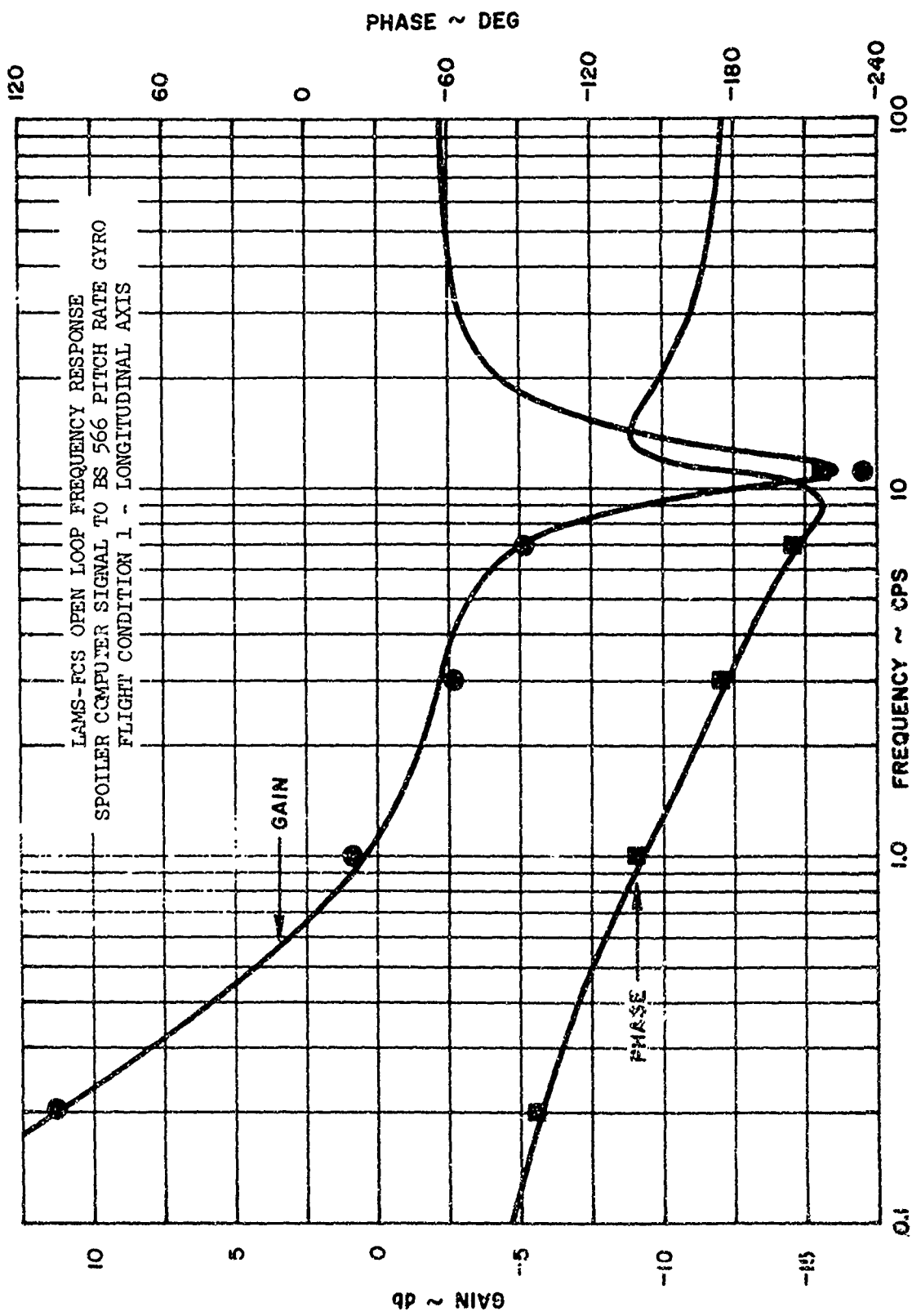


FIGURE 100

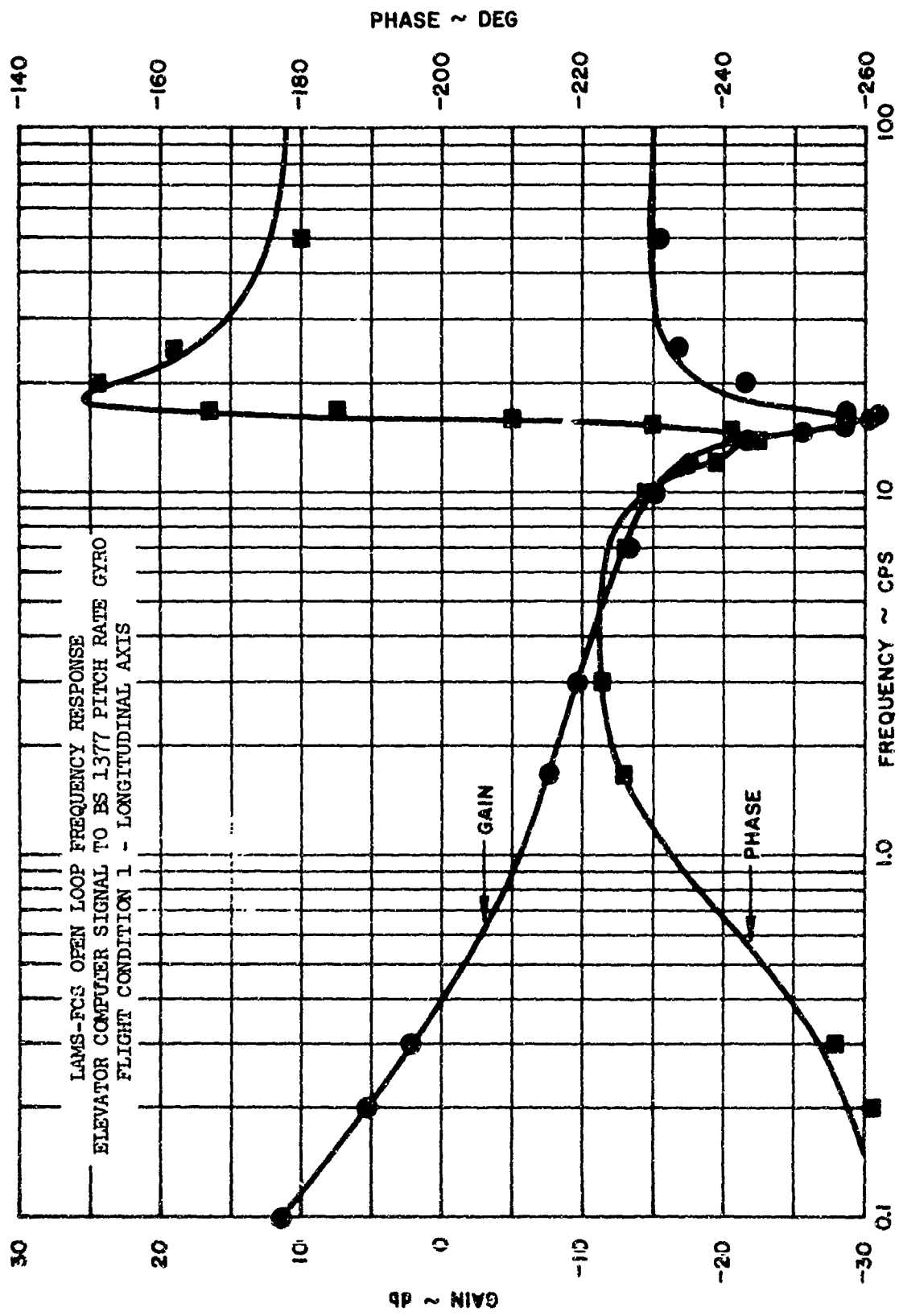


FIGURE 101

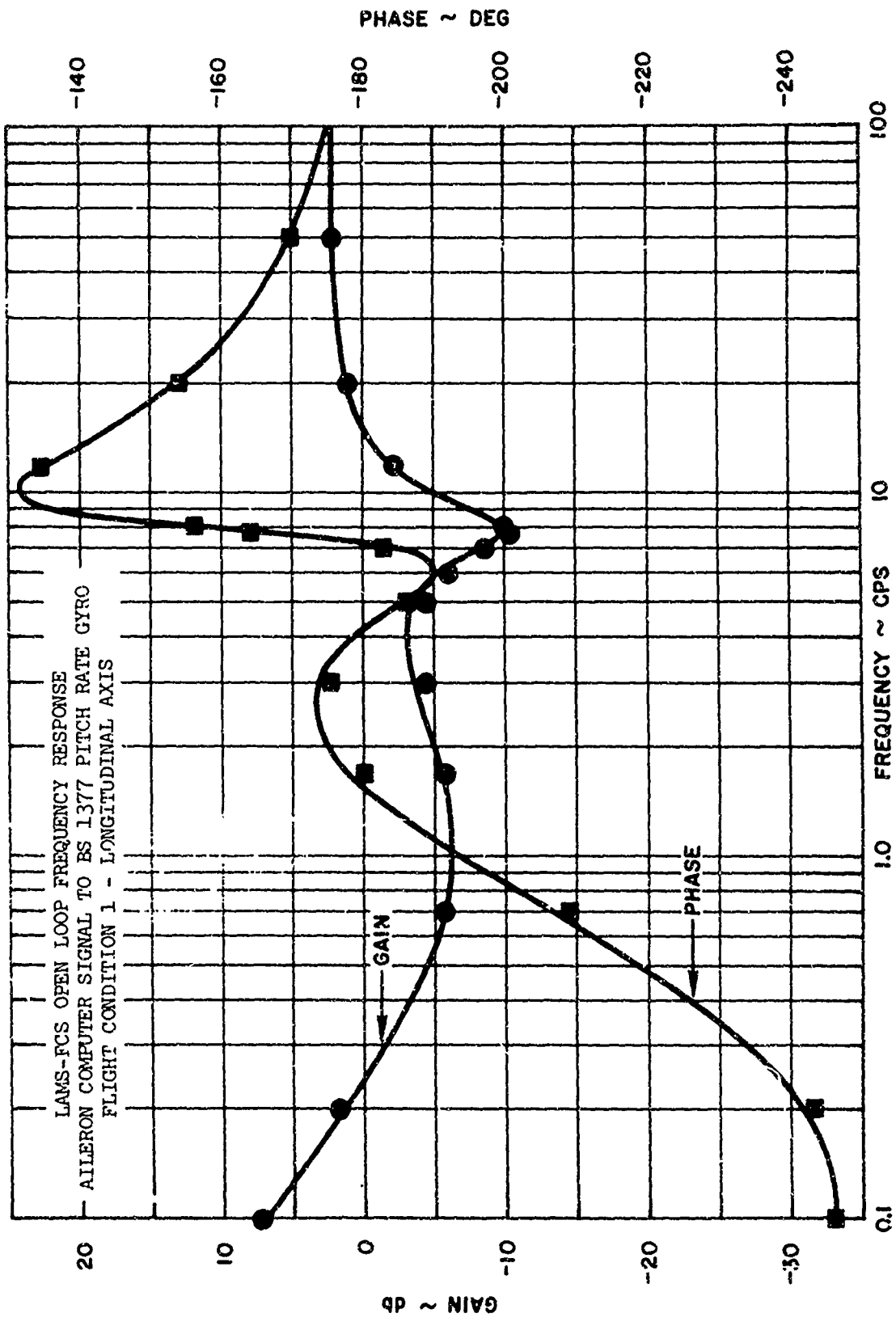


FIGURE 102

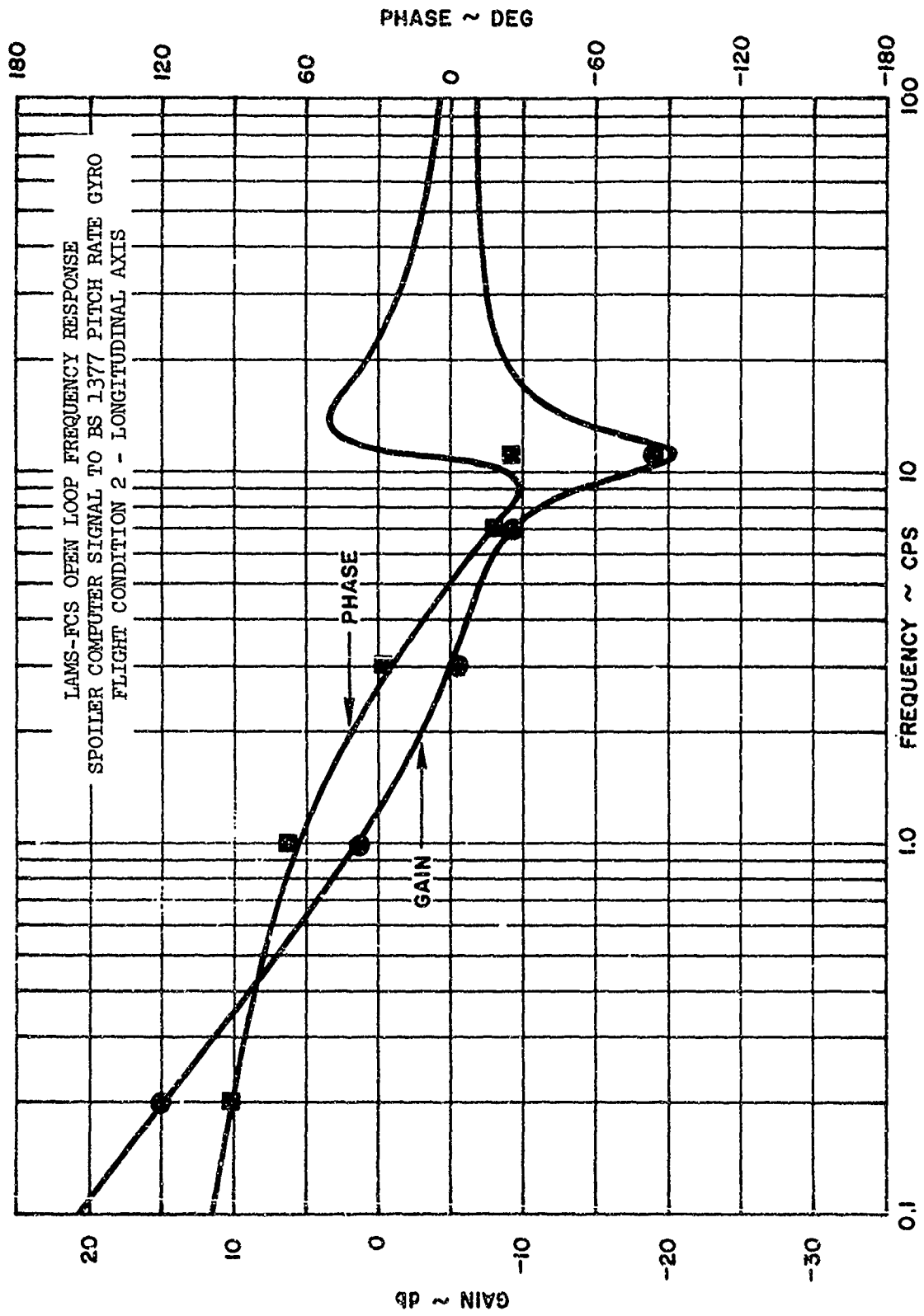
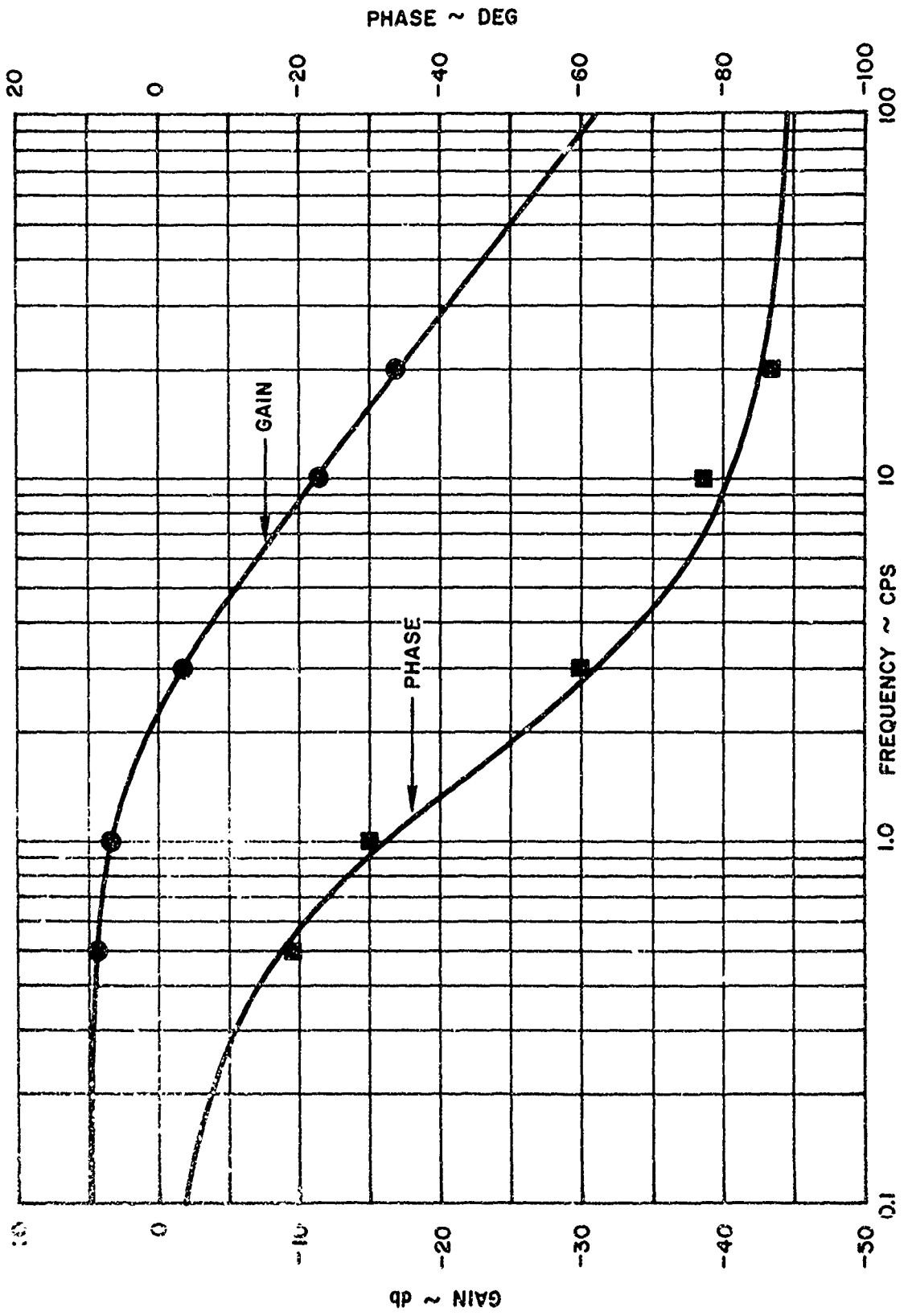


FIGURE 103



LAMS-FCS OPEN LOOP FREQUENCY RESPONSE - ELEVATOR TO EVALUATION PILOT COLUMN

FIGURE 104

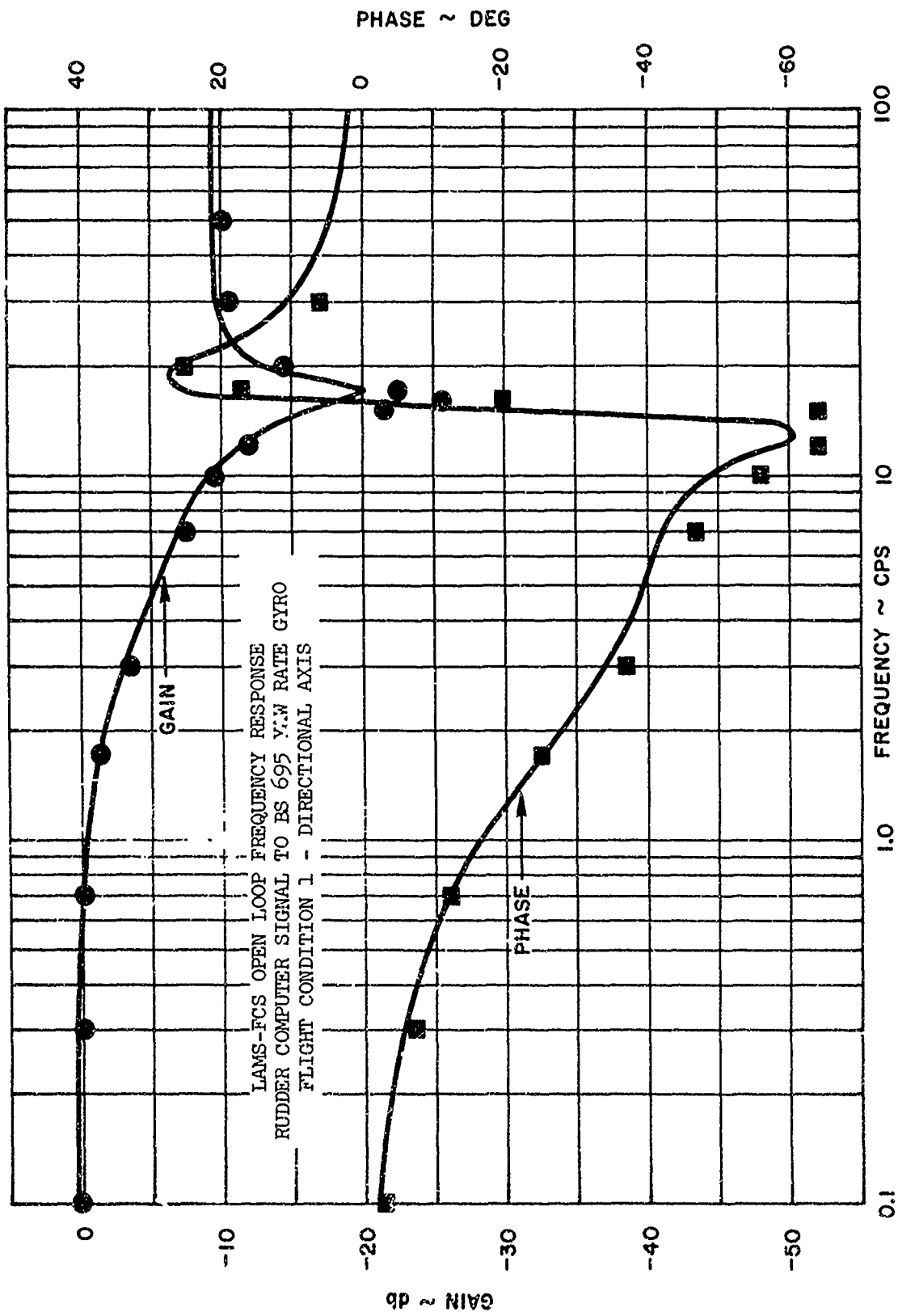


FIGURE 105

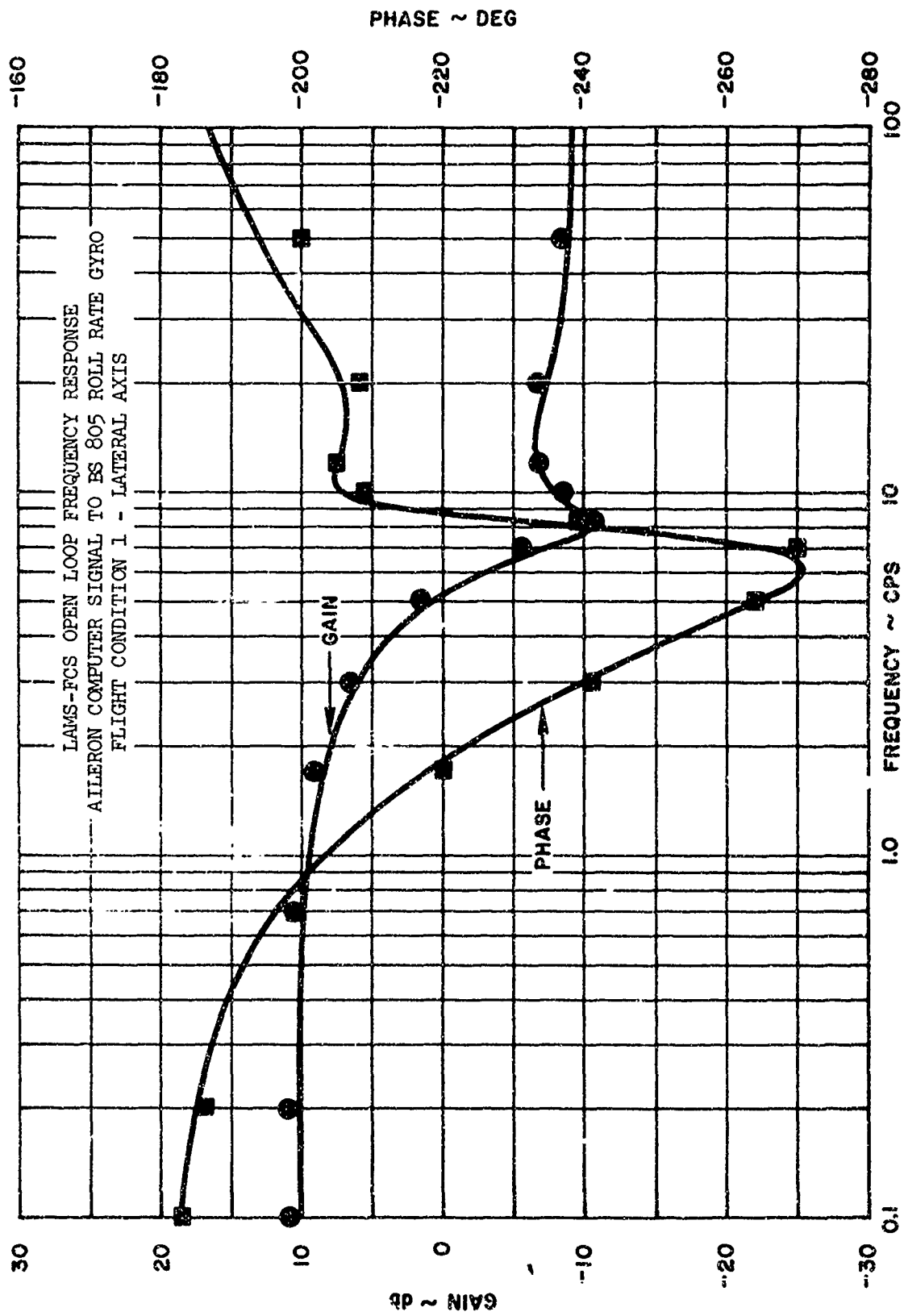
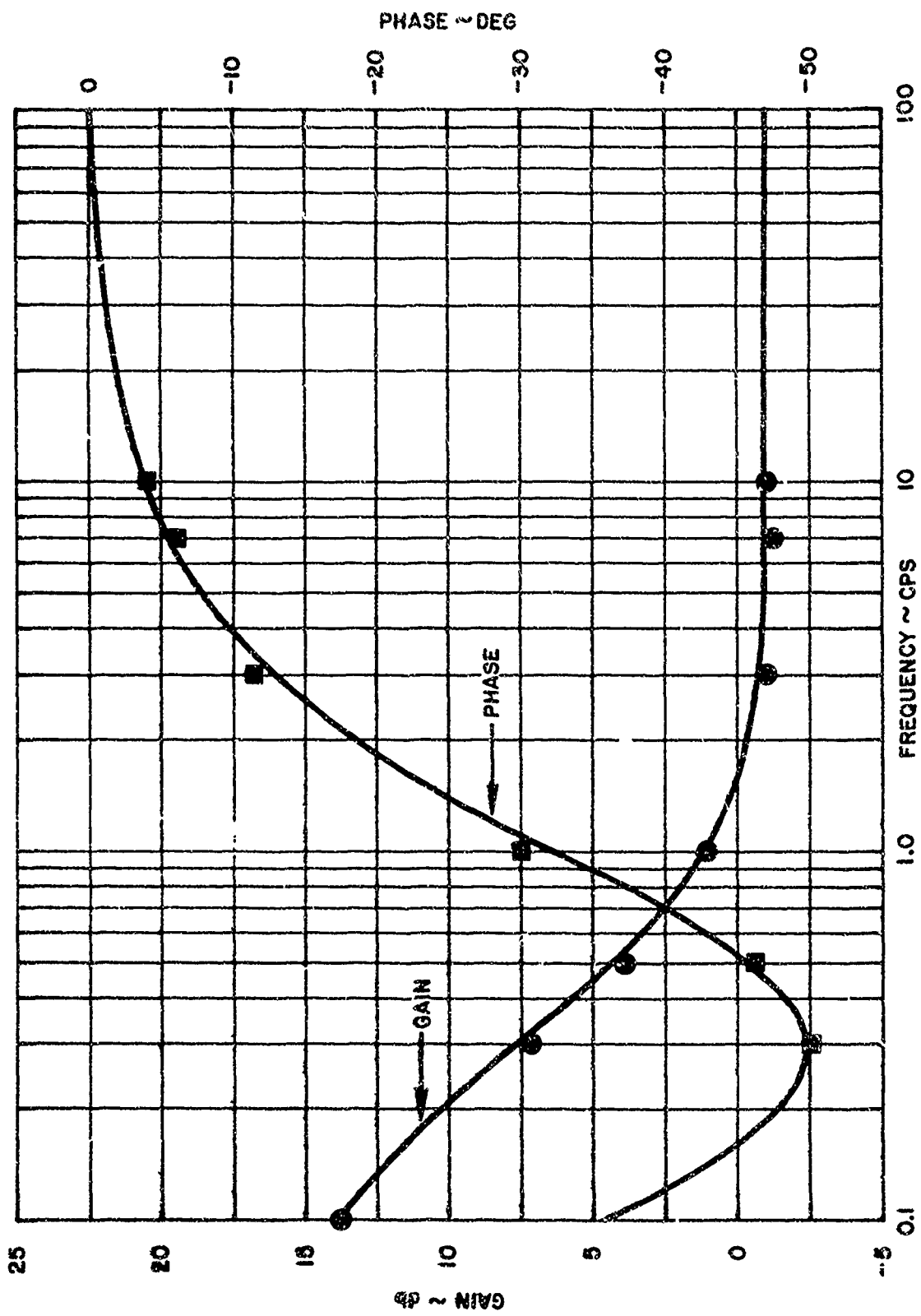


FIGURE 106



LAMS-FCS OPEN LOOP FREQUENCY RESPONSE - ALLERON TO EVALUATION PILOT WHEEL

FIGURE 107

The power supplies were monitored on the analog computer DVM. The power supplies were required to be within 1 to 2 percent.

The function generator was checked for waveform, number of cycles, amplitude, and frequency, using the oscilloscope. Wiring continuity from the function generator to each control surface auxiliary actuator was verified.

The two analog computers are slaved together and either computer can be used as the master unit at the discretion of the flight engineer. The slave mode for each computer was checked.

The safety monitor comparators and lights were checked. This was accomplished by engaging a switch which puts a large voltage on each comparator and trips the disengage switch causing all the safety monitor lights to illuminate.

G-limits for normal acceleration at the aircraft c.g. can be set by a switch on the aisle stand between the pilots and is part of the safety monitor. G-limit values were checked and system disengagement, when G-limits were exceeded, was verified. All other accelerometers, which are part of the safety monitor, were torqued to verify that the safety monitor disengaged the system at proper acceleration limits. Nulls for these accelerometers were checked and accelerometer signals were renulled as required.

Rate gyro motor speeds were checked for all rate gyros used in the Baseline SAS and LAMS-FCS. Null outputs from these rate gyros were checked and the signals were renulled as required.

Monitor pilot controls were checked by verifying that all control surfaces were in a neutral position when the monitor pilot controls were in a neutral position and that full surface deflection was attained for full monitor pilot control inputs in each axis. Evaluation pilot signals were nulled and the control surface nulls were checked with the fly-by-wire system engaged. Evaluation pilot input to control surface output gains were checked in each axis.

The Baseline SAS and LAMS-FCS were checked by obtaining a frequency response at four frequencies for the Baseline SAS and for the rudder and elevator channels of the LAMS-FCS. Five frequencies were sampled for the LAMS-FCS aileron and spoiler channels. These channels are the same as those described in the functional test of the LAMS-FCS in Section 5.7 except that frequency responses were not run for the evaluation pilot controls.

In addition, each rate gyro is torqued to provide step input responses for each axis of the Baseline SAS and each channel of the LAMS-FCS. This provides an additional check on system phasing and SAS circuit wiring continuity as well as checking the rate gyro torquing circuits. Proper operation of the torquing circuits was verified because they are required during the prior to flight checkout and as aids in "trouble shooting", if problems should occur during flight.

### 5.8.2 Prior to Flight Checkout

The prior to flight checkout is accomplished shortly before take-off and is done with the aircraft engines running and the crew on board.

A check is made to insure that the proper interpatch panel board and analog computer boards are installed and that all the LAMS system switches at the pilot station and flight engineer station are positioned properly. Power supplies are checked to insure that all are within operating tolerance.

The interlock system is checked to assure that all system status lights and switches operate properly. The safety monitor system comparators and indicator lights are checked to verify that any exceeded limit will cause the system to disengage.

The evaluation pilot controls are checked to insure that all control surfaces move in the right direction and that the evaluation pilot has full authority for all control surfaces. The monitor pilot controls are checked during the handbook prior-to-flight checkouts.

The Baseline SAS and the LAMS-FCS configurations are checked by torquing each gyro and verifying that each control surface moves in the proper direction.

## 6.0 CONCLUSIONS

The conclusions are presented in two parts. The first part refers to the total LAMS program effort as documented in four volumes. The second part deals with the conclusions obtained from the ground and flight test demonstration analysis presented in the foregoing material.

### 6.1 Conclusions, LAMS Program

Contemporary analysis and synthesis techniques were successfully applied in the Load Alleviation and Mode Stabilization (LAMS) program to a B-52 test vehicle. Using these techniques, an operable flight control system (FCS) was defined and produced in hardware. The LAMS-FCS successfully controlled selected structural modes and alleviated gust loads due to turbulence during flight demonstration.

Similar techniques were analytically applied to a low altitude and high speed flight condition for the C-5A aircraft. Significant reductions in fatigue damage rates and fuselage accelerations were predicted.

### 6.2 Conclusions, LAMS B-52 Flight Demonstration

#### 6.2.1 Aircraft Configuration

Modifications to NB-52E, AF56-632, provided an adequate test vehicle for demonstrating the LAMS system concepts.

#### 6.2.2 LAMS Flight Control System (FCS)

The LAMS-FCS was adequate to demonstrate the LAMS concept functions. Hardware flexibility was included in design of the flight control which permitted minor modifications required in flight demonstration.

#### 6.2.3 System Ground Test Evaluations

The system ground testing accomplished during this program confirmed the theoretical design analyses and provided basis for proceeding into the flight phase of the program.

#### 6.2.4 Flight Demonstration

##### 6.2.4.1 Stability

The LAMS test vehicle with powered controls with or without the Baseline SAS has an adequate flutter boundary. The aircraft with the LAMS-FCS has an adequate flutter boundary at design conditions.

##### 6.2.4.2 Airframe Response Testing

A method of introducing repeatable sinewave and step function transients into the control surfaces at selected frequencies and amplitudes was used in confirming functional operation of the control systems. Data derived from transient testing was required to define open and closed loop responses of the aircraft and system.

#### 6.2.4.3 Performance

The control surface authority and effectiveness data obtained during the test agreed well with the predicted analytical values.

Handling qualities performance was retained while improving structural performance.

Repeatable test results were obtained using statistical data reduction methods to evaluate the control system performance during flight through a turbulence environment. The LAMS-FCS provided reductions in stress and fatigue damage rates equal to or greater than that predicted by the analyses. Also, the ride qualities with the LAMS engaged was as predicted by the analyses.

The LAMS-FCS, one of a family of controllers that could be proposed meets the design and performance criteria.

7.0 REFERENCES

1. Boeing Document D3-6657, "B-52 E/ECP-1128 Ground Vibration Test (AF 56-632)."
2. Boeing Document D3-6951-4, "GVT-B-52H/ECP-1195 Prototype."
3. Boeing Document D3-7877, "LAMS Airplane Preflight Checkout Procedure."
4. Boeing-Honeywell Report D3-7901-1, "Aircraft Load Alleviation and Mode Stabilization (LAMS) B-52 System Analysis, Synthesis, and Design."
5. Boeing-Honeywell Report D3-7902-1, "Aircraft Load Alleviation and Mode Stabilization (LAMS) Flight Demonstration Test Activities."
6. Boeing Document D3-7902-4, "LAMS Aerodynamic Flight Evaluation - Handling Qualities and Control Surface Effectiveness."

UNCLASSIFIED

Security Classification

DOCUMENT CONTROL DATA R & D

(Security classification of title, body of abstract, and indexing information shall be entered when the report is classified)

1. ORIGINATING ACTIVITY (Corporate author)		2a. REPORT SECURITY CLASSIFICATION	
The Boeing Company Wichita Division Wichita, Kansas 67210		UNCLASSIFIED	
3. REPORT TITLE		2b. GROUP	
Aircraft Load Alleviation and Mode Stabilization (LAMS) Flight Demonstration Test Analysis		N/A	
4. DESCRIPTIVE NOTES (Type of report and inclusive dates)			
Final Technical Report			
5. AUTHOR(S) (First name, middle initial, last name)			
The Boeing Company and Honeywell, Inc.			
6. REPORT DATE		7a. TOTAL NO. OF PAGES	7b. NO. OF REFS
December 1969		179	6
8a. CONTRACT OR GRANT NO.		9a. ORIGINATOR'S REPORT NUMBER(S)	
AF33(615)-3753		APFDL-TR-68-164	
8b. PROJECT NO.		9b. OTHER REPORT NUMBER (Any other numbers that may be assigned this report)	
683E		D3-7902-2	
10. DISTRIBUTION STATEMENT			
This document is subject to special export controls and each transmittal to foreign governments or foreign nationals may be made only with prior approval of the Air Force Flight Dynamics Laboratory (FDCS), WPAFB, Ohio 45433.			
11. SUPPLEMENTARY NOTES		12. SPONSORING MILITARY ACTIVITY	
		Air Force Flight Dynamics Laboratory Wright-Patterson AFB, Ohio 45433	
13. ABSTRACT			
<p>The Load Alleviation and Mode Stabilization (LAMS) program was conducted to demonstrate the capabilities of an advanced flight control system to alleviate gust loads and control structural modes on a large flexible aircraft using existing aerodynamic control surfaces as force producers.</p> <p>The analysis, design, and flight demonstration of the flight control system was directed toward three discrete flight conditions contained in a hypothetical mission profile of a B-52E aircraft. The FCS was designed to alleviate structural loads while flying through random atmospheric turbulence.</p> <p>The B-52 LAMS-FCS was produced as hardware and installed on B-52E, AF56-632. The test vehicle modification included the addition of hydraulically powered controls, a fly-by-wire (FEW) pilot station, associated electronics and analog computers at the bombardier-navigator station, instrumentation for system evaluation, and the LAMS flight controller.</p> <p>A flight demonstration of the B-52 LAMS-FCS was conducted to provide a comparison of experimental to analytical data. The results obtained during the LAMS program showed that the LAMS-FCS provided significant reduction in fatigue damage rates similar to that predicted.</p> <p>In addition to the above, a LAMS C-5A study was included in the program. This portion of the program was to analytically demonstrate that the technology developed for the B-52 would be applied to another aircraft. The C-5A study was conducted for one flight condition contained in the C-5A mission profile and predicted significant reductions in fatigue damage rates and fuselage accelerations.</p>			

DD FORM 1473  
1 NOV 58

UNCLASSIFIED

Security Classification